Note that the vertical accuracy at larger scales converges to the same value regardless of the model of the POS/AV™. This indicates that at the larger scales the vertical ground accuracy is limited by the GPS accuracy, not the angle accuracy. Hence when using direct georeferencing at larger scales it is absolutely critical that the proper mission planning and base station layout be used in order to ensure maximum possible accuracy in the GPS solution.

As previously mentioned, some calibration issues have not been considered in the theoretical study presented herein. Two calibration parameters are important, those being camera and boresight calibration. The former is the determination of the camera interior geometry (principal point offsets and focal length) as well as lens distortion parameters (which are calibrated in a lab). The latter is the orientation offset between the image coordinate system and the IMU coordinates system (which is done using a ground target field). Residual errors of these two calibration parameter sets are kept to a minimum by checking on a regular basis - especially the boresight.

3. ANALYSIS OF AIRBORNE DATA

In order to verify the theoretical error analysis presented in Section 2, an airborne data set provided by HJW of Oakland, California is presented here. It includes image data, precisely surveyed GCPs, POS/AV™510 GPS/IMU raw observables and a post-processed GPS-assisted aerotriangulation reference.

For this flight, the POS/AV™ 510 system was used, coupled with a Zeiss RMK Top camera. A 1:6000 scale, four-strip flight was flown with minimum banking angles (to avoid GPS cycle slips) and resulting in a block of 4 strips of 11 images each (a 44-image block). The flight lines were flown in opposite directions in order to achieve good boresight calibration. A total of 27 well-distributed GCPs were included in the block.

Using the POSPac™ post-processing package, a smoothed best estimate trajectory was produced. Then, using the POSEO™ package the interpolated camera exposure station position and image orientation angles, at the moment of each camera exposure, were extracted for each photo from the trajectory, coordinated in the US state-plane mapping frame.

The constant boresight angles between the camera and the IMU were removed so that the practical error analysis could be compared with the theoretical one presented in Section 2. This was done by processing the POS/AV™ derived position and orientation angles along with the image measurements in the POSBST™ software package. After removing the boresight angles, the camera station positions and image orientation produced independently by aerotriangulation were differenced with the exterior orientation generated by the POS/AV™510. The camera exposure station position differences are shown in Figure 9, while the image orientation angle differences are shown in Figure 10. Their statistics are shown in Table 3. The results are consistent with the POS/AV™ 510 system specifications listed in Table 1.

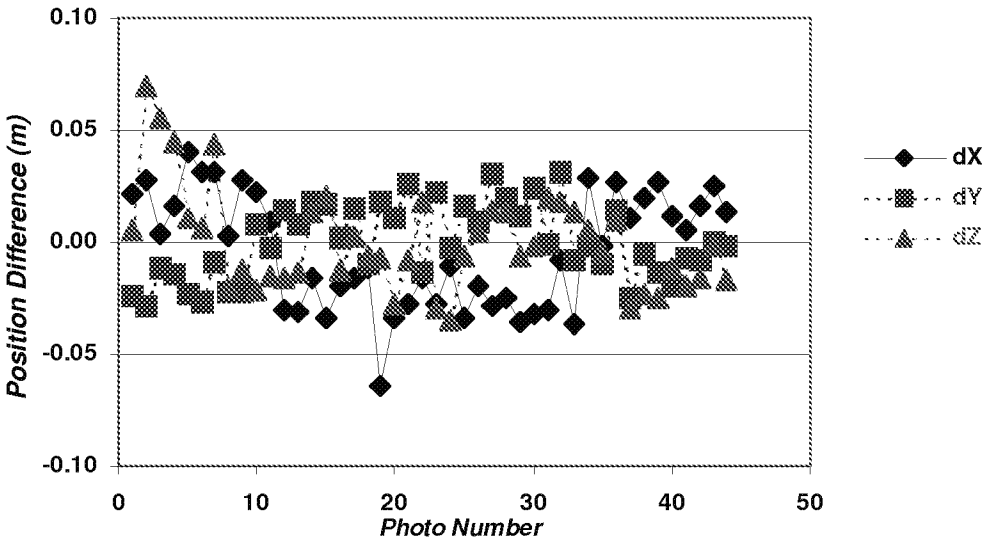


Figure 9. Camera Exposure Station Position Difference Between Aerotriangulation and POS/AV™ 510

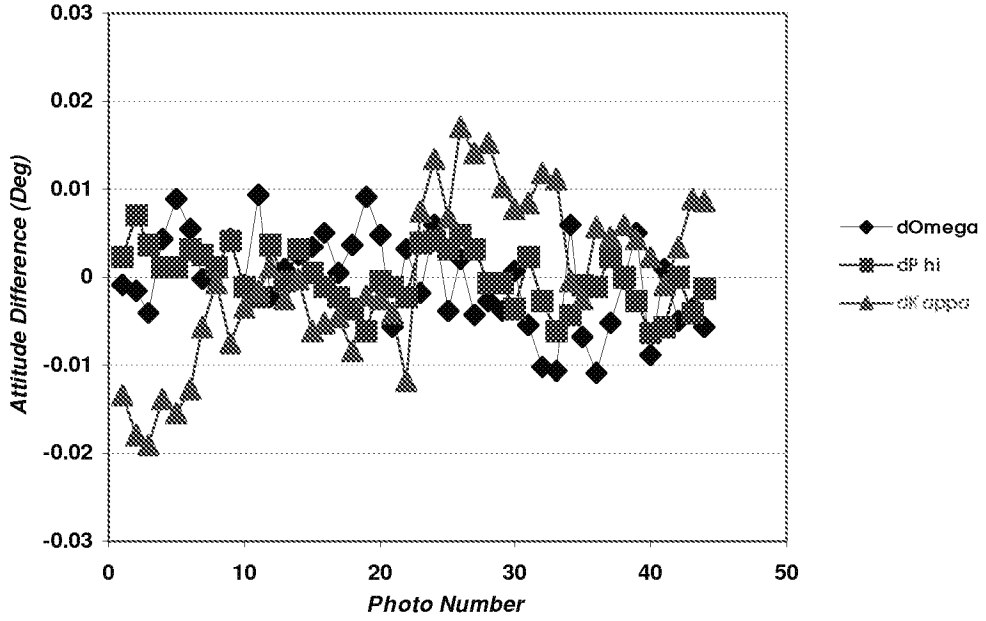


Figure 10. Camera Attitude Difference Between Aerotriangulation and POS/AV™ 510

Table 3. The Difference between Aerotriangulation and POS/AV^{TM}510

Stats.	dX (m)	dY (m)	dZ (m)	dOmega (ArcSec)	dPhi (ArcSec)	dKappa (ArcSec)
Min	-0.064	-0.029	-0.034	-39.2	-22.7	-68
Max	0.040	0.031	0.070	33.1	25.2	61
Mean	***-0.004***	***0.000***	***0.000***	***-1.4***	***-0.3***	***0.4***
Std Dev	0.026	0.017	0.023	19.1	11.9	33.1
RMS	0.03	0.02	0.02	19.2	11.9	33.1

To determine the absolute ground accuracy of the direct georeferencing approach using POS/AV^{TM} exterior orientation without GCPs, 36 models were processed individually using only one image point (with known ground coordinates) per model. In each model, the exterior orientation data derived by POS/AV^{TM} were used, along with the image point coordinates on both model photos, to determine the conjugate ground point position using the space intersection concept. The determined ground coordinates were then compared to the reference land-surveyed values. The checkpoint residuals are shown in Figure 11, while their statistics are depicted in Table 4. It is obvious from the checkpoint residuals that the accuracy of direct georeferencing using POS/AV^{TM} 510 is consistent with the theoretical accuracy presented in Figures 7 and 8 for the model case, thus validating the analysis.

Table 4. Statistics of Checkpoint Residuals

Stats.	East (m)	North (m)	Height (m)
Min	-0.19	-0.08	-0.24
Max	0.18	0.14	0.36
Mean	***0.02***	***0.01***	***0.09***
Std. Dev.	0.07	0.05	0.13
RMS	0.08	0.05	0.16

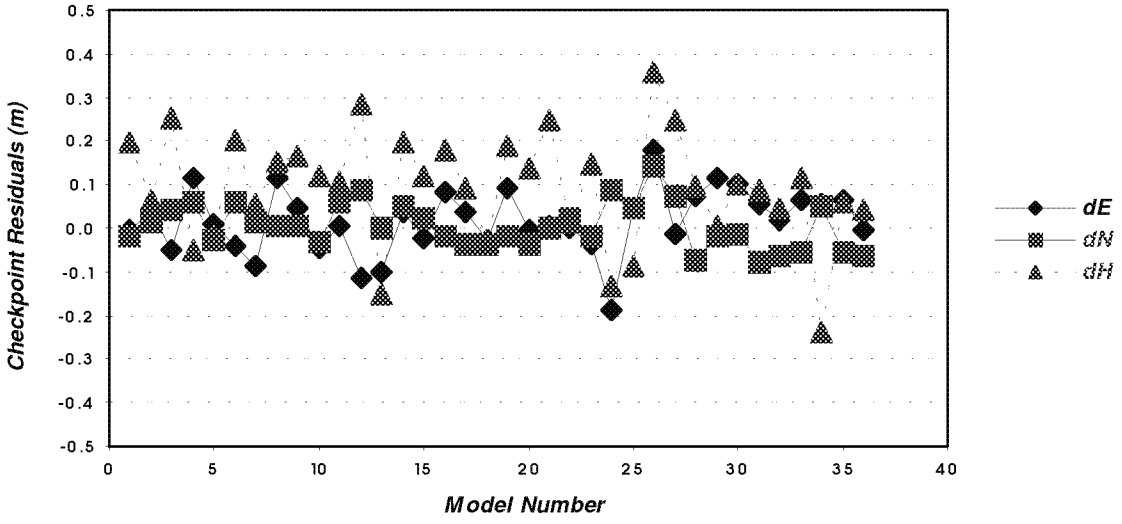


Figure 11. Check Point Residuals Derived Using Individual Models

SUMMARY AND OUTLOOK

In this paper both a theoretical and practical error analysis were presented.

The main objective of the theoretical error analysis is to extrapolate the POS/AV^{TM} system accuracy capabilities in the mapping industry, under variable conditions, for the different POS^{TM} systems and for different image scales. The airborne data error analysis was used to verify the theoretical one.

Hence, the theoretical accuracy plots presented herein can be used as guidelines for designing a multi-sensor system for data acquisition. However it should be noted that additional error sources such as boresight and camera calibration will degrade the overall integrated system accuracy. Since overall integrated system calibration and individual sensor calibration are very important in the direct georeferencing approach, the effect of residual calibration errors is currently under investigation.

ACKNOWLEDGMENT

HJW, Oakland, California, is gratefully acknowledged for providing image data, precise GCP data, and AT reference for the analysis presented here.

REFERENCES

Ackermann, F., and H. Schade, 1993. Application of GPS for Aerial Triangulation, *Photogrammetric Engineering & Remote* Sensing, 59(11):1625-1632.

ASCE, 1996. Photogrammetric Mapping - Technical Engineering and Design Guides as Adapted from The US Army Corps of Engineers, No. 14, American Society of Civil Engineers Press.

Cramer, M., D. Stallmann, and N. Halla, 1997. High Precision Georeferencing Using GPS/INS and Image Matching, Proceedings of the International Symposium on Kinematic Systems in Geodesy, Geomatics and Navigation, Banff, Alberta, Canada, June 3-6, pp. 453-462.

FGDC, 1998, Geospatial Positioning Accuracy Standards, FGDC-STD-007.3-1998, Part 3: National Standard for Spatial Data Accuracy (NSSDA).

Fraser, C.S., 1997. Digital Camera Self Calibration, ISPRS Journal of Photogrammetry & Remote Sensing, 52(1997): 149-159.

Grejner-Brzezinska, 2000. Direct Exterior Orientation of Airborne Imagery With GPS/INS Systems: Performance Analysis, Navigation, 46(4): 261-270.

Lechner, W., and P. Lahmann, 1995. Airborne Photogrammetry Based on Integrated DGPS/INS Navigation, Proceedings of the 3rd International Workshop on High Precision Navigation (K.Linkwitz and U. Hangleiter, editors), Dümmler Verlag, Bonn, Germany pp. 303-310.

Merchant, D.C., 1982. Analytical Photogrammetry - Theory and Practice, Part II, Department of Geodetic Science and Surveying, The Ohio State University.

Moffit, F., and E.M. Mikhail, 1980. Photogrammetry, Harper and Row, Inc., New York, 648 p.

Mostafa, M.M.R., K.P. Schwarz, and P.Gong, 1998. GPS/INS Integrated Navigation System in Support of Digital Image Georeferencing, Proceedings, Institute of Navigation 54th Annual Meeting, Denver, Colorado, USA, June 13, pp. 435-444.

Mostafa, M.M.R. and K.P. Schwarz, 1999. An Autonomous System for Aerial Image Acquisition and Georeferencing, American Society of Photogrammetry and Remote Sensing Annual Meeting, Portland, Oregon, May 17-21.

Reid, D.B., E. Lithopoulos, and J. Hutton, 1998. Position and Orientation System for Direct Georeferencing (POS/DG), Proceedings, Institute of Navigation 54th Annual Meeting, Denver, Colorado, USA, June 1-3, pp. 445-449.

Schwarz, K.P., M.A. Chapman, M.E. Cannon, and P. Gong, 1993. An Integrated INS/GPS Approach to the Georeferencing of Remotely Sensed Data, Photogrammetric Engineering & Remote Sensing, 59(11): 1167-1674.

Škaloud, J., M. Cramer, and K.P. Schwarz, 1996. Exterior Orientation by Direct Measurement of Position and Attitude, International Archives of Photogrammetry and Remote Sensing, 31(B3): 125-130.

BIOGRAPHICAL NOTES

Mohamed Mostafa is responsible for R&D in Airborne Applications at Applanix. He obtained a Ph.D. in Geomatics Engineering from The University of Calgary in 1999. His research interests are in the field of kinematic geodesy and digital photogrammetry.

Joseph Hutton obtained a Master of Applied Science in Aerospace Control from the University of Toronto in 1991. He has been with Applanix since 1991 as Product Manager of Airborne Applications, where he worked in the area of inertial/GPS sensor integration for airborne survey and mapping applications.

Erik Lithopoulos obtained a Master of Applied Science in Electrical Engineering from the University of Toronto in 1981. He is responsible for exploring and developing new markets for Applanix's GPS/Inertial products and technology. He has been with the company since 1991 as Manager of Business Development.

Airborne Kinematic Positioning and Attitude Determination Without Base Stations

Mohamed M. R. Mostafa and Joseph Hutton

Applanix Corporation
85 Leek Cr., Richmond Hill
Ontario, Canada L4B 3B3
Phone: (905) 709-4600 ext 274
e-mail: mmostafa@applanix.com

BIOGRAPHY

Mohamed Mostafa is responsible for Research and Development in Airborne Systems at Applanix Corporation and is the Chair of the Direct Georeferencing Committee of the American Society of Photogrammetry and Remote Sensing. He obtained a Bachelor of Science and a Master of Applied Science from Alexandria University in 1991 and 1994, respectively and a Ph.D. from The University of Calgary in 1999. His research interest is mapping using multi-sensor systems.

Joseph Hutton is the Product Manager of Airborne Systems at Applanix, and has been with the company since its inception in 1991. He obtained a Bachelor of Applied Science in Aerospace Engineering and a Master of Applied Science in Aerospace Control from the University of Toronto in 1989 and 1991, respectively. He has over 10 years experience in the areas of inertial/GPS integration, Kalman filtering, airborne photogrammetry and LIDAR. His research interest is optimal design of airborne GPS/inertial systems for mapping by multi-sensor systems.

ABSTRACT

One of the limitations of using integrated inertial/GPS systems to Directly Georeference airborne sensor data (c.f., Mostafa and Hutton, 2001), is the necessity of using a GPS base station or stations in order to obtain the positional accuracy required to meet the accuracy standards of certain mapping products. In some precise large-scale aerial survey applications having to place a number of GPS base stations in a remote or inaccessible location becomes quite problematic. In some other occasions, such as in a real production environment, the GPS base station data is lost. In this paper, the potential of using GPS with no base station for aerial survey applications is discussed. The NGS CORS network stations are processed in conjunction with the airborne GPS raw observables to determine the aircraft position which is then used to aid the inertial data processing in a closed loop fashion to end up with a full resolution of the trajectory parameters, namely position, velocity and attitude, which are then used to generate Exterior Orientation data to support aerial mapping. Flight test data were collected in January 2001 using the Applanix POS/AV™ system (S/A is off). Test results and analysis are presented in some detail.

1. INTRODUCTION

Aerial survey industry has been using airborne GPS as a standard procedure to assist map production for the past decade. More recently, GPS-aided inertial systems such as Applanix POS/AV™ have been successfully used to provide the full resolution of trajectory parameters, namely position, velocity, and attitude. This way, the entire set of translational, and rotational parameters of any airborne acquired image or laser scan line can be measured with respect to some mapping frame.

Data acquisition procedure plays a role in the success of this method. Separation between the airborne and base station GPS receivers, satellite geometry as reflected by the Position Dilution of Precision (PDOP), signal multipath and many other parameters must be considered in order to achieve the maximum possible GPS positioning accuracy. Many times it is difficult or not practical to optimize these parameters.

Proceedings, International Symposium On Kinematic Systems in Geodesy, Geomatics, and Navigation (KIS 2001)
Banff, Alberta, Canada, June 4-8, 2001

For example, since the sun angle required for aerial photography and the PDOP required for strong geometric positioning by GPS do not necessarily occur at the same time, aerial flight missions sometime inadvertently compromise the GPS PDOP in order to get a good sun angle.

Hence for high accuracy mapping applications where the highest GPS positioning accuracy is required, careful mission planning is therefore mandatory. A usual outcome of this is the requirement for a series of GPS base stations to be deployed in order to support the project. In inaccessible regions this can be very difficult.

In other applications such as corridor surveying where the accessibility is usually quite good and the positional accuracy is often relaxed, a major problem is the cost of laying out base stations at regular intervals along the corridor, which can often be thousands of km in length. In some other occasions, (as often is the case in a real production environment), the GPS base station data may simply be lost due to equipment problems or human error.

Therefore, the focus of this paper is on the accuracy that can be obtained using the NGS CORS (c.f., www.ngs.noaa.gov/CORS) stations as base stations for airborne GPS positioning, and the possibility of using these stations to supplement, back up, or even replace the base stations usually deployed for a given project.

2. THE NGS CORS

The CORS (continuously operating reference station) system is run by The US National Geodetic Survey (NGS). CORS comprises a network of 219 sites, (as of April 2001), containing geodetic quality GPS receivers.

This network is currently growing at a rate of about 3 sites per month. NGS collects, processes, and distributes data from these sites in support of high-accuracy 3D positioning activities throughout the United States and its territories. For details about CORS, see Snay (2000) and Spofford and Weston (1998). Figure 1 shows a number of CORS stations in southern US, some of which were used in the analysis presented here.

3. REFERENCE TRAJECTORY

To establish a reference trajectory for comparison purposes, a set of photogrammetric data was collected. The photogrammetric data included a number of overlapped photographs acquired over the mapping area and a number of land-surveyed ground points that appear in the acquired images.

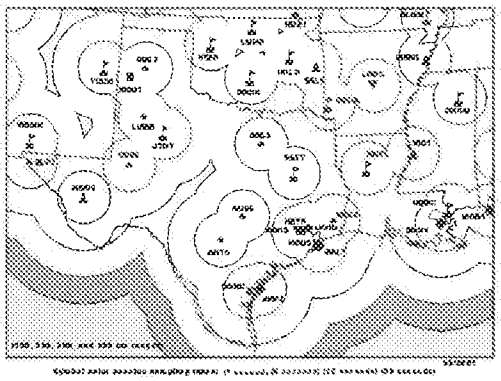


Figure 1 The CORS Stations in Texas/Oklahoma Area (courtesy of CORS website)

The ground point coordinates used together with their measured locations on the imagery, allow for the determination of each photo centre position. Although they only provide a discrete version of the trajectory, the photo centre positions establish a reference trajectory determined by a technique completely independent from GPS.

The resulting photo centres were compared to a 200 Hz Smoothed Best Estimate of Trajectory (SBET) determined by POSPac™, which is produced using GPS/inertial data and a base station at the airport.

The resulting position differences at the photo centres were about 15 cm in horizontal and about 20 cm in height. Having validated its accuracy in this manner, the SBET, computed using the GPS base station located at airport, (shown in Figure 2), is taken as a reference for the remainder of the paper. For details on the subject, see Hutton, et al (1997); Mostafa and Hutton (2001); Scherzinger (1997).

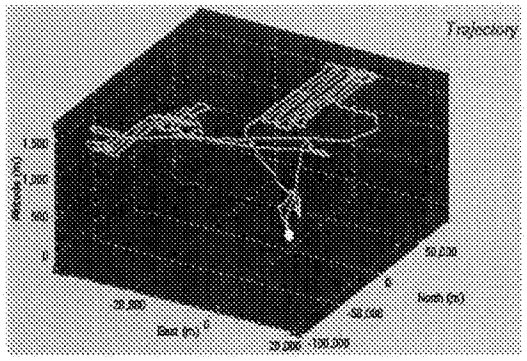


Figure 2 Smoothed Best Estimate of Trajectory (SBET) derived by GPS/inertial Data and a Base Station at Airport for Jan 26 Flight in Texas

4. GPS DATA PROCESSING USING DIFFERENT CORS STATIONS

As Shown in Figure 3, six CORS stations were independently used as base stations to allow for differential GPS positioning. Each of the derived trajectories was then compared to the reference SBET trajectory (see Section 3). In the following the, results of these comparisons are presented in some detail.

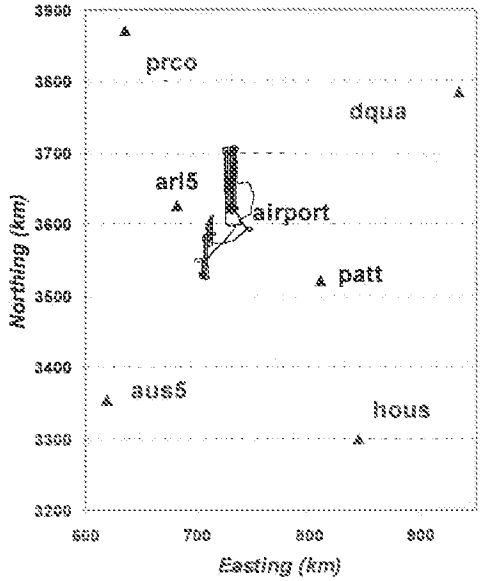


Figure 3 Aircraft Trajectory and six Surrounding CORS Stations

4.1 DGPS PROCESSING USING ARL5

The ARL5 station, which data is collected at 5-second intervals, was used as a base station to determine the trajectory of the aircraft. The master-to-rover separation varied from 30 to 110 km as shown in Figure 4. For details on ARL5; see Texas/texas_arl5.html under the CORS website listed in Section 1.

The raw data was interpolated to 1-sec intervals and then processed in differential mode. The derived trajectory was compared to the reference SBET. Figure 5 shows the differences in east, north, and down position components. Table 1 shows the RMS values.

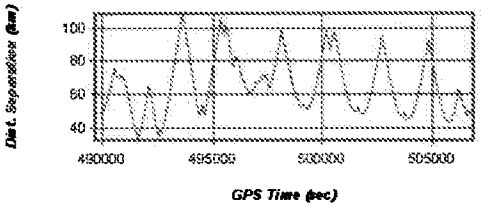


Figure 4 Distance Separation between ARL5 Station and Aircraft

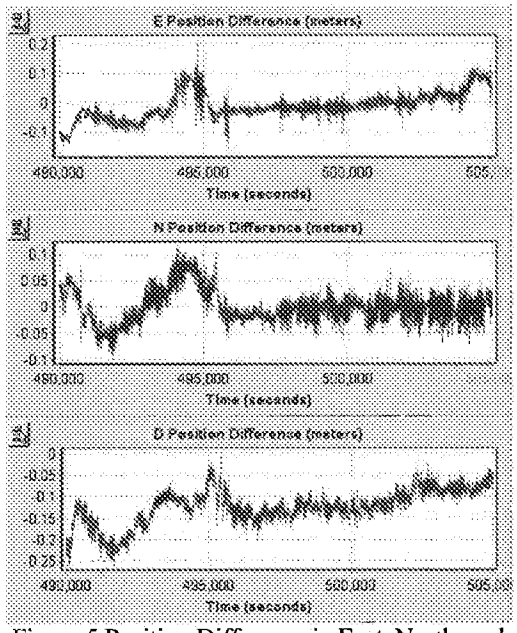


Figure 5 Position Difference in East, North, and Height Between Reference SBET and GPS-derived Trajectory using ARL5

Table 1. Position Difference Statistics ARL5 solution

Position Component	Max (m)	RMS (m)
Easting	0.21	0.11
Northing	0.11	0.12
Height	0.29	0.25

4.2 DGPS PROCESSING USING PATT

The PATT station, which data is collected at 30-second intervals, was used as mentioned above. For details on PATT; see Texas/texas_patt.html. The master-to-rover separation ranged from 100 – 200 km, as shown in Figure 6.

The raw data was interpolated to 1-sec intervals and then processed in differential mode. The derived trajectory was compared to the reference SBET. Figure 7 shows the position difference, while Table 2 shows their statistics.

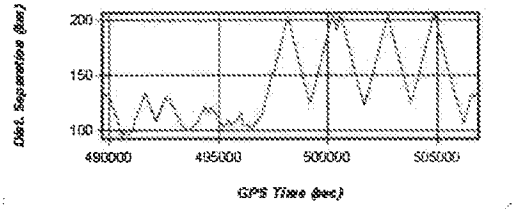


Figure 6 Distance Separation between PATT Station and Aircraft

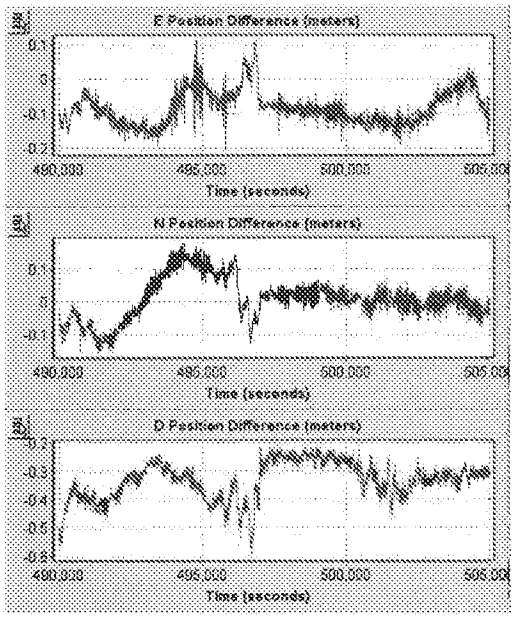


Figure 7 Position Difference in East, North, and Height Between Reference SBET and GPS-derived Trajectory using PATT

Table 2. Position Difference Statistics PATT solution

Position Component	Max (m)	RMS (m)
Easting	0.22	0.10
Northing	0.19	0.07
Height	0.61	0.34

4.3 DGPS PROCESSING USING DQUA

The DQUA station, which data is collected at 30-second intervals, was used as previously mentioned. For details on DQUA station; see Arkansas/arkansas_dqua.html.

The master-to-rover separation was 210-350 km, as shown in Figure 8. The derived trajectory was compared to the reference SBET. Figure 9 shows the position difference, while Table 3 shows their statistics.

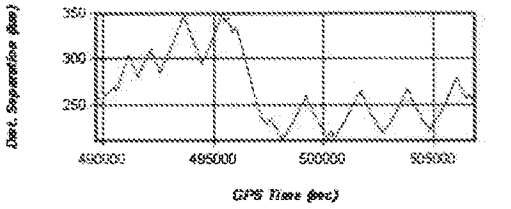


Figure 8 Distance Separation between DQUA Station and Aircraft

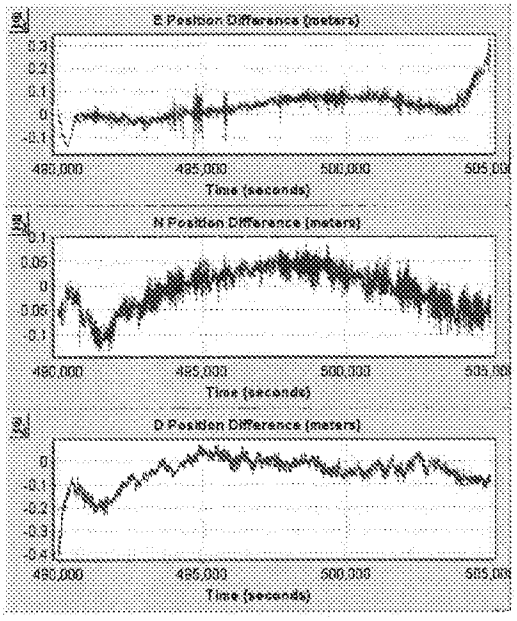


Figure 9 Position Difference in East, North, and Height Between Reference SBET and GPS-derived Trajectory using DQUA

Table 3. Position Difference Statistics DQUA solution

Position Component	Max (m)	RMS (m)
Easting	0.35	0.18
Northing	0.14	0.05
Height	0.42	0.09

4.4 DGPS PROCESSING USING AUS5

The AUS5 station, which data is collected at 5-second intervals, was used as previously mentioned. For details on AUS5 station; see Texas/texas_aus5.html.

The master-to-rover separation was 190-370 km, as shown in Figure 10. Figure 11 shows the position difference, while Table 4 shows the statistics of the difference.

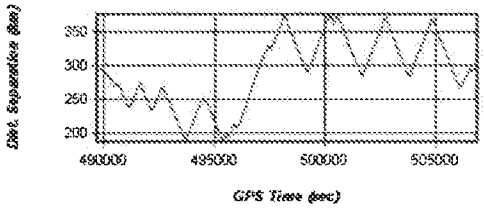


Figure 10 Distance Separation between AUS5 Station and Aircraft

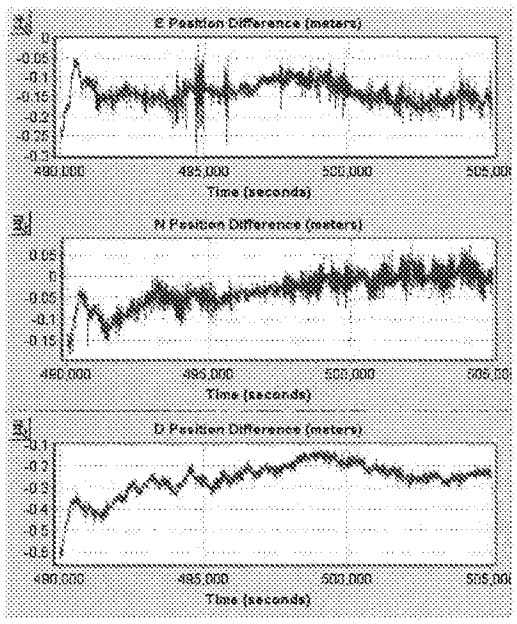


Figure 11 Position Difference in East, North, and Height Between Reference SBET and GPS-derived Trajectory using AUS5

Table 4. Position Difference Statistics AUS5 solution

Position Component	Max (m)	RMS (m)
Easting	0.30	0.18
Northing	0.21	0.07
Height	0.67	0.28

4.5 DGPS PROCESSING USING PRCO

The PRCO station is used as described previously. The GPS raw data was collected at 30-second intervals. For details on PRCO station; see Oklahoma/oklahoma_prco.html.

The master-to-rover separation was 190-360 km, as shown in Figure 12. Figure 13 shows the position difference, while Table 5 shows their statistics.

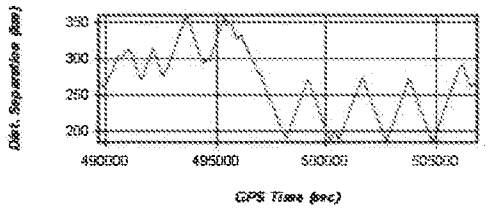


Figure 12 Distance Separation between PRCO Station and Aircraft

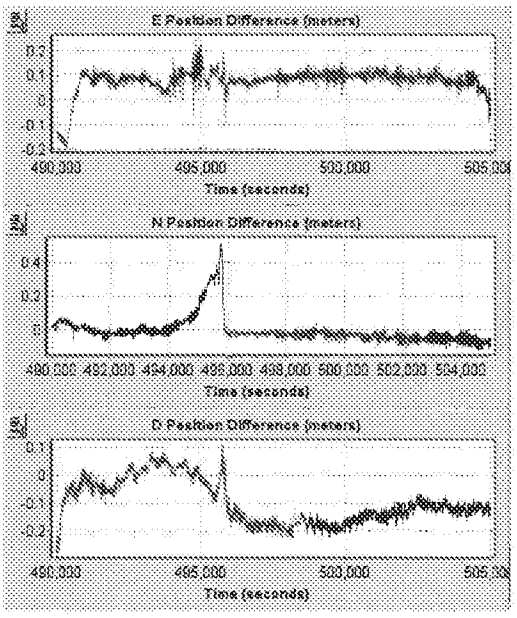


Figure 13 Position Difference in East, North, and Height Between Reference SBET and GPS-derived Trajectory using PRCO

Table 5. Position Difference Statistics PRCO solution

Position Component	Max (m)	RMS (m)
Easting	0.22	0.10
Northing	0.47	0.08
Height	0.29	0.13

4.6 DGPS PROCESSING USING HOUS

The HOUS station is used as described previously. The GPS raw data was collected at 5-second intervals. For details on HOUS station; see Texas/texas_hous.html. The master-to-rover separation was 260-420 km, as shown in Figure 14. Figure 15 shows the position difference, while Table 6 shows their statistics.

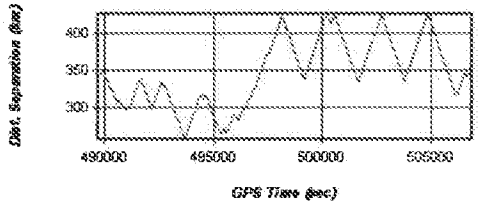


Figure 14 Distance Separation between PRCO Station and Aircraft

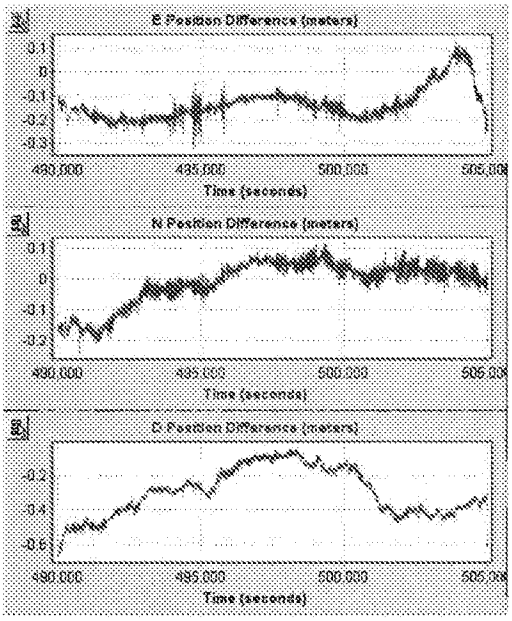


Figure 15 Position Difference in East, North, and Height Between Reference SBET and GPS-derived Trajectory using HOUS

Table 6. Position Difference Statistics HOUS solution

Position Component	Max (m)	RMS (m)
Easting	0.30	0.23
Northing	0.21	0.08
Height	0.67	0.38

5. COMBINED DGPS PROCESSING USING MULTIPLE CORS STATIONS

All six CORS stations were used to produce a combined GPS profile using POSGPS™ Batch Processing utility. The resulting GPS profile was then compared to the reference SBET. The position difference showed a similar pattern and magnitude to that shown when ARL5 station was used individually as a base station. This is due to the fact that the combined solution is mainly dominated by the ARL5 station since it is the closest to the airborne vehicle, as shown in Figure 4.

Therefore, only the five other CORS stations were combined to produce a GPS profile which when compared to the reference SBET resulted in the differences shown in Figures 16.

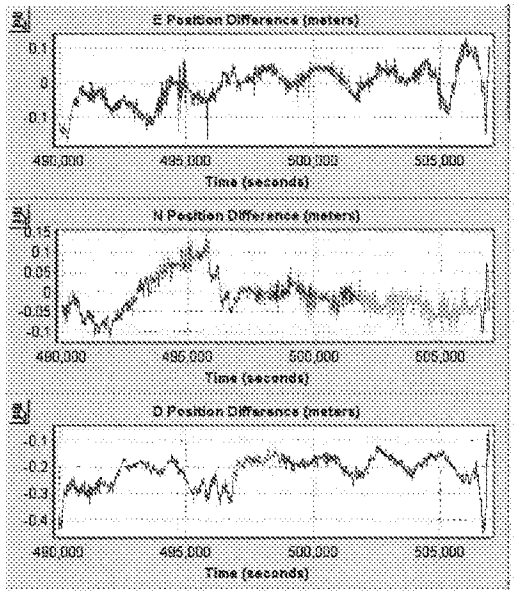


Figure 16 Position Difference in East, North, and Height Between Reference SBET and Combined GPS-derived Trajectory using Multiple CORS Stations

Table 7. Statistics of Position Differences The Combined solution

Position Component	Max (m)	RMS (m)
Easting	0.16	0.05
Northing	0.21	0.05
Height	0.46	0.22

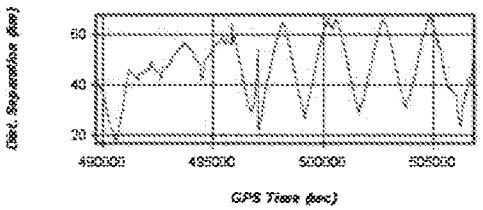


Figure 17 Virtual Mater-To-Rover Separation Using The Combined CORS Base Stations

Note that the CORS stations are well distributed around the flight trajectory. Consequently, they provide a geometrically strong combined solution, which can be considered as creating a single virtual base station closer to the rover than any of the CORS station used in the combined solution. For instance, using the combined solution, the resulting master-to-rover separation, shown in Figure 17, varies only between 18 and 65 km, while the closest CORS station to the airborne vehicle was 100 km away (PATT station; see Figure 6). Therefore, the combined solution provided the best solution when compared to the reference trajectory. Table 7 shows the statistics of the differences.

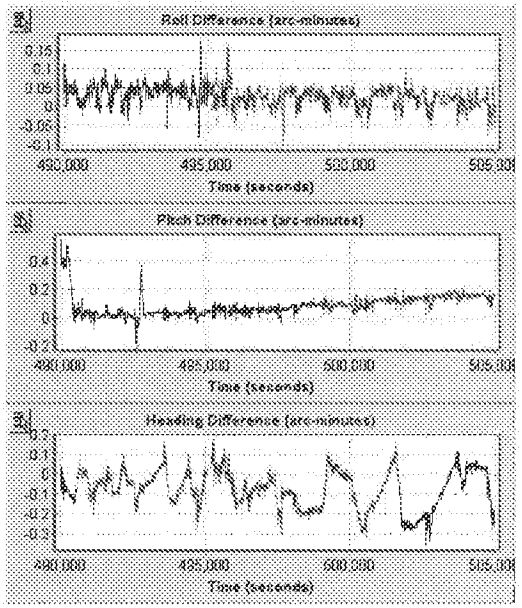


Figure 18 Attitude Difference

6. POSITIONING ACCURACY EFFECT ON ORIENTATION ACCURACY

Since airborne mapping depends on position and orientation accuracy, the effect of DGPS data processing using long baselines on the orientation accuracy is analyzed.

The GPS profile using farthest CORS station (HOUS) was used to generate another SBET file, which was then compared to the reference SBET.

Figure 18 shows the differences in roll, pitch and heading, while Table 8 shows their statistics.
Note that the effect of GPS accuracy on the orientation accuracy is minimal and is well within the Applanix POS/AV™ 510 accuracy specifications (c.f., Mostafa et al, 2001). Hence, the resulting mapping accuracy would not be affected.

Table 8. Attitude Difference Statistics HOUS SBET solution

Attitude Angle	Max (arcmin)	RMS (arcmin)
Roll	0.18	0.08
Pitch	0.47	0.07
Heading	0.37	0.14

7. EFFECT ON MAPPING ACCURACY

There are three ways of georeferencing airborne images to some mapping frame of reference. The first (traditional) is completely dependent on ground control points, which is obsolete. The second method is dependent on airborne GPS and minimal ground control using some aerial triangulation scheme and is, therefore, referred to as GPS-assisted aerial triangulation. The third method is referred to as direct georeferencing, which is completely dependent on GPS/inertial data that identifies the location and orientation of each aerial image at the moment of its exposure.

Using the CORS stations individually showed that the horizontal accuracy varies from 0.05 to 0.23 m RMS in east or north, while the height varies from 0.09 m to 0.38 m RMS. These accuracies are generally acceptable for either of the two new georeferencing methods.

In small-scale photography applications (high altitude photography), the GPS accuracy presented here is acceptable for both GPS-assisted aerial triangulation and for direct georeferencing, since positional accuracy requirement is generally relaxed. In large scale mapping projects (low altitude photography), the mapping error budget is dominated by GPS errors and, therefore, the accuracy shown in Section 4, is not good enough for direct georeferencing purposes, but acceptable for GPS-assisted aerial triangulation since in the

latter case, the geometry of image networks together with the accuracy of ground control points improve the image positional accuracy, when all airborne, image, and ground information is processed simultaneously. For airborne remote sensing applications and resource mapping, the GPS accuracies presented using individual CORS stations are adequate.

Combined DGPS processing using multiple CORS stations, showed a significant accuracy improvement when compared to DGPS processing using individual stations, as shown in Section 5. A number of researchers showed similar results when operating in a multi-receiver configuration (c.f., Shi, 1994). For a complete list of references, see Raquet (1998).

SMMARY AND OUTLOOK

In this paper, the potential of using the US National Geodetic Survey (NGS) continuously operating reference stations (CORS) as base stations for airborne GPS surveys is studied. Six CORS stations were used individually and in combined configurations as base stations for an airborne GPS data set. All individual six GPS profiles were compared to an independent photogrammetrically derived reference trajectory, and the results were analysed. Generally speaking, the CORS stations have a great potential to serve the aerial mapping industry in USA, especially when the stations are densified and the data frequency is increased to 1-2 seconds interval instead of the 5-30 seconds intervals.

ACKNOWLEDGEMENTS

- Darren Cosandier is gratefully acknowledged for providing the CORS data interpolation software and for his valuable discussions.
- Aeromap US is gratefully acknowledged for airborne data acquisition.
- Scott Miller of LH-Systems is gratefully acknowledged for providing Socet Set package for research purposes.
- Roman Kathofer is thanked for performing image coordinate measurement on Socet Set.

REFERENCES

Hutton, J., Savina, T., and Lithopoulos, L., 1997. Photogrammetric Applications of Applanix's Position and Orientation System (POS). ASPRS/MAPPS Softcopy Conference, Arlington, Virginia, July 27 - 30.

Mostafa, M.M.R., J. Hutton, 2001. Direct Positioning and Orientation Systems: How Do They Work? What is The Attainable Accuracy? Proceedings, The American Society of Photogrammetry and Remote Sensing Annual Meeting, St. Louis, MO, USA, April 23 – 27.

Mostafa, M.M.R., J. Hutton, and E. Lithopoulos, 2001. Direct Georeferencing of Frame Imagery - An Error Budget. Proceedings, The Third International Mobile Mapping Symposium, Cairo, Egypt, January 3-5.

Raquet, J.F., 1998. Development of a Method for Kinematic GPS Carrier-Phase Ambiguity Resolution Using Multiple Reference Receivers, UCGE Report # 20116, Department of Geomatics Engineering, The University of Calgary, Alberta, Canada, 259 p.

Scherzinger, B., 1997. A Position and Orientation Post-Processing Software Package for Inertial/GPS Integration (POSProc). Proceedings of the International Symposium on Kinematic Systems in Geodesy, Geomatics and Navigation (KIS 97), Banff, Canada, June 1997

Shi, J., 1994. High Accuracy Airborne Differential GPS Positioning Using a Multi-Receiver Configuration, UCGE Report # 20061, Department of Geomatics Engineering, The University of Calgary, Alberta, Canada, 129p.

Snay, R.A., 2000. The National and Cooperative CORS Systems in 2000 and Beyond, Proceedings of ION GPS 2000, 19-22 September 2000, Salt Lake City, UT, pp. 55-58.

Spofford, P.R., N.D. Weston, 1998. National Geodetic Survey Continuously Operating Reference Station project. Status and Plans. *ACSM Bulletin*, 172: 20-25.

Airborne DGPS Without Dedicated Base Stations for Mapping Applications

A.M. Bruton, M.M.R. Mostafa, and B. Scherzinger, *Applanix Corporation, Ontario, Canada*

BIOGRAPHIES

Dr. Alex Bruton recently joined Applanix Corporation where he works in the Advanced Technology Group. He holds a Ph.D. in geomatics engineering and a B.Sc. in surveying engineering from the University of Calgary. His research interests include modeling and estimation for inertial navigation, and the development and use of integrated systems for applications in mapping and geodesy.

Dr. Mohamed Mostafa is responsible for Research and Development in Airborne Systems at Applanix Corporation and is the Chair of the Direct Georeferencing Committee of the American Society of Photogrammetry and Remote Sensing. He obtained a B.Sc. and a M.Sc. from Alexandria University in 1991 and 1994, respectively, and a Ph.D. from the University of Calgary in 1999. His research interest is mapping using multi-sensor systems.

Dr. Bruno Scherzinger obtained a B.Eng degree from McGill University in 1977, and M.A.Sc. and Ph.D. degrees from the University of Toronto in 1979 and 1983, respectively. He is a founding partner and the Chief Scientist at Applanix Corporation.

ABSTRACT

This paper evaluates the potential of deriving reliable and accurate estimates of the position of a survey aircraft without the establishment of dedicated GPS base stations. Although there are several approaches to doing this, the concept studied herein is to make use of data available from existing permanent GPS reference systems to estimate the position of the aircraft. While such stations have been established to support static or low dynamic land based GPS surveying and can be at a considerable distance from the survey area (e.g. 100 to 500 km), they are often large in number and their data is usually freely available. In this research, position is determined using data collected as part of the NGS CORS network in conjunction with the measurements made by the receiver on the survey aircraft.

The success of the approach is evaluated empirically based on data collected using the Applanix POS/AV™. Analyses of the test results show that when using five network stations at average distances between 160 and 420 km, it is possible to achieve an accuracy of 25 cm (RMS) in 3D position while not deviating from the dedicated solution by more than 42 cm at any time during the survey. It is also seen that when the network solution is augmented to include three stations at average distances of between 40 and 90 km, the quality of the 3D positioning information can reach the level of better than 12 cm (RMS) while never deviating from the dedicated solution by more than 28 cm. It is then observed that when positioning information from any of these scenarios is used (in place of that coming from dedicated GPS base stations) as an update to the IMU in the POS/AV™ system, the maximum differences in roll and pitch can reach the level of 3 arc seconds and the maximum difference in heading can be as low as 10 arc seconds. Finally, comments are made regarding the application of this method in practice.

1. INTRODUCTION AND METHODOLOGY

Positioning information derived from GPS measurements has become a reliable component of many of today's aerial mapping systems. However, one of the logistical limitations commonly faced when using GPS for airborne mapping is the need for continuous data collected by a GPS receiver at one or more base stations in the area of the survey (e.g. having a station within 30 km of the aircraft at all times). While the use of such data is a means of meeting the accuracy requirements of today's most demanding applications, the establishment of the base stations is often a difficult task when surveys take place over remote or inaccessible terrain. Further, even when dedicated base stations are established, the continuity of the data is not always guaranteed as a result of environmental effects, receiver error, or human error.

With these comments in mind, this paper contributes to research being carried out at Applanix Corporation to evaluate the accuracy with which the position of an aircraft can be estimated in post-mission for scenarios in which dedicated GPS base stations are not available within the immediate vicinity of the survey. Specifically, the objective is to explore the capabilities of a method that estimates position via an optimal combination of solutions obtained from the stations in an existing permanent GPS reference system. The method is evaluated empirically using data collected by an Applanix POS/AV™ 510 system and data made available by the United States (US) National Geodetic Survey (NGS) as part of their Continuously Operating Reference Stations (CORS), see Snay (2000) and Spofford and Weston (1998). The utilities and batch processing options available within the Applanix POSPac™ software (version 3.0) are used to do the data processing, and the resulting solutions are evaluated by comparing them to a reference solution that has been validated against ground control points (GCP) using aerial triangulation (AT), and that is considered to have an absolute accuracy of 10 cm in position and between 20 and 30 arc seconds in attitude.

This research is intended to complement the analysis carried out in Mostafa and Hutton (2001) in which a network of NGS CORS stations (with an average distance from the aircraft of 216 km) was used to estimate position and attitude of an aircraft in a different survey. Comments about that survey, the survey presented herein, and the consistency of the two surveys will be discussed in section 5.

In the next section of this paper, the data set used in the analyses is described, and the method used to derive the reference for the position and attitude estimates is outlined. This is followed in section 3 by an evaluation of the position estimates that are obtained via various combinations of the CORS network solutions, and in section 4 by an assessment of the corresponding attitude estimates. As mentioned above, the results obtained herein are compared in section 5 to refined results based on the data that were presented in Mostafa and Hutton (2001). Comments are also made in section 5 regarding the general applicability of the method. Finally in section 6, the paper is summarized and conclusions are drawn in light of the use of this method in practice for a variety of applications.

2. THE FIELD TEST, THE CORS DATA, AND THE REFERENCE SOLUTION

The new analyses presented in this research are based on data collected by HJW GeoSpatial Inc. using an Applanix POS/AV™ 510 system during a survey that took place on June 21 2000 between Oakland and San Jose California in the US. As shown in Figure 1, a dedicated base station (labeled TOMS) was established directly below the centre of the flight track and a CORS reference station (labeled CHAB) was available at a location very close to the airport. Local cities are labeled for reference, but GPS data are not available at those sites. The flight took place between approximately 14:30 and 18:30 local time and the ellipsoidal flying height was 1155 metres for approximately one third of the flight lines and 995 metres for the remainder.

The CORS stations that were operating on June 21 2000 are shown in Figure 2 for the area within 400 km of the flight track. Notice that there are many CORS stations in the California area; five within 90 km of the survey site and eight others between 160 and 420 km of the site. The data collected at the stations marked by an unfilled square are all subject to 2 to 5 minute periods of missing data immediately after 18:00 and are therefore not used in these analyses. As shown, there are therefore three useable stations within 90 km of the survey site and five useable stations between 160 and 420 km of the site. With the exception of the CHAB station, those marked with a solid circle are used in the combined network solutions that are discussed later in section 3. Note again that the cities are only shown for reference. Also note that although other California CORS stations exist for the area shown in Figure 2, they are not shown because data are not available for them on June 21 2000.

As mentioned above, the results obtained in the following sections are evaluated by comparing them to a reference trajectory. That trajectory was derived from differential GPS solutions obtained by using the TOMS and CHAB stations in a dedicated fashion. Specifically, both stations were used independently to estimate the trajectory of the aircraft using fixed integer carrier phase techniques. These estimates were then combined using the POSGPS™ component of POSPac™ and used as an update to the IMU in the POS/AV™ system, resulting in a smoothed best estimate of the trajectory (SBET). Under the conditions of this survey the absolute accuracy of the POS/AV™ 510 system is at the level of 10 cm RMS for position and 20-30 arc seconds RMS for attitude. This is documented in Cramer (1999) and Mostafa and Hutton (2001), for example. The absolute accuracy of the solution in this specific case was established by comparing it to the position and orientation derived from a set of photogrammetric data using aerial triangulation. The accuracy was confirmed to be 10 cm RMS for position and 20-30 arc seconds RMS for orientation. Thus validated, this solution is considered to be the ideal solution and the objective of the research is to consider how closely it can be approximated using the solutions based on the other CORS stations.

Although data processing was done using the whole data set in all cases, the analyses presented in the following only consider the time period during which the aircraft was at survey altitude (i.e. all maneuvers are considered except during the periods of ascent and descent).

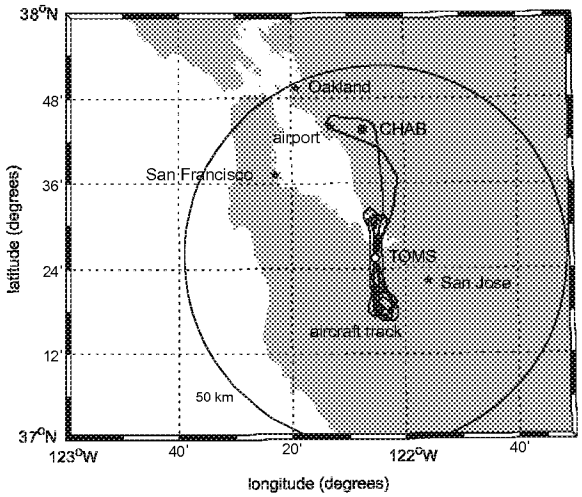


Figure 1: The trajectory and the dedicated base stations used to generate the reference solution

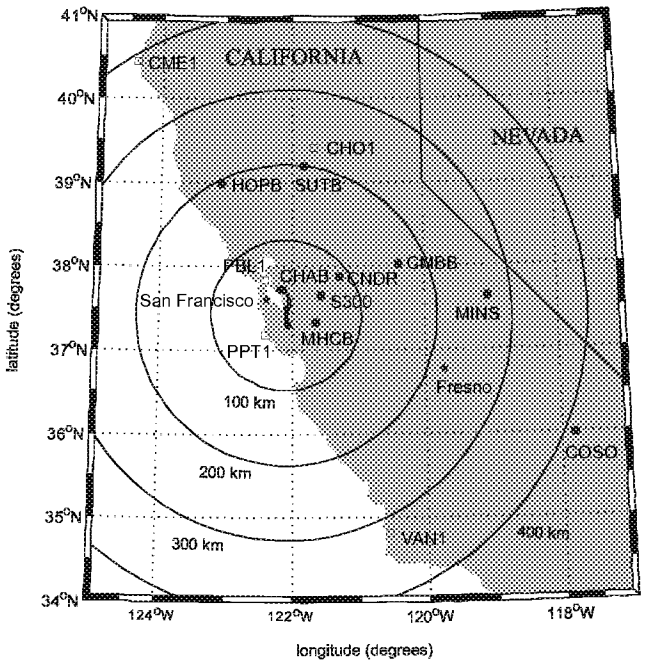


Figure 2: The CORS base stations for which data is available during the survey

3. EVALUATION OF THE ESTIMATED POSITION SOLUTIONS

The goal of this section is to evaluate the position estimates coming from various combinations of the estimates that were in turn obtained by processing between each of the CORS stations and the aircraft. In all cases, differences in position are evaluated by comparing an estimated position to the one given by the reference solution that was described in the last section.

As a starting point, briefly consider the individual solutions between the CORS base stations and the aircraft that are discussed in the Appendix. It is seen therein that as expected, the differences are generally smaller for stations closer to the aircraft, and that they can be quite large for longer baselines. Notice from Table A1 (also in the Appendix) that the RMS of the observed differences in the 3D position vector varies between 9 and 51 cm, and that the maximum observed difference varies between 25 and 87 cm, depending on the station used.

Next, consider Figure 3 and Table 1 that show the differences between the reference trajectory and trajectories obtained via three different combinations of the solutions to the individual CORS stations. The top plot in Figure 3 and the first entry in Table 1 show the differences between the reference trajectory and estimates of position obtained using all eight of the CORS stations available. The agreement for the 3D position vector is at the level of 12 cm RMS and the largest difference at any point in time is 28 cm. This is clearly very good and implies that estimates of position derived from such a network can be used to estimate position at or near the noise level of those derived from dedicated GPS base stations.

The differences shown in the other plots of Figure 3 and the other entries in Table 1 were computed in order to assess the role that stations close to the survey area play in such a combined solution. The middle plot shows the differences in position for a solution that is based only on the three CORS stations closest to the survey area (MHCB, S300 and CNDR), and the bottom plot shows the differences for the solution based on the remaining five CORS stations. The usefulness of having stations close to the survey areas is clear. Because it is likely that surveys will take place in areas with no GPS reference stations within 90 km of the survey area, it is important to note the quality of the combined solution that is based on the five stations further than 160 km: the agreement for the 3D position vector is at the level of 25 cm RMS and the largest difference at any point in time is approximately 42 cm.

Before concluding this section, note that for this data set, the solution obtained using only the three CORS stations closer than 90 km is slightly better than the solution obtained using all eight CORS stations. This implies that if such stations are available, then the inclusion of others does not help. Unless that level of proximity to the aircraft is available for a number of CORS stations, however, it will be desirable to process all available stations in the vicinity of the flight area.

4. ACCURACY WITH WHICH ATTITUDE CAN BE DETERMINED

The goal of this section is to evaluate the differences in attitude estimates made by the POS/AV^{TM} 510 system when positioning information from the solutions discussed in the last section is used in place of that coming from dedicated GPS base stations.

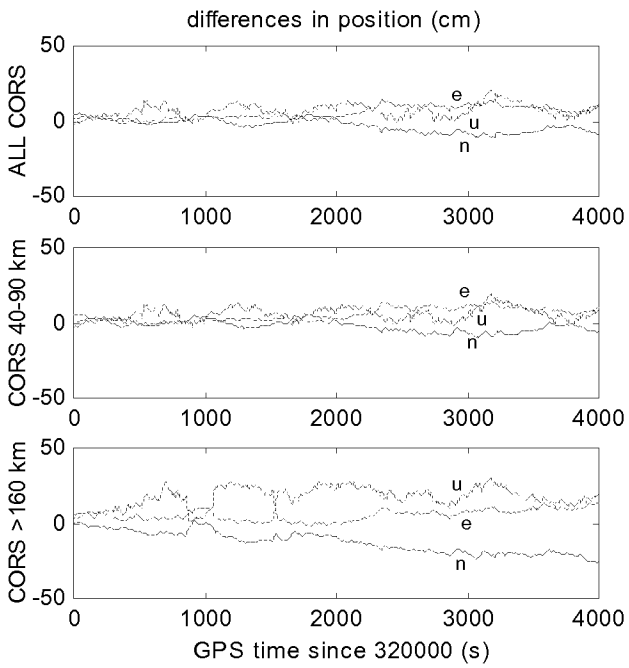


Figure 3: Differences in position for various combined solutions

Table 1: The statistics for differences in position for the combined solutions (cm)

station	statistic	component of difference			
		north	east	up	3D
All CORS stations	RMS	5.0	6.8	8.1	11.7
	largest	11.2	14.4	21.0	27.8
3 CORS stations (40-90 km)	RMS	4.2	6.8	7.3	10.9
	largest	9.7	15.0	19.9	26.7
5 CORS stations (>160 km)	RMS	14.4	6.5	18.8	24.5
	largest	26.4	13.5	30.0	42.2

Differences in attitude are evaluated by comparing estimated attitude values to those given by the reference solution that was described in section 2.

Processing was carried out using four different position estimates as updates to the IMU in the POS/AV™ 510 system; the three combination solutions that were treated in Figure 3, and the single baseline solution that was obtained by processing between the MINS CORS station and the aircraft. Because the latter exhibited the largest differences in position (see the Appendix), it is considered a worst-case scenario. The differences in attitude corresponding to these processing instances are shown in Figure 4 and Table 2.

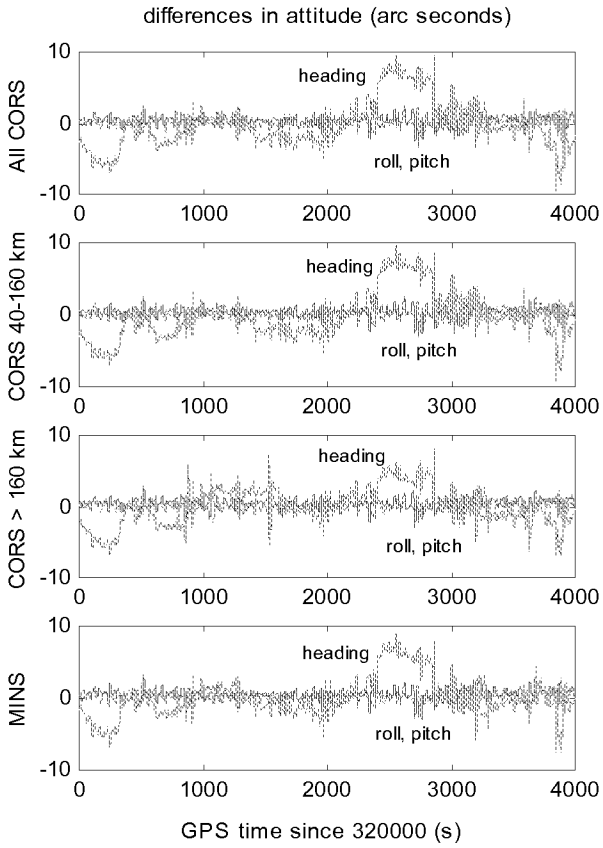


Figure 4: Differences in attitude for various combined solutions and for the MINS solution

Table 2: The statistics for differences in attitude for the combined solutions (arc seconds)

station	statistic	component of difference		
		roll	pitch	heading
All CORS stations	RMS	0.60	0.87	3.32
	largest	3.45	3.35	9.74
3 CORS stations (40-90 km)	RMS	0.60	0.89	3.27
	largest	3.22	3.11	9.74
5 CORS stations (>160 km)	RMS	0.71	0.97	2.68
	largest	5.83	5.97	8.20
MINS (268 km)	RMS	0.63	0.94	2.84
	largest	3.20	3.28	9.06

In all of these cases, the differences in attitude are at the level of just under 1 arc second (RMS) in roll and pitch and approximately 3 arc seconds (RMS) in heading. Clearly then, the effect of the various position solutions on attitude is within the noise level of the reference solution. Further, there are no visible long-term (drift-

like) differences in attitude for this data set, implying that the observed differences are due to short and medium-term differences in the position solutions. In turn, these may be due to the fact that the solutions based on dedicated GPS base stations use fixed ambiguity carrier phase observables, while all of those based on the CORS stations use ionospheric-free carrier phase observables.

Although the behaviour of the attitude estimates made based on all four of these position solutions is similar, the following observations follow from Figure 4 and Table 2:

- The maximum differences in roll and pitch for the solution that is based on only on the three closest CORS stations (MHCB, S300 and CNDR) are very slightly smaller than those for the solution based on all of the CORS stations. This is to be expected from the last section, where it was seen that the differences in position are also slightly smaller for the solution based on the three closest stations.
- The maximum differences in attitude for the solution that is based on the five farthest CORS stations are different from the others; the differences in roll and pitch are larger and the differences in heading are smaller. It is possible that this is due to different quality factors being assigned to the position estimates by the batch processor in the POSGPS™ component of the POSPac™ package. In turn, this could imply that different weights (i.e. confidence levels) are being assigned to the position updates.

5. DISCUSSION OF THE APPLICABILITY OF THIS METHOD

This section of the paper is included for completeness with the goal of commenting on the applicability of this method in general. For this purpose, the analysis using a different POS/AV™ 510 system that was presented in Mostafa and Hutton (2001) is briefly recalled. It will be referred to as the Dallas project. Consider Figure 5 in which the flight path and the locations of the CORS and dedicated GPS base stations are shown for that data set. One dedicated GPS base station and six CORS stations were considered in the area. As in the analysis presented in this paper, the dedicated GPS base station was used to generate a reference position trajectory, and the five CORS stations marked with solid circles were used to generate a combined estimate of the position. The ARL5 solution was not included in the combined solution because it was considerably closer to the survey area than the others and would therefore dominate that solution. As such, the average distance between the aircraft and the five remaining stations is 216 km. These were then each used as an update to the IMU in the POS/AV™ system to compute the corresponding SBETs.

Figure 6 and Table 3 are included so that the results from that analysis can be directly compared to those of the analyses presented so far in this paper; they show the differences between the reference trajectory and selected solutions obtained using the CORS stations for the period of time during which the aircraft was at survey altitude during that flight test. The top plot in Figure 6 and the first entry in Table 3 show the differences between the reference trajectory and estimates of position obtained using all five CORS stations. The agreement for the 3D position vector is at the level of 23 cm RMS and the largest difference at any point in time is 42 cm. This is clearly consistent with the results presented in the current research and supports the conclusion that estimates of position derived from such a network can be used to estimate position near the noise level of those derived from dedicated GPS base stations. The second plot in Figure 6 and the second entry in Table 3 are included for completeness to show the differences obtained when using the furthest CORS station alone (HOUS which is 347 km away on average).

In Figure 7 and Table 4, the plots and statistics can be found for the attitude estimates that correspond to the position solutions in Figure 6 and Table 3. Note that the attitude results for the Dallas project have been refined since they were presented in the earlier publication. As such, these attitude results are also consistent with the results presented in the current research.

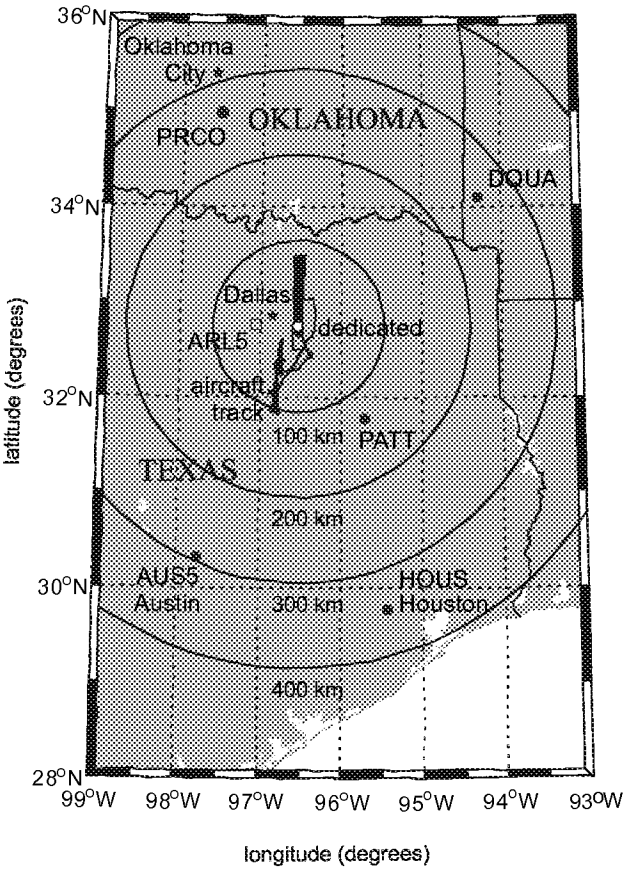


Figure 5: The trajectory and the GPS base stations used in the Dallas data processing

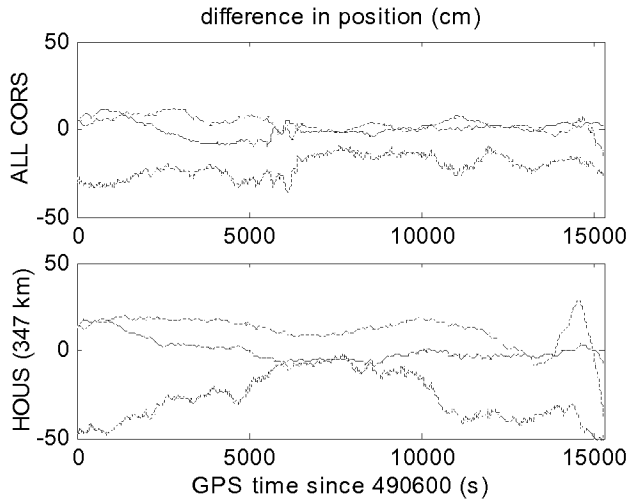


Figure 6: Differences in position for the combined solution and for the HOUS solution for the Dallas project

Table 3: Statistics for differences in position (cm) for the solutions in Figure 6

station	statistic	component of difference			
		north	east	up	3D
All CORS stations	RMS	5.0	5.1	22.2	23.2
	largest	11.6	15.2	37.8	42.3
HOUS (347 km)	RMS	6.4	14.4	30.2	34.0
	largest	18.1	37.8	52.4	67.1

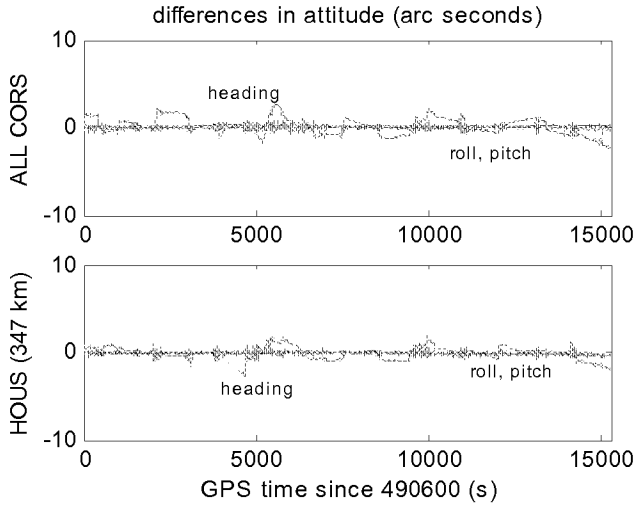


Figure 7: Differences in attitude for the combined solution and for the HOUS solution for the Dallas project

Table 4: Statistics for differences in attitude (arc seconds) for the solutions in Figure 7

station	statistic	component of difference		
		roll	pitch	heading
All CORS stations	RMS	0.18	0.20	0.97
	largest	0.85	0.95	2.89
HOUS (347 km)	RMS	0.16	0.22	0.76
	largest	0.67	1.07	2.73

Based on the high level of consistency that is observed between the results of these two studies, it is proposed by the authors that this method can provide a viable alternative for estimating the position of an aircraft in post-mission for scenarios in which dedicated GPS base stations are not available within the immediate vicinity of the survey.

6. SUMMARY AND CONCLUSIONS

It was seen in this research that a combination of solutions from permanent GPS reference stations can be used very successfully in place of dedicated base stations for positioning a survey aircraft. Analyses of the test results show that when using five network stations at average distances between 160 and 420 km, it is possible to achieve estimates with a quality of 25 cm (RMS) in 3D position while not deviating from the dedicated solution by more than 42 cm at any time during the survey. It was seen that when the network solution is augmented to include three stations at average distances of between 40 and 90 km, the quality of the 3D positioning information can reach the level of 12 cm (RMS) while not deviating from the dedicated solution by more than 28 cm. It was also seen that if data are available from a sufficient number of GPS reference stations within 90 km of the survey area, then it is unlikely that data from stations further away than that will add anything to a combined solution.

It was observed with the data sets studied herein that the quality of attitude estimates is not greatly affected by the type of position solution being used (including single baseline solutions with position differences as high as 75 cm), as long as those position solutions are appropriately weighted when used as an update to the IMU in a mapping system such as the Applanix POS/AV™. The combination solutions considered here were observed to provide attitude solutions with maximum differences of 10 arc seconds in heading and 3-5 arc seconds in roll and pitch.

These observations are very encouraging for mapping applications taking place under conditions in which dedicated GPS base stations are not available in the area surrounding a survey. Immediate potential benefits of

this approach include precise positioning for aerial survey applications such as GPS-assisted aerotriangulation, and the generation of Exterior Orientation parameters for direct georeferencing for aerial film or digital cameras, LIDAR, and SAR.

As an example, this paper used data sets from the US, where data from the CORS reference network could be used in place of dedicated GPS base stations. Before concluding, the authors would like to point out there exist a number of other such networks throughout the world. As well as many permanent GPS reference networks existing at state or provincial levels, examples include many national networks. Among those are the Canadian Active Control System (CACS), the EUREF Permanent Network (EPN) in Europe, the Australian Regional GPS Network (ARGN), and two networks maintained by the Geographical Survey Institute of Japan.

Finally, in conclusion, the authors would like to point out that if a surveyor plans to use this method for estimating position, there exists a responsibility on his or her part to carefully plan the survey. For example, it is important to make sure that there is a sufficient number of baselines close enough to the survey area to ensure redundancy. The five CORS stations with periods of missing data discussed in section 2 are good examples of why this is so.

ACKNOWLEDGMENTS

HJW GeoSpatial Inc. of Oakland California, is gratefully acknowledged for providing image data, precise GCP data, and the AT reference for the analysis presented herein.

Aeromap US and Mark Hurd are gratefully acknowledged for providing airborne navigation data and imagery, respectively.

Scott Miller of LH-Systems is gratefully acknowledged for providing Socet Set package for research purposes.

Roman Kathofer is thanked for performing image coordinate measurement on Socet Set.

Joe Hutton is thanked for his contributions.

REFERENCES

Cramer, M. (1999) Direct exterior orientation of airborne sensors, GIM - International 13 (9), 46–49.

Mostafa, M. and J. Hutton (2001) Airborne Kinematic Positioning and Attitude Determination Without Base Stations, Proceedings of International Symposium on Kinematic Systems in Geomatics and Navigation (KIS 2001), Banff, Canada, June 5-8.

Mostafa, M.M.R., J. Hutton, and E. Lithopoulos (2001) Direct Georeferencing of Frame Imagery - An Error Budget. Proceedings, The Third International Mobile Mapping Symposium, Cairo, Egypt, January 3-5.

Snay, R.A., 2000. The National and Cooperative CORS Systems in 2000 and Beyond, Proceedings of ION GPS 2000, 19-22 September 2000, Salt Lake City, UT, pp. 55-58.

Spofford, P.R., N.D. Weston, 1998. National Geodetic Survey Continuously Operating Reference Station project. Status and Plans. *ACSM Bulletin*, 172: 20-25.

APPENDIX: THE POSITION ESTIMATES FROM THE INDIVIDUAL CORS BASE STATIONS

This Appendix is included for completeness for two reasons. The first is to demonstrate the behaviour of the position solutions obtained by processing between each CORS station and the aircraft, and the second is to describe the important processing parameters that were used in generating each of them. As usual, the differences in position are evaluated by comparing a given estimate to the position given by the reference solution that was described in section 2.

Figure A1 shows the differences in position for the solutions obtained using the measurements for the five CORS stations that are at an average distance of greater than 160 km from the survey area. The average distances are shown on the left hand side of the figure (in brackets following each station name) and the differences are labeled with the letters e, n, and u to represent the east, north and upward components, respectively. The stations shown at the top of the figure are closer to the aircraft than those at the bottom. In all of these cases, processing was done using the batch processor in the POSGPS™ component of POSPac™. Default settings were used as a starting point for each processing instance. The basic approach was to use the ionospheric-free model and to process the data forward and backwards in time. Only minor changes to the default settings were made as necessary to minimize the differences between the forward and reverse solutions in each case. The solutions shown are based on an optimal combination of the forward and reverse solutions. Table A1 gives the statistics of the differences for each of these stations.

Figure A2 shows the data for the CORS stations that are at an average distance of less than 90 km from the survey site. The basic approach to processing these somewhat shorter baselines was also to use the ionospheric-free model and to process the data forward and backwards in time. For the two shorter baselines (MHCB and S300), it was also possible to aid the float ambiguity solution by initializing the processing with a "quick static" solution during the static periods at the beginning and end of the survey. Otherwise, only minor changes to the default settings were made as necessary to minimize the differences between the forward and reverse solutions

from each station. Table A1 gives the statistics of the differences for each of these stations.

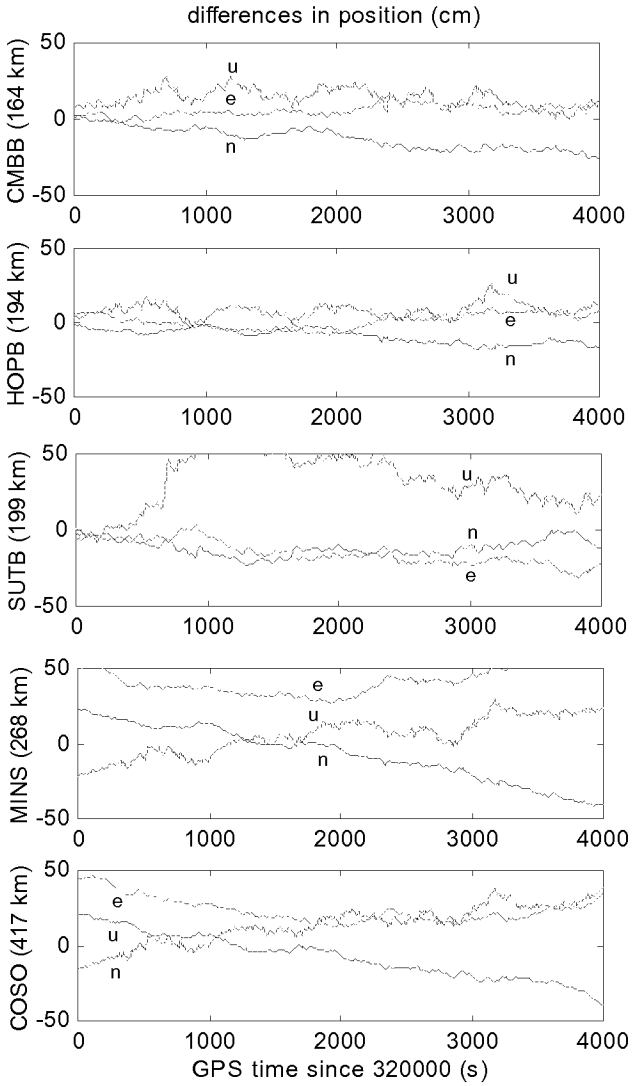


Figure A1: Differences in position for solutions from CORS stations more than 150 km from the aircraft

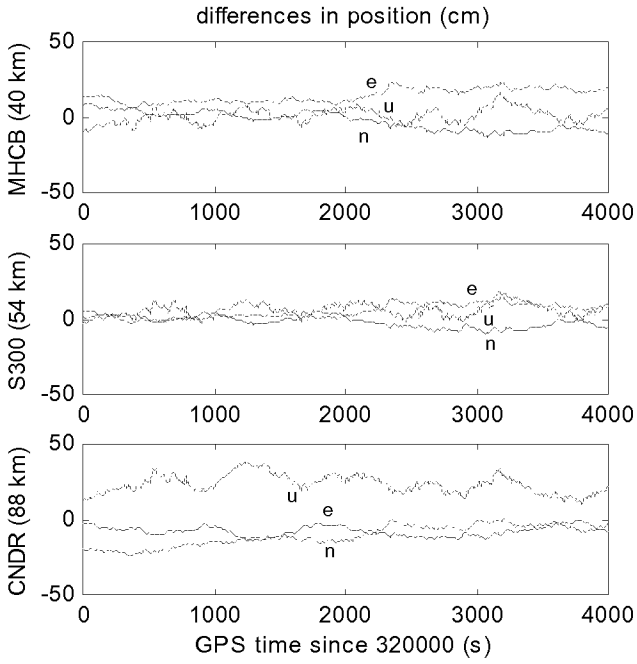


Figure A2: Differences in position for solutions from CORS stations more than 90 km from the aircraft

Table A1: The statistics for differences in position observed for solutions derived from each CORS station (cm)

station	statistic	component of difference			
		north	east	up	3D
MHCB	RMS	6.5	14.9	4.9	17.0
(40 km)	Largest	13.3	23.5	16.7	31.7
S300	RMS	3.8	3.2	7.2	8.7
(54 km)	largest	9.2	8.5	21.5	24.8
CNDR	RMS	8.5	12.9	24.1	28.6
(88 km)	largest	14.9	23.9	38.5	47.7
CMBB	RMS	14.4	6.9	14.9	21.8
(164 km)	largest	25.9	16.3	27.7	41.3
HOPB	RMS	10.0	5.0	9.8	14.9
(194 km)	largest	18.3	10.4	26.1	33.5
SUTB	RMS	12.9	16.8	37.4	43.0
(199 km)	largest	23.5	31.5	63.3	74.5
MINS	RMS	19.3	44.6	13.5	50.5
(268 km)	largest	41.2	70.3	29.7	86.7
COSO	RMS	16.4	24.9	18.7	35.2
(417 km)	largest	39.4	46.3	38.4	72.0

ISAT Direct Exterior Orientation QA/QC Strategy Using POS Data

Mostafa Madani[1] and Mohamed Mostafa[2]

[1]Z/I Imaging Corporation
301 Cochran Rd, Suite 9
Huntsville, Alabama 35824
E-mail: msmadani@ziimaging.com

[2]APPLANIX Corporation
85 Leek Cr., Richmond Hill
Ontario, Canada L4B 3B3
E-mail: MMostafa@applanix.com

ABSTRACT

This paper describes the quality assurance and quality control (QA/QC) tools currently planned and under implementation in the Z/I ImageStation Automatic Triangulation (ISAT) product for imagery acquired by an aerial camera and Applanix POS/AV™ navigation system. First, a description of the ISAT product with its user interface with the Applanix POSEO package is given. Then, a description on using the EO data in mapping applications is presented. Instead of using the full capabilities of an automatic aerial triangulation, the QA/QC procedure is designed to lessen the amount of work needed to check the quality of the GPS, IMU, and GCP data using different schemes, such as performing a statistical analysis on image/object space intersection using digital images and the GPS/IMU data. Numerical results of using the ISAT's QA/QC strategies on the OEEPE data set are also presented.

1. INTRODUCTION

In an aerial triangulation process, the image coordinates of all tie, control, and check points appearing on all photographs are measured and then a least squares bundle adjustment is performed. This process ultimately provides exterior orientation parameters for all photographs and three-dimensional object coordinates for all measured image points. Until recently, all photo measurement was done manually. Furthermore, the block adjustment was a completely separate step (Madani, 1996).

New advances in digital photogrammetry permit automatic tie point extraction using image-matching techniques to automate the point transfer and the point mensuration procedures. Automatic Aerial Triangulation (AAT) is already in production rather successfully. The AAT solution has reached the accuracy level of a conventional aerial triangulation. It has been proven, that the AAT solution is much more economical than a conventional one. However, like any new products, AAT systems need to be improved to fit increasing demands of the users (Schenk, 1996).

In 1997, the European Organization for Experimental Photogrammetric Research (OEEPE) and the International Society for Photogrammetry and Remote Sensing (ISPRS) initiated a test of different existing commercial and experimental AAT systems to study the stability of the block geometry, the accuracy of the tie points and the derived orientation parameters, and the limitations of the products (Heipke, Eder, 1998). Results of the OEEPE-ISPRS test showed that the existing AAT systems have some limitations; therefore, any new AAT approach must incorporate following features:

- Embedding reliable and efficient mechanisms to detect and eliminate blunders in the tie point measurements
- Increasing the number of multi-ray points and ensuring an even point distribution to guarantee a stable block geometry
- Applying combined approaches of image matching to improve both the computation time and the accuracy of point measurement
- Including special techniques to process poorly textured areas by increasing the success rate of automation
- Including an intuitive and instructive interface for the operators who must intercede in the case of automation failure
- Keeping the tuneable procedure control parameters to the very minimum or, even, to achieve an autonomous operation.

GPS photogrammetry has already helped to improve the accuracy/performance of the conventional aerial triangulation process. Directly derived exterior orientation parameters using combined GPS and high-performance INS systems offer the possibility of eliminating conventional aerial triangulation in the long run. Consequently, these changes significantly impact all the steps of the data reduction and measurement processes. For example, the possible elimination of a complete aerial triangulation process will result in substantial savings while increasing the need for more sophisticated quality control procedures.

The early experiments with GPS/INS-derived exterior orientation data were related to analytical plotters. The objective was to set up models very quickly for map compilation without the usual orientation process. Now that GPS/INS technology has evolved, interest is already shifted toward softcopy systems too.

The use of GPS and INS systems in photogrammetry can, on the one hand, support the existing aerial triangulation (AT) packages by providing highly accurate exterior orientation parameters from the beginning and improve the quality and reliability of the orientation results. It is also possible to perform camera and/or self-calibration and simplify the point measurement process of automatic aerotriangulation by reducing the number and necessary tie points and the distribution of the tie point areas. On the other hand, AAT solutions operate as a method where camera, GPS, IMU and ground control observation are checked for consistency, gross errors, and statistical properties.

Cross flights introduced into many GPS supported AT projects served just for the determination of additional drift parameters caused by various factors. Using the INS-derived image orientation angles as additional orientation information helps to reduce and eliminate the necessary cross flights for aerial triangulation projects. This has resulted in an important cost reduction for many GPS supported AT projects.

So the question is raised if the aerial triangulation (AT) will soon become obsolete? The determination of the exterior orientation parameters by the GPS/INS systems has been significantly improved. However, these parameters are not still accurate enough to be used directly in large scale and engineering photogrammetry applications (Greening, et al, 2000). There are still good reasons to keep AT or AAT:

- The self-calibrating block adjustment serves to compensate for systematic image errors based on available tie points;
- The condition of ray intersections which underlies the AT as well as the image plotting serves to be the geometric constraint for compensation of both random and systematic errors in an image. Errors in the parameters of interior orientation can also be compensated for by the exterior orientation. Thus, the orientation parameters determined by an AT could best fit the image for further processing;
- IMU (Inertial Measurement Unit) system alignment based on ground control points (GCP) is essential for the GPS/INS application;
- GPS-derived camera exposure station coordinates are not always available at the precision required for mapping.
- Geodetic consideration regarding underlying coordinate system and datum bias.

Nevertheless, the GPS/INS technology benefits the AT and thus the next generation of AAT systems. Therefore, they should be used in a combined block adjustment.

Facing these new technical challenges Z/I Imaging, as a photogrammetry system provider, has recently upgraded and enhanced its existing AAT system (Madani, 2001).

This paper describes the main features, the major functionality, and the workflow of the newly developed ImageStation Automatic Triangulation (ISAT) product. A number of QC/QA methods are designed to let the operators very quickly evaluate the quality of the directly derived EO parameters (GPS/IMU data) for a particular application and scale. Numerical results of using the ISAT's QA/QC methods on the OEEPE data set are also presented.

2. ISAT MAIN FEATURES

Special emphasis has been given to the ISAT's user friendliness, reliability, and integration. Some of the main features of the ISAT product are (Madani, et al, 2001):

- Comprehensive and flexible photogrammetric project set-up
- Footprint selection, which lets the user graphically select footprints of photos/models/blocks
- Unlimited project size through division into sub-blocks
- Several Import/Export translators and raster utility options for photogrammetric data
- Automatic and interactive image manipulation and enhancement tools
- Automatic and manual Interior Orientation and Relative Orientation
- Single Photo Resection and Absolute Orientation
- Multiphoto measurement in monoscopic and/or stereoscopic modes
- Semi-automatic and manual tie point measurement in a Multiphoto environment
- Real-time panning for image movement in mono and stereo and dynamic coordinate system read out
- Well-connected image block by high-quality multi-ray points
- High performance image matching by using efficient algorithms and by restricting tie points to a reasonable limit
- Automatic weak-area detection and interactive handling mechanism
- Comprehensive bundle block adjustment utilizing (see Figure 1)
    - Relative ("free network") and Absolute bundle block adjustments
    - Robust estimators for blunder detection
    - GPS/INS data processing -- It is tightly integrated with the Applanix POSEO system (see Figure 2)
    - Camera and self calibration capability
    - Variance-covariance (precision) estimation
- Display of vector residuals (image/object) to facilitate the error analysis process
- Several easy-to-use editing tools for image measurements
- Merging and editing sub-blocks to allow users to merge multiple blocks into a new block
- On-line bundle block adjustment with and without control points (relative and absolute modes)

3. GRAPHICAL ERROR ANALYSIS

ISAT provides graphical displays and error analysis tools to facilitate detection of blunders, weak areas, and problem photos after an AAT run and a bundle adjustment. These graphical displays consist primarily of vector residual displays that interact with the operator:

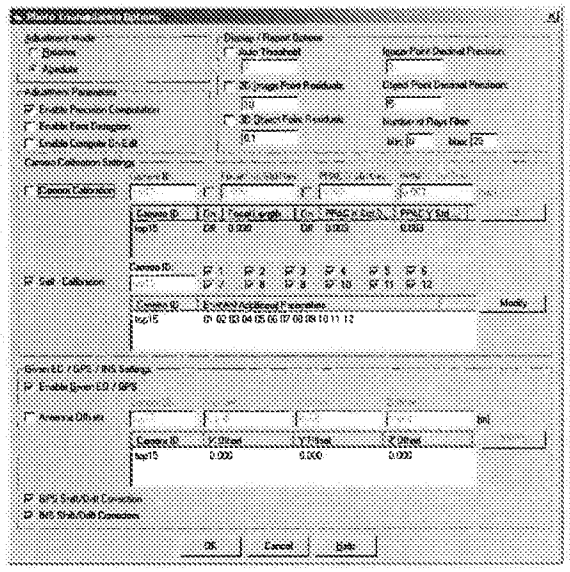


Figure 1. Bundle Block Adjustment Options

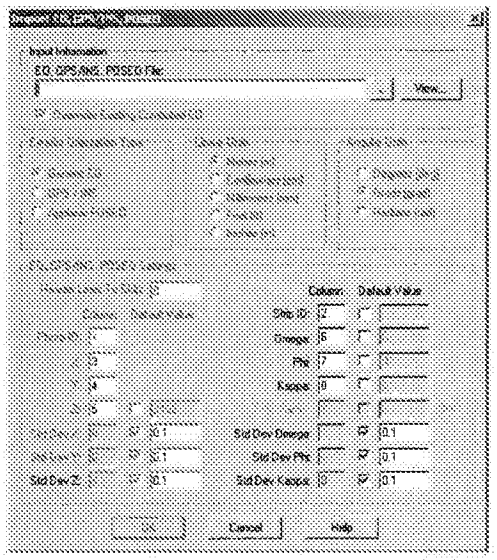


Figure 2. Import EO, GPS/INS, POSEO

- Display vector residuals of control, check points, and photo positions
- Display vector residuals of image points per photo and per block
- Display image systematic errors using significant additional parameters derived by self calibration
- Allow the user to threshold the display to show only vector residuals above a known value or based on number of rays
- Allow the user to scale the magnitude of the vector residuals on the graphical display
- Display dynamic readouts of point ids, XY, and Z residuals
- Display dynamic readouts of photo ids when photo footprints are displayed along with the vector residuals
- Allow the user to perform all the basic viewing commands on the vector residual (Zoom In, Zoom Out, Fit, Pan)

- The numerical point list and the graphical vector residual display will interact. Selecting a point in the list will highlight the point in the graphic display. Selecting a vector in the graphic view will select that point in the listview and scroll to it in the view
- Double-clicking a vector residual will do a window centre about that point and select it in the listview
- Double-clicking a vector residual will drive the image views to that point in the Multiphoto environment
- Error analysis dialog provides pre-filter values to limit the number of points displayed in the list and in the vector display
- Display photo position residuals residual vector between computed and given EO parameters

4. WORKFLOW DESCRIPTION

In general, the user will typically perform following steps, shown in Figure 3, when running ISAT.

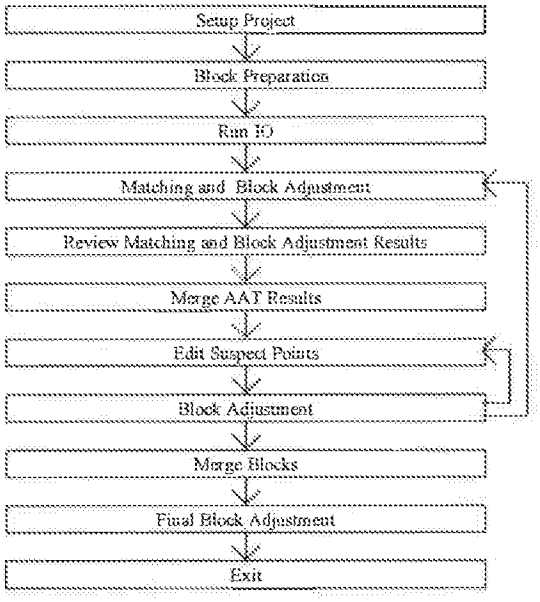


Figure 3: ISAT Workflow

The user sets up a project. This will involve setting up project, strip and camera parameters and optionally entering control coordinates (but not necessarily measuring the control before the automatic tie point generation), GPS/INS data (exterior orientation parameters), if available, and other specific project and users defined parameters.

The user may wish to run image matching and block adjustment on only part of the project. ISAT allows the user to create a sub-block for AAT processing. This will be via a graphical interface that shows flight lines with photo centers, from which the user can select the photos to include in the block. ISAT allows the user to use photo and block footprints to create, edit, delete, and measure blocks. Creating, editing, and merging blocks can be done in a variety of ways: graphically by selecting photo footprints or existing block footprint, by selecting photos or existing blocks from list, or by any combination of these. Later in the workflow the user will be able to tie overlapping blocks together (Merge Blocks).

After performing automatic interior orientation, ISAT's image-matching module generates optimized and well-distributed tie points for the selected images. At the end of image matching, an internal bundle adjustment is called to check the quality of the extracted tie points and to remove blunders using a robust estimator technique.

The user is able to review all the weak areas where insufficient matched points were not generated by AAT. The AAT dialog includes a graphical view for these weak areas. The user may manually measure additional points in those images that do not have strong connections with the overlapping images. After the user has measured new points in weak areas, he will need to run a block adjustment to incorporate these changes into the solution. The user is able to review all the statistics from the image matching and block adjustment steps. In addition to the usual block adjustment statistics, this includes statistics from the point matching procedures. The statistical information also includes a graphical view (vector residuals) of point statistics on the Photo, Object, and Point tabs of the dialog. From this, the user determines whether the adjustment succeeded or failed.

If multiple sub-blocks are run, their measurements may be merged into "master block". This command allows the user to merge multiple blocks into a single block. This allows the user to work with blocks of a manageable size to perform the sub-block

matching and block adjustments and ultimately merges all blocks together into a single large block. A final post processing bundle block adjustment is then performed without any further matching.

5. HOW THE POS/AV™ SYSTEM WORKS

The key component of the POS/AV™ system is the Integrated Inertial Navigation (IIN) software. This software runs in real-time on the POS Computer System (PCS) and in post-processing in the POSPac™ software suite, and performs the integration of the inertial data from the IMU with the data from the GPS receiver. The functional architecture of the software is given in Figure 4. For details see, Mostafa and Hutton (2001b). For details on GPS-aided inertial positioning and attitude determination, see Scherzinger (1997), Schwarz et al (1993), Hutton et al (1998) and Reid et al (1998). The software consists of the following components:

- Strapdown inertial navigator
- Kalman filter
- Closed-loop error controller
- Smoother (POSPac™ only)
- Feed forward error controller (POSPac™ only)
- In-flight Alignment

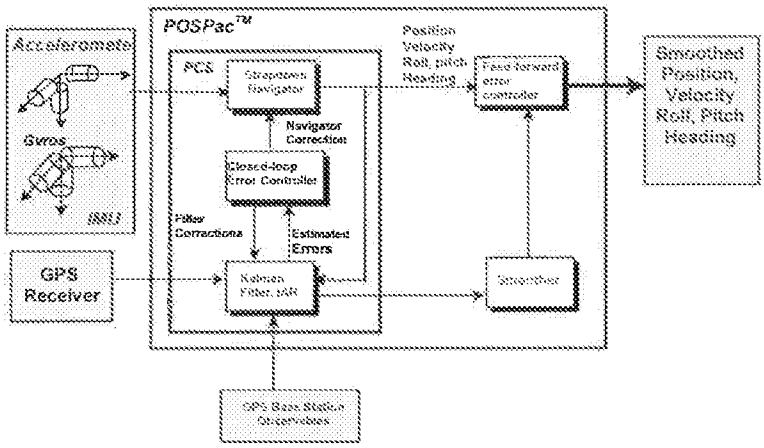


Figure 4. Functional Architecture of the POS/AV System

6. DIRECT EXTERIOR ORIENTATION DETERMINATION

As shown in Figure 5, Photo positioning and attitude data is processed using POSPAC™ in an Earth-Centred Earth-Fixed (ECEF) frame of reference, typically WGS84, to produce a smoothed best-estimated trajectory (SBET). Then POSEO™ is used to interpolate the position and attitude information at each image exposure time, calibrate the boresight, and determine the exterior orientation parameters in a local mapping frame of reference that is required for map compilation. Figure 6 shows POSEO™ interface, while Figure 7 shows the POSEO™ data output options, which includes a special format option for Z/I Imaging ISAT (see also Figure 2).

7. DIRECT EO QUALITY ASSURANCE AND QUALITY CONTROL (QA/QC)

The quality of the exterior orientation data generated by a POS/AV system becomes directly apparent when it is combined with the imaging system data. On the other hand, the mapping process using directly measured exterior orientation parameters is different from the traditional one (c.f., Jacobsen, 2001). Therefore, generally, the entire process of quality control becomes a process of managing each step in the data acquisition and post-mission processing phases to achieve a consistent and reliable quality assessment. Consequently, the process of quality control of directly measured exterior orientation data by POS/AV is categorized into two main categories which are done sequentially, namely, quality control using navigation data and quality control using navigation and imaging data simultaneously by ISAT. In the following, each of these will be discussed in some detail.

7.1 QA/QC Using Navigation Data

Proper mission planning goes a long way towards obtaining repeatable results. Once the mission begins, the POS/AV system must be monitored frequently for GPS dropouts or other data acquisition failures. A severe failure such as loss of GPS data for an extended time period may be grounds for aborting the mission. Once the aircraft has landed, the recorded data should be checked for outages and other immediate indications of bad or missing data. This allows the mission to be re-flown possibly the same day.

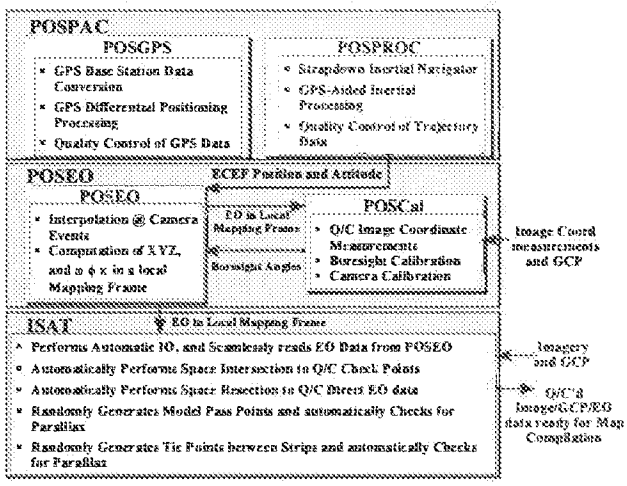


Figure 5. General Processing and Q/C Data Flow

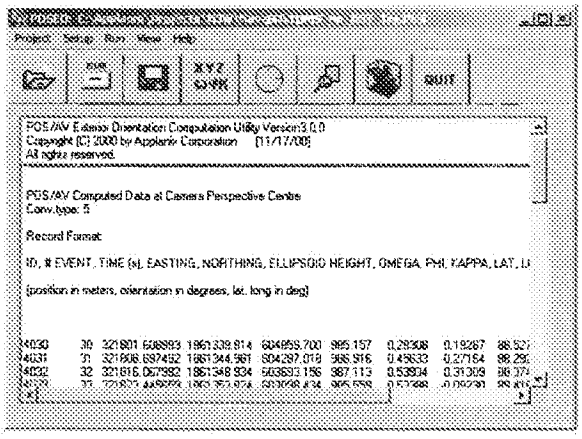


Figure 6. POSEO™ Software Interface

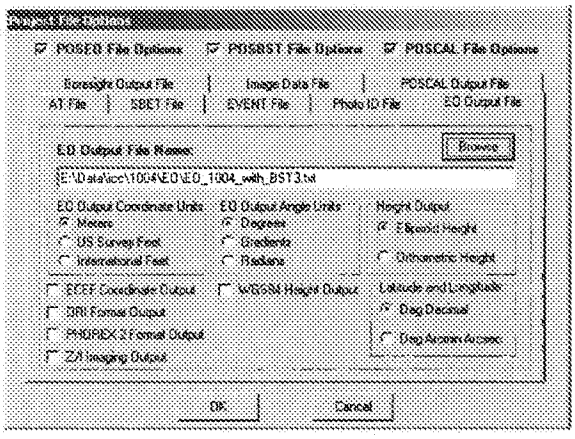


Figure 7. POSEO™ Output File Including Z/I Imaging Output

If the recorded data are seemed to be acceptable, then the data are handed over to post-mission processing. POSPAC™ has several quality assessment indicators. The most basic of these are the inertial-GPS residuals. These are the corrected differences between the inertial and GPS position solutions at each GPS epoch, and indicate the consistency between the solutions. The residuals will appear to be random in a successful inertial-GPS integration, indicating that the integration process has removed all sources of bias errors in the data. The processing software will typically perform a statistical analysis on the residuals and report a simple quality indicator to the user (c.f., Scherzinger, 1997).

7.1.1 Mission Planning

The absolute accuracy of the blended position of a GPS/inertial system is limited to the absolute positional accuracy of the GPS. Hence it is important that proper mission planning be conducted to ensure that the best possible GPS accuracy is achieved. The best GPS positioning accuracy (5 to 15 cm) is achieved using carrier phase DGPS techniques. To obtain this accuracy, a mission must be planned to provide conditions for reliable ambiguity resolution throughout the mission. Error sources that can prevent maintenance or re-fixing of integer ambiguities include ionospheric delays, multipath, and poor satellite geometry. Even if the correct ambiguities are found and maintained for the entire mission, these error sources can, if not properly managed, still degrade the accuracy of the solution. Airborne mission planning should therefore include the following components.

7.1.2 Static Data Collection

A mission should begin and end with a static data acquisition each lasting a minimum of 5 minutes. The static data allows the GPS post-processing software uses the constant position information to obtain the correct initial and final ambiguities with high probability of success.

7.1.3 Minimizing Multipath

Multipath reflections can be a major source of position error and cause for integer ambiguity resolution failures. All base receivers should use antenna choke rings or ground planes to attenuate low elevation signals, and should be mounted at least 100 m away or above all reflecting surfaces.

7.1.4 Limiting Baseline Separation

If the mission requires the 2-10 centimetre position accuracy that a kinematic ambiguity resolution solution can provide, then the maximum baseline separation must be limited to 10 to 50 km depending on the diurnal and seasonal solar activity. This allows the GPS processing software to recover fixed integer ambiguities following cycle slips or loss of phase lock at any time during the mission. For missions with flight lines greater than 100 kilometres, multiple base receivers must be used to ensure the maximum separation between the aircraft and any base receiver is less than 50 kilometres. Currently, POSGPS™ processing software package processes data from multiple base receivers to produce an optimal combined solution (c.f., Mostafa and Hutton, 2001a).

7.1.5 Planning for PDOP

The mission should be planned during times of good satellite coverage so that PDOP is 3 or less throughout the mission. At the time of writing, the GPS constellation comprises 29 satellites, which provides for a poor PDOP relatively infrequently. A simple satellite prediction software tool provides the information needed to plan for best PDOP. Figure 10 shows the double differenced PDOP during an aerial photography flight. Flight missions should be planned to avoid such spike centred at GPS time of 390,000 for about 10 minutes, although the PDOP is less than three ($< \sqrt{9}$). In that case, the pilot could have been instructed to fly away from the mapping area during that ten-minute period of time to avoid the resulting inconsistent GPS accuracy.

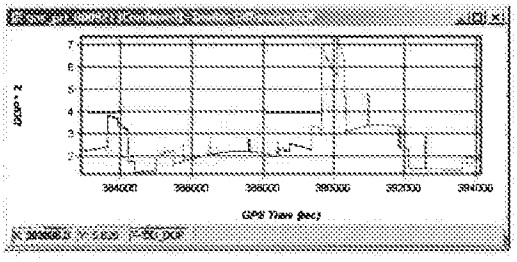


Figure 8. GPS DD-PDOP During an Aerial Photography Flight

7.1.6 Inertial Navigator Alignment

POS/AV can align itself while stationary or in motion. In fact, the in-air alignment is accelerated and the quality of the alignment improved if the aircraft performs an accelerating manoeuvre such as take-off or a turn. An in-air alignment requires about 3 minutes of nominally straight and level flight to allow POS/AV to compute an initial roll and pitch, followed by a series of turns to align the heading. Thereafter POS/AV improves its alignment with every manoeuvre. A typical zigzag survey pattern provides the manoeuvres required by POS/AV to maintain a high quality alignment. Figure 9 shows a frequently changed velocity of an aircraft due to manoeuvres and Figure 10 shows the total acceleration due to such manoeuvres.

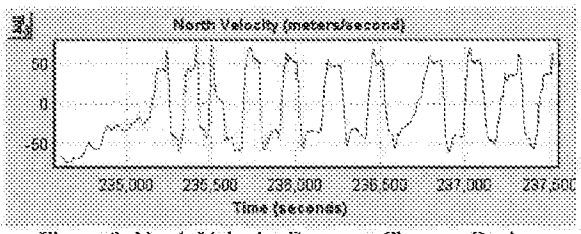


Figure 9. North Velocity Frequent Changes During Manoeuvres

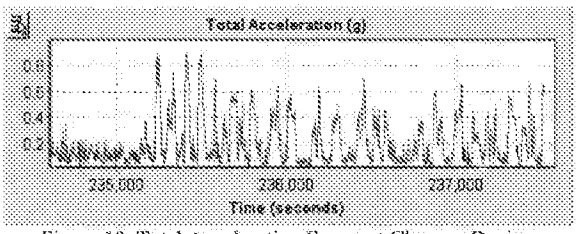


Figure 10. Total Acceleration Frequent Changes During Maneuvers

7.2 QA/QC Using Navigation/Imagery Data – The DLC™ Concept

Detection, Location, and Correction (DLC™) is the concept behind the direct EO QA/QC process in ISAT. POS (GPS/IMU) data, project aerial imagery, and available GCP (control/check points) are simultaneously used to efficiently perform DLC. By 'detection' we mean, to automatically detect whether or not there is a perfect fit (according to some predefined threshold) between the directly derived EO parameters, the images, and the available GCP. If there is no perfect fit then 'Location' is performed, where ISAT tries to automatically identify the location and possibly the reason for erroneous EO parameters. 'Correction' is where the erroneous (inaccurate for some reason) EO parameters are corrected.

Figure 11 shows the DLC workflow in the ISAT product. Typically, the raw GPS and IMU data are processed in POSGPS, POSProc, and POSEO, where the derived trajectory parameters are translated into camera exposure station coordinates and image orientation angles with respect to a local mapping frame. ISAT then reads the information where it first performs the automatic interior orientation (IO) then checks in the POSEO output file whether or not the EO parameters have high standard deviations. If the standard deviations are higher than what is suitable for the project at hand, then it will issue a warning to the operator that the EO data should be improved by reprocessing the GPS data.

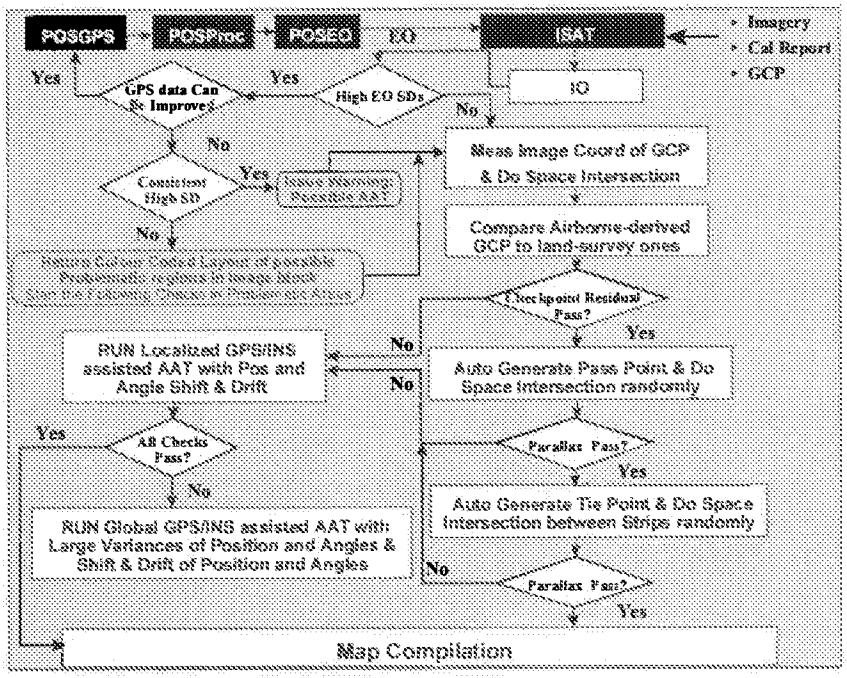


Figure 11. Detection, Location, and Correction Concept (DLC™)

The operator is then becomes responsible to improve the GPS data processing quality, then run the data through POSProc and POSEO, respectively and import the improved X, Y, and Z and ω, φ, and κ, data in ISAT. If the GPS data cannot be improved, ISAT will check whether the standard deviations are consistently too high for the project at hand or not. If the data is consistently high, then ISAT will issue a warning that there might be a possibility to use a ISAT's automatic aerotriangulation engine to its fullest. If the EO standard deviations are not consistently high, ISAT will then return a colour-coded footprint of the project layout to show and distinguish the problematic areas in the project. Then, ISAT will run the following checks on those areas of the project that have high EO standard deviation.

1. ISAT will manually or semi-automatically measure image coordinates of the ground points (check points). The user can then revisit the ground point locations manually to make sure that they are precisely located on the imagery.
2. ISAT will then perform the space intersection using the given EO data and the image coordinates of all available checkpoints.
3. ISAT will compare the computed checkpoint coordinates with the given values. If the checkpoint residual test passes, ISAT will issue a statement that all checkpoint residuals are within the required accuracy.
4. If checkpoint residual testing did not pass, ISAT will issue a warning and let the user decide on running a local automatic aerial triangulation using GPS/INS assisted triangulation concept applying the shift and drift parameters.
5. If the checkpoint residual test passed, ISAT will automatically generate model pass points and performs space intersection to check analytically if model pass points have any parallax. If parallax is evident, the user is given an option to eliminate the parallax by using the localized GPS/INS-assisted AAT option.
6. If the pass point test passed, ISAT will move on to automatically generate tie points between strips. These points will be used again in the space intersection mode to determine whether or not there is remaining parallax between the image strips. If no parallax is discovered, then the software will issue a statement that no errors are found in this project and the EO data can then be used directly in the map compilation mode.
7. If parallax is evident, the user is given an option to eliminate the parallax by using the localized GPS/INS-assisted AAT option.
8. Each time there is any need to run a localized GPS/INS-assisted AAT, all the check listed in steps 1 to 7 will be checked again. If all those checks are passed, ISAT will issue a statement that all errors found in this project are fixed and the EO data can then be used directly in the map compilation mode.

If any of the check failed, the user will be given the option to run the entire project using ISAT's GPS/INS-assisted automatic aerotriangulation engine, to fix the remaining problems.

8. EXAMPLES OF NUMERICAL RESULTS

8.1 Test Data Description

The 1:10,000 photo scale data of the Fredrikstad, Norway test field, flown by Fotonor AS using a wide angle Leica RC30 camera equipped by an Ashtech GPS receiver and the Applanix POS/DG system, was used in this study (for detail, see Heipke, et al, 2000). This test field is about 5 x 6 km^2 and has 51 well distributed signalized control points with the accuracy of about 0.01 cm. The control point coordinates and raw and refined direct EO parameters were given in UTM/EuroRef80 coordinate system with ellipsoidal heights. This data set is comprised of five parallel strips and two cross strips and 13 control points (Figure 12).

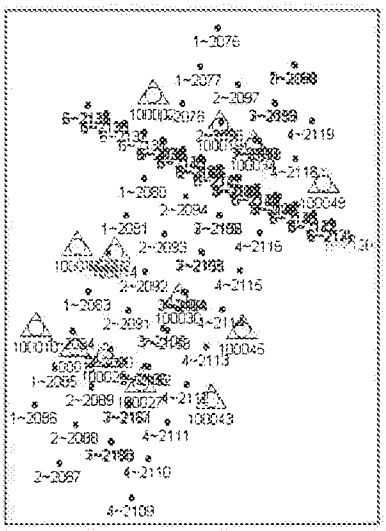


Figure 12: Calibration Flight in Southern Norway, Image Scale 1:10,000

Applanix POSEO data, uncorrected and corrected for boresight (misalignment between camera IMU coordinate frames) computed in the phase one of the OEEPE study, along with the provided control points coordinates and the image coordinates of all 85 photos were used to investigate the results obtained by the ISAT bundle block adjustment and its DLC capability for analyzing the quality of the derived EO parameters.

For quality control purposes, error detection is experimented using the 1:10,000 block of photos. The purpose of examining this scenario is to investigate the following:

1. Can the boresight errors be detected using the shift and drift parameters in ISAT?
2. What is the effect of block geometry in detecting any boresight errors?
3. What is the effect of boresight errors on camera exposure station coordinates and orientation angles if a block is adjusted using the boresight-corrupted exterior orientation data ignoring boresight errors

Therefore, POSEO was used to produce an exterior orientation file for the block with boresight angles set to zeros. This is done this way to simulate a scenario where the calibrated boresight values were not input to the software by mistake. Then, the corrupted exterior orientation data files were read in ISAT. The entire block was triangulated using the original photo coordinate measurements, the boresight-corrupted exterior orientation data and all available ground control points. The whole 85 photos were used in this scenario. Angular shift and drift option was used to answer the first question on the previous list. The standard deviations of the camera exposure station coordinates and orientation angles were set to the POS system specifications, namely 0.1 m for each component of the camera exposure station coordinates and 0.005°, 0.005°, 0.008° for image ω, φ, and κ, respectively. This implies that the intentional boresight error is not accounted for in the standard deviations of image orientation angles. This is done on purpose in order to simulate a production environment.

The computed shift angles were very close to the boresight angles. In other words, ISAT was capable of absorbing almost all the intentional boresight errors by the angular shift parameters. The computed exterior orientation parameters were then compared to those given by POSEO. Figures 13, 14, and 15 show the difference in camera position in X, Y, and Z components, respectively. In these Figures the difference is shown twice, once in red diamonds where no angular shift and drift were used, and the other time in blue squares where the angular shift and drift option was used. It is clear that any boresight error will affect the camera exposure

station coordinates if the data is triangulated neglecting the boresight error without properly choosing the necessary math model required to recover the boresight error. . Figures 16, 17, and 18 show the differences in image orientation angles in ω, φ, and κ, respectively. Note that the same observation can be made in Figures 16-18, too Although it is evident that ISAT will absorb the boresight errors, it will issue a warning that there is possible calibration issue and the operator should go back and double-check entering the correct boresight values in POSEO. Tables 1 and 2 show the statistics of the differences presented in Figures 16 - 18. Although it is evident that ISAT will absorb the boresight errors, it will issue a warning that there is possible calibration issue and the operator should go back and double-check entering the correct the boresight values in the POSEO.

Table 1. Statistics of Image Orientation Differences from POSEO Using ISAT With INS Shift and Drift Option to recover a Boresight-Corrupted Data - Full Block 1: 10,000 photo Scale

	Omega (deg)	Phi (deg)	Kappa (deg)
Minimum	-0.019	-0.006	-0.020
Maximum	0.003	0.013	0.011
Mean	-0.008	0.003	-0.002
Std Dev	0.005	0.005	0.005
RMS	**0.010**	**0.005**	**0.008**

Table 2. Statistics of Image Orientation Differences from POSEO Using ISAT Without INS Shift and Drift Option to recover a Boresight-Corrupted Data - Full Block 1: 10,000 photo Scale

	Omega (deg)	Phi (deg)	Kappa (deg)
Minimum	-0.042	-0.028	-0.041
Maximum	0.037	0.027	0.005
Mean	-0.008	-0.002	-0.013
Std Dev	0.017	0.015	0.009
RMS	**0.019**	**0.015**	**0.015**

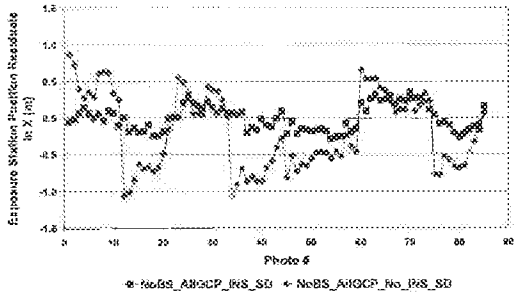


Figure 13. Exposure Station Position Residuals (X Component) Using ISAT With and Without INS Shift and Drift Option to Recover a Boresight-Corrupted Data - Full Block 1: 10,000 photo Scale

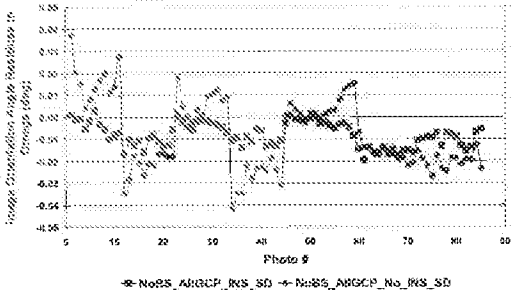


Figure 16. Image Orientation Residuals (in Omega) Using ISAT With and Without INS Shift and Drift Option to Recover a Boresight-Corrupted Data - Full Block 1: 10,000 photo Scale

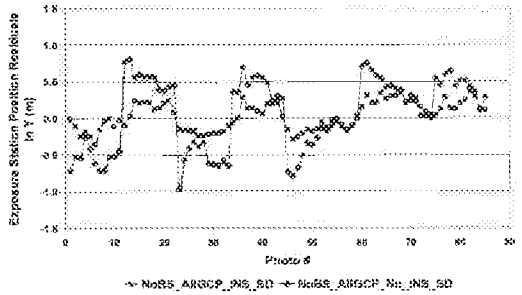


Figure 14. Exposure Station Position Residuals (Y Component) Using ISAT With and Without INS Shift and Drift Option to Recover a Boresight-Corrupted Data - Full Block 1: 10,000 photo Scale

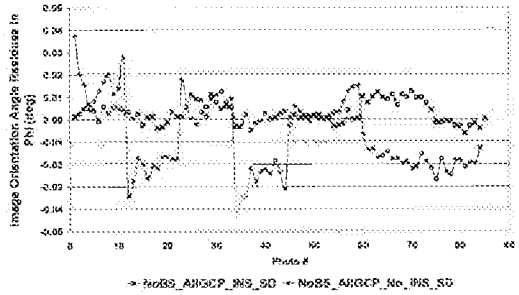
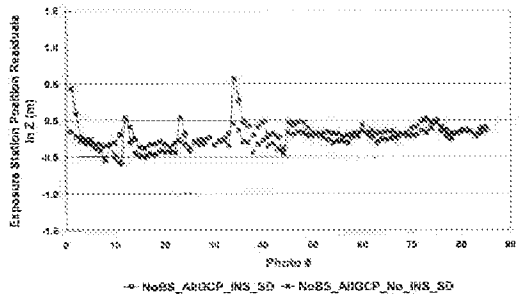


Figure 17. Image Orientation Residuals (in Phi) Using ISAT With and Without INS Shift and Drift Option to Recover a Boresight-Corrupted Data - Full Block 1: 10,000 photo Scale



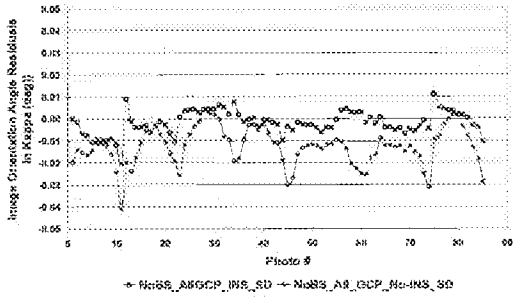


Figure 15. Exposure Station Position Residuals (Z Component) Using ISAT With and Without INS Shift and Drift Option to Recover a Boresight-Corrupted Data - Full Block 1: 10,000 photo Scale

Figure 18. Image Orientation Residuals (in Kappa) Using ISAT With and Without INS Shift and Drift Option to Recover a Boresight-Corrupted Data - Full Block 1: 10,000 photo Scale

The second scenario is similar to the aforementioned one, except that error detection is experimented using only two image strips. This is to investigate whether or not a two-strip image block is geometrically stable enough to detect any boresight errors by ISAT. ISAT was then used to run the two-strip block using the angular shift and drift option. This required the use of four ground control points. ISAT was able to absorb the intentional boresight error by the shift parameters for the two sets of data. The refined image angles by ISAT were then compared to those derived by POSEO (where the boresight angles are accounted for). The results are shown in Figure 19 for the strip 1 and 2 block, and in Figure 20 for the strip 1 & 4 block.

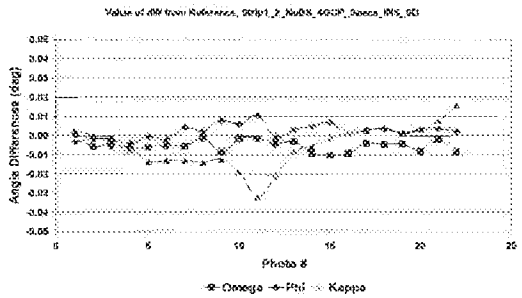


Figure 19. Image Orientation Difference Between POSEO and ISAT using INS Shift and Drift for Boresight-Corrupted Data Strip 1 & 2 Photo Scale 1: 10,000

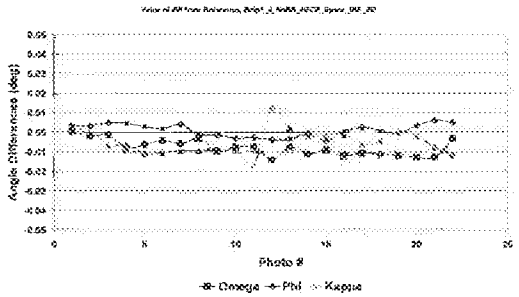


Figure 20. Image Orientation Difference Between POSEO and ISAT using INS Shift and Drift for Boresight-Corrupted Data Strips 1 & 4 Photo Scale 1:10,000

Tables 3 and 4 show the statistics of the differences shown in Figure 19 and 20. It is clear from Tables 1 and 2 that ISAT absorbed almost all of the boresight error by the angular shift parameters. More importantly, ISAT detected the boresight error. Typically, the next step in the ISAT data processing chain in such a scenario is to warn the user to go back and correct for that boresight mistake in POSEO.

Table 3. Statistics of Attitude Differences using Strips 1 & 2

	Omega (deg)	Phi (deg)	Kappa (deg)
Minimum	-0.010	-0.004	-0.032
Maximum	0.001	0.011	0.016
Mean	-0.005	0.002	-0.006
Std Dev	0.003	0.004	0.011
RMS	0.006	0.004	0.012

Table 4. Statistics of Attitude Differences using Strips 1 & 4

	Omega (deg)	Phi (deg)	Kappa (deg)
Minimum	-0.014	-0.004	-0.016
Maximum	0.001	0.006	0.013
Mean	-0.008	0.001	-0.004
Std Dev	0.004	0.003	0.006
RMS	0.009	0.004	0.008

10. CONCLUDING REMARKS

Directly observed EO parameters from a well-planned mission and correctly operating GPS/IMU systems are accurate enough to be used in many photogrammetric applications. However, the critical issue is the QC/QA of the data. If images are to be processed in stereo then AT followed by bulk model orientation is essential in order to solve the parallax problem. Check points measured in AT provide information on the quality of the direct EO data. Performing AT also permits modeling the unaccounted systematic errors using self-calibration techniques.

The DLC concept currently implemented in ISAT is an attempt to reduce or eliminate remaining errors. In that sense, the function of AT can be viewed as changing from the determination of EO parameters to the QC/QA of direct EO data. For large-scale engineering surveys, it is still the case that ground control points are necessary in order to achieve the required accuracy in the AT.

- The ISAT product covers all the mandatory requirements for automated aerotriangulation, and avoids those drawbacks found in the OEEPE-ISPRS report.
- The ISAT product delivers fully and automatically the best-matched multi-ray tie points, without blunders. This is achieved by a robust built-in bundle block adjustment during all phases of the image matching operation.
- ISAT contains improved search algorithms to find sufficient and well-distributed tie points in the overlapping regions.

- ISAT has s number of tools for the QC/QA of the directly measured EO parameters by Applanix POS/AV system. These tools and methods allow the operator to analyze very quickly the accuracy of the directly derived EO parameters.
- Since the quality of the EO parameters depend on the quality of the GPS data (e.g., number and distribution of satellites, etc.) the IMU data (the quality of the inertial navigator alignment), the quality of lever arm calibration, and boresight calibration. ISAT is currently being augmented by the necessary tools to automatically isolate the EO errors due to any of the aforementioned reasons, to eventually inform the operator about the possible reason of any EO errors
- The DLC concept is introduced briefly, where ISAT will automatically to answer the following questions 1) where is the error? Of which magnitude is the error?, and What is the most probable reason of that error.
- The OEEPE Phase I data of the 1:10,000 flight was used to analyze one part (boresight errors) of the new DLC concept, namely the automatic detection and isolation of the boresight error and then correcting it.

11. FUTURE WORK

ISAT will be augmented with numerous tools to aid the operator control the quality of the directly measured EO data by Applanix POS/AV system.

12. REFERENCES

Ackermann, F., Schade, H. (1993): Application of GPS for Aerial Triangulation, Photogrammetric Engineering & Remote Sensing, 59(11): 1625-1632.

FGDC (1998): Geospatial Positioning Accuracy Standards, FGDC-STD-007.3-1998, Part 3: National Standard for Spatial Data Accuracy (NSSDA).

Ebner H. (1976): Self-Calibrating Block Adjustment. *Bildmessung und Luftbildwesen* 44, 128-139.

Heipke C., Eder K. (1998): Performance of tie-point extraction in automatic aerial triangulation, OEEPE Official Publication No 35, 125-185.

Heipke C., Jacobsen, K., Wegmann, H., Anderson, O., Nilsen, B. (2000): Integrated Sensor Orientation – An OEEPE Test, IAPRS, Vol. XXXIII, Amsterdam.

Hutton, J., Savina, T., and Lithopoulos, L., (1997): Photogrammetric Applications of Applanix's Position and Orientation System (POS). Proc. ASPRS/MAPPS Softcopy Conference, Arlington, Virginia, July 27 - 30.

Greening, T., Schickler, W., Thorpe, A. (2000): The Proper Use of Directly Observed Orientation Data: Aerial Triangulation is not Obsolete. 2000 ASPRS Annual Conference, Washington, DC, May 22–26.

Madani, M., Dörstel, C., Zeitler, W., Tang, L. (2001): Z/I Imaging New Automatic Aerial Triangulation System 2001. ASPRS Annual Conference, ST. Louis, MO, April.22–26.

Madani, M. (1996): Digital Aerial Triangulation - The Operational Performance, Presented at the XVIII ISPRS Congress, Vienna, Austria, July 9-19, 1996.

Mostafa, M.M R., Hutton, J. (2001a): Airborne Kinematic Positioning and Attitude Determination Without Base Stations. Proceed. Int. Symposium on Kinematic Systems in Geodesy, Geomatics and Navigation – KIS 2001, Banff, Canada, June, 5-8.

Mostafa, M.M.R., Hutton, J. (2001b): Direct Positioning and Orientation Systems - How Do They Work? What is The Attainable Accuracy? Proceed. American Society of Photogrammetry and Remote Sensing (ASPRS) Annual Meeting, ST. Louis, MO, USA, April 22-27.

Mostafa. M.M.R., J. Hutton, and E. Lithopoulos (2001): Direct Georeferencing of Frame Imagery - An Error Budget. Proceedings, The Third International Mobile Mapping Symposium, Cairo, Egypt, January 3-5.

Mostafa, M.M.R. and K.P. Schwarz (2000): A Multi-Sensor System for Airborne Image Capture and Georeferencing. PE&RS, 66 (12): 1417-1424.

Reid, D.B., E. Lithopoulos, and J. Hutton (1998): Position and Orientation System for Direct Georeferencing (POS/DG), Proceedings, Institute of Navigation 54th Annual Meeting, Denver, Colorado, USA, June 1-3, pp. 445-449.

Scherzinger, B. (1997): A Position and Orientation Post-Processing Software Package for Inertial/GPS Integration (POSProc). Proceedings of the International Symposium on Kinematic Systems in Geodesy, Geomatics and Navigation (KISS 97), Banff, Canada, June 1997.

Schwarz, K.P., Chapman, M.A., Cannon, M.E., and Gong, P (1993): An Integrated INS/GPS Approach to the Georeferencing of Remotely Sensed Data, PE& RS, 59(11): 1167-1674.

Škaloud, J., Cramer, M. Schwarz, (1996): Exterior Orientation by Direct Measurement of Position and Attitude, International Archives of Photogrammetry and Remote Sensing, 31 (B3): 125-130.

Schenk T. (1996): Digital Aerial Triangulation. In: *International Archives of Photogrammetry and Remote Sensing*, (31), Part B3, 735-745.

Camera/IMU Boresight Calibration: New Advances and Performance Analysis

Mohamed M. R. Mostafa, Applanix Corporation
85 Leek Cr. Richmond Hill, Ontario
Canada L4B 3B3
MMostafa@applanix.com

ABSTRACT

Camera/IMU boresight calibration is a critical element in the mapping process when using GPS/IMU in the direct georeferencing mode of mapping or even when using the aerotriangulation mapping. Several researchers proved the need for an optimal boresight calibration process, procedure, and software tools. Therefore, this paper is focused on presenting the latest development in the field of boresight calibration using the newly released POSCal™ software of Applanix Corporation. First, a brief discussion is presented to summarize the software capabilities in a descriptive fashion. Then, a number of analytical tools implemented in the software, which are needed to do quality assurance and quality control of the GPS, IMU, image, ground control, and datum issues, are briefly introduced. An analytical study has been done to test the analytical tools of the software. This study has been done using real sets of data collected by HJW GeoSpatial Inc of Oakland California, and by the pilot centre (University of Hannover) of the European Organization for Experimental Photogrammetric Research (OEEPE). All data sets were acquired by a 9" x 9" film camera equipped by a 6" lens cone and by Applanix POS/AV™ 510 system. In addition, all data sets had a good number, distribution, and accuracy of ground control points, quality image measurements, and good GPS and IMU data. This allowed starting off with good quality data sets where biases and noises were introduced intentionally for analysis purposes. Different imaging configurations have been studied. All data sets have been run with and without ground control points where their effect is analysed. A summary of the results and analysis is presented together with the relevant references that discussed this topic.

1. INTRODUCTION

The airborne boresight calibration is currently done by flying over a calibration field that has well distributed and accurate ground control points. Image measurements are collected using an analytical plotter or a SoftCopy workstation. An airborne GPS-assisted aerotriangulation is then done to determine each image attitude matrix with respect to some local mapping frame. For each image frame, the IMU-derived attitude matrix is then compared to the photogrammetric attitude matrix to derive the boresight matrix, from which three boresight angles are derived. Averaging the boresight over a number of images in a block configuration is the last step done to provide accurate calibration and the necessary statistics. This method has been followed successfully for the past few years using the traditional aerotriangulation approach (c.f., Hutton et al, 1997; Mostafa et al, 1997; Schwarz et al, 1993; Škaloud et al, 1996). In the map production environment, the separation between processing the photogrammetric data and the GPS/inertial data results in the following disadvantages:

1. Airborne trajectory data is slaved to some base station which coordinates are referenced to a global datum, while the photogrammetric data is normally referenced to a local Datum or a national grid. This results in datum errors that have to be compensated for during the triangulation process. These errors should be dealt with during the boresight calibration process to ensure a good fit between the airborne GPS coordinates and the ground coordinates.
2. The angular sequence of rotations of the photogrammetric data can be different from that of the inertial data, which might lead to erroneous results. Strictly speaking, this can take place due to inconsistency in the definition of frames of references between the aerotriangulation packages and the Applanix POSPac post processing software.
3. There is no access to the different data streams in the boresight calibration process. Therefore, if the quality of the boresight calibration results does not meet the required specifications, the quality control process takes place backwards.
4. If there is any miscommunication between the aerotriangulation operator and the boresight calibration operator, it can take longer time to be satisfied with the results of boresight calibration
5. Difference in data format between various aerotriangulation packages makes it difficult to directly access the data and takes time to decode the data.

The main objective of this paper is to present the POSCal™ software, which has been recently, released by Applanix Corporation for boresight calibration and camera calibration purposes. In the following sections, a brief description of the software capabilities is presented, the results of a study conducted at Applanix Corporation to determine the effect of different parameters on the boresight determination accuracy.

2. POSCAL™ FOR BORESIGHT CALIBRATION

POSCAL™ is a new software package released in April 2002 by Applanix Corporation. POSCal™ stands for Position and Orientation System Calibration. It is embedded in the POSEO software package to do boresight and camera calibration and a number of other functions to compensate for datum errors, GPS shifts and drifts, and timing errors. It is equipped with a number of analytical tools to do a quality assurance and quality control of the image coordinates, ground control point data, GPS data, inertial data, and camera calibration data. POSCal™ uses the least squares concept to simultaneously estimate boresight angles, adjust camera calibration parameters, compensate for datum distortions, correct GPS shifts and drifts, and control the quality of image coordinates and ground control point coordinates.

The graphical user interface (GUI) is designed to be a user-friendly, and project oriented. For example, Figure 1 shows the GUI of the camera parameters (left) and for the ground control point wizard (right). After camera parameters are input to POSCal™, they are saved in the Favourites for any subsequent use so that the user does not have to re-input these values once more for the same camera unless it is re-calibrated. The ground control point wizard enables the user to import ground control point data from different files, projects. It also allows manually importing or editing the ground control point data. Then the ground control point data is colour-coded according to their status. Ground control point status can be set to either full, horizontal, or vertical control, or to check points as shown in Figure 1. Ground control point precision can be either globally set to a certain value or locally (one point at a time) to different precision.

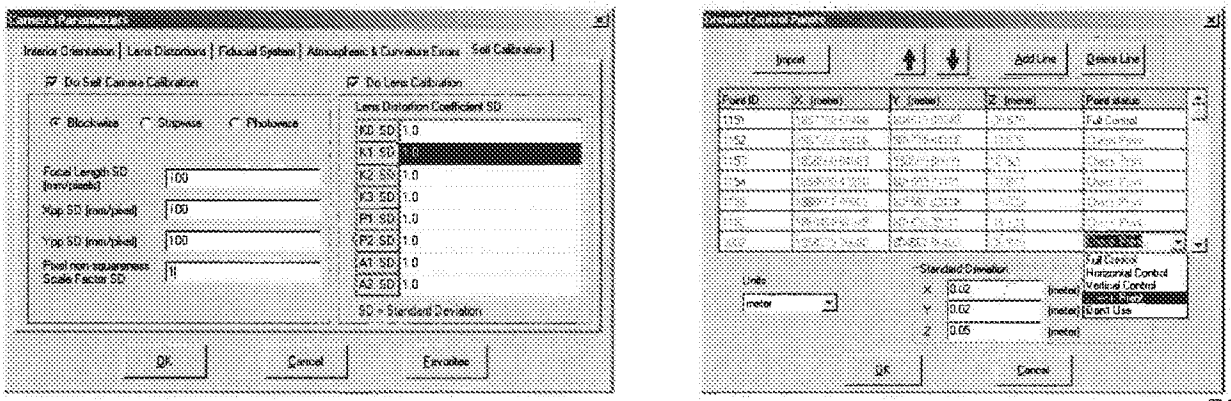


Figure 1. Graphical User Interface for Camera Wizard (left) and User Interface for Ground Control Point Wizard (right) of POSCal™

POSCal™ deals with imagery captured by either film cameras (analogue) or digital cameras as shown in Figure 2. In the case of an aerial film camera, POSCal™ accepts the image coordinates measured on both analytical and digital plotters. In the case of a digital camera, image coordinates are always measured on a digital plotter and therefore handled easily by POSCal™. Unlike film cameras, no government organization offers digital camera calibration. Therefore, digital camera calibration is usually done by the mapping firm. Consequently, digital camera calibration is implemented in POSCal™ using both close range and airborne approaches. For details, see Beyer (1992), Fraser (1997), and Lichti and Chapman (1997). Figure 3 (left panel) shows the digital camera calibration GUI in POSCal™. Furthermore, Local datum shifts are modeled in POSCal™ as shown in the right panel of Figure 3, where a 7-parameter transformation is provided absorb local datum distortions and/or make the airborne GPS-derived height consistent with the local datum heights.

An important feature in POSEO™ package is the ability to handle data processing in a number of global, regional or local datums. Figure 4 shows, for example, a number of datums implemented in POSEO™, while Figure 4 shows the various mapping frame projections implemented in POSEO™. This allows the user to do all the necessary coordinate transformations of the GPS/inertial data so that, once image coordinates, ground control points, camera calibration parameters are input to POSCal™, all the information are automatically referenced to the same mapping frame of reference.

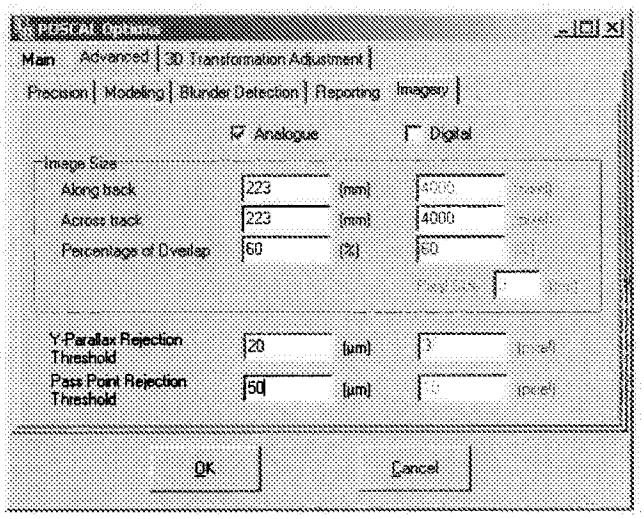


Figure 2 Film or Digital Camera Options

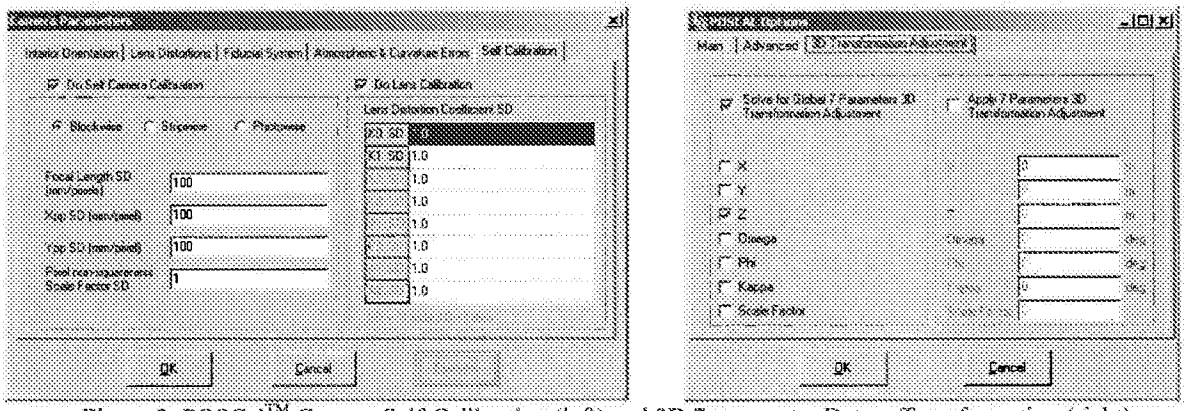


Figure 3. POSCal™ Camera Self-Calibration (left) and 3D 7-parameter Datum Transformation (right)

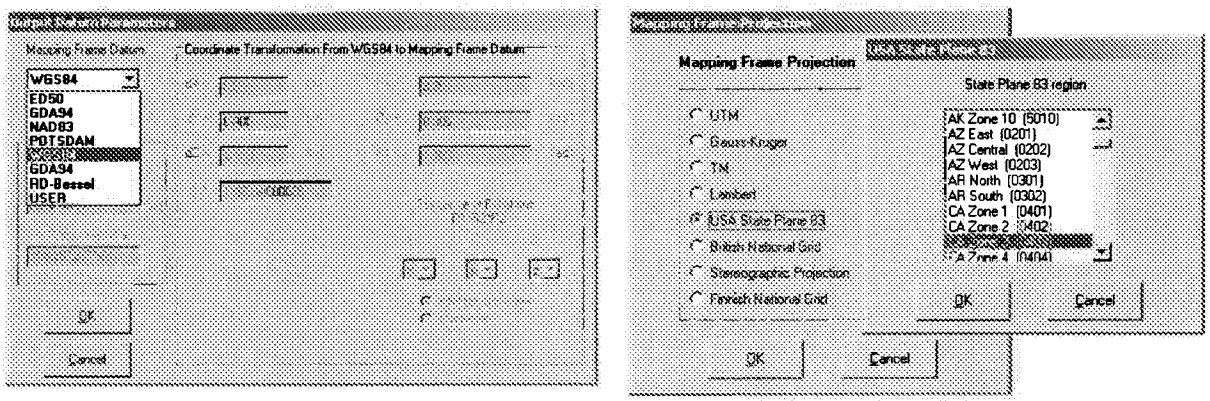


Figure 4. Datums and Mapping Frame Projections Implemented in POSEO

3. A DESCRIPTION OF DATA SETS USED FOR ANALYSIS

Two flight campaigns are used herein to analyse the performance of the new software and to analyse the effect of different parameters on boresight calibration accuracy. In this section, a brief description of these two data sets is presented.

3.1 The HJW Project

HJW GeoSpatial Inc. collected this data set for the first of these two campaigns to be considered herein. The flight took place on June 21, 2000 between Oakland and San Jose, California in the USA using an Applanix POS/AV 510 system. This data set will be referred to as the HJW Project. It includes image data, precisely surveyed GCPs, POS/AV™ 510 GPS/IMU raw observables and a post-processed GPS-assisted aerotriangulation reference. A Zeiss RMK Top camera of a 9" x 9" format equipped with a 6" focal length was used.

A 1:6000 photo scale, four-strip flight was flown with minimum banking angles (to avoid GPS cycle slips) resulting in a block of 4 strips of 11 images each. The flight lines were flown in opposite directions in order to achieve good boresight calibration. A total of 27 well-distributed GCPs were included in the block. Using the POSPac™ post-processing package, a smoothed best estimate trajectory was produced. Then, the POSEO™ new software package (including POSCal™) was used to do the analysis presented in Section 4. Figure 5 shows the flight pattern and the layout of the ground control points.

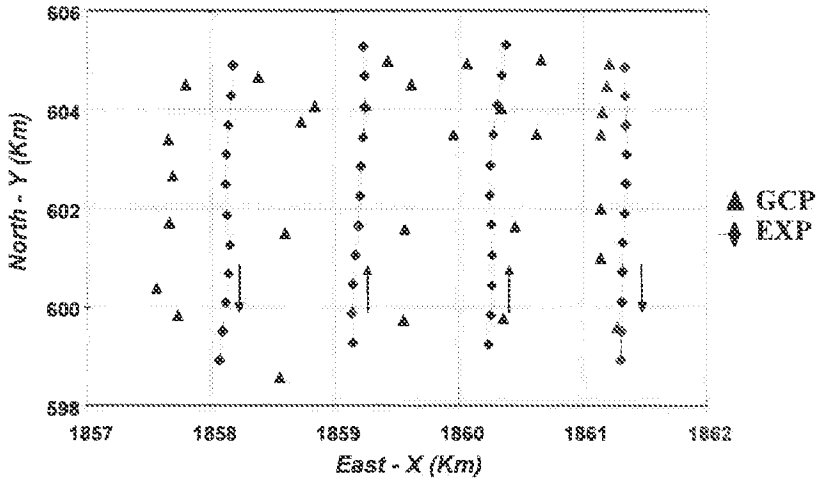


Figure 5. Flight Layout of the HJW Project

3.2 The OEEPE Project

Two data sets of the Fredrikstad, Norway test field, flown by Fotonor AS using a wide angle Leica RC30 camera equipped by an Ashtech GPS receiver and the Applanix POS/AV 510 system, were used in this study. For detail on the OEEPE project, see Heipke et al (2001).

This test field is about 5 x 6 km^2 and has 51 well distributed signalized control points with the accuracy of about 0.01 m. The control point coordinates and raw GPS/IMU data were provided by the OEEPE pilot Centre (IPI, University of Hannover, Germany) in UTM/EuroRef80 coordinate system with ellipsoidal heights. Two photo scales were flown namely; 1:5000 photo scale which flight pattern is shown in Figure 6, and 1:10,000 photo scale which flight pattern is shown in Figure 7.

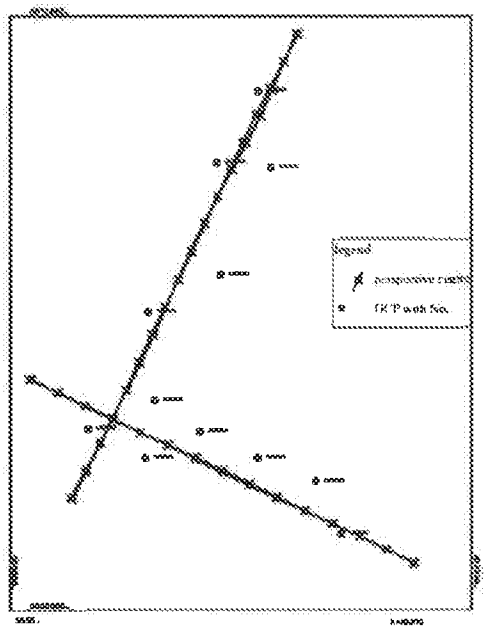


Figure 6. OEEPE 1:5,000 Photo Scale Flight Pattern In Norway (after Heipke et al, 2001)

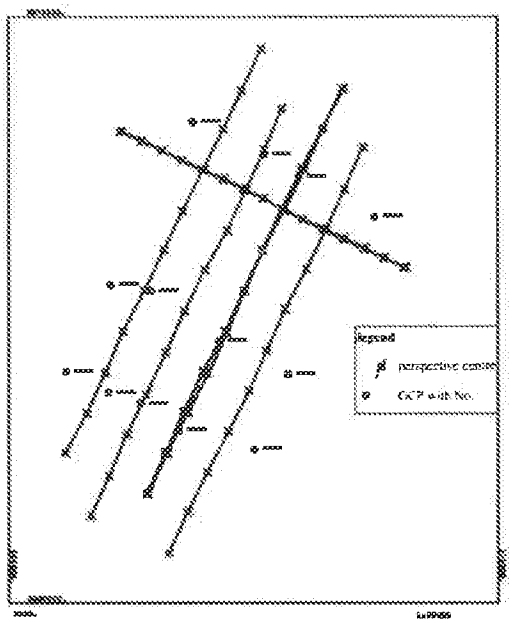


Figure 7. OEEPE 1:10,000 Photo Scale Flight Pattern In Norway (after Heipke et al, 2001)

4. DATA RESULTS AND ANALYSIS

This section is dedicated to introduce summary of the analysis conducted to analyse the performance of the newly developed software (POSCal™). In addition, the effect of a number of parameters on boresight calibration accuracy is analysed. The results are presented in some detail in the following subsections.

4.1 Performance Analysis of POSCal™

POSCal™ is equipped with a number of analytical tools to help understanding the data and the results. One of the tools is the residual analysis of ground checkpoints; exposure station coordinates; IMU angles; and image coordinate residuals. Figure 8, for example, shows the RMS of the checkpoint residuals of a number of POSCal™ experiments to calibrate the boresight of the OEEPE project. Different configurations were used such as boresight calibration using the entire block (labelled BS), simultaneous boresight/camera calibration (labelled BS_CB), boresight calibration for each single strip (BSS) or camera calibration for each single strip (CS). Note that the height bias has been significantly reduced using the datum error compensation tool in POSCal™. Figure 9, on the other hand, shows the RMS of the checkpoint residuals for the 1:10,000 photo scale block, the 1:5,000 photo scale block, and for the combined block. In addition to ground checkpoint residuals, the IMU-derived angular residuals give an indication of how the boresight and the IMU angles fitted the overall least squares solution as shown in Figure 10. The RMS values of the IMU residuals are 0.16, 0.17, 0.21 arc minutes for boresight roll pitch and heading components, respectively. Figure 11 shows the residuals of the exposure station coordinates, which is the expected from a well-planned GPS flight, which is processed using a number of base stations.

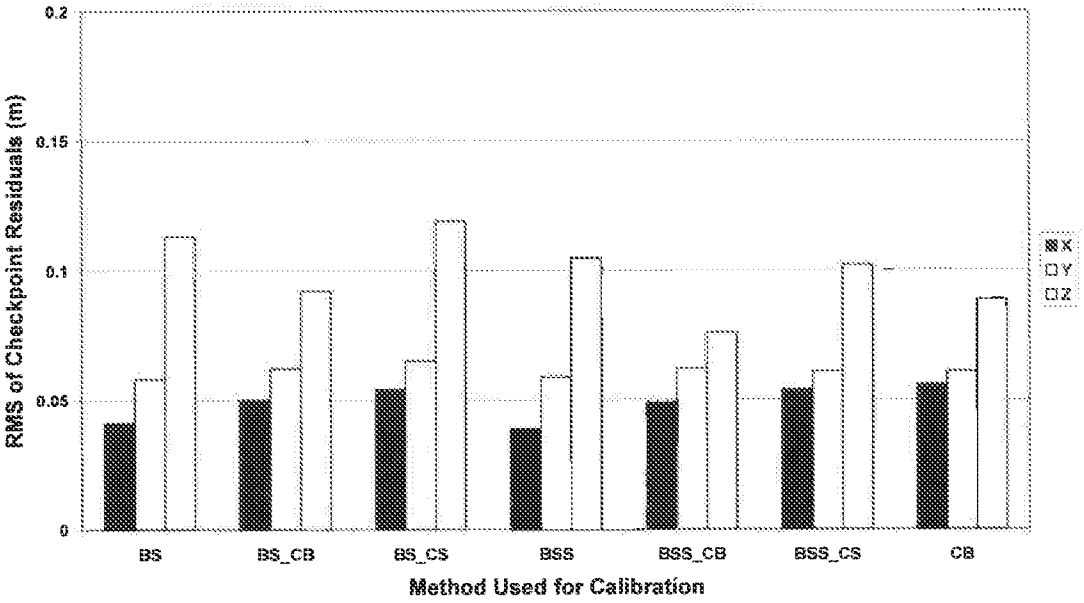


Figure 8 RMS of Checkpoint Residuals Using Different Software Options (The OEEPE Project)

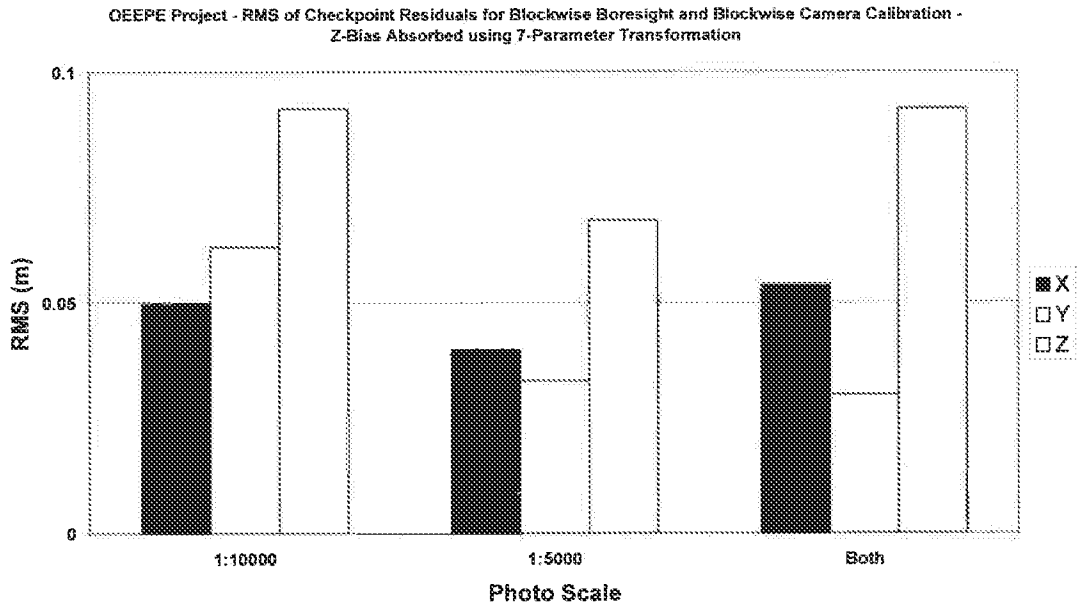


Figure 9 RMS of Checkpoint Residuals Using Different Block of images (The OEEPE Project)

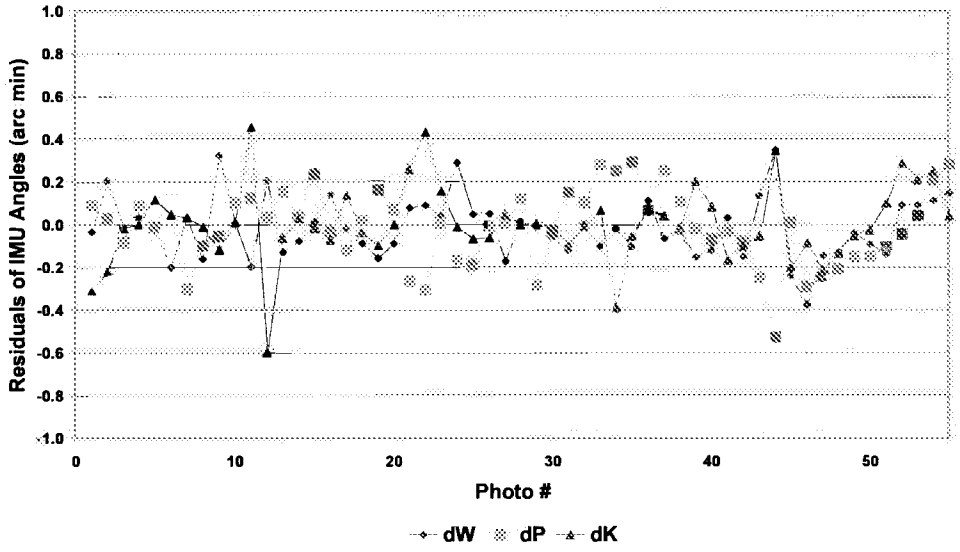


Figure 10 IMU Angular Residuals After the Simultaneous Least Squares Adjustment and Boresight Calibration

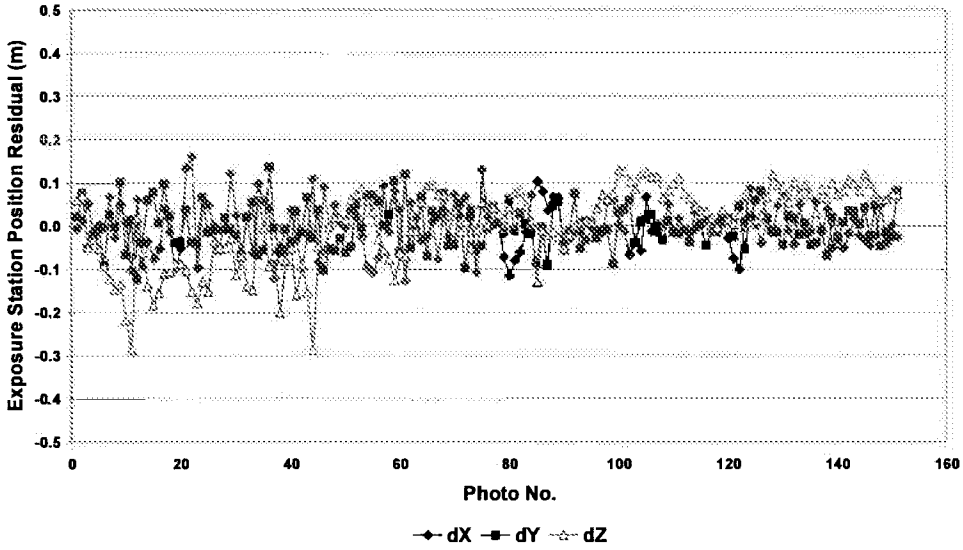


Figure 11 Exposure Station Residuals After the Simultaneous Least Squares Adjustment and Boresight Calibration

4.2 Evaluating Boresight Calibration Without Ground Control

The traditional way of boresight calibration is based on using ground control points in the aerotriangulation process. In POSCal™, however, the boresight calibration is done simultaneously with the aerotriangulation process; therefore, the quality of image coordinates and the accuracy of GPS-derived exposure station positions are the critical factors in the boresight calibration process. Figure 12 shows a comparison between the boresight angles determined using different methods by POSCal™ using the 1:10,000 photo scale flight of the OEEPE project. The reference boresight angles in this case are those determined simultaneously using both 1:10,000 and 1:5,000 photo scale flights and using all available ground control points.

The first entry in Figure 12 shows the differences between the boresight angles determined by the reference solution and those determined using only the 1:10,000 photo scale flight (labelled BS.) The second entry in Figure 12 (labelled BS/CB) shows the difference between the reference boresight angles and those determined using the 1:10,000 flight data to calibrate both the boresight and camera interior orientation parameters simultaneously. The third entry in Figure 12 (labelled BS/CS) shows the difference between the reference boresight angles and those determined using the 1:10,000 flight data to calibrate both the boresight and an individual set of camera interior orientation parameters for each strip simultaneously. The three solutions presented in Figure 12 were produced without ground control points. All ground control points were therefore used instead as checkpoints. Note that the differences are almost zero for the first method, which is a direct comparison between using or not using ground control points in the calibration process. The second and third entries showed a minimal deviation from zero, in the omega and phi components of the boresight, while the difference in kappa is almost zero. These slight deviations from zero can be attributed to the camera calibration influence in the second and third entries in Figure 12. In summary, there is no effect of the ground control points on boresight calibration accuracy using the approach implemented in POSCal™. However, it is always an advantage to use a minimal number of ground control points at the corner of the calibration field for quality control purposes.

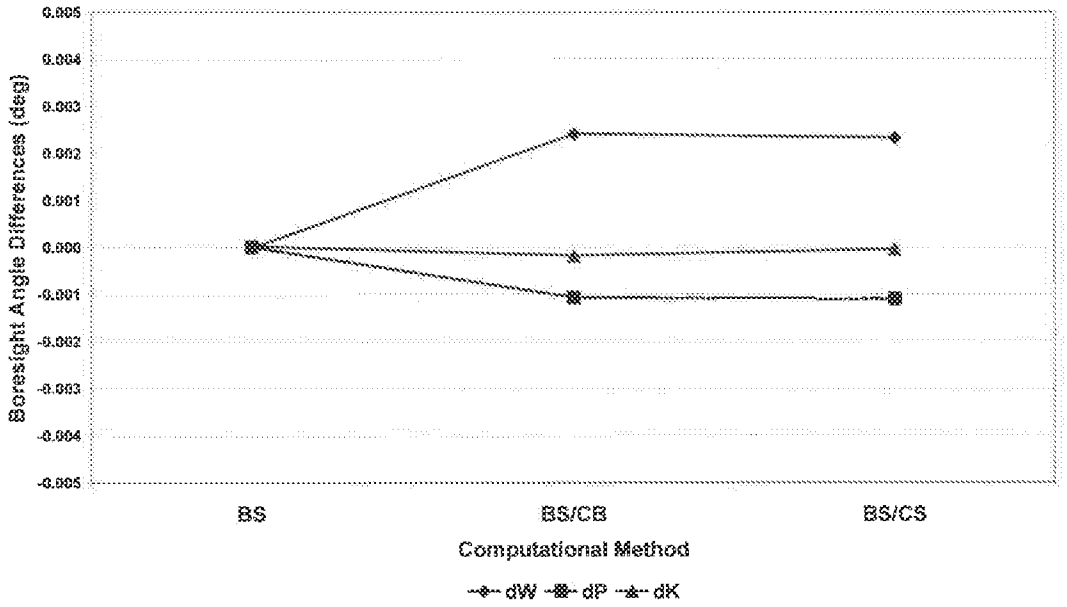


Figure 12 Boresight Angles Determined by Different Methods – The OEEPE Project – Photo Scale 1: 10,000

4.3 Effect of Number of Image Points per Photo

The number of tie points per image is not a limiting factor when digital workstations are used in the mensuration process, especially when using automated tie point matching. However, using analytical plotters to measure image coordinates of tie points, the more the number of tie points, the longer it takes to complete the measurement process. If the boresight angles are needed to be computed only for quality assurance purposes, it is essential to analyse the time required to collect the necessary image coordinates for boresight calibration, especially if an analytical plotter is used to measure image coordinates. Even when using a digital workstation and an automated tie point matching engine, the more tie points needed to be generated automatically, the longer it takes to collect them. In the following, a brief summary of a study conducted to analyse the effect of the number of tie/pass points per photo on boresight calibration accuracy. In this study, a reference boresight was computed using all available data from the OEEPE project by POSCAL™. Then, a set of boresight angles is determined once when the number of tie points is reduced to the Van Gruber points (6 points per stereo model or 9 points per single photo) and once more when the number of tie points is reduced to 4 points per photo. Note that the reference boresight angles are computed using all the available imagery, while the new boresight angles for each of the previously mentioned tie point configurations is determined using only a 2-strip block. In fact this test therefore shows the effect of both number of strip and number of image points per photo on the boresight calibration.

Figure 13 shows the typical number of tie points per photo as measured by Fotonor AS. Figure 14 shows the intentionally reduced number of tie points (9 points per photo or Von Gruber points). Figure 15 shows the configuration of 4 points per image. Note that 4 points per image is not enough number of pass or tie points for relative orientation. However, they are adequate for boresight calibration and the fastest to compute in a photogrammetric workstation. Figure 16 shows the accuracy of boresight using the 3 aforementioned configurations of tie points. The difference between the newly computed boresight angles and the reference boresight is shown to vary among the different components. The roll component for example does not exceed 0.001°, which equals about 4 arc seconds. This is well within the noise level of the IMU. The worst deviation is the kappa component of the boresight, which is at the level of 0.005°. Again this is well within the noise level of the POS AV system. Note that the differences between the different methods is less than 0.001°, which shows how the number of tie points is not a limiting factor for the boresight accuracy. On the other hand, the difference between the reference boresight and the computed boresight is due to using 2 strips instead of 4 in producing the new boresight values.

In summary, using only 2 strips of images will yield an accuracy of better than 0.002° in boresight roll and pitch components and 0.005° for boresight heading component, respectively. On the other hand, the effect of number of tie points per image is very minimal and does not exceed 0.001°. The latter conclusion is important from the quality control perspective.

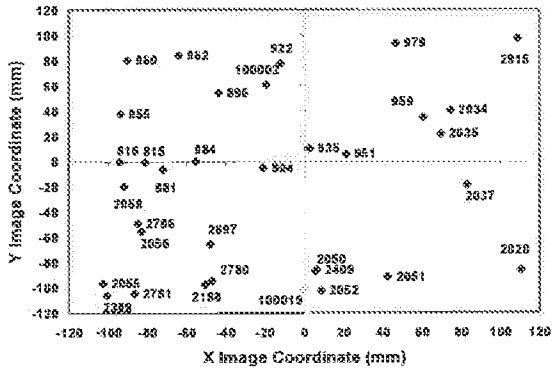


Figure 13. Original Tie Points

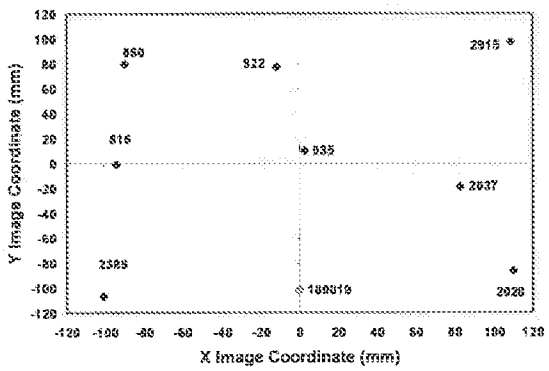


Figure 14. Van Gruber Points

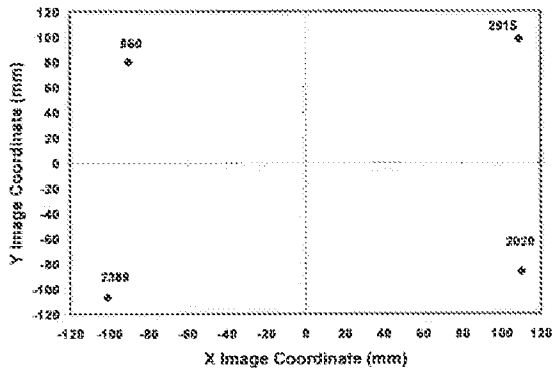


Figure 15. The Reduced 4 Tie Points per Photo

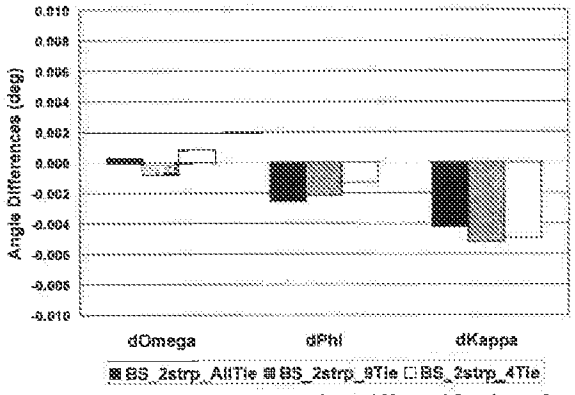


Figure 16. Boresight Accuracy Using Different Number of Tie Points per Photo

4.4 Effect of Number of Strips on Boresight Calibration Accuracy

The number of image strips is important to increase the observablity of the boresight. In addition, increasing the number of image strips results in increasing the volume of data, which helps in averaging other errors such as the IMU-derived heading. In some cases, there is a need to calibrate boresight using a minimum number of images from the actual mapping project for quality assurance purposes. In that case, one strip of photos is an attractive alternative to a well-conditioned block for boresight calibration. The disadvantage of using one strip of images is the observablity of the different components of the boresight. For example, when only a single strip is used in the calibration, the entire strip becomes very easy to roll.

Two strips of imagery therefore will increase the rigidity of the image block and eliminate this strip rolling effect. However, if there is only one strip to be used, one could think of using ground control points as an alternative to increasing the number of strips. Table 1 shows the differences between a reference boresight solution computed by POSCal using the HJW project and a number of boresight angles using one strip at a time in different configurations. As shown in Table 1, the first entry is for strip # 1 of the HJW project (strp_1) where the boresight values where computed once using no ground control points, once with all ground control points, and once using only two ground control points. The results depict that calibrating boresight using one strip with no ground control points yields significantly poorer accuracy in the boresight roll component. The pitch component of the boresight does not seem to be affected by the ground control points at all. The boresight heading component is similar to the boresight pitch component except that the heading component is close to 1.0 arc minute. This is twice poorer than the POSAV system accuracy. Moreover, there is no difference between using only 2 ground control points or using all of them as far as the boresight accuracy is concerned. As a partial conclusion, a single strip of photographs can be used to calibrate the boresight if two ground control points are used. This way, if there is a need to calibrate the boresight angles for quality assurance purposes, a single strip of images can be used together with two ground control points at the end of the strip, which can be surveyed after the mapping mission. The only disadvantage in this approach is the rather poorer boresight heading accuracy.

Table 1 Boresight Analysis Using Single Strip of Images (arc minute)

Strp_1	No_GCP	-12.8	0.6	1.1
	All_GCP	-0.1	0.2	0.9
	2GCP	-0.1	0.2	0.9
Strp_2	No_GCP	-25.9	-0.2	0.4
	All_GCP	0.0	-0.1	0.2
	2GCP	-0.1	-0.1	0.1
Strp_3	No_GCP	-8.9	0.3	-0.9
	All_GCP	0.1	0.2	-0.9
	2GCP	-0.3	0.2	-0.9
Strp_4	No_GCP	-15.8	-0.1	-0.2
	All_GCP	0.2	-0.2	-0.3
	2GCP	0.1	-0.1	-0.3

Using two strips of photos to calibrate boresight increases the observablity of different boresight components, especially if the two strips are flown in opposite directions. Therefore it is a viable approach to calibrate boresight using a 2-strip block without the need for ground control. For instance, Figure 17 shows the results of comparing the boresight calibrated using only two strips to a reference boresight solution, which is computed using the entire set of data of the HJW project. The first entry in the three plots of Figure 17 shows the result when comparing the boresight computed using strip # 1 and # 2 without GCPs to the reference boresight. The next entry depicts the results when comparing the boresight computed using strip # 1 and # 2 using GCPs to the reference boresight. The next two entries show the results of comparing the boresight computed using strip # 2 and # 3, respectively to the reference boresight, while the last two entries show the results of comparing the boresight computed using strip # 3 and #4 to the reference boresight. It is evident from these comparisons that calibrating the boresight using only two strips of images without ground control points is a viable approach. The resulting accuracy is well within the POS AV accuracy specifications in the roll and pitch components while marginal in the heading component.

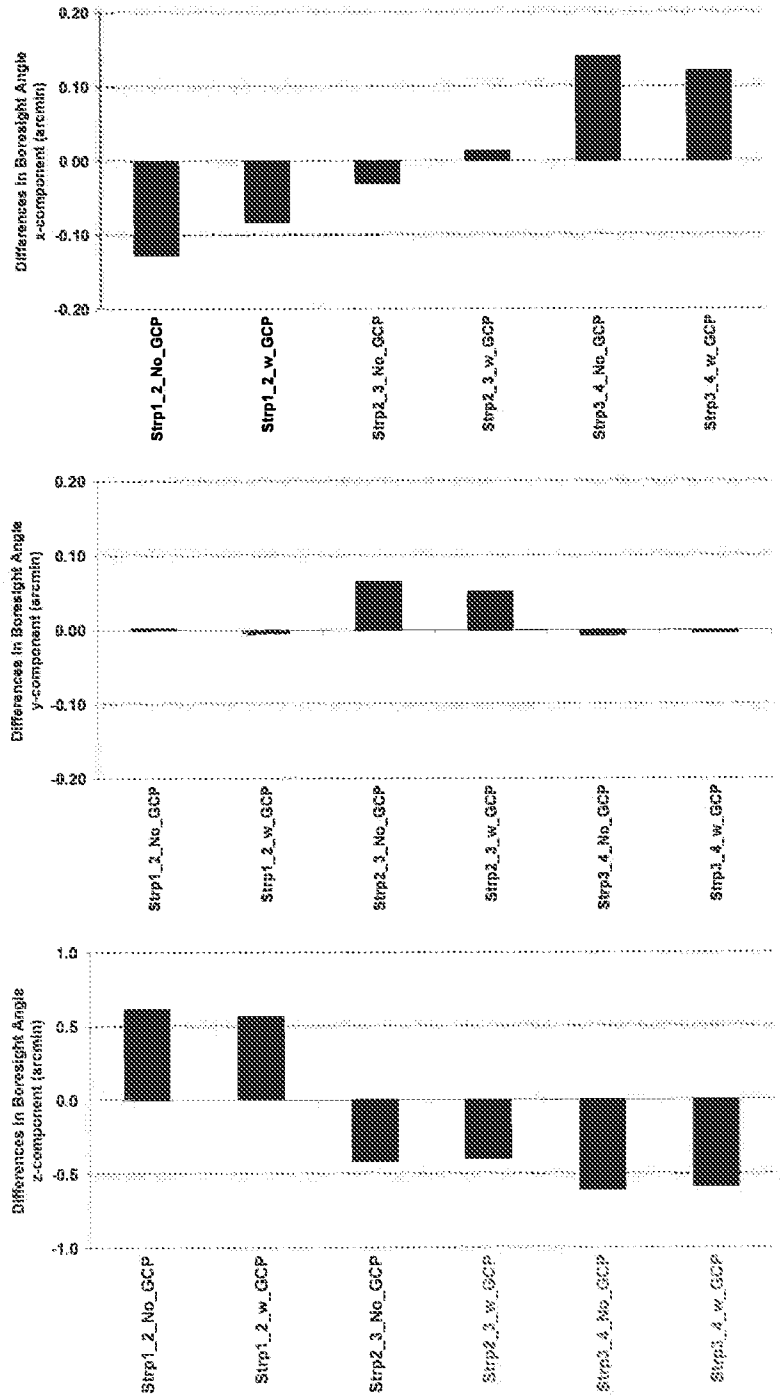


Figure 17 Boresight Angle Differences Using Different Flight Configurations in x-component (upper), y-component (middle) and z-component (lower), respectively - HJW Project

5. CONCLUSIONS

The POSCal™ software is introduced and the results from a number of studies are briefly presented. It is shown that using POSCal™, one can calibrate both boresight, and digital camera simultaneously using different imaging configurations without the need for ground control points. It is also shown that for quality control purposes, boresight can be checked using only the minimum number of tie/pass points in POSCal™. A number of analytical tools are provided in POSCalTM to help check the quality of the data, detect data blunders, and control the quality of the data.

ACKNOWLEDGEMENTS

The OEEPE Pilot Centre (University of Hannover), Fotonor AS and HJW GeoSpatial Inc. are gratefully acknowledged for providing the Applanix POS/AV 510 data and the photogrammetric data for the research presented here. Joe Hutton is thanked for his valuable discussions, assistance with data processing and for proofreading this manuscript. Alan Ip of Applanix Corporation is thanked for assisting with data processing in the OEEPE project.

REFERENCES

Beyer, H.A., 1992. Geometric and Radiometric Analysis of a CCD-Camera Based photogrammetric Close-Range System, *Ph.D. Thesis, Institut für Geodäsie und Photogrammetrie, ETH-Hönggerberg, CH-8093 Zürich, Mitteilungen Nr. 51.*

Cosandier, D. and M. A. Chapman, 1995. Precise Multispectral Airborne Pushbroom Image Georectification and DEM Generation, Proceedings of ISPRS/IAG/FIG Workshop on Integrated Sensors Orientation, Barcelona, September, 4 - 8, pp. 91-100.

Fraser, C.S., 1997. Digital Camera Self Calibration, ISPRS Journal of Photogrammetry & Remote Sensing, 52(1997): 149-159.

Heipke, C., Jacobsen, K, and Wegmann, H., 2001. OEEPE Test on Integrated Sensor Orientation - Status Report. CD-ROM Proceedings, ASPRS Annual Meeting, St. Louis, MO, USA, April 23 – 27.

Hutton, J., Savina, T., and Lithopoulos, L., 1997. Photogrammetric Applications of Applanix's Position and Orientation System (POS). ASPRS/MAPPS Softcopy Conference, Arlington, Virginia, July 27 - 30.

Lichti, D.D. and M. A. Chapman, 1997. Constrained FEM Self-Calibration, PE&RS, 63(9): 1111-1119.

Moffit, F. and E.M. Mikhail, 1980. Photogrammetry. Harper and Row, Inc, New York.

Mostafa, M.M.R., J. Hutton, and E. Lithopoulos, 2001. Direct Georeferencing of Frame Imagery - An Error Budget. Proceedings, The Third International Mobile Mapping Symposium, Cairo, Egypt, January 3-5.

Schwarz, K.P., M.A. Chapman, M.E. Cannon and P. Gong, 1993. An Integrated INS/GPS Approach to The Georeferencing of Remotely Sensed Data, PE&RS, 59(11): 1167-1674.

Scherzinger, B., 1997. A Position and Orientation Post-Processing Software Package for Inertial/GPS Integration (POSProc). Proceedings of the International Symposium on Kinematic Systems in Geodesy, Geomatics and Navigation (KIS 97), Banff, Canada, June 1997

Sensor Integration Aids Mapping at Ground Zero

Mary E. Hiatt, USA

Hours after the September 11, 2001, attack on the World Trade Center, the New York Office for Technology (NYSOFT) was tasked with gathering and managing the airborne data collection over Ground Zero. On September 14, they enlisted the help of EarthData, an airborne mapping and remote sensing company headquartered in Washington, D.C.

The EarthData team quickly determined that the combined use of three airborne imaging sensors – integrated with airborne GPS and inertial measurement systems — would provide the most detail to the recovery workers on the ground. The EarthData team therefore decided to use the three following sensors:

1. The lidar (LIght Detection and Ranging) system, which provides highly accurate 3-D maps of the site and allows measurement of the rubble and shifts in the surrounding buildings.
2. A high resolution digital camera to complement the lidar and enable rescue and recovery workers to monitor the movement using geometrically corrected digital images
3. A thermal camera to complement the lidar and enable rescue and recovery workers to monitor the temperatures of the fires burning below.

No ground control was used in any of the mapping missions. Sensor exterior orientation parameters were obtained using an Applanix POS/AV system, which uses integrated GPS/IMU technology. The NOAA/NGS Liberty Island Station was used as the GPS base station.

The aircraft, which at the time was southwest of Washington D.C., had to be outfitted for the project at EarthData Aviation's hangar in Hagerstown, Maryland. With airspace closed to all flights, special permission and coordination were a must. Concurrently, preparations were made to relocate a subset of EarthData's data processing team, complete with computers and all peripherals, to the NYSOFT offices in Albany, New York. By early afternoon on September 15, the EarthData team had established a capable data processing center in Albany.

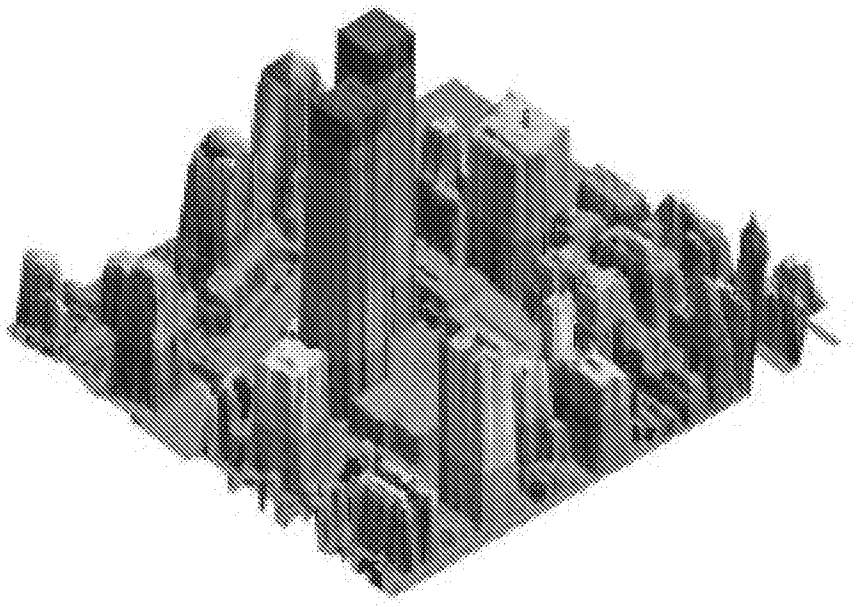
The Navajo Chieftain, with a two-man crew of a pilot and an airborne operations coordinator, flew from Hagerstown on the morning of the 15th to conduct the first flight over Ground Zero, collecting lidar and digital photography data. The plane landed in Albany in the early afternoon and the data was rushed to the processing center where several mapping products were generated for the rescue and recovery teams. The lidar provided a Digital Elevation Model (DEM) that gave a three-dimensional perspective of the scene. Elevations were determined from the DEM to within six inches accuracy. Simultaneously, the digital images were merged together to provide one large, high-resolution, geometrically correct image over the disaster site. Because no ground control was available for the mapping missions, EarthData used existing vector data to verify mapping accuracy. Based on this method, an estimated accuracy of six inches vertically and better than 12 inches horizontally was achieved.

The final map products were transferred to NYSOFT within eight to 12 hours after landing. At sunrise on September 16, the Navajo Chieftain was again flown over Ground Zero to collect thermal imagery. The data was immediately processed in Albany, and delivered to NYSOFT. The New York State police escorted the images to New York City's Pier 92 where the Emergency Mapping and Data Analysis Center had been set up.

After the two initial data collections were complete, EarthData established a routine that involved thermal data collection in the morning, with lidar and digital imagery collected midday. A total of 43 missions were flown between September 15 and October 22, 2001.

At Pier 92, EarthData's continually updated products were imported into New York City's Geographic Information System (GIS), which contains the NYCMAP (pronounced "nice map"), a digital database of highly detailed geographic information of the entire city accurate to within 18 inches. The NYCMAP was created over a period of five years by the New York City Department of Information, Technology and Telecommunications; the Department of Environmental Protection; and Hunter College's Center for the Analysis of Spatial Information (CARSI). The database contains information on New York City's buildings, curb lines, streets, parks, and transportation features. After September 11th, more than 50 GIS professionals from government, academia, and industry worked around the clock with the database

continued on page 879



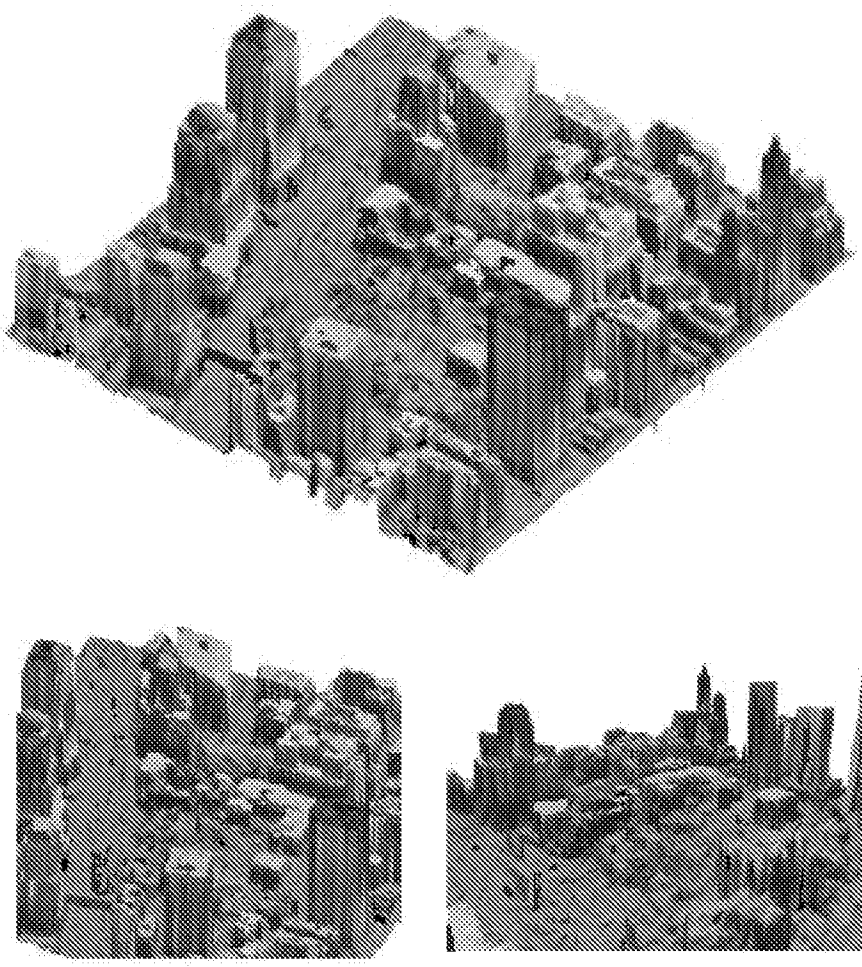
3-dimensional lidar data captured over World Trade Center site during July of 2001.

continued from page 877

to generate the maps and analysis needed by many departments of New York City. With the historic data in the database, as well as up-to-the-minute mapping data provided by EarthData, this team played a vital effort at Ground Zero.

Since October 22nd, EarthData has flown over a dozen additional missions for NYSOFT as well as the Federal Emergency Management Agency, and the Environmental Protection Agency aimed at assessing conditions that would impact the re-opening of homes, schools, and businesses in and around Ground Zero.

For more information on EarthData's role at the World Trade Center or EarthData's services, please contact Mary Hiatt at 301-948-8550 or visit our website at www.earthdata.com.



3-dimensional lidar data captured over World Trade Center site after September 11, 2001.

Mary E. Hiatt, Senior Vice President, Corporate Marketing, EarthData Holdings, Inc.

Edited By Mohamed M.R. Mostafa, Applanix Corporation

Precision Aircraft GPS Positioning Using CORS

By Mohamed M.R. Mostafa

One of the limitations of using integrated inertial/GPS systems to Directly Georeference airborne sensor data is the necessity of using a GPS base station or stations in order to obtain the positional accuracy required to meet the accuracy standards of certain mapping products. In some precise large-scale aerial survey applications having to place a number of GPS base stations in a remote or inaccessible location becomes quite problematic. The aerial survey industry has been using airborne GPS as a standard procedure to assist map production for the past decade. More recently, GPS-aided inertial systems such as Applanix POS AV have been successfully used to provide the full resolution of trajectory parameters, namely position, velocity, and attitude. This way, the entire set of translational, and rotational parameters of any airborne acquired image or laser scan line can be measured with respect to some mapping frame. Data acquisition procedure plays a role in the success of this method. Separation between the airborne and base station GPS receivers, satellite geometry as reflected by the Position Dilution of Precision (PDOP), signal multipath and many other parameters must be considered in order to achieve the maximum possible GPS positioning accuracy (see Table 1 for details on residual DGPS errors). Many times it is difficult or not practical to optimize these parameters. For example, since the sun angle required for aerial photography and the PDOP required for strong geometric positioning by GPS do not necessarily occur at the same time, aerial flight missions sometime inadvertently compromise the GPS PDOP in order to get a good sun angle.

Table 1. DGPS Residual Errors

Error	Error Characteristics
Orbital	• Correlated between satellites • Significantly reduced by between-satellite differencing (DGPS) • Using precise orbits and satellite clock corrections improves positioning accuracy for long baselines
Ionospheric	• Frequency-dependent, thus, dual frequency data eliminates the error for long baselines. • Broadcast model reduces the error by 50% • In double difference airborne kinematic case error is typically 1-2 PPM for mid-latitudes between sunspot highs
Tropospheric	• Frequency-independent, thus, cannot be removed by dual-frequency data • Dry component can be modeled and removed • Wet component needs meteorological data and more difficult to model because of the variable nature of water vapor • Over long baselines the wet component effect on positioning can be estimated for airborne applications
Multipath	• Site-dependent and, thus, cannot be removed using differential GPS • In kinematic applications, the multipath signature has a strong correlation with vehicle speed • Therefore, multipath gets random (and less) for higher speed

Hence for high accuracy mapping applications where the highest GPS positioning accuracy is required, careful mission planning is therefore mandatory. A usual outcome of this is the requirement for a series of GPS base stations to be deployed in order to support the project. In inaccessible regions this can be very difficult. In other applications such as corridor surveying where the accessibility is usually quite good and the positional accuracy is often relaxed, a major problem is the cost of laying out base stations at regular intervals along the corridor, which can often be thousands of kilometers in length. On some other occasions, (as often is the case in a real production environment), the GPS base station data may simply be lost due to equipment problems or human error.

Therefore, the focus of this article is on the accuracy that can be obtained using the NGS CORS stations as base stations for airborne GPS positioning, and the possibility of using these stations to supplement, back up, or even replace the base stations usually deployed for a given project.

The USA Continuously Operating Reference Stations (CORS) is run by The National Geodetic Survey (NGS). CORS comprises a network of 253 sites (as of January 2002), containing geodetic quality GPS receivers. This network is currently growing at a rate of about 4 –10 sites per month. The NGS collects, processes, and distributes data from these sites in support of high-accuracy 3D positioning activities throughout the United States and its territories. For details about CORS, see www.ngs.noaa.gov. Figure 1 shows a map of the CORS stations in The USA.

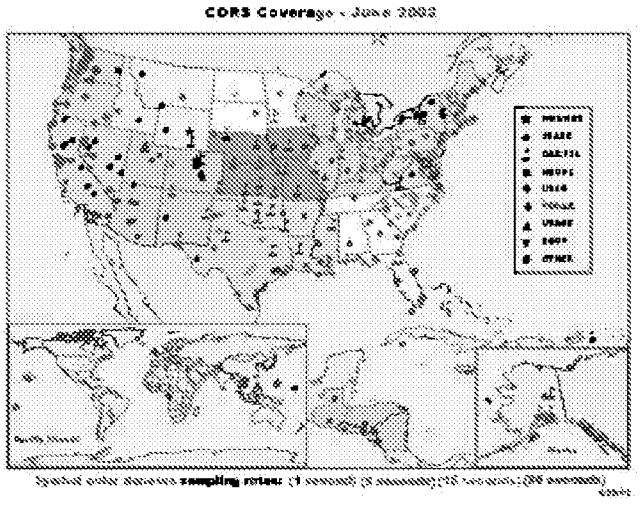


Figure 1. CORS in The USA

Accuracy Analysis

Two mapping projects have been recently used to assess the quality, reliability, repeatability, and feasibility of using the CORS in airborne mapping missions. These are called here the Aeromap Project and the HJW Project. In both projects the CORS stations in the proximity of the mapping area together with the airborne GPS data were

continued on page 1126

continued from page 1125

used to analyze the accuracy achieved when using the multiple-base approach implemented in POSGPS, which incorporates the data from any available base station in the processing of the airborne GPS data. The separation between different CORS stations and the mapping area varied between 30 and 400 Km. The achievable accuracy in both projects is summarized in Table 2.

Table 2. Camera Exposure Station Position Accuracy Using CORS data (The Multiple-base Station Approach).

Position Component	Aeromap Project		HJW Project	
Statistics	Maximum (m)	RMS (m)	Maximum (m)	RMS (m)
Easting	0.16	0.05	0.14	0.07
Northing	0.21	0.05	0.12	0.05
Height	0.46	0.22	0.21	0.08
3D	0.53	0.23	0.28	0.12

Summary and Outlook

Briefly, in this article, the results and analysis from real mapping projects were presented to show the great potential of using the CORS for airborne GPS positioning in the United States. Other CORS networks are already established in different countries. Ongoing experiments with the foreign CORS networks will be presented in the direct georeferencing column. In addition, other methods of airborne GPS positioning will be presented in the direct georeferencing column.

Acknowledgments

Dr. Richard Snay of the United States NGS CORS program is gratefully acknowledged for his valuable discussions. Thanks to A. Bruton of Intermap Technologies and J. Hutton and E. Roy of Applanix Corporation for helping with data processing and analysis. HJW GeoSpatial Inc. and Aeromap US are gratefully acknowledged for providing the POS AV 510 data and the photogrammetric data for the research presented here.

Further Reading

Bruton, A.M., Mostafa, M.M.R., and Scherzinger, B.M., 2001. Airborne DGPS Without Dedicated Base Stations for Mapping Applications. Proceedings of ION-GPS 2001, Salt Lake City, Utah, USA, Sept 11-14.

Lachapelle, G., E.M. Cannon, W Qiu, and C. Varner, 1995. An Analysis of Differential and Absolute GPS aircraft Positioning. ION NTM, Anaheim, CA, January 18-22

Mostafa, M.M.R., J. Hutton, 2001. Direct Positioning and Orientation Systems: How Do They Work? What is The Attainable Accuracy? Proceedings, The American Society of Photogrammetry and Remote Sensing Annual Meeting, St. Louis, MO, USA, April 23 – 27.

Snay, R.A., 2000. The National and Cooperative CORS Systems in 2000 and Beyond, Proceedings of ION GPS 2000, 19-22 September 2000, Salt Lake City, UT, pp. 55-58.

Dr. Mohamed M.R. Mostafa, Chief Technical Authority - Airborne Systems Applanix Corporation

SYSTEM PERFORMANCE ANALYSIS OF INS/DGPS INTEGRATED SYSTEM FOR MOBILE MAPPING SYSTEM (MMS)

A. W. L. Ip [a], N. El-Sheimy [a], M. M. R. Mostafa [b]
[a]Mobile Multi-Sensor Research Group
Department of Geomatics Engineering, University of Calgary,
2500 University Drive NW, Calgary, Alberta, T2N 1N4 Canada
awlip@ucalgary.ca, naser@geomatics.ucalgary.ca
[b] Applanix Corporation, 85 Leek Crest, Richmond Hill, Ontario, L4B 3B3, Canada – mmostafa@applanix.com

Commission VI, WG VI/4

KEY WORDS: Aerial Mapping, Aerotriangulation, GPS, INS, Direct Georeferencing, Boresight Calibration

ABSTRACT:

Major progress has been made in Mobile Mapping Systems (MMS) over the last few years in terms of sensor resolution, size, data rate, power requirements, and cost, besides the advances in sensor integration and data post-processing and filtering techniques. Thus, the use of such systems in different mapping applications has become cost-effective, and an enabling technology in some applications. This paper examines several topics that are critical for properly operating a mobile mapping system for different platforms and for different applications. Sensor placement, sensor synchronization, system calibration and the sensors' initial alignment are discussed in some detail. Features common to most systems will be identified and a unified model for MMS integration for airborne and land mapping application is presented where the suitable observables are assessed, and factors affecting system performance are discussed. An example from a commercial airborne MMS will be presented in some results.

1. INTRODUCTION

The parameters of exterior orientation, three translations and three rotations, essentially describe rigid-body motion in space. If a system that measures rigid-body motion can be installed on a vehicle, then the translations and rotations of the vehicle can be directly determined as time varying vectors. The process of determining these values by independent sensors is often called geo-referencing. Today, georeferencing is most easily accomplished by integrating the measurements of an inertial measuring unit (IMU) with those of GPS receivers used in differential mode (DGPS). The IMU/DGPS integration gives translation and orientation parameters for the vehicle as solutions of a system of differential equations, i.e. as functions of time.

Mobile mapping systems (MMS) consist of two major components, an imaging component and a geo-referencing component. The imaging component may be an optical or digital camera, a multi-spectral pushbroom scanner, an interferometric radar system, or a scanning laser system. If digital cameras are used as the imaging component and are fixed to the same rigid body as the IMU and the GPS antenna (i.e. to the aircraft), then the parameters of exterior orientation can simply be determined by interpolating the translation and rotation vectors at the moment of exposure. These parameters can be stamped on each digital image. In this way, the complex time-dependent positioning problem is transformed into a spatial problem from which time has been eliminated as a variable. This obviously requires very accurate time synchronization between the different sensors. The resulting geo-referenced digital images obtained in this way become the building blocks for the digital mapping program. It should be noted that a multi-sensor system defined in this way is completely self-sufficient, i.e. only data collected in the vehicle are needed to solve the georeferencing problem. It is independent of ground control because GPS, by linking into a system of Earth- orbiting satellites, will output all its results in an Earth-fixed, Earth-centered coordinate frame – the WGS 84, see Figure 1 for an example of the concept of airborne-bases MMS. MMS thus provides an integrated problem solution, rapid data acquisition, fully digital data storage, and great flexibility in post-mission data processing. Some important parameters play a role in that case such as sensor placement, sensor synchronization, system calibration, and initial alignment, which will be discussed in some details in the next few sections.

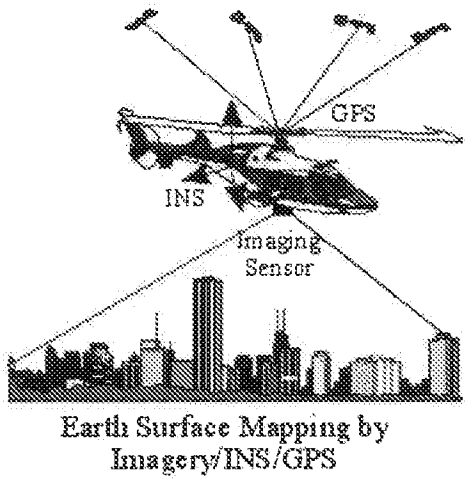


Figure 1. An Airborne MMS

2. DIRECT GEOREFERENCING USING INS/GPS INTEGRATION

The main components of a direct georeferencing system for mobile mapping use different technologies. GPS uses range measurements from satellites and INS uses gyros and accelerometers to measure angular velocity and specific force. Table 1 lists the characteristics of a stand-alone GPS, a stand-alone INS and an integrated GPS/INS.

Table 1. General difference between GPS and INS

	Advantage	Disadvantages
INS	• Self contained and independent system • Continuous data acquisition • Three positioning and three attitude components • High data sampling rate (up to 256 Hz)	• Sensor errors grow with time causing positioning error divergence
DGPS	• High accuracy of position and velocity estimation • Time-independent error model	• Losses of lock causing gaps in positioning • Low data sampling rate (1-10 Hz) • Slow ambiguity resolution time over long baseline and/or in presence of higher ambient noise
INS / DGPS	• Combine all advantages of both systems • Redundant and complementary data (both systems' errors are separately observable) • Navigation through GPS outages • GPS fixes allow INS error estimation	• No significant limitations • Precise time synchronization needed

As depicted in Table 1, the low noise and high bias INS and the higher noise and low bias GPS are complementary systems. Their integration, therefore, reduces or eliminates their limitations.

2.1 The Unified Georeferencing Model

Direct georeferencing mathematical model has been used for numerous applications in land, airborne and marine applications (c.f., Schwarz, el al, 1993, El-Sheimy, 1996a, Mostafa, 2003). Several forms of the mathematical model have been previously presented to accommodate a certain application. In this Section, the basic unified formula is re-visited. As shown in Figure 2, the georeferencing basic model can be expressed by:

$$r_p^m = r_{INS}^m(t) + R_b^m(t)(sR_c^b r^c - a_1^b) \qquad (1)$$

where, $r_{INS}^m(t) = r_{GPS}^m(t) - R_b^m(t)a_2^b$ (2)

therefore $r_p^m = r_{GPS}^m(t) + R_b^m(t)(sR_c^b r^c - a_1^b - a_2^b)$ (3)

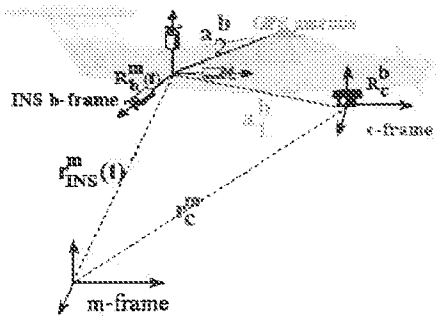


Figure 2 The Direct Georeferencing Model

The different terms in Equations 1, 2, and 3 are explained in Table 2.

Table 2. Terms of georeferencing equation

Variable	Description
r_p^m	Position of the point of interest represented in mapping frame
$r_{GPS}^m(t)$	GPS antenna position represented in mapping frame
$R_b^m(t)$	Rotation matrix between INS body frame and mapping frame
s	Scale factor between camera image space and object space
R_c^b	Rotation matrix between camera frame and body frame
r_c	Location of the point of interest represented in camera frame
a_1^b	Lever arm offset between INS body frame and camera frame
a_2^b	Lever arm offset between INS body frame and GPS antenna

For a MMS system, a number of parameters play a role when the system performance, accuracy, and reliability are concerned. These parameters can be summarized as:

1. Sensor placement – It is imperative that relative sensor placement in the carrier platform be taken into account. This includes the different sensor position and orientation offsets as previously presented in Table 2 by the lever arms and the rotation matrix between the camera frame and the INS body frame
2. Synchronization – the synchronization is the process by which the different sensors in a MMS are relatively brought to one unique time frame.
3. Calibration – the calibration is the process by which the relative positions and orientation of each sensor with respect to a reference frame is established. Once calibration is done, all different streams of sensor data can be properly fused.
4. Initial alignment – all sensor generates errors, it must be minimized before mapping mission starts.

Next, the aforementioned issues will be discussed in some detail.

2.2 Sensor Placement

For a mobile mapping system used in land or airborne, GPS, IMU, and an imaging sensor tend to be the common sensors to be used efficiently. In some other instances, such as in a land-based application, some dead reckoning systems might be integrated with the three main sensors to help improve the overall performance in case of GPS signal blockage in urban canyons. However, this paper will only focus on the integration of the first three sensors. The inter-relationship between these primary sensors is defined by lever arms and mis-alignment angles; these calibration terms are discussed in the following:

Imaging Sensor Installation

This sensor usually has a fixed location because it normally is located where the scene of interest is visible for image acquisition. Therefore, imaging sensor is placed on the front roof of the vehicle in land applications, and is placed at the bottom of the aerial photography aircraft in airborne applications.

GPS Antenna Installation

The GPS antenna has to be always visible to all satellite antennas for proper GPS signal reception at all times. Therefore, the GPS antenna is placed outside of the platform for proper signal reception. In land applications, it can be placed anywhere on the rooftop of the vehicle. But for calibration efficiency, it is usually mounted as closely as possible to the imaging sensor. In airborne applications, the same concept applies. It is preferable to even mount the GPS antenna directly above the centre of the imaging sensor lens. In addition, the aircraft wings are also taken into consideration, in order to prevent GPS blockage during large banking angles. Practically, pilots will have to take wider turns to minimize banking angles. Thus, the location of the GPS antenna is more flexible and can be located as closely as possible to the INS sensor.

IMU Installation

An IMU is a self contained instrument and does not have a specific installation requirement except for rigidly mounting it to the imaging sensor. Rigid mounting the IMU is a key factor in all mobile mapping systems because of the assumption made in the georeferencing formulae which is the constant rotation matrix between the IMU body frame and the camera frame. It, therefore, established a critical calibration parameter called boresight (the angular misalignment between the IMU and camera frames). Boresight calibration is done at system installation and periodically as a quality control of the entire mobile mapping system, for details on boresight calibration see Mostafa, 2001 for airborne applications and El-Sheimy, 1996b. Figure 3 shows an airborne example of IMU mount on the camera head in the Applanix DSS, while Figure 4 shows the entire system installation onboard an aircraft. A number of other airborne digital systems has been designed to rigidly install the IMU directly on the camera head such as the Leica ADS40 and the Z/I Imaging DMC cameras. In land-based applications, multiple imaging sensors are normally used for coverage purposes. Therefore, the INS is rigidly mounted on a platform that holds all imaging sensors together, to allow for constant boresight matrix at all times. Figures 5 and 6 shows sensor installation onboard The VISAT of The University of Calgary.

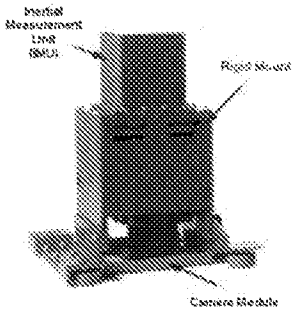


Figure 3. Rigid Mount for Camera/IMU of the DSS

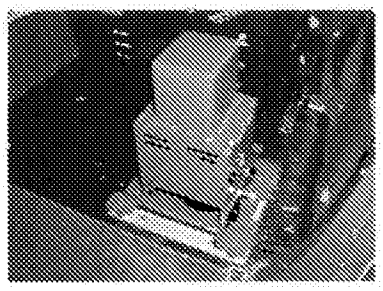


Figure 4. DSS Aircraft Installation



Figure 5. VISAT of The University of Calgary

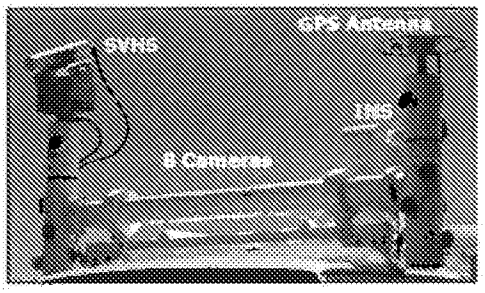


Figure 6. Sensor Installation onboard of the VISAT

2.3 Synchronization

For high accuracy position and orientation determination by MMS, precise synchronization is very important. The three

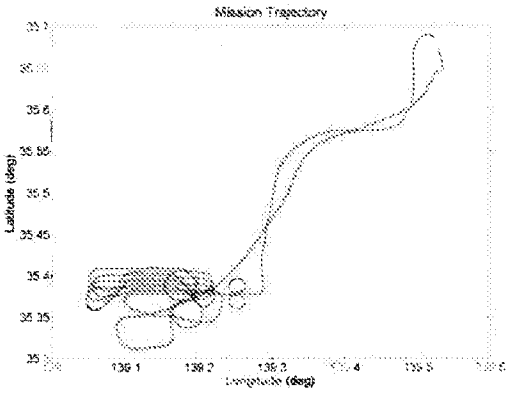
sensors: GPS, INS and imaging sensor operate at their own time frame. In addition, data logging is typically done using computer components that have their own frequency oscillators. The synchronization of all different components is an essential assumption in the direct georeferencing case. In principle, GPS provides the best time reference with GPS time. INS comes with an integrated timing module, but is rarely directly synchronized with GPS On the other hand, imaging sensors do not come with any timing module, and the acquisition of imagery does not occur at a fixed time interval. Resolving this timing problem, newer imaging sensors provide a linkage to the GPS receiver, in order to time-tag the imagery exposure time.

Whether it is real-time or post-processing integration, interpolation will be used to synchronize all the measurements from the different sensors. Since all measurements are collected by the controlling computer system with physical connections, data transmission delays must be considered. Such delays can result from cable length, computer clock error or A/D conversion. For precise system design, these delays can be determined easily and calibrated from synchronization.

Synchronization error (δt) introduces both position and attitude error. Position error is a function of velocity and attitude error is a function of angular velocity. Therefore, synchronization error is directly proportional to application dynamics. The combined error presented in direct georeferencing can be formulated by modifying Equation 3 to replace the GPS antenna position with a platform velocity v(t) and to replace the rotation matrix between INS body and mapping frames with an angular velocity vector w(t). This results in:

$$\delta r_p^m = \delta t[v(t) + w(t)(sR_c^b r^c - a_1^b - a_2^b) \qquad (4)$$

For demonstration purposes, a simulation has been done using a DSS flight with an average speed of 180 km/h. Figure 7 presents the flight trajectory and the dynamics of the aircraft during image acquisition on two flight lines over a span of 15 minutes. A 1 millisecond of synchronization error has been introduced. The corresponding position and attitude errors are shown in Figure 8 and the statistic report is listed in Table 3.



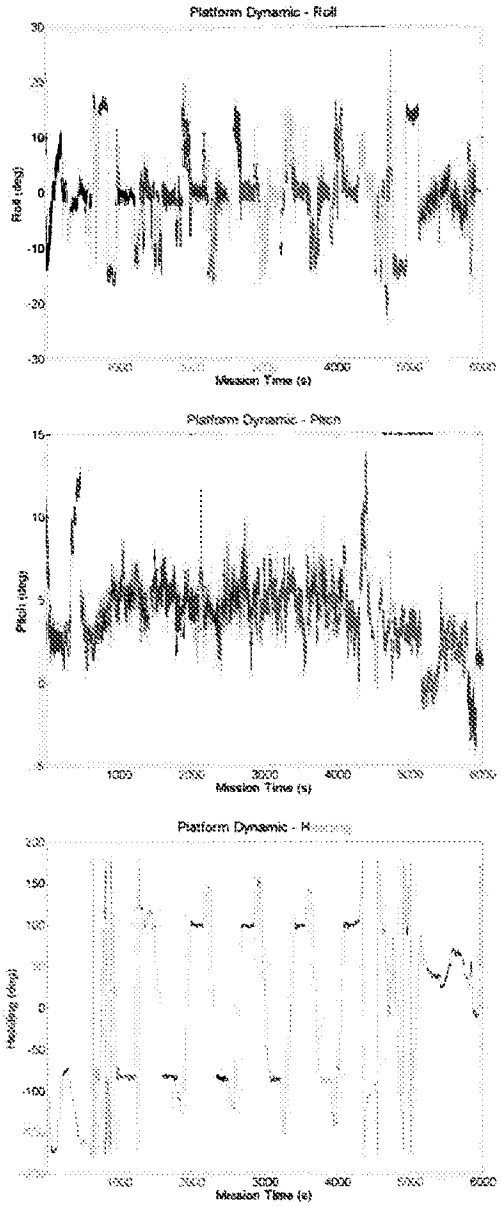
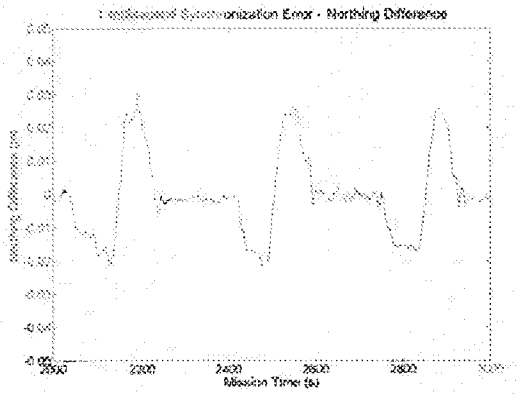
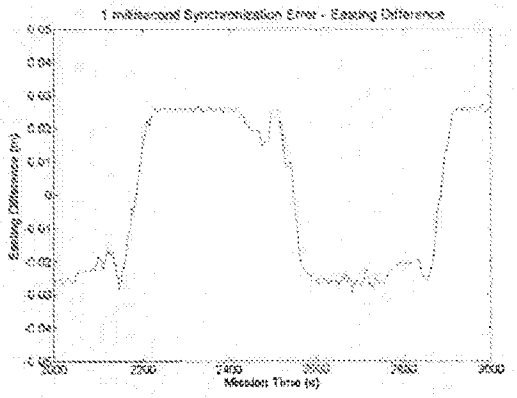
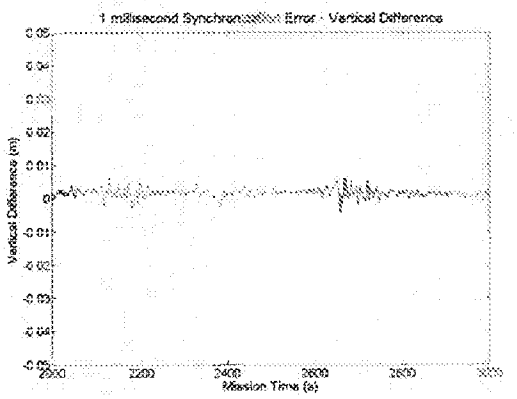
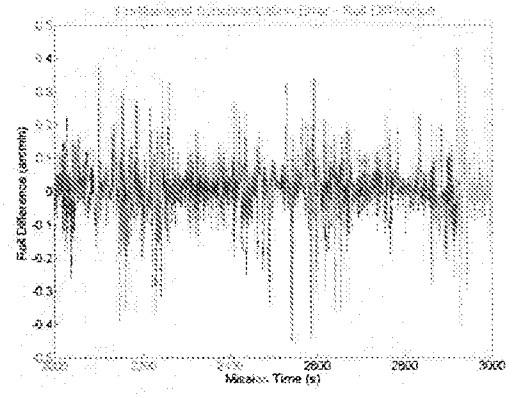


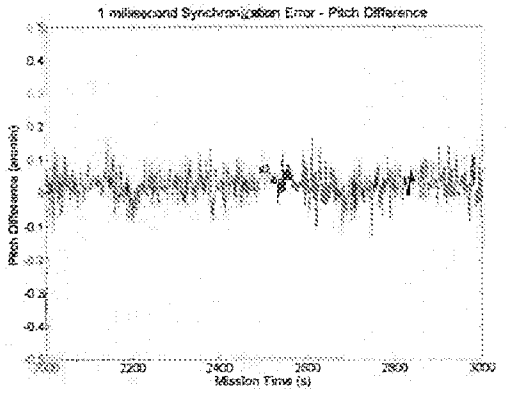
Figure 7. DSS Flight Trajectory and dynamics during image acquisition











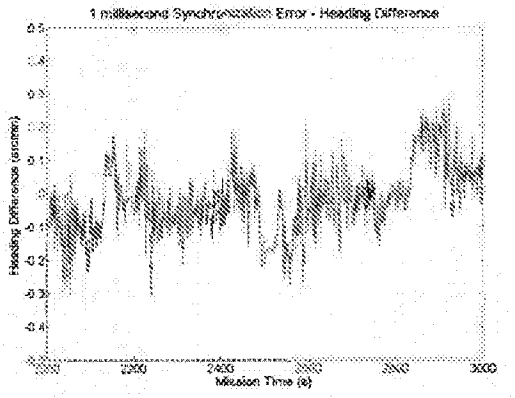


Figure 8. Navigation error due to 1 ms synchronization error

Table 3. Statistics of Synchronization Error Influence on Navigation Position and Attitude in Post-Processing, 1 millisecond simulation

Navigation error	Min	Max	Mean	RMS
Northing (m)	-0.021	0.031	0.000	0.012
Easting (m)	-0.030	0.027	0.000	0.023
Vertical (m)	-0.004	0.007	0.002	0.002
Roll (amin)	-0.840	0.700	0.000	0.140
Pitch (amin)	-0.280	0.320	0.020	0.060
Heading (amin)	-0.390	0.340	-0.020	0.110

Notice that Table 3 reflects the absolute value of the simulation results. Although the original data was available at 200Hz data rate, Figure 8 was plotted using a 1Hz data rate.. This down-sampling method has been applied to all figures in this paper.

1 millisecond is chosen to be used in the simulation because it is a small quantity when compared to a typical 1 MHz of the data logging computer. This value is far less than the actual IMU data rate reported (typically 200Hz). Although the statistics shown in Figure 8 and Table 3 are insignificant, these only reflect a simulation where synchronization error is small in the system. Due to the nature of electronic systems, some CCDs require up to several seconds for a single image acquisition; in this case synchronization error is relatively large. In addition, these errors will be projected to the ground which is directly related to system dynamic and project scale. Therefore synchronization error is very important especially in large scale project and missions with high dynamics. For example, in

Applanix DSS, there is a known delay (through calibration) in the CCD chip of about 2 milliseconds. When this delay is inserted in Equation 4 with the same simulation data, a 2 millisecond synchronization error should introduce twice of the error as in the 1 millisecond simulation. The result of the 2 milliseconds simulation is presented in Table 4.

Table 4. Statistics of Synchronization Error Influence on Navigation Position and Attitude in Post-Processing, 2 milliseconds simulation

Navigation error	Min	Max	Mean	RMS
Northing (m)	-0.043	0.058	0.000	0.025
Easting (m)	-0.060	0.056	0.000	0.047
Vertical (m)	-0.006	0.012	0.004	0.004
Roll (amin)	-1.690	1.400	0.000	0.280
Pitch (amin)	-0.510	0.610	0.050	0.120
Heading (amin)	-0.740	0.630	0.000	0.200

From Table 4, expected results are achieved with twice of navigation error experienced under 2 milliseconds synchronization error. As notice from both Table 3 and 4, mean values in navigation error is close to zero. This is a result of opposite flight lines where the errors are cancelled by each other. This proves that synchronization error is flight direction related and it helps to capture synchronization error in flight environment. In existence of synchronization error, change of sign will appear in difference of navigation solution on each opposite flight lines. However, when project is flown in the same direction on each flight line, synchronization can not be captured directly as it is correlated with datum shift. Therefore, calibration of synchronization error is usually carried in lab environments where static mode can be achieved. Using accurate timing equipments, synchronization error can be captured in static mode without influence from system dynamics.

2.4 System Calibration

A mobile mapping multi-sensor system calibration is critical for a successful image georeferencing. Overall system calibration is kept in mind when choosing the system installation. Equation 3 shows that there are several parameters which must be determined through calibration. There are a total of three calibration parameters, namely: Lever arm offset, Boresight misalignment, and Camera calibration. In the following subsections, these items are discussed in some detail.

2.4.1 Lever Arm Calibration:

The Lever arm describes the spatial vector difference between two coordinate frame origins of two sensors. For the case at hand, three lever arms exist between the GPS, IMU and the imaging system. However, the direct georeferencing equation deals with sensor positions and attitude angles projected from the INS body frame onto the mapping frame. Therefore, it comes down to calibrating the lever arm between the GPS antenna the IMU centre and the lever arm between the imaging system coordinate frame origin and the IMU centre.

Lever arm calibration is done using either of the following approaches:

1. Measuring the lever arms using land-survey techniques. The ease and simplicity of such an approach makes it a common process in airborne and land applications. In the airborne case, however, it's preferred to mount the GPS antenna directly above the lens centre of the imaging sensor in use.
2. Indirectly computing the lever arms using photogrammetric bundle adjustment. This way, the lever arms are modelled as unknown parameters. It, however, increases the complexity of the bundle adjustment algorithm and might introduce correlation with the GPS-derived antenna position. Therefore, such an approach is not entirely favourable from the photogrammetric stand point.
3. Indirectly computing the lever arms using the GPS and IMU measurements during data collection. Kalman filter is used for that purpose in either real-time or more accurately in post-mission. Figure 9 shows the lever arm between GPS antenna and INS, which is shown to be settled to a constant value after about 15 minutes of data collection. In this experiment, initial lever arm values for all axes are set to zero to illustrate the efficiency of Kalman Filtering. Since the resolved value of lever arm in z axis is quite away from initial value, it takes more time to converge. In actual application, initial values of lever arms are roughly determined (by tape measurements) and provided to data post-processing softcopy. Note that this method is only valid for the estimation of the lever arm between the GPS antenna and the IMU center. The lever arm between the imaging sensor and the IMU center or GPS antenna cannot be computed. In land application, this is not a problem since it can be determined using a total station. In aerial application, where the IMU is normally installed closely to the imaging sensor, the lever arm is typically measured and provided by the manufacturer.

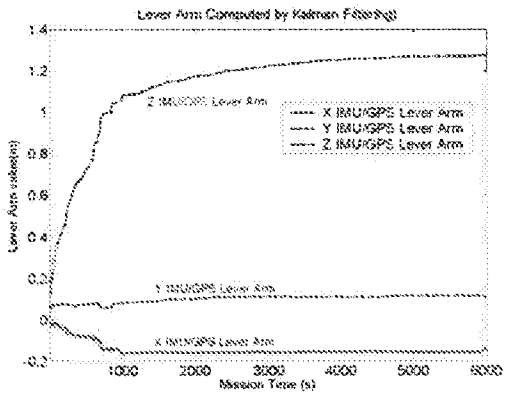


Figure 9. Lever Arm Computed by Kalman Filtering

Although a lever arm between different sensor components in a mobile mapping system is constant vector. Therefore, by intuition, any error in lever arm causes a constant bias of the image position. However, such a constant bias is projected onto the mapping frame by the time dependent rotation matrix between INS body and mapping frames, $R^m_b(t)$. Therefore, the lever arm error is also time dependent with respect to the mapping frame. It is, therefore, affected by the dynamics of the MMS platform. The lever arm error can be expressed by:

$$\delta r^m_p = R^m_b(t)(\delta a^b_1 - \delta a^b_2) \quad (5)$$

For demonstration purposes, a simulation has been done using the same DSS flight shown in Figure 7. An error of 10 cm is introduced to the x-axis lever arm (which points in the flight direction). The resulting imaging sensor position error is shown in Figure 10 and the statistic report is presented in Table 5.

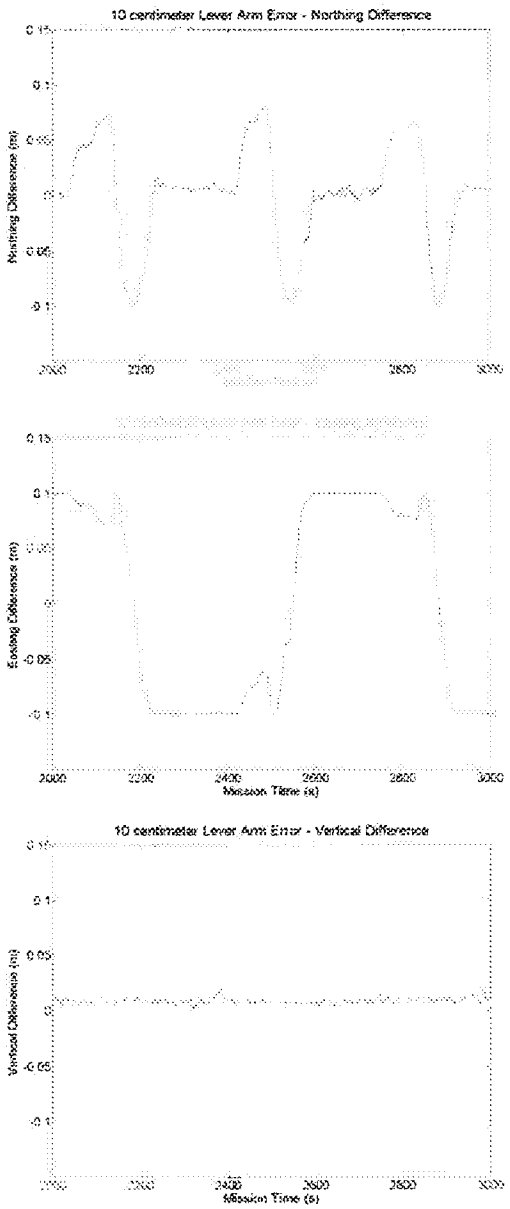


Figure 10. Position error due to 10 centimeter Lever Arm Error in flight direction

Table 5. Statistics of Lever Arm Error Influence on Navigation Position in Post-Processing, 10 centimeter simulation

Navigation error	Min	Max	Mean	RMS
Northing (m)	-0.110	**0.078**	0.001	0.046
Easting (m)	**-0.100**	**0.100**	0.003	0.009
Vertical (m)	0.000	0.002	0.008	0.009

The reason for choosing the 10 cm lever arm error in the simulation is because this is an average value in the DSS system. Although lever arm can have a value of sub-meter level, especially in z axis, this simulated result can provide relative influence of lever arm error. From Figure 10, lever arm error is only projected to Northing component during aircraft banking, and the rest of lever arm error is introduced to Easting component when the flight direction is parallel to x-axis. Therefore, lever arm error can be projected in both Easting and Northing components depending on the dynamics of the flight. Similar to synchronization error, lever arm error is flight direction related and there it can be captured through opposite flight lines. Further, aircraft pitching occasionally in this DSS flight, the vertical position component has also been influenced but with insignificant magnitude. Since lever arm error is a constant vector, this error is independent when determining attitude information of the platform. Therefore, no attitude error is being introduced in this simulation.

2.4.2 Boresight Calibration:

Although most care is typically done to install the IMU in perfect alignment with the imaging sensor. A residual mis-alignment angle between the two frames will take place. This is called boresight as shown in Figure 11.

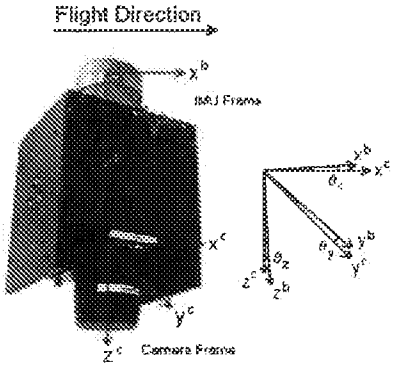


Figure 11. Camera/IMU Boresight

There are two methods to calibrate the boresight, namely:

1. Comparing the GPS/INS-derived angles with those independently computed using Aerial Triangulation (c.f., Skaloud, 1999). The constant difference between the two sets of angles is extracted as the three components of the boresight angles.
2. Computing the boresight angles as additional unknown parameters in GPS/INS-assisted Bundle Adjustment (c.f., Mostafa, 2001).

When comparing the two methods, the first method is more costly, and requires a lot more effort than the second method. On the other hand, the second method allows a ground control point – free solution. Geometrically, the second method is more

stable and therefore, camera self-calibration parameters are decorrelated easily and thus camera calibration is feasible simultaneously with the boresight calibration.

Since the IMU and the imaging sensor are typically installed in a rigid mount, boresight is assumed constant over time. This is a key assumption in the direct georeferencing technique. However, boresight angular errors are projected onto the mapping frame. Therefore, it depends on the MMS platform dynamics and is also amplified by the scale of the project; which is directly related to the flying height (h). The boresight error can be expressed by Equation 6 and an illustration of the error is shown in Figure 12.

$$\delta r_p^m = R_b^m(t)(s\delta R_c^b r^c) \tag{6}$$

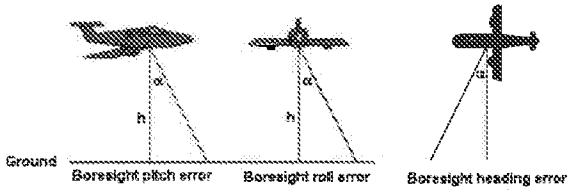


Figure 12. Illustration of Boresight Errors in Airborne Applications

For demonstration purposes, a simulation has been done using a DSS flight with a photo scale of 1:22000. A 10 arc-min boresight error is introduced on each INS axis independently. This value is chosen based on the typical boresight angle found on a DSS system. Specification of a DSS is summarized in Table 6.

Table 6. Specification of DSS

Array size	4092 X 4077 pixels, 9 micron pixel size
Lenses	Standard: 55mm – Color & CIR Optional: 35mm – Color only
Shutter Speed	1/125 – 1/4000 sec
Max Exposure Rate	2.5 or 4 sec
GSD	0.05 to 1 meter (platform dependent)
Smear	< 10% typical
Housing	Ruggedized exoskeleton with lens stabilization
Positioning accuracy	0.05 – 0.3 meter, post mission
Navigation error	0.008 – 0.015 deg, post mission
FMS	TrackAir EZtrack or external third-party
Northing (cm)	80 GB removable hard drive and pressurized data brick

The resulting exterior orientation parameters are then used to perform space intersections for 7 ground control points within the project area shown in Figure 13. Table 7 lists the RMS of the checkpoint residuals computed as the difference between the check point coordinates computed by space intersection and their values measured by land surveying techniques. The first entry of the table which is labelled "no error" shows the RMS of check point residuals of the 7 points without any intentional boresight error. The second entry labelled "x-axis" shows the RMS when an error in the boresight x-component is introduced to be 10 arc minutes. Note that the Northing component has increased by about twenty times due to the intentional simulated boresight error. Similarly, the introduction of a boresight error of 10 arc minutes on the y-component of the boresight results in increasing the Easting error by about 16 times and increasing the error in the vertical component by twice as much. This is due to the fact that the intentional boresight error is projected on the mapping frame and it affected all coordinate components. In the third entry, labelled "z-axis", an intentional boresight error of 10 arc minutes has been introduced to the z-component of the boresight angle and it resulted in degrading the Easting and Northing components by 2-3 times.

Table 7. Statistics of Boresight Error Influence on GCP Coordinate Computational Accuracy by Direct Georeferencing

Boresight error on	GCP RMS		
	Easting (m)	Northing (m)	Vertical (m)
no error	0.153	0.145	0.656
x-axis	0.141	**2.890**	0.740
y-axis	**2.455**	0.192	**1.202**
z-axis	0.494	0.401	0.762

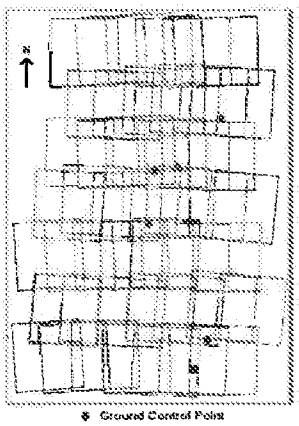


Figure 13. Block Configuration of the DSS 1: 22000 Flight

Note that, since the boresight error influence is photo scale-dependent, it is more severe in the case of airborne applications than that of the land-based applications.

2.4.3 Camera Calibration

Camera calibration is the process of determining the internal geometric and optical characteristics of the camera. This is also referred as the interior orientation of a camera system.

Interior orientation includes focal length, of principal point location, and lens distortion. Metric camera is calibrated in

laboratory periodically through certified agencies to ensure stable geometry. Except for the airborne commercial digital cameras, current cameras are not designed for photogrammetric operation and therefore the internal geometry is normally unknown. This is typical in the case of land-based applications and some airborne applications, where the user develops their own camera. In order to provide cost effective procedure for frequent self-calibration, camera calibration is normally done together with boresight calibration through a quality control of the overall system.

2.4.4 Initial Alignment

Alignment is the process of estimating the attitude information of the IMU, i.e. the direction cosine matrix (R_b^m) of the IMU with respect to the mapping frame. Static alignment is accomplished by two steps, levelling and gyro-compassing. Levelling refers to obtaining the roll and pitch of the IMU using the accelerometer outputs and gyro-compassing refers to obtaining the heading information using the gyroscope outputs. The attitude information (roll, pitch and heading) are referenced to the navigation or local-level frame (l-frame), which is an arbitrary frame and is not compatible with the mapping frame. Therefore, the alignment angles resolved through accelerometer output and gyro-compassing is instead represented by R_b^l which is the rotation matrix between the body frame and the l-frame. In order to align the IMU with respect to the mapping frame, a transformation (R_l^m) must be applied (from roll, pitch and heading to omega, phi and kappa, respectively). R_l^m defines the relationship between the two frames and therefore R_b^m can be determined from Equation 7. The resulting part is the attitude information of the IMU (R_b^m) in mapping frame with its components are as described in Equation 8.

$$R_b^m = R_l^m R_b^l \tag{7}$$

$$R_b^m = R_3(\kappa)R_2(\rho)R_1(\omega) \tag{8}$$

$$R_b^m = \begin{pmatrix} \cos\rho\cos\kappa & -\cos\omega\sin\kappa + \sin\omega\sin\rho\cos\kappa & \sin\omega\sin\kappa + \cos\omega\sin\rho\cos\kappa \\ \cos\rho\sin\kappa & \cos\omega\cos\kappa + \sin\omega\sin\rho\sin\kappa & -\sin\omega\cos\kappa + \cos\omega\sin\rho\sin\kappa \\ -\sin\rho & \sin\omega\cos\rho & \cos\omega\cos\rho \end{pmatrix}$$

Note that the time component (t) of $R^m{}_b(t)$ is neglected as the initial alignment process is performed in static mode. R_3, R_2 and R_1 correspond to the rotation along the axes: z (kappa), y (phi) and x (omega), respectively. Due to the angler random walk of the inertial gyroscopes, initial alignment accuracy is dependent on alignment time, especially on the Kappa angle (κ). Equation 9 expresses the relationship between alignment error in Kappa angle ($\delta\kappa$) with Angular Random Walk (ARW) in the z-gyro, the alignment time (T_a), the latitude (ϕ) at location of initial alignment and the earth rotation (ω_e). Error in initial alignment is treated as attitude error throughout the mission, and the error model is expressed in Equation 10. Since attitude errors will be amplified by the altitude of aircraft, their behaviour is similar to the boresight errors (shown in Figure 12). Note in Equation 9, Kappa accuracy is indirectly proportional to the square root of alignment time. Therefore, to achieve better Kappa accuracy, longer the alignment is required (typically 15 to 20 minutes).

$$\delta\kappa = \frac{ARW}{\omega_e \cos\phi\sqrt{T_a}} \tag{9}$$

$$\delta r_p^m = \delta R_b^m(t)(sR_c^b r^c) \tag{10}$$

After initial alignment, $R_b^l(t)$ will be updated/integrated through angular velocity measurements of the gyros. Each time $R_b^l(t)$ is updated, $R_l^m(t)$ must be applied to determine the corresponding $R_b^m(t)$, and the attitude information can be extracted through the recursive form in Equation 11.

$$R_b^m(t) = \begin{pmatrix} r_{11} & r_{12} & r_{13} \\ r_{21} & r_{22} & r_{23} \\ r_{31} & r_{32} & r_{33} \end{pmatrix}$$

and

$$\begin{aligned} \omega &= \tan^{-1}(r_{32}/r_{33}) \\ \rho &= \tan^{-1}(r_{31}/\sqrt{r_{11}^2 + r_{22}^2}) \\ \kappa &= \tan^{-1}(r_{21}/r_{11}) \end{aligned} \tag{11}$$

Since the above attitude information is referenced to the IMU center with respect to the mapping frame; for the interest of mapping application, attitude information in the EO parameters must be referenced to the center of the imaging sensor. Therefore, boresight angle and lever arm between the imaging sensor and the IMU center must be considered and applied to complete the Direct Georeferencing equation as presented in Equation 3.

3. CONCLUSION

Direct Georeferencing is an effective tool for mapping application through multi-sensor integration. Due to the different definition of these sensors, integration parameters of these sensors must be considered and well calibrated. Certain parameters include sensor placement and synchronization, system calibration and initial alignment. For both airborne and land application, the basics behind the integration method is similar, in which the integration of three primary sensors are considered: GPS, INS and imaging sensor. However, the operating environment controls how these sensors are related to each other, especially in the sensor placement. Therefore, the weights of calibration parameters for these two applications are different from each other, resulting different design of Kalman Filtering for implementation. Throughout the examples from the paper, it has shown that system synchronization and calibration are the most important factors to be considered. Error in system synchronization will be magnified through MMS dynamics in the Direct Georeferencing equation. However, this error is still relatively small comparing to system calibration error; also, it can be captured and calibrated through

lab environment. In system calibration, lever arm is important with its magnitude (up to sub-meter level). Error in lever arm can be projected to any position vector depending on platform dynamics. With the help of sensor specification, lever arm can be determined through installation. In addition, with the help of Kalman Filtering, lever arm with uncertainty can be calibrated throughout the mission. In boresight calibration, it is an important part on using a Direct Georeferencing system. Being an attitude error, boresight mis-alignment decreases the accuracy of EO parameters and introduces magnified ground error through operating height. Therefore, this parameter must be well-calibrated and monitor constantly through proper quality analysis/control procedures. Finally, initial alignment under static mode is important to provide accurate DGPS/INS data through out the mission. Although aligning during dynamic motion is possible with Kalman Filtering, longer epochs are required for alignment process; this lengthens mission time and is not cost efficient. Therefore, MMS is a complex system which requires knowledge on each parameters, each of them must be well calibrated/controlled to provide accurate EO parameters for direct georeferencing in either airborne or land application.

4. ACKNOWLEDGEMENTS

The authors would like to thank the financial support by NSERC and Applanix for supporting this research work.

5. REFERENCES

Elium, C.M., N., El-Sheimy, 2002. The Calibration of Image-Based Mobile Mapping Systems. Department of Geomatics Engineering, University of Calgary, Calgary, Canada.

Elium, C.M., N., El-Sheimy, 2001. Land-Based Integrated Systems for Mapping and GIS application. Department of Geomatics Engineering, University of Calgary, Canada.

El-Sheimy N., 1996a. A Mobile Multi-Sensor System For GIS Applications In Urban Centers. The International Society for Photogrammetry and Remote Sensing (ISPRS) 1996, Commission II, Working Group 1, Vol. XXXI, Part B2, pp. 95-100, Vienna, Austria, July 9-19.

El-Sheimy, N., 1996b. The Development of VISAT-A Mobile Survey System for GIS Applications, UCGE Report #20101, Department of Geomatics Engineering, The University of Calgary, Canada.

Grejner-Brzezinska, D.A., 2001. Direct Sensor Orientation in Airborne and Land-based Mapping Application. Report No. 461, Geodetic GeoInformation Science, Department of Civil and Environmental Engineering and Geodetic Science, The Ohio State University, Ohio, United States.

Lithopoulos, E., D.B., Reid, B., Scherzinger, 1996. The Position and Orientation System (POS) for Survey Applications, International Archieves of Photogrammetry and Remote Sensing, ISPRS Comm. III, Vol. XXXI, Part B3, pp. 467-471.

Mostafa, M.M.R., 2003. Design and Performance of the DSS. Proceedings, 49th Photogrammetric Week, Stuttgart, Germany, September 1-5, 2003.

Mostafa, M.M.R., 2001. Digital Multi-Sensor Systems – Calibration and Performance Analysis. OEEPE Workshop, Integrated Sensor Orientation, Hannover, Germany, Sept 17 – 18, 2001.

Reid, D.B., E., Lithopoulos, J., Hutton, 1998. Position and Orientation System for Direct Georeferencing (POS/DG), ION 54th Annual Meeting, Denver, Colorado, June 1-3, pp. 445-449.

Skaloud, J., 1999. Problems in Direct-Georeferencing by INS/DGPS in the Airborne Environment. ISPRS Commission III, WG III/1 Barcelona, Spain, November 25-26.

Skaloud, J., D., Cosandier, K.P., Schwarz, M.A., Chapman, 1994. GPS/INS Orientation Accuracy Derived From A Medium Scale Photogrammetry Test, International Symposium on Kinematic Systems in Geodesy, Geomatics and Navigation – KIS94, Banff, Alberta, Canada, August 30-September 2, pp. 341-348.

Skaloud, J., M. Cramer, K.P., Schwarz, 1996. Exterior Orientation by Direct Measurement of Camera Position and Attitude, International Archieves of Photogrammetry and Remote Sensing, Vol. XXXI, Part B3, pp. 125-130.

Schwarz, K.P., M.A., Chapman, M.E., Cannon, and P., Gong, 1993. An Integrated INS/GPS Approach to The Georeferencing of Remotely Sensed Data, PE&RS, 59(11): 1167-1674.



GPS AND INERTIAL NAVIGATION - DELIVERING

FRANK ARTÉS AND JOE HUTTON EXPLAIN THE BENEFITS OF DIRECT GEO-REFERENCING

GPS aided inertial navigation systems have been available for commercial mapping applications for approximately a decade, pioneered by Canadian-based Applanix Corporation with their POS (Position and Orientation System) technology. The impact on the aerial survey and remote sensing industry has brought about a re-assessment of traditional photogrammetric methodology and the potential elimination of two fundamental mapping components, the ground control survey and corresponding aerotriangulation process.

By merging the GPS and inertial navigation technologies, accurate position and orientation of the airborne imaging sensor, with respect to the Earth, can be determined directly. Such an approach is referred to as Direct Georeferencing. This approach is opposite to that of aerotriangulation, which requires accurate control points to be surveyed on the ground and then identified in the stereo imagery. These are then used to "back-out" the position and orientation of each photo through a geometric adjustment. One main advantage of Direct Georeferencing is that it can be used with any type of airborne imaging sensor, such as an aerial camera, hyperspectral scanner, Synthetic Aperture Radar or LIDAR. This method of calculating airborne position and orientation data is now a proven and reliable technology that is becoming more robust and accurate every year with the ongoing development in GPS and inertial equipment.

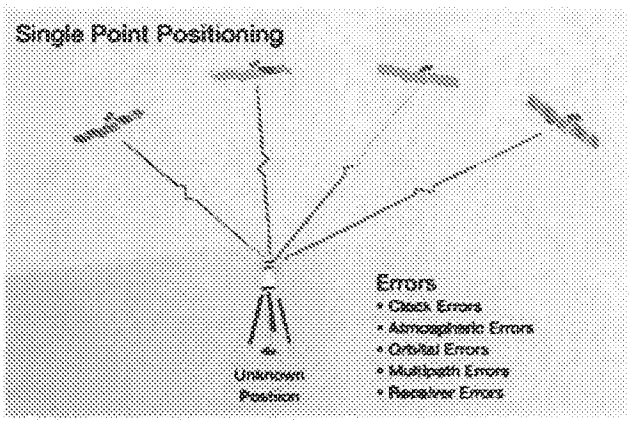
GPS and IMU Basics

Since its inception in the 1980's, the 12 billion dollar GPS project, developed by the US Department of Defense, has matured to become an extremely valuable resource for those organizations which rely on accurate geopositioning information. The concept of GPS positioning is based on triangulation using a minimum of ranges to four satellites (whose positions are known) to determine the precise location of a point anywhere on the Earth's surface. Using a single receiver, this methodology is referred to as single point positioning and is the simplest but least accurate way of generating position data. Typical accuracies can vary from 2m to 10m, though for many mapping applications this level of accuracy is less than suitable.

The ranges between the GPS receiver and satellites are computed by measuring the precise time it takes the radio signal to leave the satellite and hit the GPS antenna, multiplied by the speed of light. Errors in the receiver's clock and the Satellite's clock cause errors in the ranges. Also, the signals can reflect off nearby surfaces before hitting the antenna, causing an incorrect range to be computed (called the Multipath effect). In addition, atmospheric conditions affect a GPS signal's ability to penetrate the Ionosphere and Troposphere, slowing them down as they travel earthwards. Finally there are residual errors in the positions of the satellites themselves.

A standard methodology, known as Differential GPS (DGPS), is used to eliminate the majority of these errors. By using multiple base stations set up over known surveyed locations, to collect satellite data at the same time as the mobile GPS receiver, very accurate positioning of the mobile receiver can be achieved. Since the locations of the base stations are known, the common errors in the ranges to each satellite can be calculated and removed from the mobile receiver. Accuracies at the cm level are then possible.

A number of countries have established their own network of base stations, such as CORS (Continuous Operating Reference Stations) in the United States, and ANN (Australian National Network) in Australia. Also, the IGS (International GPS Service) volunteer organization provides precise orbit and satellite clock corrections with a worldwide



LEFT: SINGLE Point Positioning
BELOW LEFT: Differential GPS Positioning
BELOW RIGHT: Direct Georeferencing with GPS/INS

GPS permanent tracking network using the combined systems of various nations.

For centimeter-level positioning accuracy required for precise photogrammetric applications, both the base station and the mobile receiver must be operating simultaneously, and receiving GPS data from at least four common satellites. The GPS datasets can then be post-processed off site to generate an extremely accurate position and orientation solution for the imaging sensor. The raw measurements produced by the GPS are processed together with inertial navigation data to calculate accurate position and orientation for each image.

The inertial navigation solution provides high rate measurements of position, velocity and orientation (roll, pitch, heading) by integrating the output from accelerometers and gyros. Accelerometers measure linear acceleration, while gyros measure angular rates. The accelerometers and gyros are contained in a unit called the Inertial Measurement Unit (IMU), which is physically attached to the imaging sensor. A common misconception within the airborne industry is that an IMU is the same as an INS (Inertial Navigation System). The IMU is actually one of the two components in an INS, the other being an inertial navigator, which turns the sensor measurements into position and orientation. The INS is a self contained autonomous system that does not rely on external signals for information to produce a full navigation solution. One drawback of inertial navigation systems is that over time their position and orientation errors grow unbounded.

Having accurate GPS positions however, means they can be used to aid the inertial navigation solution by controlling the position error, which in turn controls the orientation error.

The Benefit for Photogrammetry

With the introduction of GPS aided inertial navigation technology, the aerial survey and remote sensing industry has seen a change in the way geospatial data is now generated. Standard applications such as topographic mapping, corridor surveys, DTM generation, and environmental monitoring have all benefited from the technology's particular attributes, which translate into an increase in operational efficiency and a decrease in time-to-data-delivery.

The non-intrusive technology has simplified topographic mapping applications and made accessibility problems of little concern, particularly in rough terrain or disaster-prone locations. For example, generating photogrammetric data for a coal stockpile inventory, where surface contrast causes problems for traditional aerotriangulation tasks, the use of direct georeferencing can be very effective. Even from a safety standpoint, there is now no need for survey personnel to be working in and around heavy mining or construction equipment.

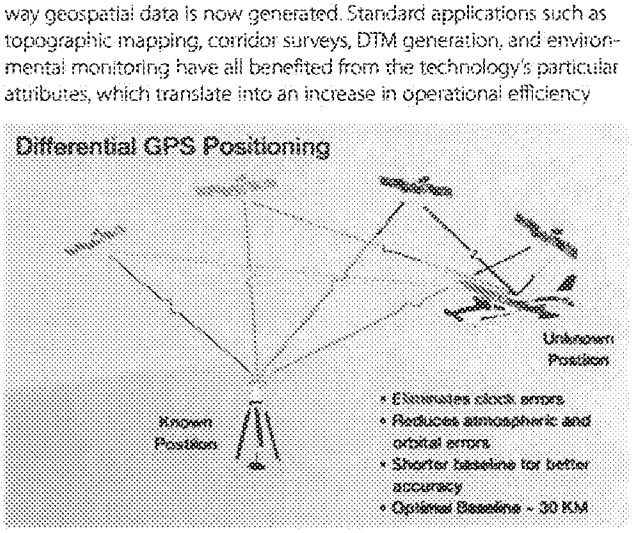
Also, with the heightened interest in Homeland Security, there is a recognized need for rapid response mapping to generate usable geospatial data in the wake of a national emergency, or in the case of natural disasters such as hurricanes, earthquakes and floods etc. Making current, georeferenced imagery available to first-responders and emergency personnel as quickly as possible cannot be overstressed. So without the requirement for ground control, integrated inertial/GPS technology can offer a significant advantage under these circumstances. In many cases it is the enabling technology behind various imaging sensors such as LIDAR, SAR (Synthetic Aperture Radar), and IfSAR (Interferometric SAR), providing the georeferencing component to the data.

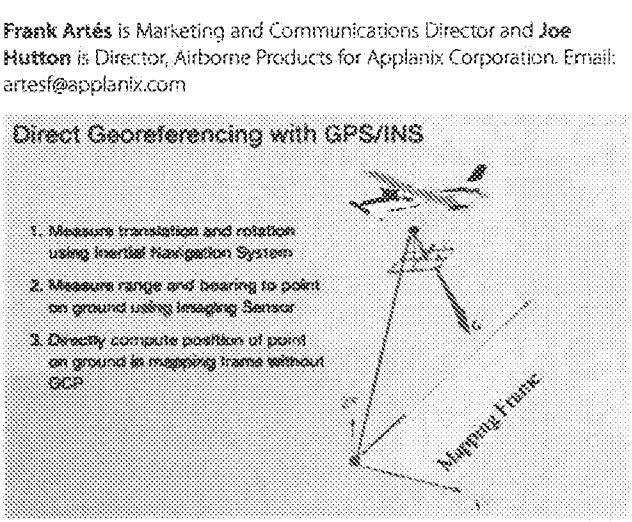
Future Trends

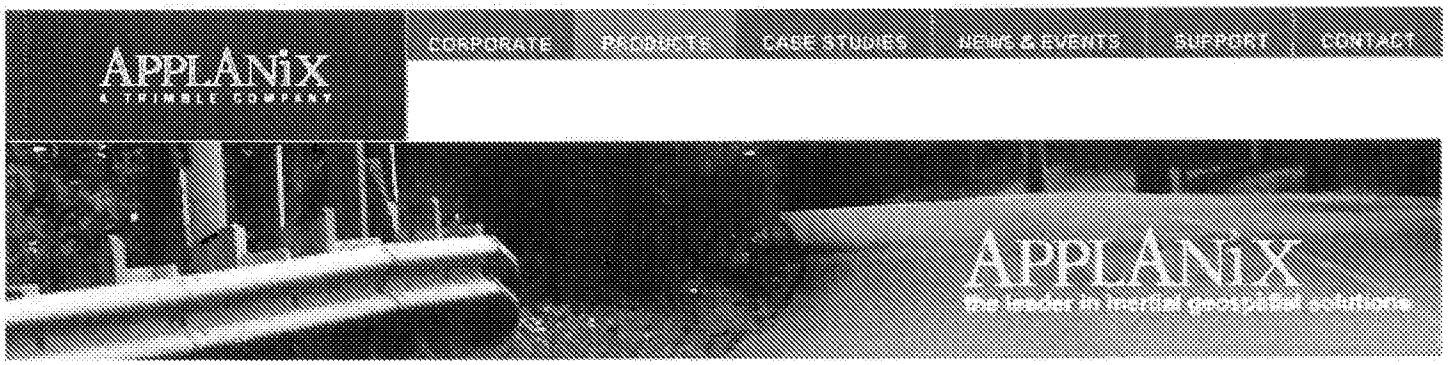
With continued improvements in GPS technology and the move towards MEMS-based (Micro-Electro-Mechanical Systems) inertial components, integrated inertial/GPS systems are becoming more mainstream in being able to offer the airborne geospatial community the necessary accuracy levels they require.

By the year 2010 it is expected there will be a full constellation of next generation satellites to bolster the GPS numbers currently in use. The introduction of Galileo from a European consortium will make a major difference in accuracy and accessibility, with 30 new satellites in orbit. The Galileo system of satellites and ground stations will complement the existing GPS system in the same way that GLONASS is presently being used. A number of other countries, such as India and Japan, are looking at initiating their own satellite programs so the future of satellite positioning for the geospatial community looks very positive.

Frank Artés is Marketing and Communications Director and **Joe Hutton** is Director, Airborne Products for Applanix Corporation. Email: artesf@applanix.com



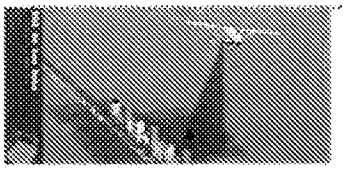




Land | Marine | Airborne

- POS AV
  - **Product Outline**
  - POS AV 210
  - POS AV 310
  - POS AV 410
  - POS AV 510
  - POS AV 610
  - POSTrack 210
  - POSTrack 310
  - POSTrack 410
  - POSTrack 510
  - POSTrack 610
  - Download POS AV Brochure
  - Download POSTrack Fact Sheet
  - Articles and Papers
  - Download FAQs
- DSS
- POSPac

Additional Resources



Directly Georeferenced Aerial Imagery
Learn how direct georeferencing of digital aerial imagery works in this interactive tutorial.
More...

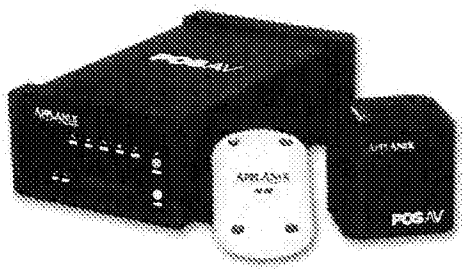
POSTrack
The Applanix POSTrack System



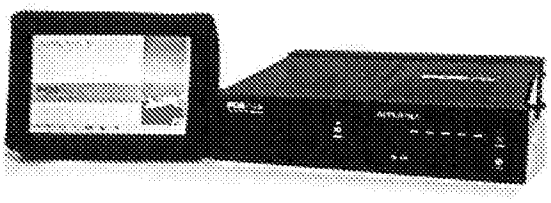
AnOverview of the Applanix POSTrack System
For a complete overview of the POSTrack System and how it can

Product Outline

POS AV



POS AV is a hardware and software system specifically designed for direct georeferencing of airborne sensor data. By integrating precision GPS with inertial technology, POS AV enables geospatial projects to be completed more efficiently, effectively, and economically. Supported by Applanix' industry expertise and technological innovation, POS AV is engineered for aerial cameras, scanning lasers, imaging sensors, synthetic aperture radar, and LIDAR technology.



POS AV is also available with an integrated flight management system, in a new product called POSTrack (above). POSTrack is the first fully integrated, real-time direct georeferencing and flight management system designed for the airborne geospatial community. Purpose-built to reduce the costs associated with the preparation and implementation of airborne surveys, POSTrack minimizes mission planning and operational workload. Utilizing a combination of specifically developed software and hardware tools, the system combines the best of both technologies with all the functionality necessary to simplify and streamline today's aerial survey and remote sensing

Applications

- Aerial Camera Systems (Film and Digital)
- LIDAR
- Synthetic Aperture Radar (all-weather capability)
- Digital Scanner

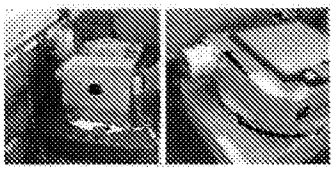
More Applications...

Case Studies

Film Camera Survey
AeroMap utilizes POS AV direct georeferencing technology to survey challenging areas in Alaska and quickly produce georeferenced imagery for orthophoto production.
More...

LIDAR Survey
MD Atlantic undertakes an extensive LIDAR mapping project, incorporating POS AV technology to generate sensor-specific position and orientation information.
More...

Examples



significantly reduce your mission planning and operational workload.
More...

operations.

For more information about POS AV or POSTrack, contact airborne@applanix.com

Related Products

POSPac
Post-processing Package

Utilize the latest in processing software to improve productivity, improve data accuracy and improve reliability.

Contact Us

For detailed information on how POS AV can streamline your airborne operations, please contact airborne@applanix.com

Inertial Factoids

An accelerometer is a device which can measure acceleration, the rate of change of velocity with respect to time. (Source)

Applanix News

Subscribe to receive the latest news and information on Applanix geopositioning solutions, innovation and technology working for you. Subscribe Now!

Benefits

Top of Page

- Provides an accurate real-time and post-mission solution for all motion variables including sensor-specific Exterior Orientation (EO) parameters using Direct Georeferencing
- Eliminates the requirement for aerotriangulation and a complete ground control survey (often only check points for quality control are needed)
- Streamlines and automates the data workflow and quality control processes
- Allows for single stereo model mapping and single photo orthorectification using an existing Digital Elevation Model
- Improves productivity in traditional aerial mapping applications, which translates into operational time and costs savings, with increased accuracy
- Easily integrated with digital cameras, film cameras, LIDAR systems, SAR systems, and digital scanners
- Ideally suited to inhospitable environments and rapid response applications where ground control is not available

Applications

Top of Page

Aerial Camera Systems (Film and Digital)
- Topographic mapping
- DTM (Digital Terrain Model) generation
- High-resolution digital imagery
- Orthophoto production
- Resource industry volumetrics

LIDAR
- Erosion monitoring
- Topographic mapping
- Forestry ground and canopy measurements
- Bathymetry data generation for shallow water and shoreline mapping

Synthetic Aperture Radar (all-weather capability)
- DTM (Digital Terrain Model) generation
- Environmental monitoring (oil/chemical spills etc)
- Deforestation
- Radar-based topographic imagery
- Reconnaissance, surveillance

Digital Scanner
- Topographic mapping
- DTM (Digital Terrain Model) generation

Technology

Top of Page

POS AV provides the aerial survey and remote sensing industry with a revolutionary method of georeferencing data. **Direct Georeferencing** is the direct measurement of sensor position and orientation (also known as the exterior orientation parameters), without the need for additional ground information over the project area. These parameters allow data from the airborne sensor to be georeferenced to the Earth or local mapping frame. Examples of airborne sensors include: aerial cameras (digital or film-based), multi-spectral or hyper-spectral scanners, SAR, or LIDAR. All POS AV systems integrate seamlessly with the Track'Air Flight Management System (www.trackair.com).

Components

Top of Page

- PCS: POS Computer System. Ruggedized, low-power, light-weight, small format, with built-in logging. Includes embedded state-of-the-art survey grade GPS receiver.
- IMU: Inertial Measurement Unit. Ruggedized, state-of-the-art, small format, light-weight, with high measurement rates
- POSPac: Post-processing software bundle. Includes Carrier Phase DGPS processing, integrated Inertial/GPS processing, and optional photogrammetry tools for EO

generation, IMU boresight calibration and quality control.
* Optional integrated Track'air Flight Management System: Mission planning, pilot display, and in-air POS AV and sensor control for maximum in-flight task automation and operational efficiency

Legal | Subscribe to Newsletter | Contact Us
©2007 Applanix Corp., All Rights Reserved

POSTrack

One Compact System, One Complete Solution



Combining the precision of POS AV of Direct Georeferencing with the Flight Management System expertise of TRACK'AIR

POSTrack is the first fully integrated, real-time direct georeferencing and flight management system designed for the airborne geospatial community. Purpose-built to reduce the costs associated with the preparation and implementation of airborne surveys, POSTrack minimizes and streamlines mission planning and in-flight operational workload.

Utilizing a combination of specifically developed software and hardware tools, the system combines the best of both technologies with all the functionality necessary to simplify and streamline today's aerial survey and remote sensing operations.

POSTrack's Complementary Technologies (POS AV & XTRACK)

POSTrack incorporates the latest integrated inertial/GPS direct georeferencing technology from Applanix, with the Flight Management System (FMS) expertise of Track'air, the industry's leading FMS manufacturer. Unlike other IMU/GPS/FMS configurations, which utilize independent components for in-flight task automation and mission planning, POSTrack is engineered as a single system, compact, convenient, and easily installed on all types of aircraft without a complicated network of cables and connectors.

POS AV

The POS AV component integrates precision GPS with inertial technology to enable geospatial projects to be completed more efficiently and effectively. Supported by Applanix industry expertise and technological innovation, POS AV is engineered for all types of aerial sensors to produce directly georeferenced data. The system generates an accurate solution for all motion variables, and precise, image-specific Exterior Orientation parameters without the requirement for a complete ground control survey and corresponding aerotriangulation processing.

XTRACK

As the most sophisticated flight management system available, XTRACK covers all the aspects of flying an airborne mission, from preparation, to image acquisition, to data archiving. It incorporates flight planning, navigation and reporting software with an external sensor interface and pilot display. Combining the two technologies offers seamless integration to provide automated airborne mission control for consistent project success.

The POSTrack Advantage

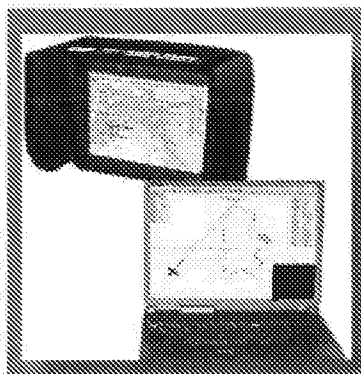
The complete POSTrack system has been configured to handle the GPS/IMU functions and control and trigger the airborne sensors to ensure the highest levels of precision are maintained. The in-flight automation provided by the system enables exact flight path guidance and accurate sensor positioning, which translates into optimized airtime over the target area for the most economical and efficient mission capability.

Compact Design and Simplified Cockpit Configuration

The system comprises a single box solution incorporating a POS AV computer (PCS) module and an FMS computer system (FCS) module, manufactured using Applanix state-of-the-art, real-time embedded computing technology.

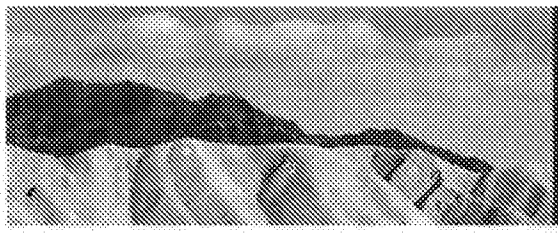
The display includes touch screen capability, allowing the pilot to operate in full standalone mode. For a two-person operation, a laptop or tablet computer can also be used to allow the second crew member (navigator) to work on the mission together with the pilot. A single Ethernet connection is all that is required. In this configuration, the XTRACK navigation software, running on the FCS, can be controlled simultaneously from either the pilot's screen or the navigation laptop.

With a maximum weight of 5.9 kg, the size of the unit does not exceed 279mm L x 330mm W x 91mm H. The compact design will easily fit all types of survey aircraft without cluttering the cockpit with cables and oversized housings and mounting brackets.



The display includes touch screen capability, allowing the pilot to operate in a full stand-alone mode.

APPLANIX
A TRIMBLE COMPANY



POSTrack™

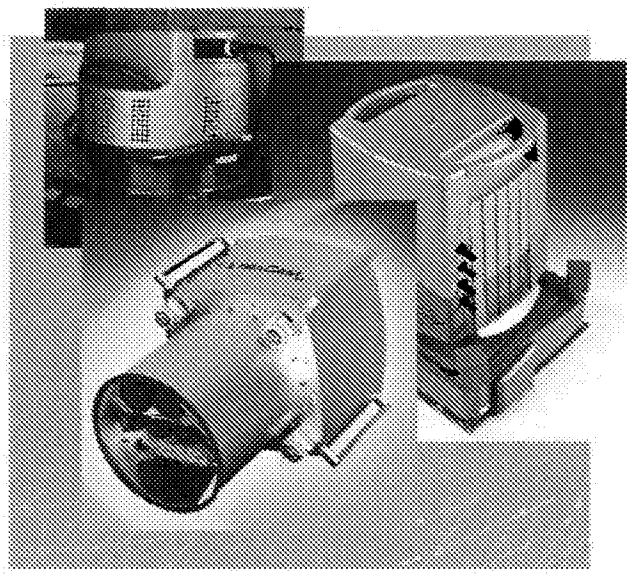
One Compact System, One Complete Solution

Tight Integration for Optimal Performance
The FCS communicates directly with the PCS via high speed Ethernet protocol. In addition to the normal GPS/IMU functions, the POS AV module has been modified to control and trigger the various types and combinations of aerial sensor. The XTRACK system monitors the real-time position and orientation of the sensors, which has been computed by the POS AV, and then instructs it to perform certain tasks to control the sensors.

Examples include the automatic triggering of frame cameras, automatic on/off control of LIDAR and push-broom scanners, and the automatic on/off control of 3-axis mount stabilization.

Flexible Interfaces for Maximum Efficiency
Although POSTrack is tightly integrated to maximize performance, it still maintains a flexible and open architecture to allow easy integration with many different types and combinations of airborne sensors.

The most common sensors are already supported, and customizations are available upon request.

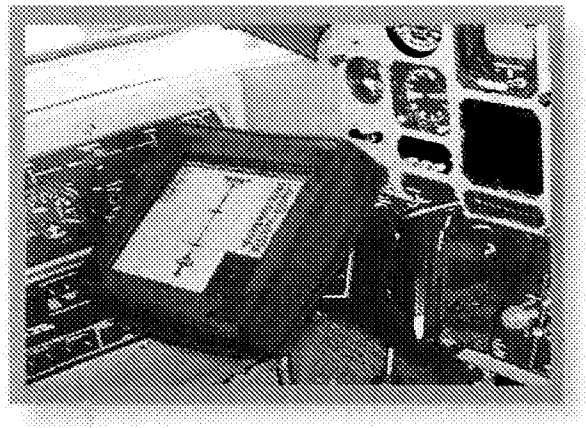


The Advantage of Real-time GPS-Aided Inertial Navigation
POSTrack computes a true real-time navigation solution for the aerial sensor 200 times or more per second. This means all motion parameters, such as position, velocity, roll, pitch, heading, acceleration and angular rate, are available for integration with the flight management software.

The real-time solution provides the pilot with feedback on the quality of the IMU and GPS data being collected for direct georeferencing. Any concerns with the data immediately appear as warnings on the pilot display.

The real-time orientation data is also used to automatically control the drift and level of a 3-axis mount, which will dramatically helof the mount. However, during turbulent conditions, the aircraft's horizontal accelerations will cause the inclinometers to generate false readings causing the mount to tilt with respect to the ground.

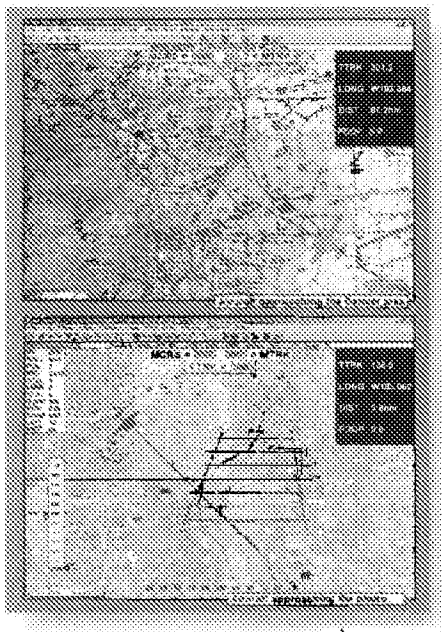
Because the POS AV is unaffected by turbulence, its real-time roll and pitch data can be fed into the mount to ensure it always remains level. Similarly, the real-time heading from POS AV can be used to automatically steer the azimuth of the mount to follow a desired track along the ground. These attributes are a tremendous advantage. Currently, POSTrack interfaces with the following 3-axis mounts: Z/I T-AS (drift control only), Leica Geosystems PAV30 (leveling and drift), SOMAG GSM3000 (leveling and drift).



Protecting Your Investment With a Complete Upgrade Path
POSTrack is a new, powerful aerial survey technology combining the best of both worlds - direct georeferencing and flight management systems.

With sensor-compatible interfaces, mission status display, low radiation LVDS pilot display screen, and planning and reporting software, POSTrack is the ideal system for single-pilot or pilot/navigator crew configurations who want a streamlined, cost-effective airborne operation.

As with all Applanix products, POSTrack has a clear upgrade path to ensure the system provides the best results and continued service.



85 Leek Crescent, Richmond Hill, Ontario CANADA L4B 3B3
Tel: 905-709-4600 Fax: 905-709-6027 Web: www.applanix.com

APPLANIX
A TRIMBLE COMPANY

Digital Frame Camera Applications

Client: 3001 Inc.

Digital Frame Camera Overview

Designed around CCD (Charged Coupled Device) imaging elements to ensure rigid image geometry, a digital frame camera uses multimillions pixel resolution to generate standard perspective, high-resolution digital imagery. Producing four color channels in red, green, blue, and near-infrared, projects can now be undertaken in low light conditions with excellent results.

3001 Inc. is an international spatial data corporation with offices located across the United States. Its geospatial expertise has been utilized in numerous projects throughout the Americas, providing technological leadership and innovative solutions to the engineering, surveying and geomatics community, with a dedicated team of aerial survey, GIS and photogrammetry professionals. Using leading-edge technology 3001 Inc. continues to harness the power of geospatial information in an everchanging world.



CHALLENGE

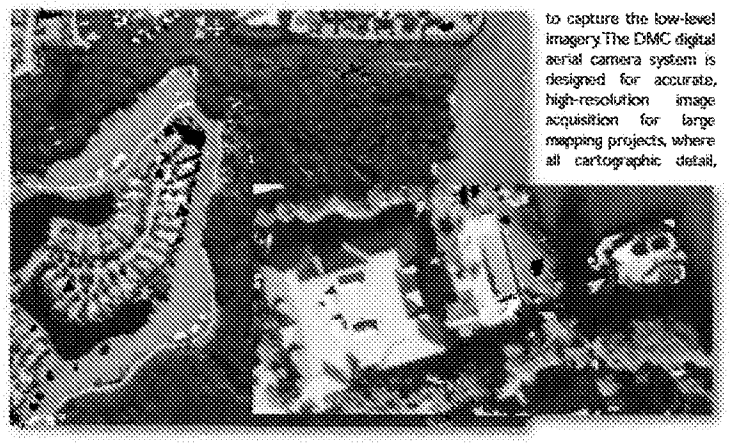
In December 2003, the company was tasked with providing a series of high resolution color digital images of Collier County in southwest Florida, as part of an on-going GIS update program involving digital orthophotography, stereocompilation, and planimetric mapping. Collier County is bordered on the west by the Gulf of Mexico, and five other counties to the north, east, and south. This portion of the project covered approximately 800 square miles of varied terrain, including large areas of swamp found along the coastal regions of western Florida. The digital imagery would be used to generate digital orthophotos and photogrammetric mapping data using stereoscopic image coverage. The final orthorectified imagery and vector mapping data would be input into the county's GIS system and accessible through the Collier County Property Appraiser's web site.

SOLUTION

To meet the project's specific requirements, 3001 inc. used their Z/I Imaging DMC (Digital Mapping Camera) equipped with an Applanix POS AV integrated inertial position and orientation system,

Digital Frame Camera Applications

Client: 3001 Inc.



to capture the low-level imagery. The DMC digital aerial camera system is designed for accurate, high-resolution image acquisition for large mapping projects, where all cartographic detail, such as vegetation, transportation networks, hydrography, and buildings, can be clearly defined. It provides excellent visibility in areas of shadow and generates a bright, sharp image, ideal for this type of application.

RESULT

Within two weeks the flying portion of the project was completed, and image processing and data capture started. Flown at an altitude of 4500', the color digital imagery generated a 0.45' pixel size and a final delivery accuracy of 0.5' for the orthophotos. The company found the POS AV system enabled them to attain a tighter aerotriangulation result by utilizing its direct georeferencing capability in areas where image tie point matching was particularly difficult.

Greg Horrall explained, "There were areas along the coast that were completely covered in swamp. Identifiable ground features, such as small islands, were few and far between, so we took advantage of the POS AV direct georeferencing capability. By taking the exterior orientation parameters for the images covering those areas, and using them as part of the aerotriangulation adjustment, we were able to achieve a much more accurate result."

> "The POS AV system enabled us generate a stable and complete aerotriangulation solution in areas where it was most needed."
>
> Greg Horrall, Aerial Triangulation Specialist, 3001 Inc.

Using the POS AV-equipped DMC system, 3001 Inc. successfully completed the Collier County project, and provided positionally-accurate and highly-detailed digital imagery, ideally suited to the orthophotography and data update requirements.

Digital Scanner Applications

Client: EarthData

EarthData is a leader in the airborne imaging, mapping, and Geographic Information Systems (GIS) field. Its fleet of specially configured survey aircraft collects a variety of information about the Earth's surface, using aerial cameras and various types of airborne sensors. The company transforms the data into customized mapping and GIS products and services. For close to 50 years, EarthData's clients have used this geospatial information for design infrastructure, terrain modeling, transportation engineering and environmental research, to better understand the Earth and its resources.

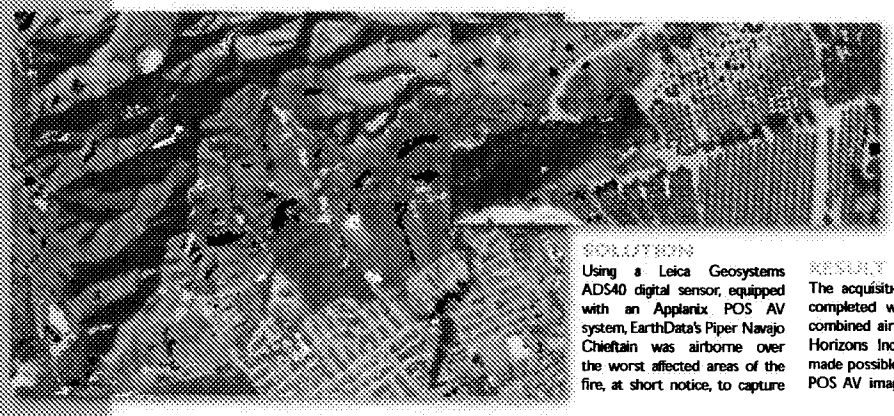
CHALLENGE

In October 2003, the State of California suffered one of the most devastating wildfires in its history. It caused extensive damage to property and the environment and posed a potential threat to the state's energy systems, which included transmission lines, major natural gas pipelines, and various oil refineries located in the immediate area. The fires were spread across more than 300,000 acres of land, with states of emergency being declared in Los Angeles, San Diego, Ventura and San Bernardino counties, where the authorities were battling fires on 10 separate fronts. EarthData, working in conjunction with ESRI and Horizons Inc., was tasked with generating accurate and detailed aerial imagery of the affected areas, to enable damage analysis to begin, in support of rapid response and recovery efforts.



Digital Scanner Applications

Client EarthData



SOLUTION

Using a Leica Geosystems ADS40 digital sensor, equipped with an Applanix POS AV system, EarthData's Piper Navajo Chieftain was airborne over the worst affected areas of the fire, at short notice, to capture color-infrared imagery. Mitch Jordan, EarthData's project manager, explains, "The POS AV system integrates very well with our airborne sensors, and its direct georeferencing capability is a big plus, especially for emergency response operations such as this one, where there is no time to carry out ground control surveys. Accurate georeferenced digital images can be generated very quickly with this system."

RESULT

The acquisition of detailed digital imagery was completed within 14 days, as a result of the combined airborne operations of EarthData and Horizons Inc. The quick data turnaround was made possible with the ADS40 digital system and POS AV image georeferencing attributes, which together prove a very efficient combination. In total 3,143 square miles of severely burned terrain were captured and processed. With the image acquisition complete, state and local authorities were able to access the data immediately for use in damage assessment and recovery. Image analysis experts at ESRI used the digital orthophotography and corresponding DTM data to map the fire-damaged environment, and analyze the drainage patterns as a precaution against the potential risk of mudslides now that ground cover vegetation had been destroyed.

Film Camera Applications

Client: AeroMap

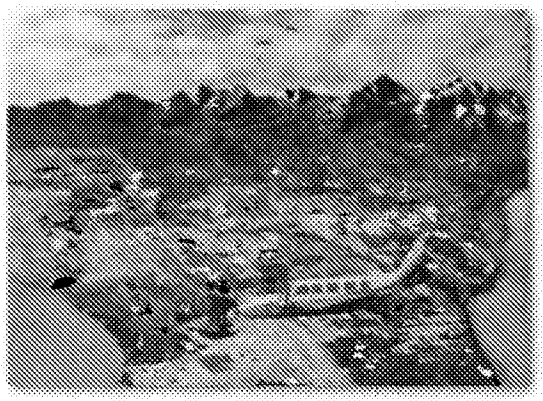
Film Camera: Overview

Producing 23cm square, high-resolution color, color infrared, and B&W photography, aerial film cameras have been a standard within the industry for many years. Stable and robust, and now fitted with FMC, gyro-stabilized mounts, and various navigation and GPS subsystems, aerial film cameras are an efficient and complete photographic unit.

AeroMap U.S. is a division of Aero-Metric Inc., one of the largest photogrammetric companies in the United States. AeroMap is based in Anchorage, Alaska, and is a full-service Geographic Information and Mapping Sciences firm, with expertise in all areas of aerial survey, airborne remote sensing, and satellite image processing. AeroMap's clients include government agencies and private sector organizations which use airborne imagery for various applications, from environmental monitoring to engineering design work.

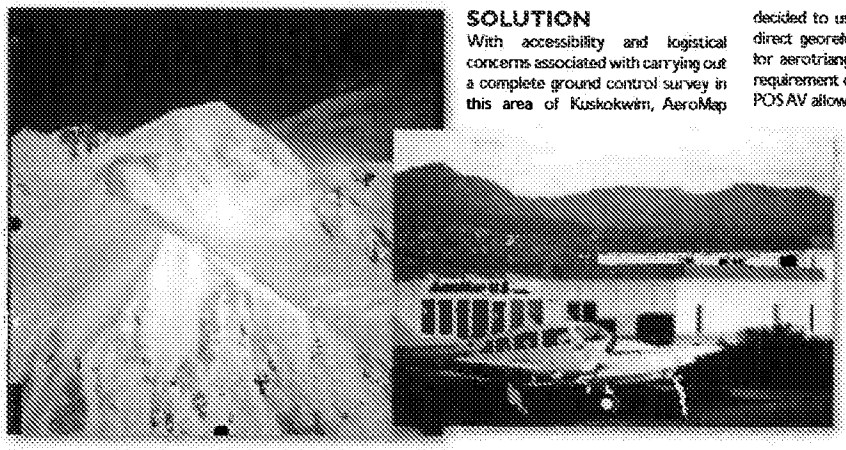
CHALLENGE

Faced with limited good flying weather and the rugged Alaskan environment, AeroMap was tasked with capturing color aerial photography for the Federal Bureau of Indian Affairs. The Class II Orthophotography project involved generating images for approximately 500 native allotments in the Calista Native Lands area of western Alaska. The allotments were scattered throughout the region, and could be as far apart as 200 miles or share a common boundary, and vary in size between 20 and 150 acres. "It was a difficult assignment in which to capture the images efficiently, so precise coordination was required," Dean Cimmiyotti explained. "As the orthophotos would be used to assess the timber stands in each allotment, positional accuracy was an important consideration, particularly as vector data was to be overlaid to show the individual property limits."



Film Camera Applications

Client: AeroMap



SOLUTION

With accessibility and logistical concerns associated with carrying out a complete ground control survey in this area of Kuskokwim, AeroMap decided to use their POS AV system to generate direct georeferenced imagery, eliminate the need for aerotriangulation, and easily meet the Class II requirement of 5' horizontal positioning. "Using the POS AV allowed us to fly single lines with as few as 3 or 4 images per allotment. To verify the accuracy of the georeferenced data we used a minimum amount of ground control as a QC check," said Cimmiyotti, "and it exceeded our expectations."

RESULT

The final georeferenced imagery was used to generate a Digital Elevation Model, which allowed the orthophotos to be produced quickly. Digital vector data, provided by the Bureau of Land Management, was then accurately overlaid to illustrate the individual allotment boundaries. Since incorporating the POS AV system into its workflow, AeroMap has found that increased productivity and additional accuracy are readily attainable under the difficult conditions encountered in Alaska, streamlining their airborne surveys into a precise and efficient operation.

> "The POS AV system enabled us to complete this project very cost effectively because we could georeference our aerial imagery without surveying multiple ground control points."
>
> Dean Cimmiyotti, Project Manager AeroMap U.S.

LIDAR Applications

Client: MD Atlantic

LIDAR Description

Light Detection And Ranging is the basis behind LIDAR, a process that uses monochromatic, laser light for the acquisition of Digital Terrain Model information. It is a very effective tool for generating accurate topographic data over large areas of flat/medium terrain.

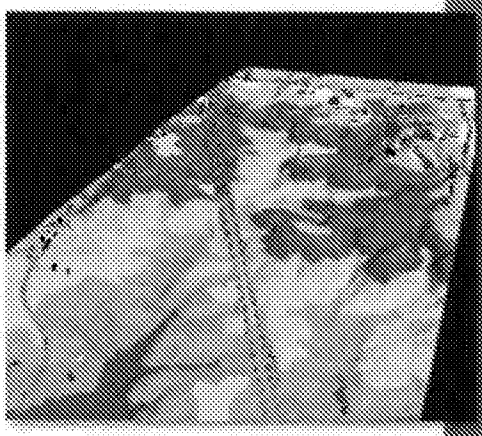
MD Atlantic Technologies is a leading supplier of geospatial information, digital aerial photography, photogrammetric mapping, airborne LIDAR data, and GIS database information. The organization provides geographic and spatial solutions to state and federal agencies, municipal governments, and the private sector. With a team of highly skilled professionals, MD Atlantic maintains its position as a leading-edge company at the forefront of the geospatial industry.

CHALLENGE

MD Atlantic was asked to undertake an extensive mapping project of Montgomery County, Alabama. A comprehensive dataset of geographic information was to be incorporated into the county's GIS system as part of its expanding GIS program. Planimetric and topographic data was required for an area covering approximately 790 square miles of rolling terrain, to include transportation networks, hydrographic features, and urban structures for all towns and cities, including Montgomery, the state capital. Color orthophotography was required together with a DTM (Digital Terrain Model), which would accurately define the topography of the county, and be used to generate 2' contour information.

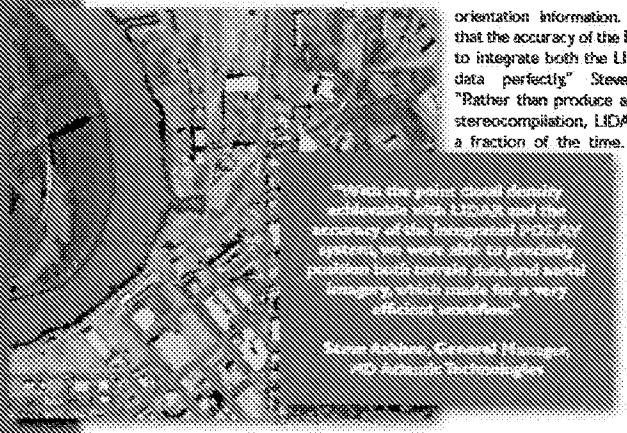
SOLUTION

To effectively complete the project, MD Atlantic's solution was to use two types of sensors to capture the information, an Optech 1210 LIDAR system, and a Leica RC30 aerial camera. Both technologies use integrated POS AV systems to generate sensor-specific position and



LIDAR Applications

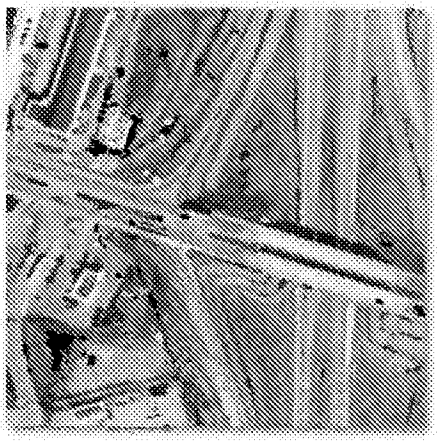
Client: MD Atlantic



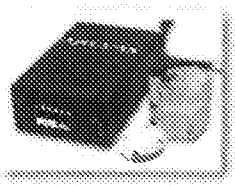
orientation information. "We were confident that the accuracy of the POS AV would allow us to integrate both the LIDAR and the mapping data perfectly" Steve Ashbee explained. "Rather than produce a complete DTM using stereocompilation, LIDAR will generate it in a fraction of the time. We then supplement the LIDAR mass point data with breaklines, road edge and hydrographic features captured photogrammetrically from the aerial photo, to produce a very accurate and true depiction of the terrain."

RESULT

Flying at an altitude of 3,280' the elevation data was acquired very quickly, with overlapping parallel swaths generating accurate XYZ point cloud information ready for mission post-processing. The terrain data was easily integrated into the project workflow and the required contour information generated. Although the LIDAR data was captured independently of the aerial photography, the accuracy of the POS AV on both systems ensured the datasets were compatible, allowing the development of a highly accurate topographic model from which 2' contour information was developed.



OEM System Specifications



The POS AV system has been successfully integrated with a number of original equipment manufacturers producing various types of sensors for the aerial survey and remote sensing industry.

The OEM version of the new POS AV has been designed with OEM requirements in mind, and contains the following features to allow for a more flexible installation and operation process:

- Light weight, smaller format
- Remote power ON/OFF capability
- Non-removable PC card for inertial data logging, or logging over the Ethernet to save power
- Designed to be used with OEM custom-manufactured cable systems

1. Physical

Temp. Range:	POS	-20 deg C to +60 deg C
Size:	POS	239 L x 158 W x 82 H mm (9.4 L x 6.2 W x 3.2 H inches)
Weight:	POS	2.54 kg
Power:	20 ~ 34	Volts DC
	POS	25 W, Max (not including IMU)

2. General - Sensors

IMU	GPS
Model dependent	12 channel dual frequency (L1/L2), low noise, DGPS ready, 10 Hz raw data

3. I/O

Ethernet (100 base-T)

Parameters	Time tag, status, position, attitude, velocity, track and speed, dynamics, performance metrics, raw IMU data (IMU rate), raw GPS data (10Hz)
Display Port	Low rate (1 Hz) UDP protocol output
Control Port	TCP/IP input for system commands
Primary Port	Real-time (up to IMU rate) TCP/IP protocol output
Secondary Port	Buffered TCP/IP protocol output for data logging to external device

Logging

Parameters	Time tag, status, position, attitude, velocity, track and speed, dynamics, performance metrics, raw IMU data (IMU rate), raw GPS data (10Hz)
Media	Embedded 1 Gbyte Flash Disk

RS232 NMEA ASCII Output

Parameters	NMEA Standard ASCII messages: Position ($INGGA), Heading ($INHDT), Track and Speed ($INVTG), Statistics ($INGST)
Rate	Up to 50 Hz (user selectable)

OEM System Specifications

RS232 High Rate Binary Output

Parameters	User selectable binary messages:Time, position, attitude, speed, track, PAV30 output,Yaw Drift Correction
Rate	Up to IMU rate (user selectable)

RS232 Input Interfaces

Parameter	Gimbal encoder input, AUX GPS Input (RTK, NavCom Starfire, OmniStar HP), RTCM104 DGPS Corrections Input.
Rate	1 Hz to IMU rate

Other I/O

1PPS	1 pulse-per-second Time Sync output, normally high, active low pulse
Event Input (2)	Time mark of external events. TTL pulses > 1 msec width, max rate 100 Hz.
Remote Power	ON/OFF control via remote signal

4. User Supplied Equipment

PC for POS Controller (Required for configuration)

- Pentium 90 processor (minimum)
- 16 MB RAM, 1 MB free disk space
- Ethernet adapter (RJ45 100 base T)
- Windows 98/2000/NT/XP

PC for POSPac Post-processing Software

- Pentium III 800Mhz or equivalent (minimum)
- 256 MB RAM, 400 MB free disk space
- USB Port (For Security Key)
- Windows 2000/XP

Synthetic Aperture Radar Applications

Client: Orbisat

Synthetic Aperture Radar Capabilities

Synthetic Aperture Radar (SAR) systems provide high resolution imaging day or night, through cloud cover, and in all weather conditions. SAR is ideal for terrain and surface mapping, and is routinely used for defense, environmental monitoring, and disaster management.

Orbisat de Amazônia is a leader in the application of Remote Sensing technology for use in mapping, geomatics, and geospatial information gathering. The company's expertise lies in its use of Interferometric Synthetic Aperture Radar (InSAR), which provides fast, accurate, and cost-effective solutions for the professional and scientific communities engaged in activities such as urban and regional planning, environmental analysis, and resource exploration and mapping.

CHALLENGE

The CartoSUR II project was established in Venezuela in 2003 as a national cartographic venture to acquire radar-based mapping data covering approximately 1/3 of the entire country. Located at the northernmost end of South America, Venezuela has a total area of 912,050 km². Included in the CartoSUR II project area was the state of Bolivar, which contains some of the oldest land forms in South America. The rugged mountains, steep cliffs, and plateaus, rise to over 3000 m in places, and contain one of the highest waterfalls in the world, Angel Falls. The terrain gradually flattens out and drops down to the Delta Amacuro on the east coast. Densely covered with forest and scored with tributaries of the Rio Orinoco, this whole region is often under thick cloud cover, and as such can be a very difficult area to map effectively.

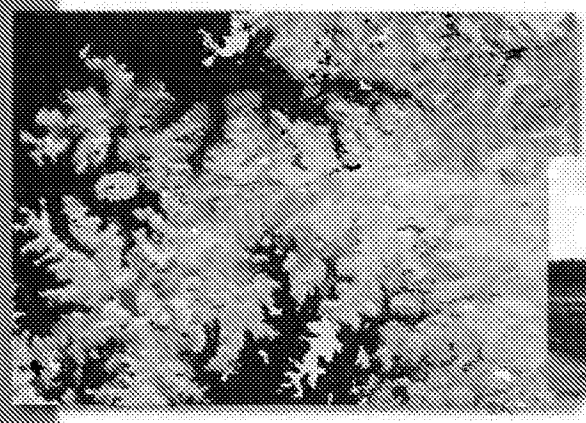
SOLUTION

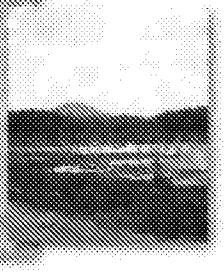
Orbisat immediately saw the solution to generating accurate cartographic data for this type of environment. The InSAR technology, with its all-weather operational capability, is unaffected by cloud, rain, poor visibility, and ground vegetation, and can very quickly produce accurate, detailed imagery, including digital terrain models. Installed aboard a Gulfstream Aerocommander aircraft, OrbiSAR-1 simultaneously uses two radar bands



Synthetic Aperture Radar Applications

Client: Orbisat





to generate image data, a result of the unique response of terrain and cultural targets to radar frequencies. The X-band reflects off surface objects such as trees, and buildings etc., to produce a Digital Surface Model, and the P-band reflects below the vegetation and produces a Digital Terrain Model.

RESULT

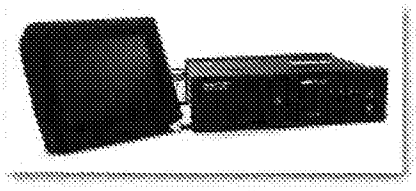
Within three months of starting the airborne operation, and 700hrs of air time, all image acquisition was completed. Flying at an altitude of 23,000', and using a dual pass for P-band interferometry with an 80 m baseline, the 3D imaging data was generated and made ready for processing. Dieter Leubeck, Project Manager, Orbisat, explained. "As well as providing position and orientation information for the radar imagery, the POS AV system also generates a real-time navigation solution that is incredibly accurate. We can fly a 120 km line and stay within a 1m horizontal variance quite easily. These attributes make the OrbiSAR-1 system extremely effective in undertaking radar mapping projects, and it's the POS AV that provides the spatial orientation accuracy." Final data delivery to the Geographical Institute of Venezuela Simon Bolivar (IGVSB) totaled 518 map sheets at a scale of 1:50,000, and covered an area of more than 263,000 km². Contour information was illustrated on the X-band orthoimage maps, and digital terrain model and full polarimetric P-band image data was made available for the complete project.

POSTrack V5 Specifications

POSTrack
One Compact Solution

Combining the precision of POS AV Direct Georeferencing with the versatility of the Track'air KTRACK Flight Management System

POSTrack is the first fully integrated, real-time direct georeferencing and flight management system designed for the airborne geospatial community.
Purpose-built to reduce the costs associated with the preparation



and implementation of airborne surveys, POSTrack minimizes mission planning and operational workload. Utilizing a combination of specifically developed software and hardware tools, the system combines the best of both technologies with all the functionality necessary to simplify and streamline today's aerial survey and remote sensing operations.

POSTrack incorporates the latest integrated inertial/GPS direct georeferencing technology from Applanix, with the Flight Management System (FMS) expertise of Track'air, the industry's leading FMS manufacturer. Unlike other IMU/GPS/FMS configurations, which utilize independent components for in-flight task automation and mission planning, POSTrack is engineered as a single system: compact, convenient, and easily installed on all types of aircraft without a complicated network of cables and connectors.

Compact, Simplified Cockpit Configuration

Configured to control and trigger various airborne sensors in addition to handling the GPS/IMU functions, POSTrack will ensure the highest levels of precision are maintained. The XTRACK component monitors the real-time position and orientation of the sensors computed by the POS AV, then instructs the system when to perform certain tasks. The in-flight automation enables exact flight path guidance and accurate sensor positioning, which translates into optimized airtime over the target area for the most economical and efficient mission capability.

With sensor-compatible interfaces, mission status display, flat panel pilot screen, and planning and reporting software, POSTrack is the ideal system for single-pilot or pilot/navigator crew configurations who want a streamlined, cost-effective airborne operation.

Complete Upgrade Path

As with all Applanix products, POSTrack has a clear upgrade path to ensure the system provides the best results and continued service.

POSTrack V5 Specifications

1. Physical

Computer System

Temp Range:	-20 deg C to +55 deg C
Size:	279 L x 330 W x 91 H mm
Weight:	5.9 kg

Pilot Touch Screen Display

Temp Range:	-10 deg C to +50 deg C
Size:	48 L x 215 W x 175 H mm
Weight:	1.34 kg
Power:	20 - 34 Volts DC, 110 W Max (including IMU, GPS, pilot display)

2. I/O

Ethernet (10G base-T)

Parameters	Time tag, status, position, attitude, velocity, track and speed, dynamics, performance metrics, raw IMU data (200 - 300Hz), raw GPS data (10Hz)
Display Port Low rate	(1 Hz) UDP protocol output
Control Port	TCP/IP input for system commands
Primary Port	Real-time (up to 300 Hz) TCP/IP protocol output
Secondary Port	Buffered TCP/IP protocol output for data logging to external device

Logging

Parameters	Time tag, status, position, attitude, velocity, track and speed, dynamics, performance metrics, raw IMU data (200 - 300 Hz), raw GPS data (10Hz)
Media	External Removable 1 Gbyte Flash Disk (2 supplied), Internal Embedded 1 Gbyte Flash Disk for redundant logging

RS232 NMEA ASCII Output

Parameters	NMEA Standard ASCII messages: Position ($INGGA), Heading ($INHDT), Track and Speed ($INVTG), Statistics ($INGST) Rate Up to 50 Hz (user selectable)

RS232 High Rate Binary Output

Parameters	User selectable binary messages: Time, position, attitude, speed, track, PAV30 output, Yaw Drift Correction.
Rate	Up to 200 Hz (user selectable)

RS232 Input Interfaces

Parameter	Gimbal encoder input, AUX GPS input (RTK, NavCom Starfire, OmniStar HP), RTCM104 DGPS Corrections input
Rate	1 to 200 Hz

Other I/O

1PPS	1 pulse-per-second Time Sync output, normally high, active low pulse
Event Input (2)	Two time mark of external events. TTL pulses > 1 msec width max rate 100 Hz

4. Sensor Interfaces

3-axis Mount

Drift Correction	T-A5 (analog/ RS232), PAV30 (RS232), GSM3000(RS232) DSS Azimuth Mount (RS232)
Levelling Control	PAV30 (RS232), GSM3000 (RS232)
Gimbal Encoder	T-A5 (RS232), PAV30 (RS232), GSM3000 (RS232) DSS Azimuth Mount (RS232)
Stab Control	GSM3000 (RS232)

Frame Camera

Triggering/MEP	RC20/30, TOP RMK, LMK 2000, Vexcel UltraCam Generic
Data Interface	RC20/30 (RC20 w/o data annotation), TOP RMK, Vexcel UltraCam, LMK2000 (requires additional interface module) Generic

LIDAR

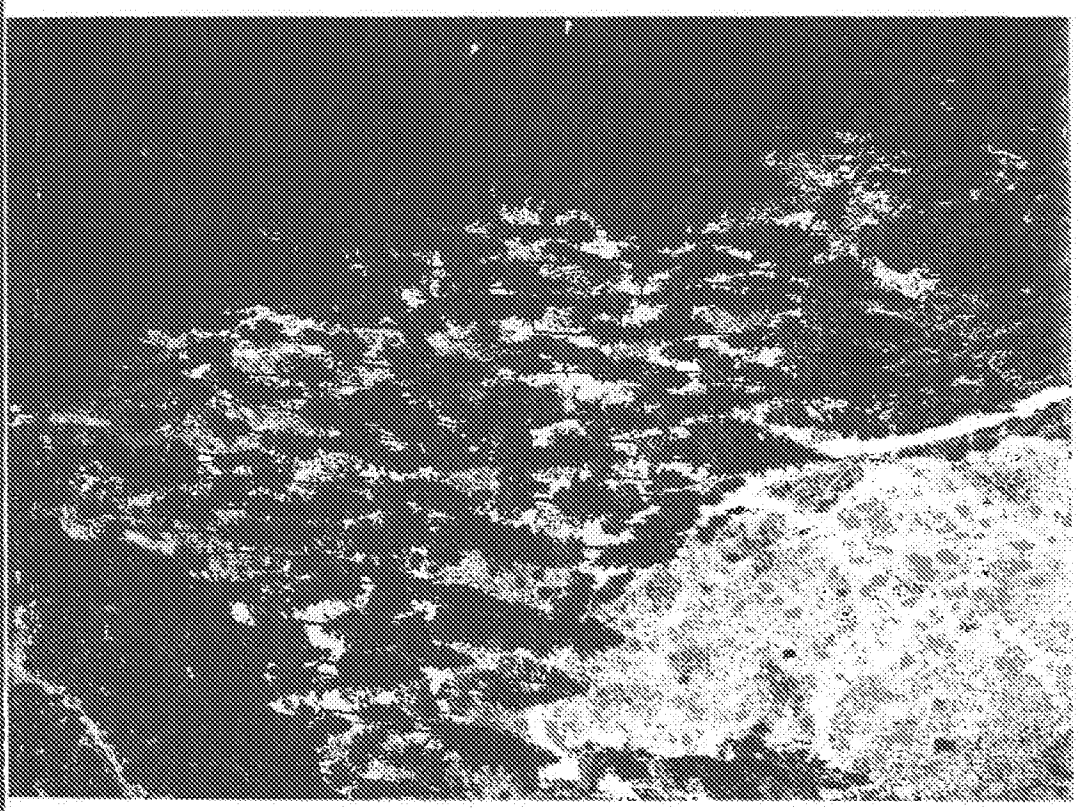
Logging On/Off	ALS40/50, Riegl Q240

5. User Supplied Equipment

PC for POSPac Post-processing Software

- Pentium III 800Mhz or equivalent (minimum)
- 256 MB RAM, 400 MB free disk space
- USB Port (for Security Key)
- Windows 2000/XP

REMOTE SENSING FOR RESOURCE INVENTORY, PLANNING, AND MONITORING



Proceedings of the Second Forest Service Remote Sensing Applications Conference — Slidell, Louisiana and NSTL, Mississippi

April 11-15, 1988

American Society for Photogrammetry and Remote Sensing

METHODS

Test Sites

The CIR video camera was field tested over sites in two regions, the Lake States (Minnesota, July 1986) and the Rocky Mountains (Wyoming, September 1986). In Minnesota, the site selected was infested by forest tent caterpillar, Malacosoma disstria (Hubner), a hardwood defoliator. In Wyoming, sites were selected which included trees attacked and killed by mountain pine beetle, Dendroctonus ponderosae (Hopkins).

Forest tent caterpillar feeds on a wide variety of hardwoods; in Minnesota the preferred host is aspen, Populus tremuloides (Michx.). The older larvae often completely defoliate the tree during outbreaks. The infestation site selected was in the north central section of the state near the town of Brookston, Minnesota.

Mountain pine beetle ranks first in destructiveness among the bark beetles of the West. It feeds on a variety of pine hosts and infests mature forests. Attacks by this insect cause a discoloration of the foliage which changes from the normal green to light greenish yellow, and finally to a reddish brown. The damaged trees in this study were all ponderosa pine, Pinus ponderosa (Laws). The bark beetle damage site was in southeastern Wyoming near Laramie Peak on the Medicine Bow National Forest.

Video Equipment

Video imagery for both areas was acquired using a CIR video camera developed by the University of Minnesota's Remote Sensing Laboratory and manufactured by E. Coyote Enterprises (marketed under the trade name Biovision)*. The camera is a modification of a broadcast-grade, three tube color camera which has been modified to simulate the response of color infrared film. Using dichroic mirrors, an internal optical beam splitter separates incoming energy into three spectral images (green, red and near infrared). The images are focused onto three 2/3 inch video tubes which are scanned simultaneously (Meisner and Lindstrom 1985).

Output from the video camera is a standard NTSC video signal which is recorded on a portable VHS standard video cassette recorder. The audio track of the VCR is tied into the aircraft intercom system to allow crew members to record pertinent information, i.e., flight conditions, LORAN coordinates, etc., as the imagery is being collected. In addition, the particular VCR utilized for this mission allows for digital numbers, i.e., date and flight line number, to be superimposed onto the video image for later reference. A 5-inch color monitor is carried for in-flight monitoring of the video output.

1840

Imagery and Data Acquisition

The acquisition of imagery and data at each test site consisted of aerial sketch mapping data, CIR aerial photography, and CIR video imagery. The aerial platform used for acquisition of imagery in Minnesota was a Cessna 206; and in Wyoming, imagery was acquired with a Forest Service Beechcraft Queen Air photo aircraft. The Minnesota site was flown in late June while the Wyoming site was flown in mid-September.

Aerial sketch mapping. Both sites were sketch mapped by experienced pest management observers for comparison with the video technique. In Minnesota, defoliation intensity was recorded on 1 1:24,000 scale USGS map base. Defoliation intensity was classified and mapped using three classes; light (<25 percent), moderate (26-50 percent), and heavy (>51 percent) categories. In the Wyoming sketch map survey, locations of groups of dying trees were recorded on USDA Forest Service 1/2 inch to the mile recreation maps.

*The use of trade, firm, or corporation names in this publication is for the information and convenience of the reader. Such use does not constitute an official endorsement or approval by the U.S. Department of Agriculture.

Aerial photography. Aerial photography was acquired to provide an accurate record of the conditions on the sites and as an aid for verification of both the video imagery and the sketch mapping information. In the forest tent caterpillar infested area photography was required with a 35mm camera (Canon F-1) equipped with a 28mm lens; for the bark beetle areas, a Zeiss mapping camera system was used. This system consisted of a RMK 21/23, 9-inch (230mm) aerial format camera with an 8-1/4 inch (210mm) focal length lens, and an NT-1 navigation telescope for visual navigation. Test sites were photographed with color infrared film, Kodak Aerochrome Infrared Type 2443. Vertical imagery was acquired along flight lines flown through the infested areas. Photo scale on the Minnesota 35mm CIR photography was approximately 1:64,000 and the Wyoming 9 by 9 inch CIR photography was 1:8,000. These photo scales were selected in order to acquire one mile wide photo coverage on the aerial photography format used.

The term "reference data" will be used to refer to the aerial photography acquired for the purpose of verifying the condition at the test sites and will be used in place of the commonly used term "ground truth'.

Video imagery. The CIR video imagery acquired for both test sites was obtained using the CIR video system owned by the University of Minnesota. The components of the aerial video system consist of a camera, portable recorder, portable color monitor, battery pack, and required power and signal cables. Vertical imagery was acquired with the video camera. Table 1 lists several flying altitudes and width of ground coverage for the video 8.5mm and 12.5mm lenses. Also listed is the equivalent ground coverage and photo scales for the 9 by 9 inch coverage.

Table 1. Flight parameter for acquisition of video imagery and the equivalent photo coverage.

Video Imagery Acquisition			Aerial Photo Acquisition	
Video Lenses	Flight Altitude (AGL)	Ground Coverage	Ground Coverage on 9 X 9 Aerial Photos	Photo Scale
8.5mm	2,550	2,640 ft (1/2 mi)	2,250 ft	1:3,000
12.5mm	3,750	2,640 ft (1/2 mi)	3,000 ft	1:4,000
8.5mm	5,100	5,280 ft (1 mi)	4,500 ft	1:6,000
12.5mm	7,500	5,280 ft (1 mi)	6,000 ft	1:8,000

Video Camera Modifications

The CIR camera has been recently modified to allow for external adjustment of signal gain for each of the individual spectral channels. This allows the response of the camera to be interactively "tuned", while airborne, to optimize the camera response for a particular application. For example, the desired near infrared sensitivity will be significantly different for studies over coniferous, as opposed to deciduous, forest stands. This is due to variations in reflectance of various cover types in the near infrared wavelengths. The camera response can be adjusted interactively to optimize it for the cover type (vegetation) and/or stress condition under study. This process is currently purely empirical, as an optimal response is selected by "tuning" the camera while observing the video output. Evaluations are currently underway which will look at the applicability of high resolution spectral measurements of cover types and stress conditions as inputs into spectral gain adjustments and narrow band filtration schemes for airborne video cameras.

1841

Imagery and Data Analysis

Sketch map, reference data (aerial photos), and video data collected on the location and intensity of pest damage on the two test sites was transferred to a 1:24,000 USGS map base. Two techniques were used for transferring the polygons of pest damage from the aerial photography and video imagery to the base maps. The first technique used a Bausch and Lomb zoom transfer scope. In the second technique, the video data was interpreted directly from the monitor screen to a topographic map. A digital freeze frame unit was used for both techniques, this allowed capturing individual frames of interest until data transfer was complete.

The maps derived from all three sources of data (aerial photography, sketch mapping, and video) were digitized and entered into a microcomputer-based geographic information system (ERDAS)*, which allows for the storage and analysis of data. The data was digitized as polygons of pest damage, which were then rasterized for input into the geographic information system (GIS). A 10 meter x 10 meter cell size was selected as being most representative of the spatial nature of the data. The results of this analysis were presented in both tabular (summary statistics) and spatial (map) format.

The video and sketch map classification results were compared for statistically significant differences. A discrete multivariate analysis procedure (Congalton et al 1983) yielding the kappa statistic was used to compare classifications. The kappa statistic measures the overall agreement between two classifications and is adjusted for chance agreement. A kappa value of +1 indicates perfect agreement between classifications; a value of 0 indicates agreement no better than that attributable to random chance; and a value of -1 indicates no agreement between classifications. The kappa statistic is estimated by KHAT and may be tested for significance with the Z statistic. This evaluation will show the trade-offs in accuracy and operational efficiency between the video technique and the sketch mapping technique.

Results and Discussion

A preliminary evaluation was conducted following the transfer of data from the imagery to the base maps. An acetate overlay was prepared for each of the three sources of damage data showing the polygons of defoliation or mortality. The individual overlays were color coded according to the source of the data. The three overlays were then registered together in order to allow a visual comparison between the sketch mapping technique and the video technique. The aerial photography was used as "reference data" in order to evaluate the accuracy of the two techniques for

detecting and mapping polygons of insect damage. Figures 1 and 2 show the individual overlays for each of the three data sources at the two test sites.

The overlays were then digitized from the base maps into a microcomputer-based geographic information system. A spatial data layer was created for each data set (photography, video and sketch map) by damage categories. Within the GIS, the video and sketch map data layers were overlayed onto the photo layer (reference map) using 10 meter cells as the units of comparison. An error matrix was produced to report site-specific errors between each data layer and the reference map.

An error matrix was produced for each of the following categories:

1. Forest tent caterpillar – A. Photography vs. video
   B. Photography vs. sketch map
2. Mountain pine beetle – A. Photography vs. video
   B. Photography vs. sketch map

Table 2. KHAT statistics for the Four Assessment Techniques.

1. Forest Tent Caterpillar:	A. Photo vs. Video	KHAT = 0.60390	P>.001
		Z = 789.51	
	B. Photo vs. Sketch Map	KHAT = 0.43598	P>.001
		Z = 546.85	
2. Mountain Pine Beetle:	A. Photo vs. Video	KHAT = 0.21074	P>.001
		Z = 39.96	
	B. Photo vs. Sketch Map	KHAT = 0.07983	P>.001
		Z = 23.11	

The overall accuracy of the error matrix for each of four comparisons was assessed by using KHAT, an estimate of the Kappa statistic. A test of significance for KHAT for each comparison was conducted to determine if the classification agreement was significantly better than that attributable to random chance. The values for KHAT and the corresponding P-values for the tests of significance are shown in Table 2. In all cases, the KHAT

statistic was significant for each matrix as indicated by the Z statistic. However, the Z statistic, which is used to test for this significance, was much greater in the forest tent caterpillar matrixes than the differences indicated by the Z statistic for mountain pine beetle.

A pairwise test of significance was performed between the two independent KHATs (i.e. for video and sketch mapping) for each insect to determine if the two error matrixes are significantly different (Cohen 1960). These statistics are:

$$Z_{FTC} = 150.31$$

$$Z_{MPB} = 20.75$$

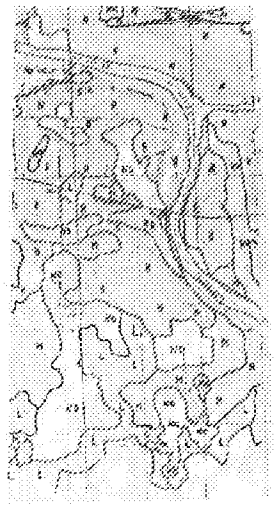
Based on these tests of significance the video technique for assessing hardwood defoliation gave a significantly more accurate assessment of damage than the sketch map technique. For mountain pine beetle, although the differences between the video technique and sketch mapping was significant, this difference was significantly less than those values associated with the forest tent caterpillar, as evidenced by the Z statistic and the corresponding KHAT values.

In regard to these differences, it should be considered that the video interpreters encountered some difficulty in locating the video coverage on the USGS topographic quad maps for the Wyoming site. This was due to the site being in a remote forest area with very few identifiable landmarks such as roads, streams, etc. This was not the case with the Minnesota site where there were many good landmarks. This problem could be greatly reduced by interfacing a Loran navigation system with the video recorder. Digital latitude and longitude coordinates would be superimposed onto the video image and displayed on the monitor screen. Since this study was undertaken, a technique for accomplishing this has been developed at the University of Minnesota (Newhurst and Meisner, 1988). When the video image is viewed in the freeze frame mode, the interpreter could quickly locate the general area by using the coordinates on the map and therefore save time in the transfer of data.

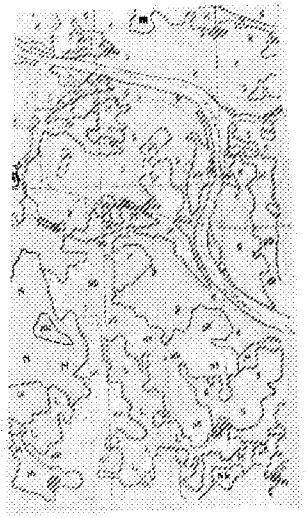
CONCLUSIONS

Two conclusions seem apparent after examination and analysis of the overlay/mapped data.

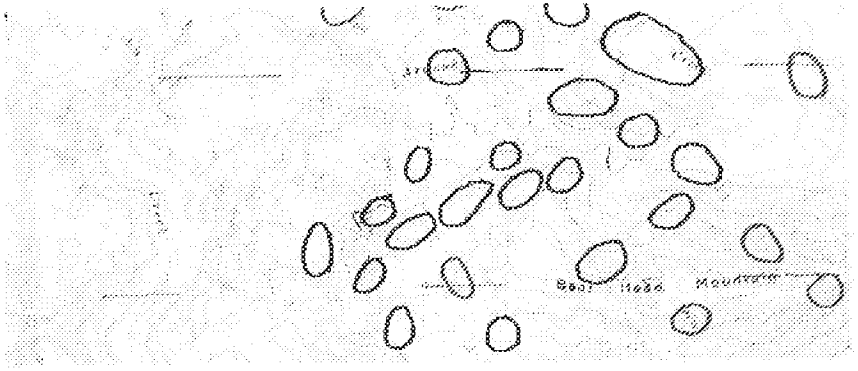
1. The degree of detail in mapping the various classes of forest tent caterpillar defoliation from the video is superior to the sketch mapped defoliation (Figure 1). An image interpreter has a definite advantage in looking at a video monitor in a freeze frame mode versus an observer in a moving aircraft.



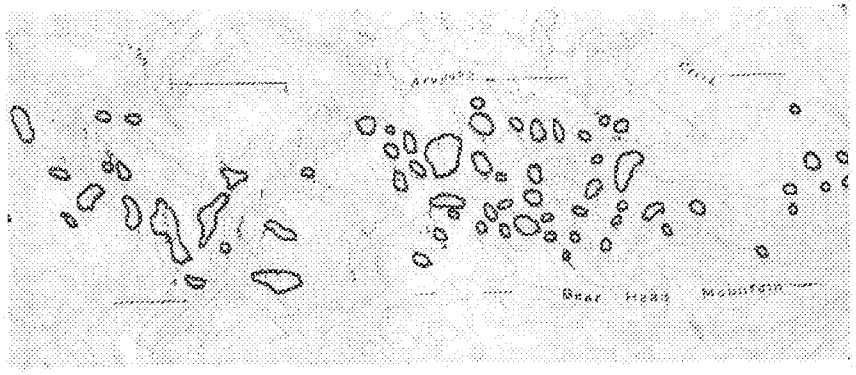
Video Map



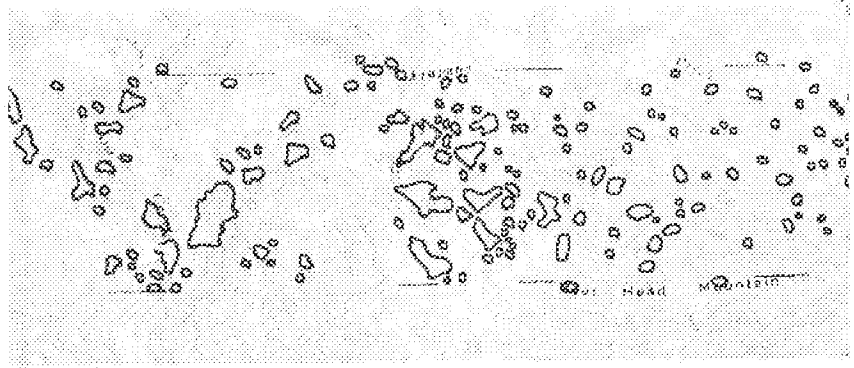
Aerial Photo Map



Sketch Map



Video Map



Aerial Photo Map

Figure 2. Mountain pine beetle mortality on a portion of the Wyoming test site. Maps were prepared from three different sources of data - sketch map survey, CIR video imagery, and CIR aerial photos (reference data base). The polygons represent groups of ponderosa pine discolored from recent beetle attacks.

1843

LOCATING OAK MORTALITY IN THE MISSOURI OZARKS WITH LOW-LEVEL COLOR INFRARED COLOR PHOTOGRAPHY

Jerry D. Gott
Forest Soil Scientist
USDA Forest Service
Mark Twain National Forest
401 Fairgrounds Road
Rolla, Missouri 65401

Jay R. Law
Timber Staff Officer
USDA Forest Service
Mark Twain National Forest
401 Fairgrounds Road
Rolla, Missouri 65401

A. Steve Munson
Forest Entomologist
USDA Forest Service
Northeastern Area State & Private Forestry
St. Paul, Minnesota 55108

ABSTRACT

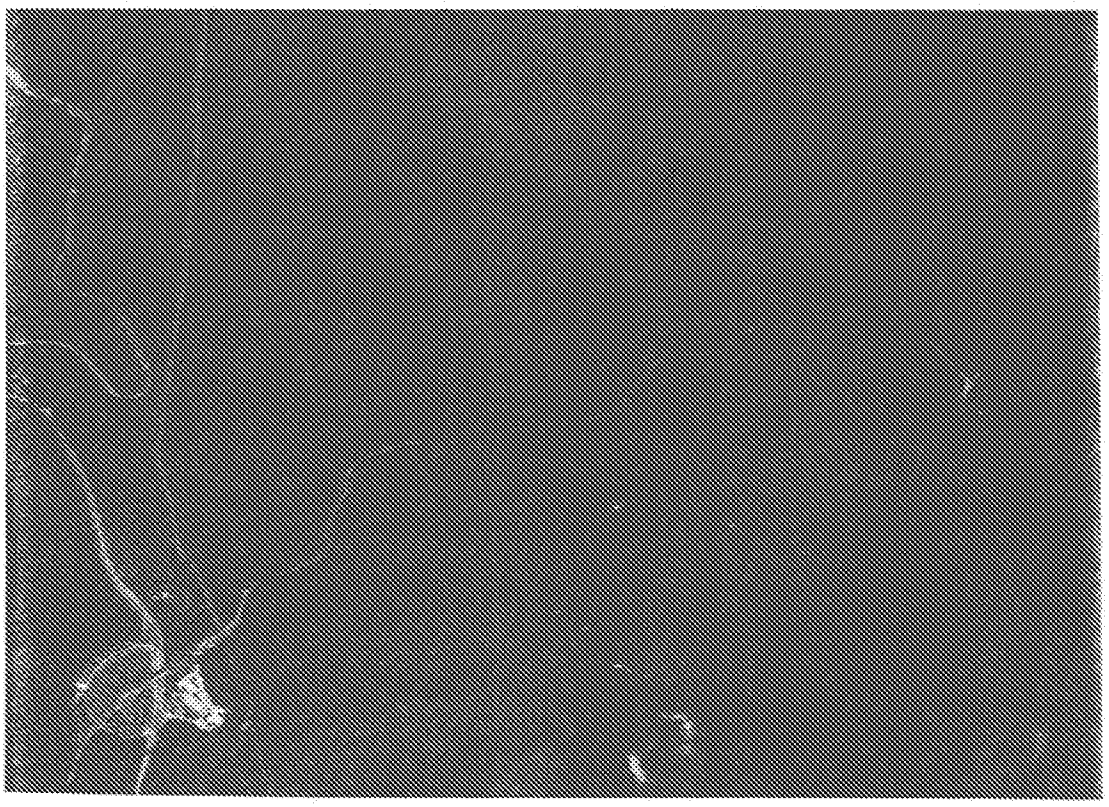
In 1980 and 1983, the Ozark Region of Missouri suffered extreme droughts. Serious mortality has occurred in the red oak group, primarily, scarlet oak (Quercus coccinea Muenchh.) and black oak (Quercus velutina Lam.). Low level, color infrared aerial photography with 100 acre photo interpreted cells on a systematic sampling design, was used to estimate the extent of the mortality within affected areas. Based on this sample, 180,000 acres of the National Forest are expected to show some signs of oak mortality. Correlation with soils, landform and aspect to the incident and extent of the mortality was also tested using the photo cells.

INTRODUCTION

The Mark Twain National Forest has been salvaging small amounts of dead and dying scarlet (Q. coccinea Muenchh.) and black oak (Q. velutina Lam.) since 1973. In 1978, Mark Twain National Forest personnel began reporting sizeable areas of dead and dying oak trees on the southeastern part of the Forest. One 28 acre area on the Van Buren Ranger District was part of a timber sale which had been marked for thinning two years earlier. When harvesting began, it was found that most of the scarlet oak and black oak sawtimber trees on the site were either dead or dying.

In 1980, because of the increase in oak mortality, the Forest initiated a major oak salvage sale program and began an investigation to describe the extent of the problem and to look into possible causes of the mortality and its effect on the timber resources of the Forest.

PROTECTING NATURAL RESOURCES WITH REMOTE SENSING



Proceedings of the Third Forest Service Remote Sensing Applications Conference — April 9-13, 1990

American Society for Photogrammetry and Remote Sensing

OTHER APPLICATIONS

The potential applications of airborne video are wide ranging. Footage acquired over the past twelve months has already been used to update GIS data, demonstrate differences between planned and harvested units, and evaluate possible timber trespasses. Requests for wildlife habitat monitoring, glacial advance/retreat documentation, and inventories for watershed restoration projects are tentatively scheduled. Other yet untested applications include identification of bald eagle nest trees, verification of "as built" construction, fire monitoring, insect damage and/or disease documentation or law enforcement evidence.

CONCLUSIONS

In the Chatham Area, this application of airborne video has already proven to be successful in meeting project specific needs for GIS data base update and other purposes in a timely and cost effective manner. The video imagery produced this year has served as a valuable resource management tool that will continue to improve with refinements in technique, improvements in equipment, and exploration of addional applications.

REFERENCES

Bergey, Robin M., 1990, Stereo Video Aerial Photography, Project Report, USDA Forest Service, Tongass National Forest, Chatham Area, Sitka, Alaska.

Bergey, Robin M., J. Caylor, W. Fieber, and R. Skillings, 1989, Stereo Video Aerial Photography Study Plan, USDA Forest Service, Tongass National Forest, Chatham Area, Sitka, Alaska.

Acknowledgements

The authors wish to acknowledge substantive advice and encouragement provided by Benn' Davis of the USDA Agricultural Research Service Remote Sensing Research Facility in Weslaco, Texas. We also wish to thank our respective units for taking the risk of supporting this work, and finally we wish to thank NFAP's Rondy Steadman for her gracious perseverance in typing and formatting the manuscript for publication.

AIRBORNE VIDEO TECHNOLOGY

Richard J. Mynre
Lee A. Graham
and
Carl R. Sumpter
USDA Forest Service
Forest Pest Management/Methods Application Group
1925 E. Mulberry St.
Fort Collins, CO 80524

ABSTRACT

Airborne videography is another potential remote sensing tool for resource managers. Airborne video technology is presently being evaluated and a total system is being developed for use by forest pest managers in the U.S. Forest Service. The package consists of two major components -- an airborne video image acquisition system and a video image analysis system. This package could have wider use in resource management disciplines other than forest pest management.

INTRODUCTION

Airborne video imagery is a potential tool for resource managers dealing with forest pest activities and problems. It provides a new mechanism for acquiring timely information to assess and evaluate the status of resources and for identifying and monitoring problem areas. This technology also shows promise for applications in other resource management domains. In forest pest management, airborne videography is not viewed as replacement for aerial photography, but can be substituted for photography where the needs do not demand the quality and cost of photography. There are many resource activities where remote sensing and aerial photography data are not being used. These gaps could be filled by initiating airborne videography techniques. This paper describes the airborne video data acquisition and analysis package currently being developed by the Methods Application Group, Forest Pest Management (FPM/MAG) of the USDA Forest Service.

The advantages of airborne video over conventional aerial photography/camera systems are:

(1) the immediate availability of imagery,
(2) error-proofing, in that what is recorded can be viewed in flight on the video monitor,
(3) provision for a straightforward pathway from tape to digital format for computerized image processing,
(4) the lower cost of video cameras/videotape relative to that of cameras/film used in conventional photography, and
(5) improved success rate in acquiring the desired coverage at a given point in time (especially important where narrow biological windows are involved).

Forest Pest Management in the U.S. Forest Service is evaluating imagery to supplement the current sketch mapping techniques used for forest pest surveys. Initial tests were conducted with a color infrared video camera over test areas containing mountain pine beetle mortality in Wyoming and forest tent caterpillar defoliation in Minnesota (Munson et al., 1988). Two general conclusions were apparent from the examination of the video imagery, sketch map data, and aerial photography. First, the degree of detail possible in mapping classes of defoliation from video is superior to that obtainable via the sketch mapping technique. Secondly, the positional accuracy of polygons (map locations) of insect damage appears to be greater when using video imagery. The discouraging part of the tests was the poor resolution of the color infrared tube camera.

An evaluation was recently conducted to determine the status of commercially available video equipment now on the market that could be adapted for airborne use. This evaluation produced the following information:

(1) new solid state (chip/CCD) cameras are superior to tube cameras for improving resolution,

(2) shuttered video cameras are available that produce higher quality imagery plus reduce image motion/blue and vibration problems that may arise in airborne systems,

(3) VHS recorders and tape will soon be supplemented by a new recording system called Super-VHS (S-VHS). S-VHS has several advantages over the present system, among them increased resolution, improved color quality and improved signal-to-noise ratio through increased band width.

Based on the findings of this evaluation, FPM/MAG personnel began development of an airborne video package suitable for addressing forest pest management applications. Planned for delivery in spring, 1991, this package consists of an airborne video acquisition module and a video image analysis module. Its components are described in the following sections.

AIRBORNE VIDEO IMAGE ACQUISITION SYSTEM

The airborne video data acquisition system assembled by FPM/MAG consists of the following components:

Video Camera
The major features of the camera are (a) S-VHS format, (b) three charge coupled device (CCD) sensors, and (c) high speed shutter system for reducing image motion and blurring, and (d) remote-controlled zoom lens.

Video Recorder
A portable S-VHS recorder unit is used for recording both audio and video data.

Video Monitor
A small monitor is used in-flight for both observing what is being recorded and to adjust the camera for image quality.

Auxiliary Equipment
This includes all cabling to link/connect all components and the power converters and inverters needed to match equipment power demands to power sources (both aircraft and portable power supplies).

Caption Generator
This unit provides a linkage between the video camera/recorder and an aircraft navigation system. Through this linkage, positional information (latitude, longitude, aircraft track or bearing) can be recorded on video frames and in microcomputer text files. Microcomputer software (IBM PC-based) controls the manner of recording these data on videotape.

Electronic Navigation Unit
A LORAN-C navigation system can provide positional data as well as time, date, and aircraft heading through an RS-232 interface to the caption generator.

Techniques are being developed to address video mission flight planning and airborne operation in order to facilitate the operational utilization of the airborne video system.

VIDEO IMAGE ANALYSIS SYSTEM

The product of a successful video mission is a videotape(s) containing the areal coverage needed for a resource management application. The first step in using these data is to review the entire tape, making note of the beginning and ending points of each flight line relative to the VCR's time or framecounting meters. Audio information recorded in-flight is particularly helpful for identifying these points as well as indicating navigation errors and/or features to be noted.

Once the tape has been reviewed, the process of interpretation can begin. There are many ways in which video imagery can be used in management applications. The simplest approach is to view the videotape and sketch features of interest directly on to hardcopy maps or mylar overlays. The positional information recorded on the videoframes is used as an aid to locating a particular frame on the reference map (usually a topographic map). No special equipment beyond the S-VHS recorder and monitor from the data acquisition module is required, although photointerpretation aids can be used to expedite the interpretation process. Templates can be constructed that approximate the areal coverage of a videoframe of a particular swath width. This tool can help the interpreter in avoiding double interpretations and estimating the position of a feature seen on the monitor compared to the aligned template on a map. Scales for measuring the approximate size and areas of features for a particular swath width can also be used.

Microcomputers equipped with special image capture graphics boards and software provide a platform for interpreting information from video imagery in a format suitable for geographic information systems (GIS) applications. Since pest and resource inventory surveys tend to cover large geographic areas, numerous images must be captured from videotape into digital computer files. FPM/MAG's survey of available image processing software indicated that although there were many image processing packages on the market, none were capable of grabbing large numbers of frames with a uniform endlap between frames.

However, most image capture board vendors supply software libraries for use in coding image capture programs. The AT&T Truevision libraries for the TARGA line of image capture boards were used to write a program called AUTOGRAB. AUTOGRAB can perform the following functions:

(1) capture images with a user-defined endlap a flight line at a time,
(2) approximately georeference each image using positional information derived from a video mission-planning program (also produced by FPM/MAG) or LORAN-C coordinate information recorded during the mission,
(3) reorient the images in an approximate North-South direction, and
(4) prepare the captured images for inclusion in a computerized indexing system called HyperIndex.

The captured images are stored in the TARGA file format, which can be easily integrated into a number of image analysis packages for subsequent processing.

As mentioned earlier, a video mission produces a large number of images that require interpretation to address the desired resource management problem. Since each captured video frame is stored in an individual computer file, a mechanism for indexing and retrieving the files in an efficient manner is desirable. For forest pest management use, some type of IBM PC/compatible platform was desired. The HyperIndex module of MIPS (Map and Image Processing System, MicroImages, Inc.) was positively evaluated by FPM/MAG as a low-cost and efficient means of indexing a wide range of geographic data, including scanned maps, photographs, and slides, vector data imported from different GIS formats or derived from interpretations, video and satellite imagery, and databases. HyperIndexed images and information are retrieved from an object hierarchy by selecting a feature of interest in the current display with a click of the computer mouse. In FPM pest survey applications, indexed video imagery is retrieved by clicking on a location within scanned topographic maps. Once an image has been retrieved, it is possible to scroll up, down, and across flight lines using the arrow keys on the keyboard.

HyperIndex can also be used to perform quick point location interpretations of pest damage from video imagery. A pilot project now underway in Texas will use the symbol overlay feature of HyperIndex to mark southern pine beetle spot locations using a 4 color symbol scheme (each color representing the severity of the outbreak in terms of number of trees infested). Each symbol is in turn linked to a record in a database, providing a mechanism for entering, retrieving, and updating management information related to that spot. The goal of the application is to provide fast-turnaround hardcopy prints of imagery and/or maps of pest locations for use by crews during ground surveys and control operations.

Other features of MIPS can be exploited to improve the quality and accuracy of geographic data interpreted from video imagery. For example, the AUTOGRAB program only approximately georeferences images at the time they are captured from videotape. Georeferencing of videoframes can be improved by adding control points to images or by using a process called

1847

vector warping. The later process involves plotting calibrated vector objects on top of video images, warping them to fit the image, then applying the resulting geometry to correct the image. The nature of video imagery does create problems in the application of these methods. Since video surveys are often flown so that an individual frame covers a very small piece of ground, identifying control points or features suitable for warping can be quite a challenge in heavily forested areas. FPM/MAG will continue to refine in-flight georeferencing techniques (by incorporating global positioning technology and/or corrections for tip and tilt of the aircraft in current LORAN-C methodologies) so that they can adequately substitute for control point and warping methods.

Finally, image processing software packages such as MIPS typically include methods for interpreting polygonal information, estimating the areas of features, and/or exporting and importing the resulting information into GIS databases. Interpretation methods may be as simple as drawing around a feature using a mouse. Alternatively, automated and semi-automated image classification techniques can be applied that use data on color signatures and feature size to interpret classes of information from imagery. It is worth noting that great caution must be taken when applying automated and semi-automated classification techniques to images derived from scanned photographs and videotape. The color signature of a a particular feature in the center of the image may be quite different than the same type feature found on the its edge. Typically, an interpretation tool which provides elements of automated image classification methods in a format permitting a high degree of interaction with the user (allowing subjective interpretations of how features are to added/deleted from a particular classification) is desirable for interpreting video imagery. The Feature Mapping process within MIPS is a one example of an interpretation tool with these capabilities and was in fact designed specifically to address the challenges posed by video imagery.

As stated earlier, there are a number of hardware and software platforms available that capable of handling video imagery. The equipment and software described in this document were evaluated, developed, and selected with forest pest management applications in mind. FPM/MAG will continue to evaluate available technologies for acquiring and processing video imagery and adapt the modules of the video package as required.

SUMMARY

A need for alternative imagery sources for detecting and evaluating forest pest insect damage has been recognized by the U.S. Forest Service. FPM/MAG has responded by evaluating video technology and by developing an airborne video package that can be used by forest pest managers in the field. This package includes a data acquisition module (consisting of video camera, recorder and monitor, and a microcomputer-controlled caption generator and geographic positioning component) and a video image processing module (providing methods for manual and computer-assisted interpretation of

forest resources and pest damage from video data). This package will be completed in Spring, 1991.

ACKNOWLEDGEMENTS

The authors wish to thank our cooperators (Don Hunter and Michael Scott) at the National Ecology Research Center, U.S. Fish and Wildlife Service, Fort Collins, CO, for assisting in the early development of the airborne video package.

REFERENCES

Munson, A.S. 1988. Assessment of a Color Infrared Aerial Video System for Forest Insect Detection and Evaluation. In Proceedings of Second Forest Service Remote Sensing Applications Conference, Slidell, LA and NSTL, MS, April 1988, pp. 242-253.

FOREST DEPLETION MONITORING WITH C-BAND SYNTHETIC APERTURE RADAR

Andrew P. Jano
Senior Scientist
Ontario Centre for Remote Sensing
Ministry of Natural Resources
90 Sheppard Avenue East, North York, Ontario M2N 3A1, Canada

ABSTRACT

The recognition and recording of changes in forest cover from growth and depletion are of prime importance for maintaining a forest resource inventory. Landsat MSS and TM imagery proved suitable for identifying and delineating burns and clearcuts, within the limits imposed by their spatial resolution. The uncertainty whether satellite imagery will be available at or near the end of the updating period is, however, a deterrent to operational use.

As satellite radar imagery will become available in the 1990s, the use of radar data is also being considered for resource inventory updating. The frequent coverage of the planned radar satellites, combined with the all-weather imaging capability of radar, promises independence from atmospheric conditions and permits inventory updating at required intervals.

In preparation for the use of spaceborne radar data, airborne C-band synthetic-aperture radar imagery, simulating the imagery expected from Canada's RADARSAT to be launched in 1994, was acquired in 1988 and 1989 over areas of clearcut and selective cuts.

Both visual interpretation and digital image analysis methods were used for the extraction of cutover boundaries. The interpreted and manually mapped boundaries would have to be digitized for inclusion in the digital forest stand map. The digital cutover map required considerable manual editing to produce the final thematic map, from which a boundary vector file may be extracted for direct transfer to the digital data base.

Attempts to detect and delineate partial cuts using single-date imagery failed. Comparison with the second set of radar imagery for detecting the subtle change caused by selective cuts yielded no conclusive results.

INTRODUCTION

With the introduction of GIS-based forest resources inventory in the Province of Ontario frequent inventory updating becomes not only necessary but possible as well, as long as information on changes is available on a frequent, regular basis. Because changes due to growth are slow, gradual and more or less predictable, modelling approaches can provide information on them. Changes due to depletion from fires and harvesting, however, are often unpredictable, and usually rapid and radical. These changes are recognizable by remote sensing.

TEST GOALS AND TEST SET UP FOR THE OEEPE TEST "INTEGRATED SENSOR ORIENTATION"

Christian Heipke, Karsten Jacobsen, Helge Wegmann, Hannover
Øystein Andersen, Barbi Nilsen Jr., Ås

ABSTRACT

The European Organisation for Experimental Photogrammetric Research (OEEPE) has embarked on a multi-site test investigating sensor orientation using GPS and IMU in comparison and in combination with aerial triangulation. The test was expected to demonstrate the extent to which direct and integrated sensor orientation are accurate and efficient methods for the determination of the exterior orientation parameters for large scale topographic mapping. Another test goal was the transfer of the recently developed technology from the research arena to potential users.

In this paper we first give some background on sensor orientation. We then describe the test goals and the expected results, followed by an explanation of the test procedure and organisation. The test consists of two phases. The first phase comprises the system calibration and direct sensor orientation. The second phase deals with the integrated sensor orientation, i e. the integration of the GPS/IMU data into a bundle adjustment. The used test data are described in Nilsen Jr. (2002), the obtained results and an in depth analysis can be found in Heipke et al. (2002).

1 INTRODUCTION

1.1 Background

Image orientation is a key element in any photogrammetric project, since the determination of three-dimensional coordinates from images requires the image orientation to be known. In aerial photogrammetry this task has been exclusively and very successfully solved using aerial triangulation for many decades. Over the years, a number of additional sensors were used to directly determine at least some exterior orientation parameters, albeit with little success until the advent of GPS (global positioning system) in the eighties and the pioneering work of Mader (1986). In this regard it is interesting to note that in the same year Ackermann predicted that "the performance of new navigation systems will allow in-flight measurements of carrier position and attitude to an accuracy which will change the photogrammetric methods fundamentally" (Ackermann 1986, p. 93).

Today, differential kinematic GPS positioning is a standard tool for determining the camera exposure centres for aerial triangulation. Using the GPS measurements as additional observations in the bundle adjustment a geometrically stable block based on tie points alone can be formed, and ground control points (GCP) are essentially only necessary for calibration, for detecting and eliminating the effect of GPS errors such as cycle slips, for reliability purposes, and possibly for datum transformations. One can distinguish between a loose coupling of photogrammetric and GPS observations, sometimes called the "shift and drift approach" (Ackermann 1994; Jacobsen 1997) and a more rigorous GPS/aerial triangulation combination (Jacobsen, Schmitz 1996; Kruck et al. 1996; Schmitz 1998).

Gyroscopes and accelerometers are the components of an inertial measurement unit (IMU)[1]. Using gyroscopes, one is able to determine the rotation elements of the exterior orientation. The accelerometers provide sensor velocity and position. Thus, in principle a GPS/IMU sensor combination can yield the exterior orientation elements of each image without aerial triangulation. This technology opens up

[1] We use the term IMU instead of INS (Inertial navigation system). Following Colomina (1999), an INS contains an IMU as a measurement device plus positioning and guidance functions, mainly realised in software.

many new applications (Schwarz et al. 1993; Colomina 1999; Skaloud 1999; Colomina 2002; for a short historical note on IMU, see Mostafa 2001).
A series of tests and pilot projects has been conducted and has convincingly shown the potential of this new technology (e.g. Skaloud, Schwarz 1998; Wewel et al. 1998; Abdullah, Tuttle 1999; Burman 1999; Colomina 1999; Cramer 1999; Toth 1999; Jacobsen 2000; Kinn 2002). At independent check points (ICP) on the ground, root mean square differences down to 0.1 to 0.2 m were obtained. These results have proven that the determination of image orientation using GPS/IMU observations is a serious alternative to conventional aerial triangulation. In addition, potential error sources have been identified. These include the Kalman filtering of the GPS/IMU data for noise reduction, the determination of parameters for systematic position and attitude corrections of the GPS/IMU data (system calibration parameters), the stability of these parameters over time (especially the stability of the attitude values relating the IMU and the camera coordinate systems), and the time synchronisation between the various sensors.

In aerial triangulation control information in the form of GCP coordinates and the object space coordinates of tie points to be determined are both located on the object surface. Therefore, the computation of the tie point coordinates can be thought of as an interpolation task. Using GPS/IMU observations, on the other hand, the control information is measured at the height of the sensors and is subsequently transferred down to object surface. Therefore, the new approach must be considered as an extrapolation, and thus a compensation of different error sources due to a strong correlation between the related parameters, is much less effective. This fact is particularly true for possible changes in the interior orientation of the camera, which can no longer be compensated by a change in the exterior orientation (e.g. Schenk 1999; Habib, Schenk 2002). In this light, the choice of the object space coordinate system also needs a closer look (see e.g. Jacobsen 2002; Ressl 2002), since the photogrammetric collinearity equations need a Cartesian system, a requirement that the curvilinear mapping systems do not fulfil.

1.2 Some comments on terminology

As is the case with many new technologies, some confusion has arisen about terminology. The traditional task of aerial triangulation is twofold, namely to simultaneously determine the parameters of exterior orientation (and possibly additional parameters for self calibration) of a block of images and the object space coordinates of the tie points and other points. The parameters of interior orientation (calibrated focal length, image coordinates of principal point) are, of course, needed but are assumed to be known and constant. Before it became possible to store and transfer exterior orientation parameters from one compilation session to the next, the tie point coordinates were the most important results, and thus the whole task was also named *point determination*. With the advent of analytical photogrammetry, the focus started to change slowly, and the orientation parameters became more important. Thus, the same task was increasingly called *determination of image orientation*. Today, we observe two new developments: (1) the exterior orientation parameters of a camera can be determined without tie points using GPS/IMU technology, and (2) the same technology is also used to determine the orientation of non-traditional sensors such as laser scanners and SAR sensors. Consequently, *image orientation* has been replaced by the more general term *sensor orientation*. *Sensor orientation* includes all related parameters, regardless of whether they are assumed to be known or unknown, and constant or changing over time. Thus, sensor orientation includes the system calibration parameters of a sensor system (i.e. calibration parameters of each sensor, e.g. the interior orientation parameters of the camera, and parameters relating the individual sensor observations in space and time to a common reference frame) and the exterior orientation parameters of the sensor system.
We further differentiate between *direct sensor orientation* and *integrated sensor orientation*. *Direct sensor orientation* stands for the determination of sensor orientation without image coordinates using only GPS/IMU observations. The system calibration parameters need to be known and thus have to be determined in a separate step beforehand. On the other hand, *integrated sensor orientation* uses all available input, namely image coordinates of tie points, control information in image and object space,

and GPS/IMU observations in a simultaneous adjustment to determine all relevant sensor orientation parameters.

In current literature, sensor orientation (whether direct or integrated) is also called *georeferencing* or *geocoding* (e.g. Schwarz et al. 1993; Cramer 2001). Ackermann writes: "A geo-reference is a global or regional coordinate system to which sensors or spatial object data are related. Hence, georeferencing or geocoding is close to the well known photogrammetric concept of exterior or absolute orientation." (Ackermann 1997, p. 28). *Georeferencing* and *geocoding* have their origin in remote sensing. G*eoreferencing* is also increasingly being used in the spatial information sciences. They emphasise the fact that the sensor orientation parameters are usually only a by-product of photogrammetric processing, and the final results in form of three-dimensional terrain coordinates, a digital terrain model (DTM), an orthoimage and/or structured vector data are needed in a global or regional coordinate system. Consequently, in remote sensing we talk about *georeferencing* or *geocoding an image* and the result is a *georeferenced* or a *geocoded image*, often used as a synonym for an orthoimage. In spatial information sciences we georeference an object (e.g. a road crossing) and mean that we provide coordinates relating to the Earth surface for this object. However, a *georeferenced* or *geocoded image* may have been generated by applying a two-dimensional polynomial rectification based on a few identical points rather than by differential rectification based on the central projection including the image orientation and a DTM. Thus, *georeferencing* and *geocoding* are more general terms, which include various mathematical models for the transformation from image to object space, and which have object space products as output.

In order to emphasise the fact that in topographic mapping from imagery (1) three-dimensional modelling of the imaging process is necessary, and (2) the image orientation parameters have a physical meaning and constitute a result by themselves (although only intermediate) we prefer to use the term *sensor orientation* as described above, when we talk about the interior and exterior orientation parameters of images and the system calibration parameters of a sensor system. We use *georeferencing* when we are concerned with determining object space quantities. Within the test these quantities are exclusively three-dimensional coordinates of terrain points.

2 TEST OBJECTIVES AND EXPECTED RESULTS

The European Organisation for Experimental Photogrammetric Research (OEEPE) has embarked on a multi-site test investigating sensor orientation using GPS and IMU in comparison and in combination with aerial triangulation (see also Heipke et al., 2000; 2001).

The focus of the test was on the obtainable accuracy for large scale topographic mapping using photogrammetric film cameras. The accuracy of the results was assessed with the help of independent check points on the ground in the following scenarios:

- conventional aerial triangulation,
- GPS/IMU observations for the projection centres only (direct sensor orientation),
- combination of aerial triangulation with GPS/IMU (integrated sensor orientation).

The test was expected to demonstrate the extent to which direct and integrated sensor orientation are accurate and efficient methods for the determination of the exterior orientation parameters for large scale topographic mapping.

A further test goal was the transfer of the recently developed technology from the research arena to potential users. This goal is in line with the mission of OEEPE, and it was the main reason for choosing a multi-site test approach. As a consequence, the duration of the test was somewhat lengthy when compared to a single-site investigation. The authors feel, that this disadvantage can be tolerated because they believe that in the long run technology transfer is more important than obtaining results quickly.

3 TEST SETUP

3.1 Preparation

The test consisted of a preparatory period and two analysis phases. It was decided at the outset to organise special test flights to control all aspects of the investigation. In order to enable a fair and meaningful comparison between the two competing technologies the following selection criteria were established for the data acquisition:

- geometrically stable photogrammetric block,
- modern photogrammetric film camera,
- dual frequency GPS receivers using differential carrier phase measurements with a data rate of 2 Hz preferably with identical receivers for the aircraft and reference station,
- a short base line between aircraft and reference station,
- high quality off-the-shelf navigation grade IMU as typically used in precise airborne attitude determination,
- different image scales suitable for large scale topographic mapping,
- a well-controlled test field with a large number of GCPs.

The Institute for Photogrammetry and GeoInformation (IPI), University of Hannover, acted as pilot centre for the multi-site test. In this capacity IPI put together and distributed the test data, and collected and analysed the results received from the test participants. The Department of Mapping Sciences (IKF), Agricultural University of Norway in Ås, carried out data acquisition including the organisation of test flights and the necessary fieldwork.

For the test the IKF test field in Southern Norway was selected. It fulfils all the mentioned criteria and had a number of additional, practical advantages. In order to ensure that potential error sources could be identified individually it was decided to perform two calibration flights at different heights/scales (1:5 000 and 1:10 000) followed by the actual test flight (scale 1:5 000) and a third calibration flight (1:10 000) at the end of the flight mission. During the test flight a GPS reference station, placed in the test field to ensure a short base line and to avoid additional errors, was operated. Details of the data acquisition can be found in Nilsen Jr. (2002).

Next, the raw GPS/IMU data of the whole flight needed to be pre-processed into object space coordinates for the centre of projection of each image accompanied by attitude information in terms of roll, pitch, and yaw values. In order to enable the system calibration (see below) and to create material for checking, the pilot centre measured the image coordinates of all visible GCPs and of a large number of tie points.

3.2 Phase I: System calibration and direct sensor orientation

The first analysis phase comprised the determination of so-called system calibration parameters, i.e. the determination of the boresight misalignment (the angular difference between the IMU and the image coordinate systems), and possibly additional parameters modelling GPS shifts, the interior orientation of the camera, GPS antenna offsets, time synchronisation errors etc. from the information of the calibration flights. Phase I also comprised the direct sensor orientation of the actual test flight based on the GPS/IMU data and the results of system calibration and – as part of the analysis of the results - the derivation of object space coordinates via a least squares forward intersection using the orientation parameters as constant values. Thus, all elements of direct sensor orientation were contained in phase I.

The test scheme of phase I is depicted in figure 1. The data to be sent out to interested test participants consisted of a subset of the measured tie point coordinates for each calibration flight image, the

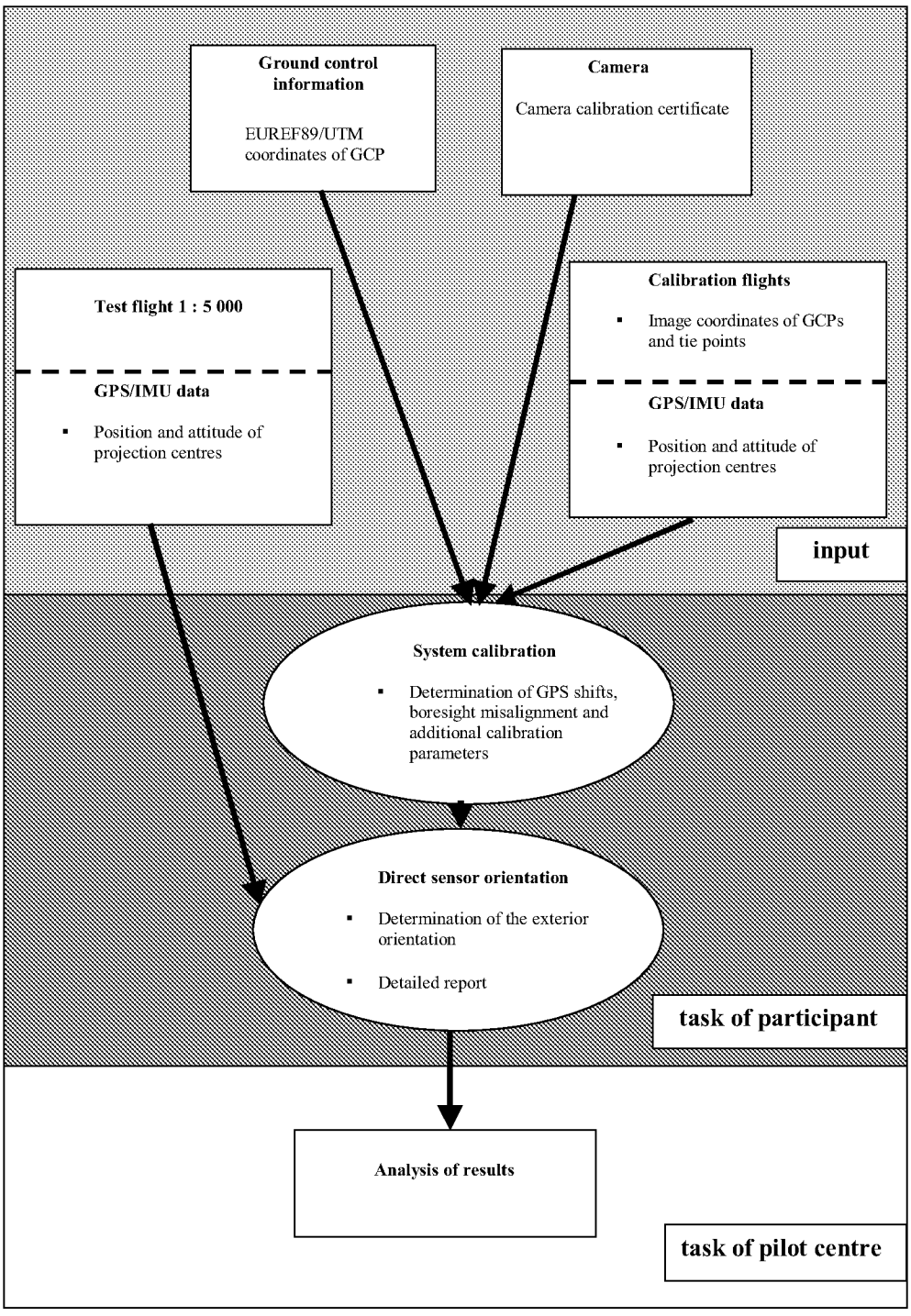


Figure 1: Flowchart of phase I

camera calibration certificates, a sufficient number of GCP coordinates in object space, and the pre-processed GPS/IMU data of the whole flight (all calibration flights and the test flight). The derived system calibration parameters together with the orientation parameters for the calibration flights and the test flight and a detailed report about the work carried out were to be delivered back to the pilot centre for the analysis of the results (see Heipke et al. 2002 for details of the analysis of the whole test).

3.3 Phase II: Integrated sensor orientation

The second phase dealt with the integration of the GPS/IMU data into the bundle adjustment i.e. the integrated sensor orientation. After having returned the results of phase I, the participants were to receive image coordinates of tie points and GCPs of a subset of the test flight images. No object space coordinates of GCPs were to be distributed, and GCPs used in phase I were not to be used as tie points in phase II. Thus, the participants were to receive only information in image space, and not in object space. This decision was taken, because we wanted to explore the advantage of combining GPS/IMU measurements with tie points alone, since (1) tie points can be generated without field work and automatically, and (2) as soon as GCPs are included, their influence may dominate the results, and thus we would run the risk of ending up with a GPS-assisted photogrammetric bundle adjustment.

Combining the information received with the system calibration parameters determined in phase I, the participants would then perform an integrated sensor orientation, refining the exterior orientation (and possibly also the system calibration parameters), and estimating the object space coordinates of the tie points and the GCPs. These values were subsequently to be returned to the pilot centre together with a detailed report describing the adopted model for the integration. The test scheme of phase II is depicted in figure 2.

4 REFERENCES

Abdullah Q.A., Tuttle M.A. (1999): Integrated GPS-inertial measurement solution as an alternative to aerial triangulation: a case study, Proceedings, ASPRS Annual Convention, Baltimore, pp. 867-876 (on CD-ROM).

Ackermann F. (1986): The use of camera orientation data in photogrammetry – a review, IAPRS (26) 1, pp. 93-99.

Ackermann F. (1994): On the status and accuracy performance of GPS photogrammetry, Proceedings, ASPRS Workshop "Mapping and remote sensing tools for the 21st Century, Washington D.C., pp. 80-90.

Ackermann F. (1997): Geo-Kodierung ohne Paßpunkte, GIS (10) 2, pp. 28-32.

Burman H. (1999): Using GPS and INS for orientation of aerial photography, Proceedings, ISPRS Workshop "Direct versus indirect methods of sensor orientation", Barcelona, pp. 148-157.

Colomina I. (1999): GPS, INS and aerial triangulation: What is the best way for the operational determination of photogrammetric image orientation?, IAPRS (32) 3-2W5, pp.121-130.

Colomina I. (2002): Modern sensor orientation technologies and procedures, in: Heipke C., Jacobsen K., Wegmann H. (Eds.), Integrated Sensor Orientation, OEEPE Official Publication No. 43.

Cramer M. (1999): Direct geocoding – is aerial triangulation obsolete?, in: Fritsch D., Spiller R. (Eds.), Photogrammetric Week '99, pp. 59-70.

Cramer M. (2001): Genauigkeitsuntersuchungen zur GPS/INS-Integration in der Aerotriangulation, DGK-C (537), 122 p.

Habib A., Schenk T. (2002): Accuracy analysis of reconstructed points in object space from direct and indirect exterior orientation methods, in: Heipke C., Jacobsen K., Wegmann H. (Eds.), Integrated Sensor Orientation, OEEPE Official Publication No. 43.

Heipke C., Jacobsen K., Wegmann H., Andersen Ø., Nilsen B. (2000): Integrated sensor orientation – an OEEPE test, IAPRS (33) B3/1, pp. 373- 380.

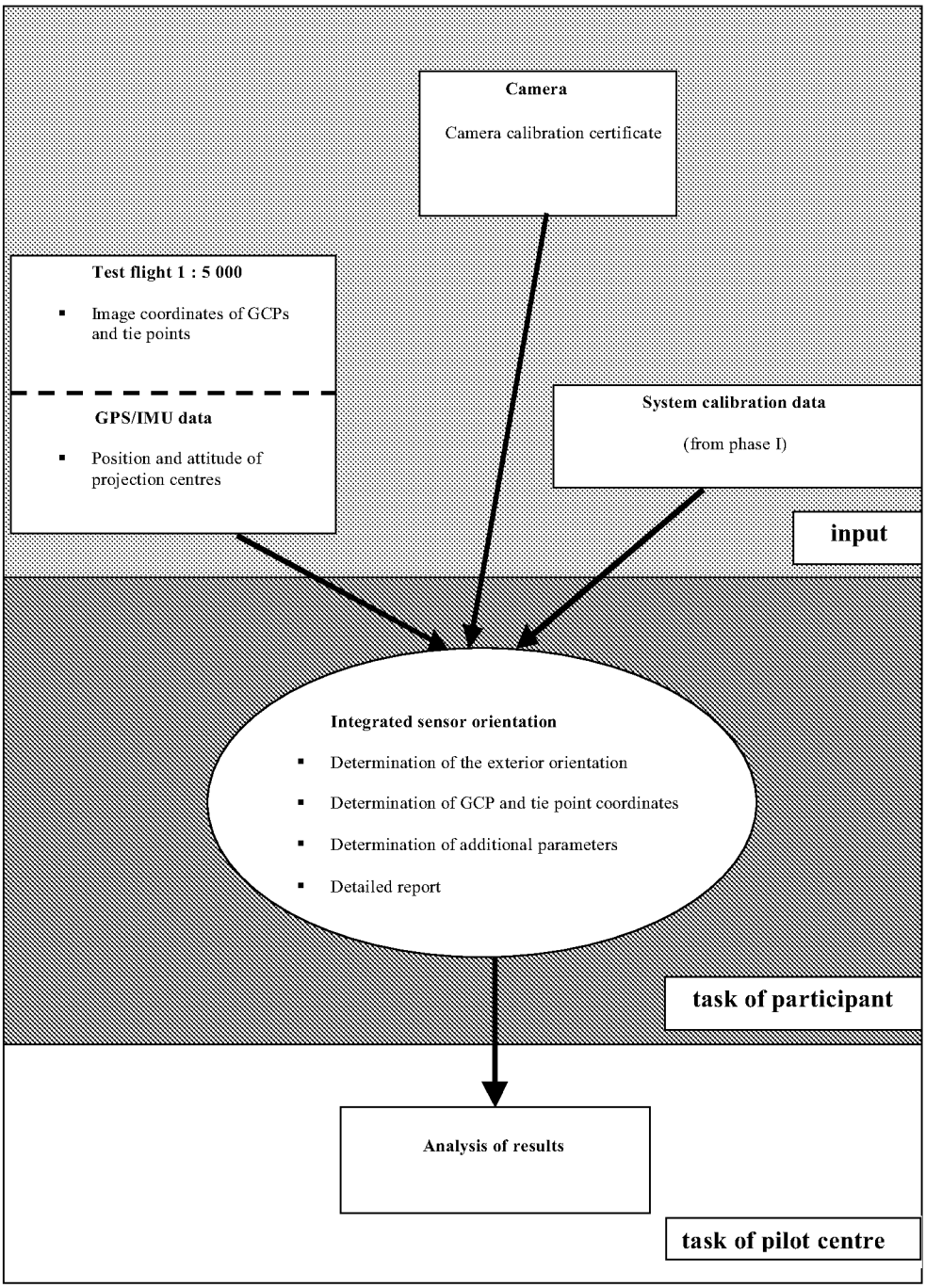


Figure 2: Flowchart of phase II

Heipke C., Jacobsen K., Wegmann H. (2001): The OEEPE test on integrated sensor orientation – Results of phase I, in: Fritsch D., Spiller R. (Eds.), Photogrammetric Week ´01, Wichmann, Heidelberg, pp. 195-204.
Heipke C., Jacobsen K., Wegmann H. (2002): Analysis of the results of the OEEPE test "Integrated sensor orientation", in: Heipke C., Jacobsen K., Wegmann H. (Eds.), Integrated Sensor Orientation, OEEPE Official Publication No. 43.
Jacobsen K. (1997): Operational block adjustment without control points, Proceedings, ASPRS Annual Convention, Seattle, Vol. 2, pp. 238-244.
Jacobsen K. (2000): Potential and limitation of direct sensor orientation, IAPRS (33), B3/1, pp. 429-435.
Jacobsen K. (2002): Transformations and computation of orientation data in different coordinate systems, in: Heipke C., Jacobsen K., Wegmann H. (Eds.), Integrated Sensor Orientation, OEEPE Official Publication No. 43.
Jacobsen K., Schmitz M. (1996): A new approach for combined block adjustment using GPS satellite constellations, IAPRS (31) B3, pp. 355-359.
Kinn G. (2002): Direct georeferencing in digital imaging practice, PE&RS (68) 5, pp. 399-402.
Kruck E., Wübena G., Bagge A. (1996): Advanced combined bundle block adjustment with kinematic GPS data, IAPRS (31) B3, pp. 394-398.
Mader G. (1986): Dynamic positioning using GPS carrier phase measurements, Manuscripta geodetica (11/4), pp. 272-277.
Mostafa M. (2001): History of inertial navigation systems in survey applications, PE&RS (67) 12, pp. 1225-1227.
Nilsen Jr. B. (2002): Test field Fredrikstad and data acquisition for the OEEPE test "Integrated Sensor Orientation", in: Heipke C., Jacobsen K., Wegmann H. (Eds.), Integrated Sensor Orientation, OEEPE Official Publication No. 43.
Ressl C. (2002): The OEEPE-test "Integrated sensor orientation" and its handling within the hybrid block-adjustment program Orient, in: Heipke C., Jacobsen K., Wegmann H. (Eds.), Integrated Sensor Orientation, OEEPE Official Publication No. 43.
Schenk T. (1999): Digital photogrammetry, Volume I, Terra Science, 428 p.
Schmitz M. (1998): Untersuchungen zur strengen GPS Parametrisierung in der gemeinsamen Ausgleichung von kinematischem GPS und Aerotriangulation, Dissertation, Wissenschaftliche Arbeiten der Fachrichtung Vermessungswesen der Universität Hannover, Nr. 225, 121 p.
Schwarz K.-P., Chapman M.E., Cannon E., Gong P. (1993): An integrated INS/GPS approach to the georeferencing of remotely sensed data, PE&RS (59) 11, pp. 1667-1674.
Skaloud J. (1999): Problems in sensor orientation by INS/DGPS in the airborne environment, Proceedings, ISPRS Workshop "Direct versus indirect methods of sensor orientation", Barcelona, pp. 7-15.
Skaloud J., Schwarz K.-P. (1998): Accurate orientation for airborne mapping systems, IAPRS (32) 2, pp. 283-290.
Toth C. (1999): Experiences with frame CCD arrays and direct georeferencing, in: Fritsch D., Spiller R. (Eds.), Photogrammetric Week ´99, pp. 95-107.
Wewel F., Scholten F., Neukum G., Albertz J. (1998): Digitale Luftbildaufnahme mit der HRSC – Ein Schritt in die Zukunft der Photogrammetrie, PFG No. 6, pp. 337-348.

Registration of video to geo-referenced imagery

Rakesh Kumar Harpreet S. Sawhney Jane C. Asmuth Art Pope Steve Hsu
Sarnoff Corporation, CN5300, Princeton, NJ 08530, USA
Email: {rkumar,hsawhney,jasmuth,apope,shsu}@sarnoff.com

Abstract

The ability to locate scenes and objects visible in aerial video imagery with their corresponding locations and coordinates in a reference coordinate system is important in visually-guided navigation, surveillance and monitoring systems. However, a key technical problem of locating objects and scenes in a video with their geo-coordinates needs to be solved in order to ascertain the geo-location of objects seen from the camera platform's current location. In this paper we present the key algorithms for the problem of accurate mapping between camera coordinates and geo-coordinates, called *geo-spatial registration*. Current systems for geo-location use the position and attitude information for the moving platform in some fixed world coordinates to locate the video frames in the reference database. However, the accuracy achieved is only of the order of 100's of pixels. Our approach utilizes the imagery and terrain information contained in the geo-spatial database to precisely align dynamic videos with the reference imagery and thus achieves a much higher accuracy. Applications of geo-spatial registration include aerial mapping, target location and tracking and enhanced visualization such as the overlay of textual/ graphical annotations of objects of interest in the current video using the stored annotations in the reference database.

1 Introduction

Aerial video is rapidly emerging as a low cost, widely used source of imagery for mapping, surveillance and monitoring applications. Visible and infrared (IR) video cameras are increasingly deployed on airborne platforms, both manned and unmanned, to provide observers with a real time view of activity and terrain. However, determining how the locations of objects in a video display relate to the geographic locations of these objects on the observed scene, remains a key technical problem in the use of video from moving vehicles. This relationship between image coordinates and geographic coordinates must be known before actions can be undertaken based on the video. The mapping between camera coordinates and ground coordinates, called geospatial registration, depends both on the location and orientation of the camera and on the distance and topology of the ground. Camera location continually changes as the airborne camera moves. Rough geospatial registration can be derived from the ESD (Engineering Support Data: obtained from the GPS and intertial navigation units etc.) stream provided by the airborne camera telemetry system and digital terrain map data (from a database) [3]. This form of registration is the best available in fielded systems today but does not provide the precision needed for many tasks. Higher precision will be achieved by correlating (and registering) observed video frames to stored references imagery. The reference imagery includes previously collected satellite images that have been precisely aligned to map coordinates. Application of precise geospatial registration include: (1) rapid updates of aerial maps, the geo-registration process enables the construction of video mosaics which may be overlaid over reference imagery, (2) geo-location of objects seen in the video for applications such as target tracking and (3) enhanced visualization, for instance it enables the overlay of maps, boundaries and other graphical features and annotations onto the video imagery.

In this paper, we present the details and results of some of the key algorithms we have developed in our laboratory towards implementing the overall system for geo-spatial registration. This work extends the previous body of work based on *still* imagery exploitation using site models [9].

1.1 Our approach

The engineering support data (ESD: GPS, camera look angle etc.) supplied with the video is decoded to define the initial estimate of the camera model (position and attitude) with respect to the reference database. The camera model is used to apply an image perspective transformation to reference imagery obtained from the database to create a set of synthetic reference images from the perspective of the sensor. This set of reference images is fed to the video processing system to be used for indexing and fine alignment[1].

The position and attitude information provided by ESD may be good enough to generate a 3Kx3K section of the relevant reference imagery with a reso-

[1]The alignment step does not require accurate knowledge of the video camera's calibration parameters.

lution of about 1-2 feet per pixel. A coarse indexing module locates the video imagery more precisely in the reference image. Subsequently, sub-pixel alignment between the video frame and reference imagery corresponding to the relevant locale is used for precise geo-location of the video frames. The current estimate of sensor attitude and position is updated based upon results of matching from registration module. This information can be used to map points from video to reference geo-coordinates or vica-versa. The information can also be used to warp the video frames to align with the reference imagery. These warped video images can then be mosaiced together to create "geo-mosaics".

To summarize, the process of precise alignment of video to reference imagery can be divided into three main steps:

- Video-to-video frame alignment and mosaic creation.
- Coarse indexing/pruning of match locations in the reference imagery to eliminate all but the best possible location of the video imagery in the reference to with a few pixels of its true location,
- Precise parametric alignment with and/or without the DEM map to obtain sub-pixel localization of the video frame in reference imagery.

In the remainder of this paper, we describe the algorithms for each of these steps and present experimental results obtained by these algorithms.

2 Lens Distortion Corrected Video Mosaicing

Video frames are typically acquired at 30 frames a second and contain a lot of frame-to-frame overlap. For typical altitudes and speeds of airborne platforms, the overlaps may range from 4/5 to 49/50th of a single frame. We exploit this overlap by converting a redundant video stream into a compact mosaic image stream. For instance, typically 30 frames in a second of standard NTSC resolution (720x480) video containing about 10M pixels may be reduced to a single mosaic image containing only about 200K to 2M pixels depending on the overlap between successive frames. The successive video frames are aligned with low order parametric transformations like translation, affine and projective transformations to create extended view mosaics. Using the mosaics for subsequent processing reduces the computational burden on the final system. Another advantage of building video mosaics at this stage is that when used at the next step for coarse indexing with respect to the reference image, they provide a much larger image context than a single video frame.

Often in aerial video streams, the lens distortion parameters must be explicitly modeled in the estimation process. A fundamental assumption made in earlier work [6, 8, 10] on mosaicing was that one image could be chosen as the reference image and the mosaic would be constructed by merging all other images to this reference image. However, in the case when lens distortion is present, this formulation and the underlying assumptions are no longer true. In [11], we extended the alignment and video mosaic creation algorithms to use a reference coordinate system but not a reference image. We compute the motion parameters which warp all images to a virtual image mosaic in this reference coordinate system. Each pixel in this virtual image mosaic is predicted by intensities from more than one image. The error measure we minimize is the sum of the variances of predicted pixel intensities at each pixel location summed over the virtual image. Formally, the unknown projective transformation parameters for each frame, $\mathbf{A}^1 \ldots \mathbf{A}^N$, and the lens distortion parameter, γ_1 (see equations 5 and 6) are solved for through:

$$\min_{\mathbf{A}^1 \ldots \mathbf{A}^N, \gamma_1} \sum_{\mathbf{p}} \frac{1}{M(\mathbf{p})} \sum_{i} (I_i(\mathbf{p}^i) - \bar{I}(\mathbf{p}))^2, \quad (1)$$

where point $\mathbf{p}^i$ in frame i is a transformation of a point $\mathbf{p}$ in the reference coordinate system, $\bar{I}(\mathbf{p})$ is the mean intensity value of all the $\mathbf{p}^i$'s that map to $\mathbf{p}$, and $M(\mathbf{p})$ is a count of all such $\mathbf{p}^i$'s. Therefore, given a point $\mathbf{p}$ in the reference coordinates, each term in the sum in Equation 1 is the variance of all the intensity values at points $\mathbf{p}^i$ that map to point $\mathbf{p}$. An example of alignment and mosaic construction using this process is provided in Figure 1, which shows three frames used for mosaic construction. The final mosaic constructed from these three frames is shown in Figure 2 (Note, the lens distortion correction).

Note that in the video mosaicing process we are not taking into account 3D parallax. However, in the overall framework, a new mosaic is constructed every second or so. In typical scenarios, the 3D parallax observed in the aerial video for such small time frames is very minimal.

3 Coarse Indexing/Matching

Coarse indexing locates a video mosaic within a reference image using visual appearance features. In principle, one could exhaustively correlate the intensities in the video mosaic and the reference image at each pixel and find the best match. However, due to the uncertainties in viewpoint computed from ESD and due to appearance changes between the reference imagery and the current video, it may not be possible to directly correlate intensities in the two images. The real changes in appearance may be due

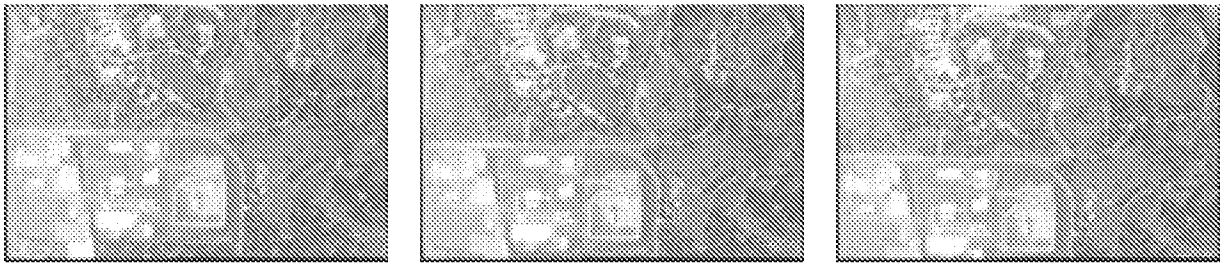


Figure 1: Top: Three frames of an aerial video clip.

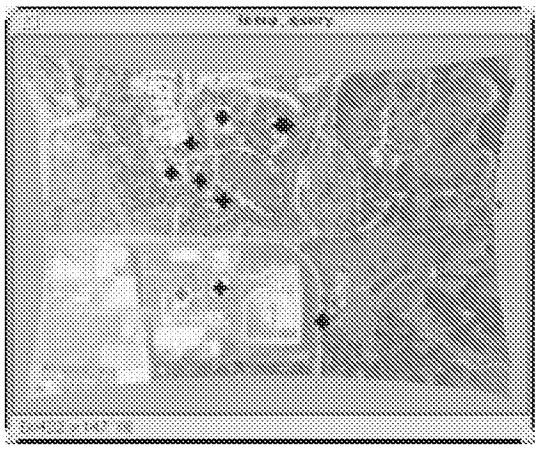


Figure 2: Lens distortion corrected video mosaic of three frames of an aerial video.
Ten salient features automatically used for indexing can be seen in the mosaic frame. The reference feature is shown as a grey cross and the remainder salient features are shown as black crosses.

to change of albedo/ reflectance of objects and surfaces in the scene (e.g. summer to fall) due to difference in illumination between the reference and the video imagery. Furthermore, since the video and reference imagery may have a large time gap between them, there may be structures (like buildings etc.) in one that may not be present in the other. Changes in appearance due to viewpoint are accounted for to a large extent by the process of warping the reference image to the ESD viewpoint. However, for robust localization, the indexing and matching processes need to be resilient to uncertainties in ESD and to real changes in the imaged scene.

We present a solution to the coarse matching problem when the relation between a video frame and the reference image is mostly translational with relatively small changes in rotation, scale and skew parameters. Global illumination changes are handled by appropriate filtering of the imagery. Geometric changes and missing/extraneous features are handled by combining local appearance matching with global consistency.

Local appearance is defined by the response of a patch to filters at multiple scales. For instance, a window that contains the response of a Laplacian filter at multiple scales is used to define the local appearance of a patch. Similarly, responses of other multi-scale multi-orientation filters (like Gabor filters) may be used. In our current implementation, salient locations where the response to the chosen filters is significant are defined. Saliency of a particular location is defined as a point in scale-space where the response to a given filter is maximal both in scale and space [7]. In other words, saliency defines a location where at the appropriate scale, a filter acts as a matched filter for the intensity structure in the patch. Thus, saliency can be applied to blob-like, corner-like and ridge-like features amongst others by defining the appropriate canonical matched filters for such features. For computational efficiency, only a small collection of scales are used to locate saliency and the salient features are subsequently represented by filter responses at a small number of scales around the optimal scale. The canonical filter is applied at multiple scales using a Gaussian pyramid [2]. The location, the scales and the filter responses at the location and scales becomes the multi-dimensional representation of a patch. For further efficiency as well as robustness to small changes in viewpoint, we choose only those locations that are salient at coarser scales. Only the mid-range scales are used. Finer scales are more sensitive to appearance and view changes whereas very coarse scales become non-distinctive.

In the matching phase, each salient feature is matched against the reference image. The same set of filters used for the video is also applied to the reference image. In our current implementation, we use normalized correlation at the appropriate scale as a match measure. Since the features are defined at coarser scales over a pyramid, the reduction in spatial resolution in the pyramid provides efficiency in matching. The matching process produces a match measure image at the appropriate scale for each of the salient features. Non-maximal suppression and dilation of the resulting local maxima are

performed for each of the match measure images. Subsequently, each of the match images is translated with respect to the coordinate of a reference feature. Let $[\mathbf{p_0}, \mathbf{p_1}, \ldots, \mathbf{p_N}]$ be the locations of the salient features, and $[C_0(\mathbf{p}), C_1(\mathbf{p}), \ldots, C_N(\mathbf{p})]$ be the correlation match images, for each of the $(N+1)$ features. Then the aggregate match image is given by:

$$M(\mathbf{p}) = \Pi_{i \in \ Best\ k} C_i(\mathbf{p} - (\mathbf{p_0} - \mathbf{p_i}))$$

In words, each match image is translated by $(\mathbf{p_i} - \mathbf{p_0})$. For each location, the top k values (where k typically is $N-2$) are selected and combined either additively or multiplicatively. Note that since each of the match images, C_i, is defined at the scale of the corresponding feature $\mathbf{p_i}$, the match images are projected to the finest scale before the combined image is generated.

The mosaic image in Figure 2 shows the location of ten features, marked by +'s, that were automatically chosen at two neighboring scales ($\sigma = 3.2, 6.4$). The reference feature location $\mathbf{p_0}$ is shown in gray and the rest are shown in black. The matching algorithm was applied between the video frame and a reference image. The location of the reference feature found in the reference image is shown in black marked by a circled + in the left image in Fig. 3. There is a displacement of about 10 pixels between the true location of the reference feature in the reference image and that of the computed one. This transformation is very much within the scope of what the fine registration algorithm can handle.

4 Fine Geo-registration

The coarse localization is used to initialize the process of fine alignment while accounting for the geometric and photometric transformations between the video and reference imagery. In general, the transformation between two views of a scene can be modeled by (i) an external coordinate transformation that specifies the 3D alignment parameters between the reference and the camera coordinate systems, and (ii) an internal camera coordinate system for image transformation that typically involves a linear (affine) transformation and non-linear lens distortion parameters. Our approach to the precise alignment problem combines the external coordinate transformation and the linear internal transformation into a single 3D projective view transformation. This along with the depth image and the non-linear distortion parameters completely specifies the alignment transformation between the video pixels and those in the reference imagery. It is to be emphasized that one main advantage to our approach is that no explicit camera calibration parameters needs to be specified. This aspect increases the scope of applicability of our proposed system to arbitrary video camera platforms. The modeled video-to-reference transformation is applied to the solution of the precise alignment problem.

4.1 Formulation

We now present the equations used for aligning video imagery to a co-registered reference mage and depth image [2]. The formulation used is the plane+parallax model developed by [5, 12, 13]. The coordinates of a point in a video image are denoted by (x, y). The coordinates of the corresponding point in the reference image are given by (X_r, Y_r). Each point is the reference image has a parallax value k. The parallax value is computed from a digital elevation map (DEM) which is co-registered with the reference image.

Twelve parameters $a_1 ... a_{12}$ are used to specify the alignment. The reference image coordinates (X_r, Y_r) are mapped to the ideal video coordinates (X_I, Y_I) by the following equations:

$$X_I = \frac{a_1 * X_r + a_2 * Y_r + a_3 * k(X_r, Y_r) + a_{10}}{a_7 * X_r + a_8 * Y_r + a_9 * k(X_r, Y_r) + a_{12}} \quad (2)$$

$$Y_I = \frac{a_4 * X_r + a_5 * Y_r + a_6 * k(X_r, Y_r) + a_{11}}{a_7 * X_r + a_8 * Y_r + a_9 * k(X_r, Y_r) + a_{12}} \quad (3)$$

Note, since, the right hand side in the above two equations is a ratio of two expressions, the parameters $a_1 .. a_{12}$ can only be determined up to a scale factor. We typically make parameter $a_{12} = 1$ and solve for the remaining 11 parameters. In the case of the reference image being an orthophoto with a corresponding DEM (digital elevation map), the parallax value k at a location is equal to the DEM value at that location. When the reference image is a real image taken from a frame camera (where the imaging is modeled with perspective projection) the parallax value k at any reference location is calculated from the depth z at that location using the following equation [5, 12, 13]:

$$k = \frac{(z - \bar{z}) * \bar{z}}{z * \sigma_z} \quad (4)$$

where $\bar{z}$ and σ_z are the average and standard deviation of the depth image values. Finally, the ideal video coordinates (X_I, Y_I) are related to the measured video coordinates (x, y) by the following equation:

$$x = X_I + \gamma * (X_I - X_c) * r^2 \quad (5)$$

$$y = Y_I + \gamma * (Y_I - Y_c) * r^2 \quad (6)$$

where

$$r^2 = (X_I - X_c)^2 + (Y_I - Y_c)^2$$

[2] The equations for aligning video imagery to a co-registered orthophoto and DEM are similar.

Note, the lens distortion parameters γ, X_c *and* Y_c are computed at the video mosaicing stage and at this stage are used to warp the video imagery to ideal coordinates.

4.2 Parameter Estimation

The reference imagery and the video are typically acquired at different times with possibly different illumination conditions and resulting intensity structures present in the imagery. To correlate the video with the reference imagery, we do the following transformations. We first compute and match the histograms [4] of the video image to the predicted section of the reference image. This allows us to match the histogram and intensity structure of the video image with the reference image. Finally, we compute the Laplacian pyramids of the reference image and the modified video image. The alignment parameters are computed by correlating the images in the two Laplacian pyramids.

To register the video image to the reference image, we extend the hierarchical, pyramid-based direct registration techniques presented in [1]. This technique first constructs filter pyramids from each of the two input images, and then estimates the motion parameters in a coarse-to-fine manner over the image pyramid. Within each corresponding level of the pyramid, the sum of squared difference (SSD) measure integrated over user selected regions of interest is used as a match measure. This measure is minimized with respect to the unknown transformation parameters $a_1..a_{12}$. The SSD error measure for estimating the transformation parameters within a region is:

$$E(\{\mathbf{A}\}) = \sum_{\mathbf{x}} (I(\mathbf{x}, ref) - I(\mathbf{Ax}, video))^2 \quad (7)$$

where $\mathbf{x} = (x, y)$ denotes the spatial image position of a point, I denotes the (Laplacian pyramid) image intensity for the reference and video images and $\mathbf{Ax}$ denotes the image transformation at each point (see equations 2 and 3). The error is computed over all the points within the region of interest. The optimization is done in an iterative manner, at each level of the pyramid using the Levenburg-Marquardt optimization technique.

4.3 Geo-mosaicing, Mapping points, Warping Images

Once the alignment parameters have been computed, the video images can be warped to coordinate frame of the reference image. A sequence of warped video images can then be merged to construct **geo-mosaics** (geo-referenced video mosaics). These mosaics can then be used to update the reference imagery. We show examples of the geo-referenced video mosaics constructed using this technique for both nadir and oblique imagery in Figure 5. The original reference image and depth image can be seen in Figure 3. The oblique video image can be seen in Figure 4. The nadir video images can be seen in Figure 1.

Finally, for annotation and other visualization tasks, it is important for the user to be able to map points from the video to the reference image and vice versa. To map points from the reference image to the video, we use equations (2,3) and (5,6) and compute the values on the right hand side. However since there is no closed form solution to map a video point to the reference image, we solve for the inverse of equations (2,3) and (5,6) using ray tracing. Similarly the video image can be warped to the reference image, directly using reverse warping with bilinear interpolation. However to warp the reference image to appear in the video image coordinates, we must use forward warping. Point mappings in the forward warping process are also computed using the ray tracing technique.

As a result of geo-registration, the user is able to determine the geo-coordinates of any object point observed in the video. The geo-registration algorithms require knowledge of a reference image and accompanying co-registered DEM (digital elevation map). The DEM may not be available at the same resolution as the reference imagery. We report on the accuracy of geo-location of video points using the geo-registration algorithms for various resolutions of DEM with a fixed resolution for the reference image.

4.4 Performance analysis and experimental results

The accuracy of geo-locating object points observed in the video depends on many factors:

1. The size of the footprint of the video pixel when projected to the geo-coordinate system. The size of the projected footprint of a 1x1 sq. pixel is a function of the look angle, altitude, field of view and other imaging parameters of the sensor. For instance, if the video is taken from an oblique view-point, the size of the projected footprint of pixels will increase with the obliquity angle of the projection ray for that pixel. The accuracy in locating objects seen from more oblique angles will be less.

2. The error in locating the object observed in the video. For the experiments described in this report, the objects are located manually in the video image. This manual operation has an inherent error of 1 or 2 pixels. Note, for computing the accuracy performance, we also manually located the object points in the reference image. Hence, the accuracy results are a function of this error.

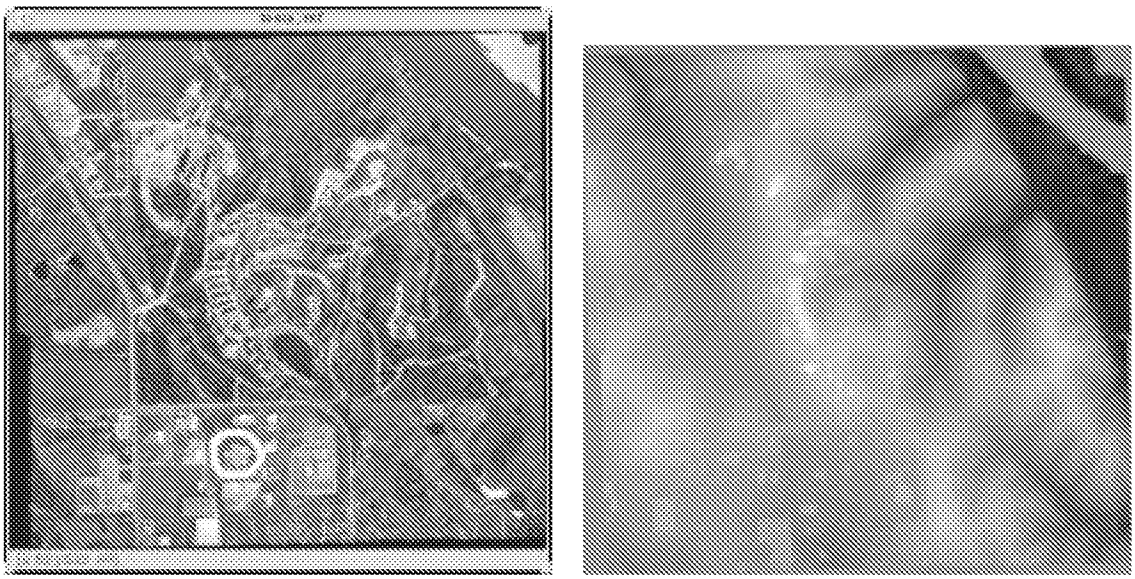


Figure 3: Left: Reference Image, Right: Digital Elevation Map.
The location of the reference feature from the video mosaic is marked by a circled gray + and can be seen on the bottom of the reference image.

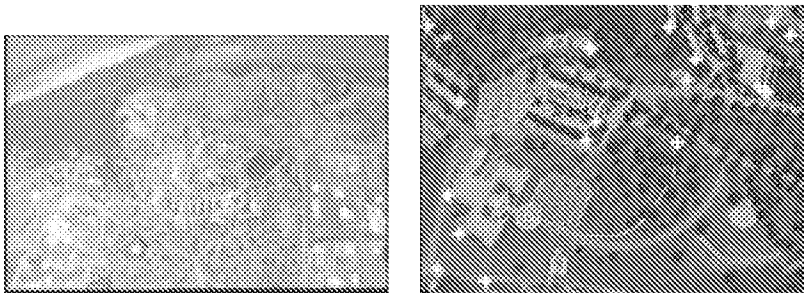


Figure 4: Left: First frame of oblique video clip. Right: First frame of video clip va4780 with marked points.



Figure 5: Left: Geo-registered nadir video mosaic, and Right: Geo-registered oblique video mosaic shown overlaid on the reference image.

Table 1: **Mapping points from video to reference using non-linear technique.** Comparision of automatic estimation vs. hand measurement

	VA4780 sequence			VA7430 sequence		
DEM res.	RMS err.	footprint err. (D1) fp. size (1x1) pixel	footprint err. (D2) fp. size (2x2) pixel	RMS err.	footprint err. (D1) fp. size (1x1) pixel	footprint err. (D2) fp. size (2x2) pixel
ft.	ft.	ft.	ft.	ft.	ft.	ft.
6	12.78	8.82	5.82	15.18	8.88	4.56
12	12.84	8.88	5.88	15.06	8.82	4.50
24	13.14	9.24	6.18	15.06	8.94	4.56
48	12.00	7.98	4.98	14.94	8.82	4.56

3. The error in estimating the camera model which maps the video frame to the geo-coordinate system. The camera model is estimated by the geo-registration software. The estimation process minimizes a non-linear function and is a function of the following factors: noise present in the video and reference imagery, the difference in view-point and time of year for acquisition of video and reference imagery, the changes which have happened in the world from the time of reference imagery acquisition to video acquisition and finally the presence or absence of features which can be used for image based registration.

4. The error in the Digital Elevation Map used in the geo-registration process. The geo-registration software assumes the digital elevation map is correct. If the elevation values are erroneous at certain pixels, then video pixels corresponding to these locations will not be mapped correctly. Note, the digital elevation map used for the experiments reported here is mostly correct. However at certain locations, some clear errors can be observed. For instance, some buildings observed in the reference image (see: right image in Figure 4) are not seen in the elevation map.

The reference imagery (reference orthophoto and elevation image shown in Figure 3) used for the experiments reported here was built using the GDE Socet Set system from stereo imagery taken in March 1985 of the VA Hospital site at Leavenworth, Kansas. The reference data includes a 1 square mile orthophoto and a digital elevation map (DEM) with 3 m post spacing. The geo-registration algorithms reported here have been tested on many video sequences using the above reference imagery. Test video sequences were acquired at multiple heights, look angles and times of year. The nadir and oblique video frames shown in Figures 4 and 1 were collected in November 1995. We now report on performance analysis experiments for two video sequences: VA4780 (see: right image in Figure 4) and VA7430 acquired in June of 1996 with the camera sensor located at a height of 2000 and 3000 ft respectively.

The geo-registration software was used to register the two sequences to the reference data. We then selected, by hand, a list of correspondence points in both the frames of the video sequences and the reference imagery. The video points were mapped to the reference coordinate system using the estimated parameters. The set of points used for the first frame of VA4780 are marked in the right frame in Figure 4 by white "+" signs. The error in locating the video points is reported in Table 1. The experiments were repeated using various resolutions of the DEM data. The various resolutions of DEM were created by blurring the original DEM data and sub-sampling at different resolutions. The registration was performed using a reference image with a 6 foot ground spacing per pixel. The following should be noted for the results described in Table 1:

- Point mapping errors were measured using sample populations of 83 hand-generated point correspondences over 5 frames in video sequence VA4780, and 50 point correspondences over 3 frames in sequence VA7430.

- Point mapping error is measured by mapping a video frame point to the reference image, and measuring its distance (and also the distance of its footprint) to the corresponding reference image point.

- DEM resolution column is the finest resolution at which the DEM is assumed available for the experimental trial. If DEM sampling resolution is coarser than reference image resolution, the DEM is interpolated by Gaussian blurring to construct a finer resolution DEM. Further interpolation was bilinear.

- All resolutions (e.g., 6, 12, 24) are in feet of inter-pixel spacing.

- Root mean square error is the average error in locating a point in reference image pixels. It does not take into account the projection of the footprint of the video pixel on the reference image.
- Footprint error (D1) is the mean of the distance (over all object points) of the measured reference image point to the corresponding bounding box of the projected footprint of the video pixel. The projected footprint is obtained by mapping a 1 square pixel box around the video frame point to the reference image.
- Footprint error (D2) is the mean of the distance (over all object points) of the measured reference image point to the corresponding bounding box of the projected footprint of the video pixel. The projected footprint is obtained by mapping a 4 square pixel box around the video frame point to the reference image.

From the first row of Table 1, we note the root mean square error for locating points for the two images varies from 12 ft to 15 ft. This corresponds to a pixel registration error of 2 to 2.5 pixels. Note, however the footprint errors are much smaller (8.8 ft or 1.2 pixels for footprints of 1x1 size video pixels). The footprint error takes into account the size of the footprint of the projected video point. Since, the location of object points in the video is done manually and only to pixel accuracy, it is important to take this into account. The footprint error decreases with the assumed size of the video footprint. In Table 1, we report results for footprint sizes of 1x1 and 2x2 pixels in the video frame.

Finally, we found that the error in locating points or footprints did not increase when we used coarse resolution DEM's. We repeated the experiment with DEM's at four different resolutions (6,12,24 and 48 ft post spacing) and found that the error in geolocating points did not increase (Table 1). It is possibly due to the slow variation in depth over the image scene and also on the choice of points used to do the experiments.

5 Conclusion

In this paper, we have presented some of the key algorithms for developing a system for georegistration of aerial video. The key image processing tasks are frame-to-frame alignment, coarse indexing and fine alignment to a reference image. These algorithms have been tested over a number of sequences. The algorithms have to date been implemented on the workstation and tested on archived digital video sequences. Currently, we are in the process of building a real time system for georegistration. The video processing steps are divided between the Sarnoff real time video processor VFE-200 (mosaicing and coarse indexing) and an SGI octane machine (fine registration of key frames).

References

[1] J. R. Bergen, P. Anandan, K. J. Hanna, and R. Hingorani. Hierarchical model-based motion estimation. In *European Conference on Computer Vision*, Santa-Margherita Ligure, Italy, 1992.

[2] P.J. Burt. Smart sensing with a pyramid vision machine. *Proceedings of the IEEE*, 76:1006–1015, 1988.

[3] D.S. Linden et. al. Automated digital mosaicking of airborne videography. Technical Report FHTET 96–12, Forest Health Technology, Enterprise Team - Fort Collins, Colorado, U.S. Dept. of Agriculture, Forest Service, 1996.

[4] David Heeger and J. R. Bergen. Pyramid-based texture analysis and synthesis. In *SIGGRAPH*, 1995.

[5] R. Kumar, P. Anandan, and K. Hanna. Direct recovery of shape from multiple views: a parallax based approach. In *Proc 12th ICPR*, 1994.

[6] Rakesh Kumar, P.Anandan, J.Bergen, M.Irani, and K.J.Hanna. Scene representation as a collection of images. In *IEEE Workshop on Visual Representations of Scenes*, Cambridge, MA, June 1995.

[7] T. Lindeberg. Detecting salient blob-like image structures and their scales with a scale-space primal sketch: A method for focus-of-attention. *International Journal of Computer Vision*, 1994.

[8] M. Irani, P. Anandan and S. Hsu. Mosaic based representation of sequences and their applications. In *International Conference on Computer Vision*, pages 605–611, Cambridge, MA, November 1995.

[9] RADIUS PI Reports and Technical papers. Proc. Darpa Image Understanding Workshop, 1996. pp. 255–525.

[10] H. S. Sawhney, S. Ayer, and M. Gorkani. Model-based 2D&3D dominant motion estimation for mosaicing and video representation. In *ICCV*, 1995.

[11] H. S. Sawhney and R. Kumar. True multi-image alignment and its application to mosaicing and lens distortion. In *CVPR*, pages 450–456, 1997.

[12] Harpreet Sawhney. 3D geometry from planar parallax. In *Proc. CVPR 94*, June 1994.

[13] A. Shashua and N. Navab. Relative affine structure, theory and application to 3d reconstruction from 2d views. In *IEEE Conference on Computer Vision and Pattern Recognition*, June 1994.

6 Acknowledgement

The reference image and DEM shown were provided to us by GDE Systems Inc.. They were produced using the GDE SocetSet photogrammetry system.

SD
144
.M9
A3
no.95-4

nited States
epartment of
griculture

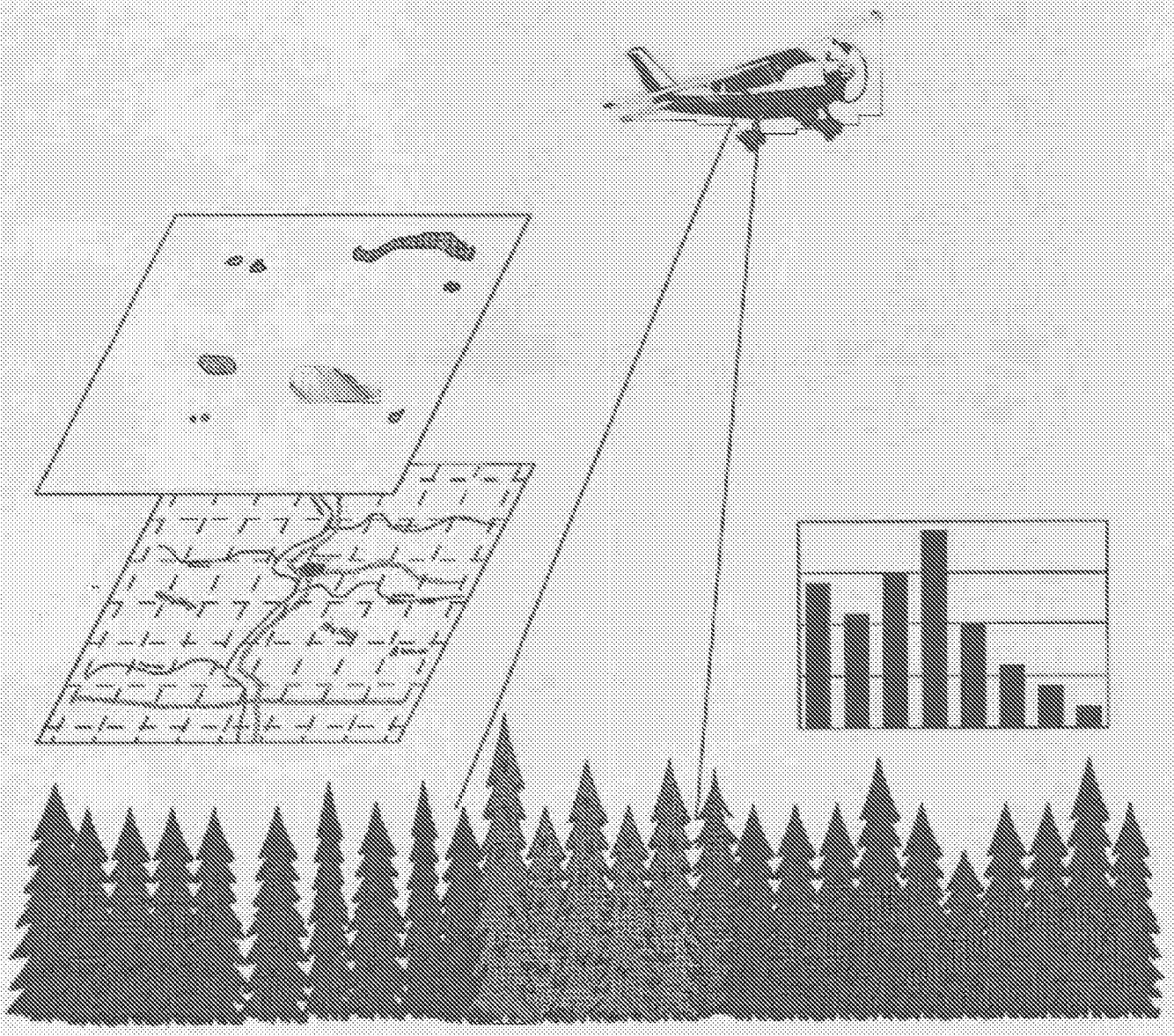
orest Service

Northern Region
Forest Pest
Management

Report 95-4

Proceedings

Aerial Pest Detection and Monitoring Workshop



Proceedings

Aerial Pest Detection and Monitoring Workshop

April 26-29, 1994
Las Vegas, Nevada

Edited by

Timothy J. McConnell
USDA Forest Service
Forest Pest Management
Northern Region
200 East Broadway
Missoula, MT 59807

Sponsored by:



USDA Forest Service
Forest Pest Management
Northern Region
Intermountain Region
Forest Insects and Diseases
Pacific Northwest Region

January 1995

INTRODUCTION

The first recorded use of an airplane to survey "pest" damage was done in Quebec and Ontario, Canada in 1920 (Swaine 1921), over an extensive spruce budworm infestation. In 1931, F.P. Keen, head of the Portland Forest Insect Laboratory and C.S. Cowan, Chief Fire Warden of the Washington Forest Fire Association, conducted the first recorded aerial survey in Washington and Oregon, delineating hemlock looper defoliation in Pacific County, Washington (Wear and Buckhorn 1955). Annual aerial surveys began in the late 1940's on a regular basis in many parts of Canada and the United States. By the late 1950's most all USDA Forest Service, Forest Pest Management (FPM) units across the country were conducting aerial surveys on an annual basis. The aerial survey technique has now become a common method of remote sensing because it is an economical and efficient means of gathering data about forest conditions over large areas.

Although programs differ around the country, due to topography, seasonal changes, different insects and diseases, budgets, personnel, available aircraft, etc., most techniques needed to perform this type of survey are common to all personnel and these techniques have been previously developed over the past 50 years. In the late 1980's, advances in the quality, portability, and affordability of video equipment were developed and video technology was adapted for use in aerial detection and monitoring surveys. Since then, many FPM units purchased and integrated airborne video systems into their existing survey programs. This workshop provided an opportunity to share methods, techniques, philosophies, priorities, safety concerns and problems associated with the responsibilities of conducting various forms of aerial surveys.

The goal of this workshop was "To provide a forum for information sharing and technology transfer to people involved in all aspects of aerial insect and disease detection and monitoring surveys." That goal was met. And from the workshop attendees came the unanimous vociferation for additional training for those people responsible for conducting aerial surveys. Most all Regions share the problem of a diminished cadre of qualified observers and increasing detection and monitoring responsibilities due to increased forest health awareness. No formal training course addressing flight safety and operations has ever been provided to aerial observers or videographers, yet the problem is of National concern. Hopefully, from this workshop, the people responsible for conducting aerial surveys, who need additional or even basic training, will be provided the tools to conduct a safe, efficient and quality aerial detection survey to supply land managers and the public with valuable forest disturbance information.

Acknowledgements

Special thanks to Linda Hastie of the Forest and Rangeland Management staff for all the word processing work to get this report in final form.

References

Swaine, J.M. 1921. A survey of our forests from the air. Agr. Gazette of Canada. 8:20-22.

Wear, J.F. and Buckhorn. 1955. Organization and conduct of forest insect aerial surveys in Oregon and Washington. USDA For. Ser. PNW Forest Range Exp. Sta., Portland, OR. 40 pp.

AERIAL PEST DETECTION AND MONITORING WORKSHOP
April 26 - 29, 1994
Las Vegas, Nevada

CONTENTS

Page

INTRODUCTION

M.J. Weiss - Aerial detection surveys, Washington Office perspective 1

S. Dudley - Airborne video, from the beginning 3

T. Valentine - Aerial detection surveys and geographic information systems (GIS) 7

AERIAL SURVEY PROGRAM PRESENTATIONS

D.R. Bridgwater - Pacific Northwest Region cooperative annual aerial insect detection survey 9

K.A. Knapp - Aerial pest detection operations in the Intermountain Region 10

S.L. Smith - Pacific Southwest Region aerial detection survey program summary 14

M.A. Roberts - Northeastern Area aerial detection survey program 15

R. Mask and R.L. Wolfe - Aerial survey of forest insect and disease activity in Alaska 17

P.J. Barry - Aerial survey methods used in the Southern Region 19

J.E. Pasek - Rocky Mountain Region aerial survey program 22

G.A. Van Sickle - Canadian aerial surveys for pest damage assessment 24

J.J. Ngasi - Use of aerial survey for monitoring cypress aphid damage in Kenya 29

D. Beckman - Aerial surveys, the good, the bad, the bumpy 36

T.J. McConnell - Northern Region aerial survey program 38

AERIAL SURVEY WORKING GROUP

K.A. Knapp - Aerial survey program questionnaire results summary 41

T.J. McConnell - Survey flight methods and logistics 43

D.R. Bridgwater - Pest/host interactions and FPM/A&FM interactions 51

GEOGRAPHIC INFORMATION SYSTEMS WORKING GROUP

M. Frank - Southwestern Region Forest Pest Management GIS summary 53

R.L. Halsey - Intermountain Region Forest Pest Management GIS operation 55

S.L. Smith - Pacific Southwest Region Forest Pest Management GIS summary 58

J.L. Johnson - Pacific Northwest forest insects and diseases GIS summary 60

T. Valentine - Southern Region Forest Health analysis team and GIS database information 62

S.J. DeLost - Northeastern Area Forest Health Protection GIS summary 66

D.J. Roschke - Update on current GIS applications in the Methods Application Group 69

AIRBORNE VIDEO OPERATIONAL SUMMARIES

S. Dudley - Airborne video western perspectives 73

M. Roberts - Remote sensing in the Northeast Area 76

J. Omer - Morgantown Field Office airborne video program 77

R.A. Spriggs, B. Silvey, and J. Knighten - Southern Region airborne video summary 78

OTHER SURVEY TOPICS

D. Overhulser - Aerial detection surveys for black bear damage 79

D.R. Bridgwater - Off plot monitoring 81

T.J. McConnell - Aerial surveys: quality, credibility, value - is it possible? 82

B. Backman - Defoliating insects that feed on western hemlock from an aerial survey perspective 88

WORKSHOP SUMMARY

T.J. McConnell (compiler) - Workshop summary; background, impressions, and recommendations; student comments; attendee list 92

AERIAL DETECTION SURVEYS, WASHINGTON OFFICE PERSPECTIVE

Melvyn J. Weiss

Acting Director, Forest Pest Management, State and Private Forestry,
USDA Forest Service, Washington DC 20090-6090

First I want to acknowledge the attendees from Canada and Kenya. We have a long-standing, excellent relationship with our Canadian couterparts. I am also pleased to see visitors from Kenya. In March, the Chief signed a long-term agreement with Kenya for exchanges in forest health. We hope to learn much through working together.

I plan to discuss five topics: surveys, exotic pests, ecosystem management, forest health monitoring and reports.

Surveys. I am glad to see here our state cooperators who participate in the Cooperative Forest Health Program. State specialists, together with our FPM specialists, are the trained observers on whom we all rely. No one else is responsible and no one else conducts systematic examinations of the Nation's forest resources for insect and disease epidemics. Although others may look, you are the ones who know what to look for and how to interpret what you see. The surveys that you annually conduct over millions of acres produce information that is highly valued and important. As we move toward ecosystem management, I am convinced that the information you provide will be even more highly valued. It will increasingly be used for interpreting the condition of our forest ecosystems.

Exotic Pests. Exotic pests continue to threaten forest ecosystems worldwide. With greater international commerce, despite the best efforts of regulatory agencies, the threat will increase. Examples of exotic insect and disease problems are Asian gypsy moth in the Pacific Northwest and now in North Carolina, white pine blister rust, dogwood anthracnose in the Southeast, and Cinara aphid in Kenya. The best way to deal with exotics is to keep them out in the first place. Working with APHIS, Agriculture Canada, and Resources Canada, we have together made major headway in the last 3 years to improve safeguards against exotic pest introductions. APHIS will soon issue the first ever regulations for the U.S. for importation of raw wood products. These regulations are based in large measure on pest risk assessments conducted by FPM and its cooperators. Canada is considering similar regulatory measures. Through the North American Forestry Commission we are developing a list of exotic pests worldwide that potentially threaten North American forest ecosystems. This list will help us plan and take proactive measures instead of only reacting after an introduction. An Asian gypsy moth monitoring system is established around Russian far eastern ports for early detection of outbreaks. This system was put in place in cooperation with APHIS, the Russian government and with the help of FPM Regional staffs. We are working with APHIS, the American military, and German officials to try to reduce the risk of further introductions of Asian gypsy moth from that country. We have to recognize that whatever we do may not be enough. Safeguards are far from perfect. Exotic pests are often widely distributed before they are detected, e.g., European pine shoot beetle on Christmas trees. As surveyors, you may be the first to spot unusual or unexpected damage that could indicate an exotic. The quicker we can detect exotics, the more we can do to respond.

Ecosystem Management. Understanding and protecting ecosystems requires information on the occurrence of insect and disease epidemics, the information you collect. I strongly believe that the success or failure of ecosystem management will be determined by how well resource managers understand and apply what is known about the combined and interacting roles of insect and disease epidemics, wildfire, and weather events in ecosystems. The information you provide is critical to this understanding. The Directors of Fire and Aviation Management, Forest Pest Management, Forest Fire and Atmospheric Sciences Research and Forest Insect and Disease Research have agreed to work together because of the significance of these factors in shaping ecosystems. We are working together to help develop national policies. To focus our work, we are using the ecological term, "Disturbance." This new, integrated approach helps us take a fresh look at how our programs are implementing ecosystem management and helps us identify realignments and new directions.

Forest Health Monitoring. FPM has significant responsibilities within the Forest Health Monitoring Program. We are responsible for "off-plot" detection monitoring and for evaluation monitoring. The Program is now in 14 states with further expansion dependent on increased budgets. This Program would not exist without the strong support and leadership of the State Foresters. When fully implemented, the Program will provide standardized data on long-term trends in the health of our Nation's forests. Canada and most European countries already have similar programs in place. I was glad to see the Forest Health Monitoring Program on your agenda. The surveys you conduct will help us meet our responsibilties in this Program. In the east and south, states have welcomed the program and the accompanying standardization of survey data. For the first time they can compare forest health data across political boundaries. We do not have to wait until the Program expands to begin to standardize data collection in other sections of the country. A new Program brochure has just been printed. It is excellent. Copies will be distributed.

Reports. This year, for the first time, we will have a nation-wide forest health report. It is entitled, "America's Forests: 1994 Health Update." The report is written in non-technical language and includes brief summaries of the several forest health problems which are currently of greatest national concern. The report includes many of the forest health problems that you are surveying and reporting. Where appropriate, the report describes the things being done to deal with the problem. The report will enable anyone with a little reading time to gain a quick overview of the nation-wide situation. We are also revising the Insect and Disease Conditions report to make it more useable and readable. Among other things, we will be including historical defoliation and other damage records on major pests for the first time so that long-term trends are apparent and the current epidemic and damage levels can be seen in perspective. Some Regions have excellent aerial survey records extending as far back as the late 1940's. We believe the display of this data will be particularly useful in better explaining the role of insects and diseases in ecosystems and understanding the current and future condition of ecosystems. The data you collect and the resulting records are, and will continue to be, essential for these reports.

What you are doing is important and essential. Keep up the good work.

AIRBORNE VIDEO FROM THE BEGINNING

Steve Dudley

Forest Pest Management, Arizona Zone Office, Southwest Region,
USDA Forest Service, Southwest Forest Science Complex,
Flagstaff, Arizona 86001

With the advent of Project 615 at hand, the Forest Service is now committed to considering remote sensing as an integral component of its information management effort, especially as a source for land cover layers. Field data collection will always remain important. However, time constraints for making decisions sometimes preclude collecting data in traditional ways. Existing databases can quickly become obsolete because of their singular purpose or narrow focus (Lachowski et al. 1992). Airborne videography is but a single remote sensing tool. In conjunction with traditional aerial photography and satellite imagery, it can provide historical, cost-effective imagery for large diverse areas which, when combined with field data, can contribute consistent and accurate vegetation information for GIS databases. Videography is a relatively new, easy-to-use remote sensing tool available to resource managers. It's readily apparent advantages are:

1. The immediate availability of imagery; film development is not needed.

2. live imagery can also be viewed by the operator as it's taken. In fact, new technological advances now make it possible to view imagery being taken in the aircraft while sitting at your office.

3. Audio tracks on video tape permit voice notation.

4. Airborne video provides a straight forward pathway from video tape to digital format for computerized image processing.

5. Video cameras and tape are cheaper then conventional aerial photo equipment.

6. Airborne videography improves the success rate of capturing temporal imagery occurring in narrow time frames.

7. Video cameras are able to efficiently operate in low light conditions.

8. Video is useful in foreign countries where aerial film and processing may be difficult to obtain.

9. Field-level personnel with little or no experience in remote sensing can be trained quickly to use the equipment efficiently (Myhre 1992).

In the early 1980's, the development and availability of cameras sophisticated enough to employ as components in airborne video image acquisition pioneered the beginnings of this technology. By the mid-1980's, significant improvement in image quality, affordability, and portability in video equipment increased the feasibility of utilizing it in remote sensing applications. In 1986, a joint project with the USDA Forest Service

(FPM/MAG) and the University of Minnesota/Remote Sensing Lab tested the operational feasibility of utilizing a color infrared video camera for forest health monitoring. Two conclusions became apparent from the project. First, it was noticed that the degree of detail possible in mapping defoliation was more precise than that obtained from sketch maps and second, that accurately locating problem areas was more precise using video imagery (Hosking et al. 1992). In 1988, the MAG staff began evaluation of video components available on the market with designs to using them in airborne operations. By 1989, further technological improvements had been made to video components including solid state cameras using chip sensors. Video cameras became available in shuttered configurations that provided higher quality imagery and reduced motion blur. With the advent of S-VHS increased resolution, (400 lines horizontal resolution compared to 240 lines horizontal resolution), improved color quality, and improved signal-to-noise ratios became available. MAG offered a consolidated procurement package in 1990 and supported it with training and technical assistance (Myhre 1992).

Prior to the availability of the supported package, and in conjunction with the work MAG was doing, the NA/FPM in St. Paul, along with R-8 FPM, National Forests, and ENG/NFAP, purchased operational systems. This brought the Forest Service into the arena of using videography as a functional remote sensing tool. The basic field package consisted of a S-VHS video camera, a lens remote controller, a camera mount, a S-VHS recorder, a power adaptor, a 10-inch monitor, an electrical junction box, and a caption generator. Platforms vary, everything from the Queen air to Cessna 180/185, 182s, 206, 207, 210s, and helicopters are being utilized. Microimages, Inc. supplied MIPS (map and image processing)--a system designed for image processing, geographic data analysis and inventory, desk-top mapping, and related computer-aided design. The original MIPS was designed to run on DOS-based 286 and 386 microcomputers where it employs a dual screen set up for program interaction and image display. When the consolidated procurement package was made available R-2 FPM, R-3 FPM and Kaibab NF, R-4 FPM, NA FPM at Durham, NH, NA FPM at Morgantown W. VA., and FPM/MAG, purchased operational systems.

Concurrently, in the late 1980's and early 1990's, several other systems were developed and utilized to aquire airborne video imagery. Differing needs and budgets led to the development and utilization of specialized and/or selective component systems. In 1988-89, U.S. Fish and Wildlife was employing airborne videography to assess the availibility of plover and tern nesting habitat at varying river flows along the Platte river. A Cessna 172 with a baggage compartment camera port and $2,900 in video equipment was utilized (Sidle and Ziewitz 1990). Simple needs for basic ground truthing of satellite imagery as well as more sophisticated systems designed to tag every video frame with GPS data such that the encoded data can be automatically retrieved using software like GMATCH were developed. Airborne videography is utilized in multi-spectral imagery and split screen displays in many places to assess crop damages. In 1991-92, in R-3 FPM and a variety of other functions began operational use of airborne videography. Numerous missions were conducted including imagery of Ips beetle outbreaks around the community of Prescott, AZ, vegetation typing for rangeland mapping on the Sante Fe NF, roundheaeded beetle outbreak on Mt. Graham, timber analysis coverage of the North Kaibab Ranger District, a roundheaded and western bark beetle outbreak on Lincoln NF, and helicopter videography of eagle habitat along the upper Verde River. Interest in utilizing airborne videography seemed to catch on rapidly as applications began to be envisioned by land managers. By late 1992, airborne videography was being employed nationwide to:

survey recreation sites,
survey riparian areas,
assess wetlands,
assess wildlife habitat,
evaluate range conditions,
do road updates,
perform snag counts,
assess forest pest damage,
assess catastrophic damages,
forest type mapping,
do forest inventory,
law enforcement,
search and rescue,
select pipeline siting (Dull et al. 1992).

Before the end of 1993, airborne videography, as developed by MAG, was demonstrated and utilized in natural resource applications in Russia, Finland, and New Zealand. Requests for videography demonstrations were received from China and Russia again.

Where does the future lie? MAG is currently evaluating the possibility of upgrading the system to tag each video frame with GPS georeferencing. Developments in SAR (synthetic aperture radar) technology enabling scientists to operate in adverse weather conditions has already been tested with the relief efforts associated with the natural disasters plaguing our own mid-west. FLIR (forward looking infrared) systems are currently being mounted and tested on Forest Service aircraft in many regions. The potential exists to offer S-VHS and FLIR imagery on a split screen display. The Boulder Public Works Department is utilizing ACCUDAT, a videography system employing an onboard 486 computer to georeference each video frame with differentiated GPS. The system platform is a Aerospatiale Gazelle helicopter capable of slowing air speeds to 40-60 mph for high quality imagery. Kodak has recently demonstrated a camera that is digital. Instead of using film, a digital file is created eliminating the need for bulky tape and video cassette recorders.

Many field units have become proficient in image acquisition. However, a rather large learning curve still confronts many of us regarding image processing and GIS. Without any defined direction due to the uncertainties created in the award of the 615 contract, many sites have utilized what analytical software is available to them to begin learning to think spatially. After all, the goal is not merely to employ a GIS as a high tech map maker, but to learn to use it as the true analytical tool it was designed as. Airborne videography will undoubtedly provide valuable data for future analysis with GIS.

References

Alban, J., Ishikawa, P., and Hoppus, M.. May-June 1992. NFAP light aircraft airborne video system with real-time differential GPS. Eng. Field Notes 24:19-23.

Dull, C.W., Weber, F.W., Carroll, R., Reed, B.J., and Bain, S.. 1992. USDA Forest Service - Remote sensing and related technologies help care for the land and serve the people. Photogram. Eng. and Remote Sensing 58:1129-1132.

Graham, L.A.. Aug. 1993. airborne video for near-real-time vegetation mapping. J. Forestry. 28-32.

Hosking, G., Shaw, W., Firth, J., and Brownlie, R.. March 1992. airborne video evaluation report, New Zealand. Forest Research Institute, Ministry of Forestry. 67pp.

Lachowski, H., Maus, P., and Platt, B.. Dec. 1992. Integrating remote sensing with GIS. J. Forestry. 16-21.

Miller, L., Martinez, R., and Whitney, J.. June 1992. An evaluation of the utility of remote sensing in range management. USDA Forest Service SW Region. 15pp.

Myhre, R.J.. 1992. An airborne video system developed within forest pest management - a demonstration. Proc. Nat. Wkshp. Taking an Ecological approach to management. Salt Lake City, Utah.

Myhre, R.J., Russell, B., and Sumpter, C.. 1992. airborne video system users guide. USDA Forest Service, Methods Application Group. 237pp.

Sidle, J.G., and Ziewitz, J.W.. 1990. Use of aerial videography in wildlife habitat studies. Wildl. Soc. Bull. 18:56-62.

AERIAL DETECTION SURVEYS AND GEOGRAPHIC INFORMATION SYSTEMS

Theresa Valentine *

Forest Health Analysis Team, Southern Region, USDA Forest Service,
Atlanta, Georgia 30367

How are Geographic Information Systems (GIS) incorporated into the management of forest health issues and aerial detection surveys? With GIS technology, it is possible to take paper maps and associated data and convert them to an electronic format. This electronic data is analyzed and used in the decision making process.

The GIS process can be divided into data definition and acquisition, data entry and storage, analysis, and display of results. All four parts are important in providing accurate and timely products to the decision makers.

Aerial survey data falls into the data definition and acquisition category. The process starts with the aerial detection survey. The sketch mapper interprets the damage onto a paper map. Airplanes allow the mapper to cover large areas and delineate many types of insect and disease damage. The data is then ready to be entered into the GIS.

Data entry and storage includes:

1. Good registration,
2. Edge matching input sheets,
3. Vertical integration,
4. Stable materials (mylar),
5. Verifying output (hard copy and attribute checks),
6. Storing each theme as a layer,
7. Clipping data to useful boundary,
8. Developing procedures for updating.

Because sketch mappers have little experience with GIS technology, problems can occur that reduce the quality of the electronic data. For example, I have received folded source maps bearing wide magic marker lines, no registration to associate with existing data sets, mislabeled polygons, and edges that did not match between quad sheets. These problems made it difficult to ensure an acceptable level of accuracy. Aerial detection specialists work hard to accurately define problem areas and it is important to build on that accuracy when the data is transferred to an electronic format.

---

* Theresa Valentine has since become the GIS Administrator for the Oregon State Service Center for Geographic Information Systems, Salem, Oregon 97310.

Data acquisition is the most expensive and important component of a GIS. You need a vision of where you want to go and how to get there. The Information Needs Assessment (INA) process can help you formulate a plan to reach your goals. The process involves identifying your present and future data needs, products, and priorities. Input is gathered from all the groups that utilize your data. This is important because you can reduce costs by sharing data. You may also find that you are duplicating efforts. Contact your local GIS specialist for more information on the INA process.

An example of why planning is important can be found in an analysis that was recently attempted by Region 8 Forest Health. They wanted to look at 1993 Gypsy Moth defoliation for the Commonwealth of Virginia and identify success rates of spray projects. The defoliation data was collected at a 1:50,000 scale using a combination of aerial photography and sketch mapping. Defoliation was lumped into areas greater than 40 acres. The spray block data was captured at 1:24,000 scale. When the two data sets were combined and the data enlarged to the county level, it appeared as if there were many spray block failures. The county cooperators became very excited when they saw the map products. When the defoliation data was mapped, areas less than 40 acres were lumped into larger polygons. Most of the spray blocks in Virginia were smaller than 40 acres. There was no intention to use the data in this manner when it was captured. One of the problems with GIS technology is that it will allow you to make these comparisons and they look accurate. If you do not understand the limitations of the data, it is possible to generate invalid conclusions. A proper INA could have prevented this problem.

Why do we need to make this data electronic? Aerial detection has been a consistent tool for mapping damage to forests throughout the United States. GIS technology makes it possible to look at changes and trends in the forest over time. The turn-around time can be fast, and the ability to look at complex combinations of forest conditions is remarkable. For example, with GIS technology it is possible to determine hazard ratings or risk factors for land not currently damaged. This can help land managers be proactive as they implement ecosystem management. The technology helps track the progression of problems over time and predict the probability of damage in the future.

The real power behind GIS technology resides in the ability to perform analysis functions. The attributes, scale, intensity of survey, original source, and method of collection of the database will determine the quality and accuracy of the analysis. Examples of analysis functions are buffering (roads, streams, spray blocks, wildlife nests), statistical information, nearest neighbor and viewshed analysis, networking, and three-dimensional modeling. For more information on spatial analysis, consult the procedings from the Spatial Analysis and Forest Pest Management Workshop (General Technical Report NE-175, June 1993).

I believe that we will soon move out of the dinosaur age and into the information age, leaving our paper maps and color pencils behind. We can provide the land use managers with quality data, quick turnarounds, and useful and accurate analysis. The analysis capabilities are the backbone of why this technology is so important in our future. The products we generate will help managers make informed and timely decisions, inform the public about proposed projects, facilitate the coordination between agencies, and provide specialists with the information they need to model pest problems.

PACIFIC NORTHWEST REGION
COOPERATIVE ANNUAL AERIAL INSECT DETECTION SURVEY

David R. Bridgwater

Forest Insects and Diseases, Natural Resources,
USDA Forest Service, Portland, Oregon 97208

In the Pacific Northwest Region, we conduct a cooperative annual aerial insect detection survey of all the major forested lands. This survey covers approximately 54 million acres and is conducted in July and August. In Oregon we fly in the Oregon Department of Forestry's Partenavia, a high wing, twin-engine aircraft, with the Department's pilot and State observer. In Washington we utilize a contracted Partenavia and pilot and have an observer from both the Forest Service and the Washington Department of Natural Resources. In Washington, about 30 percent of the flying is contour flying and 70 percent is grid flying. In Oregon, virtually all survey is grid flying.

Each observer maps the insect activity on his side of the aircraft and from these maps a master is made. The polygons and attributes from the masters are hand transferred onto mylar and scanned into the GIS and then edited in the GIS. The GIS prints the polygons and attributes onto a cronoflex from which paper copies are made and sent to the Federal, State and private land managers. In GIS, we import the data into Paradox and prepare data tables which are also made available to the land managers, and are used to track insect activity, and to prepare reports.

AERIAL PEST DETECTION OPERATIONS IN THE INTERMOUNTAIN REGION

K. Andrew Knapp

Forest Pest Management, Boise Field Office,
USDA Forest Service, Boise, Idaho 83702

Aerial pest detection surveys (ADS) are the most widely used method for detecting and monitoring forest pests and abiotic damage in the Intermountain Region. Two types of aerial surveys are currently used: aerial sketchmapping and airborne videography. Approximately 15 million acres are annually aerially surveyed using these methods. Surveys are conducted from light fixed-wing aircraft and occasionally rotor-wing aircraft.

The host's expression to pest invasion or abiotic damage, extent of damage, and management priority determines the appropriate aerial detection technique. Generally, aerial sketchmap surveys are used as the initial detection tool to locate and quantify forest pest damage. Because of the narrow swath-widths needed to obtain acceptable imagery airborne video surveys are only used over small high-priority areas with very visible pest signatures.

In the Intermountain Region symptoms of forest pathogens are difficult to detect with the exception of some needle diseases, very heavy dwarf mistletoe infections and large openings caused by root rots. Most aerially visible damage is attributed to bark beetles and/or defoliating insects. A skilled aerial observer can detect visible damage caused by these pests, estimate the degree of damage to host trees, determine probable pest involved and plot this information on a map with reasonable accuracy. Likewise a skilled video-image interpreter can accurately identify and delineate pest activity on video.

Following is a brief discussion of how aerial pest detection surveys are planned and conducted.

AERIAL PEST DETECTION SURVEYS

Planning Aerial Pest Detection Surveys

All National Forests in Region 4, National Parks, BLM state offices are contacted during April of the survey year to identify high priority ADS areas. These inputs are combined with Forest Pest Management (FPM) priority areas, such as current insect infestations or areas with a high potential of becoming infested, to develop a Regionwide survey schedule. Generally, the ADS covers major commercial timber production areas, National Recreation Areas, administrative sites and Ski areas. Low priority areas not surveyed unless specifically requested are: administrative set-asides, wilderness areas, alpine zones and extensive blocks of pinyon-juniper. Low priority areas may be surveyed on an alternate year basis.

ADS are conducted from late June through early September and insofar as possible are scheduled to coincide with optimum damage symptom expression of major forest pests and damage. Currently, FPM uses two contract aircraft and pilots, three observers to conduct surveys throughout the Region. Additionally, under a Memorandum of Understanding with the State of Idaho FPM surveys state lands intermixed with

Forest Service lands while the State of Idaho surveys Forest Service lands adjacent to state lands. Total flight time generally varies from 300 to 350 flight hours per year for Forest Service aircraft and 50 to 70 flight hours per year for State of Idaho Aircraft

Conducting Aerial Pest Detection Surveys

Aircraft: While rotor-wing aircraft make excellent survey platforms due to their slow airspeed and excellent visibility however the high hourly price of the aircraft usually precludes their use. Fixed-wing aircraft offer a cost effective and readily available aerial survey platform. Only highwing monoplanes are used because they offer acceptable downward and lateral visibility. Currently FPM uses two Cessna 206's for aerial pest detection surveys. One aircraft is equipped with a photoport for airborne videography missions.

Flying Height: For both aerial sketchmap and airborne video surveys optimum flying altitude above ground level (AGL) varies with terrain and pest activity but usually is 1,000-2,500 feet above ground level for aerial sketchmap surveys and 1,000 -3,000 AGL for airborne video surveys. We attempt to fly as high as possible while still being able to accurately identify pest activity since the greater the altitude the greater the ground coverage (with both aerial sketchmapping and airborne videography) and hence productivity. Higher elevation flight increases flight safety by increasing the glide distance in the event of an engine failure.

Airspeed: Airspeed dependent on the level of pest activity and topography but always is above 80 miles per hour at all times. Conversely, with aerial sketchmap surveys airspeeds greater than 120 miles per hour results in the aircraft passing over the ground too quickly to accurately locate and identify pest activity. Airborne video missions are generally conducted at airspeeds of 100-120 miles per hour.

Time of Flight: Because of the steep highly dissected terrain in the Intermountain Region shadows on west and north facing slopes can obscure pest activity before 0900. After 1400 hours thermally heated air can become very turbulent and make identifying and mapping observed pest activity difficult. Airborne video surveys are conducted in a narrower flight window than aerial sketchmap surveys, usually from 1000 hours to 1400 hours due to the systems sensitivity to shadowed areas and turbulence.

Flight Patterns: The topography to be surveyed, level of accuracy, and intensity of pest activity will determine the flight pattern. Two flight patterns are generally used: contour and grid.

Grid--Grid flight patterns are used when topography is generally flat with few distinguishing features. Predetermined flight lines are plotted on the flight map and while the aircraft travels down these lines two observers map pest activity from their respective sides of the aircraft. Flight lines range from one to three miles apart depending on the level of accuracy desired. Electronic navigation systems are used with grid flight patterns. Airborne video missions are conducted using grid flight patterns with swath-widths from 1/8 to 1/2 mile.

Contour--Steep, well-defined topography requires a contour flight pattern. The aircraft, usually with one observer, travels up and down major drainages in a clockwise flight pattern. Travelling up the drainage the pilot is close to the left side of the drainage allowing the aerial observer to map pest

activity to the right of the aircraft. When the top of the drainage is reached the aircraft turns around and travels down the opposite side of the drainage and the observer maps pest activity on the opposite side of the drainage. Occasionally, contour flight patterns are used on airborne video missions when it is necessary to monitor pest activity along roads, streams, etc.

In many instances a combination of grid and contour flight patterns are used to effectively survey an extensive area.

Damage symptoms which cannot be readily attributed to specific pests are plotted on sketch-maps as being of questionable cause. Location of such damage may also be entered into the aircraft's LORAN-C or GPS navigation system. These geodetic coordinates used to aid in pinpointing the ground location of tree damage during followup ground evaluations to determine causal agents.

When ADS and followup ground evaluations of each forest or survey unit are completed, information is replotted onto a single 1/2 in or 3/8 in per mile forest base map, which is then digitized into ARC/INFO Geographical Information System for data summation and map reproduction.

SAFETY/FLIGHT COORDINATION ACTIVITIES ASSOCIATED WITH AERIAL PEST DETECTION SURVEYS IN THE INTERMOUNTAIN REGION

Time	*Duty*	*Comments*
Week before flight	Call RO dispatch and inform them of week's general flight plans.	Emphasize that our plans frequently change and we are giving them a tentative schedule.
At least 24 hours before flight	Call appropriate dispatch office(s) and inform them of flight plan and aircraft manifest, check on frequencies, inquire on fire activity and aircraft on Forest. **Get name of person you talked to.**	*Flight plan*: time due on Forest, mission (pest detection), type of flight-contour or grid, starting location and general are of flight. *Manifest*: aircraft number, type of aircraft, pilot, passenger(s), color of A/C.
Day of flight	Call dispatch and repeat above, inform them of any changes in your flight plan.	
Before take-off	Radio check with dispatch, inform them of destination.	If at a controlled airport let dispatch know you will be talking to the tower and you will talk to them when leaving the TCA or ARCA.

After take-off	Radio dispatch and let them know you are off the ground and enroute.	If you are ferrying to a different Forest or area, have dispatch call with your ETA.
Every 15 minutes	Radio dispatch with location and direction or "working upsteam or down-stream" in drainage.	
After landing	Radio dispatch that you are on the ground.	If you are taking a break inform dispatch of ETD. If survey is completed inform dispatch that you are ceasing flight operations.
PM	Call with next days flight plan as above.	

PACIFIC SOUTHWEST REGION AERIAL DETECTION SURVEY PROGRAM SUMMARY

Sheri L. Smith

Forest Pest Management, Lassen National Forest,
USDA Forest Service, Susanville, California 96130

The Pacific Southwest Region (R-5) resumed aerial detection surveys in 1992 using National Forest personnel to conduct the surveys. One National Forest was flown during 1992, four during 1993, and we are anticipating flying 10 National Forests during 1994. Forest Pest Management provides the funding and survey standards and the Forests are responsible for the aerial surveys and sketch mapping. Flights are conducted between June and July by either helicopter or fixed-winged aircraft. Aircraft type varies between Forests; however, all aircraft and helicopters have been contracted.

Standardized mortality categories are used Regionwide and are based on percent of dead trees within a polygon. Mortality polygons are overlayed in GIS onto the Forest vegetation layer to determine the number of acres in each timber strata within each polygon. The number of dead trees and the volume associated with them is estimated using a Lotus 1-2-3 spreadsheet with the data for the appropriate timber strata. All maps are created on the Data General system and using LTPLUS on a PC.

R-5 has the complete airborne video package (MAG). Airborne video has been used for two projects: Modoc budworm defoliation survey and for Port-Orford-cedar root disease management. TNT MIPS version 4.4 (on an x-windows system) is available in the Region for video processing.

AERIAL DETECTION SURVEYS IN THE NORTHEASTERN AREA

Marc A. Roberts

Forest Health Protection, St. Paul Field Office, USDA Forest Service,
St. Paul, Minnesota 55108

Aerial pest detection surveys have been conducted throughout the Northeastern Area for decades. There are maps and records of aerial surveys conducted by the Forest Service dating back to the 1950's. Through the 1960's, 1970's, and into the 1980's, most aerial pest detection surveys had been driven by requests from the National Forest System or a need to assess pest conditions before or after control projects. Since the late 1980's and through the 1990's, the aerial survey programs in the Northeastern Area have been driven by a growing concern for general forest health and ecosystem conditions, and a growing appreciation for the historic value of a complete record of major pest events.

A variety of strategies are used throughout the Northeastern Area to conduct aerial pest detection surveys. Most of the States in the Northeastern Area have pest specialists, planes, and pilots available for aerial pest detection surveys. With the cooperation and coordination between Northeastern Area State and Private Forestry personnel, National Forest personnel, and State pest specialists, aerial pest detection surveys and reporting are conducted and completed in a timely and effective manner throughout the Northeastern Area. The three field offices in the Northeastern Area (St. Paul, MN field office (SPFO), Durham, NH field office (DFO), Morgantown, WV field office (MFO)) take different approaches in assuring that pest detection surveys are completed on federal lands and throughout their areas. While the federal lands in the MFO area are flown by State specialists, the DFO has a technician permanently assigned to surveying the two National Forests in their area as well as other federal lands, and the forester in the SPFO is responsible for completing the aerial surveys on the ten National Forests in their area as well as numerous National Parks, Indian Reservations, and other federal holdings. All three of the field offices rely heavily on State personnel to provide aerial survey information for State and private holdings. A network of State and National Forest personnel provide insect and disease development information which is invaluable for planning the timing of the various surveys.

The DFO and the SPFO follow Forest Service flight-following regulations while conducting aerial surveys. The DFO uses contract planes equipped with radios capable of contacting Forest dispatchers, and the SPFO uses Forest Service owned airplanes equipped with Forest Service radios, and flown by experienced Forest Service pilots who are familiar with flight-following procedures and with wilderness flying. Most of the Forests in the Northeastern Area have contracts with FAR 135 Forest Service approved private planes and pilots to fly surveys and fire patrol. These aircraft are also equipped for flight following and the pilots are usually experienced in flying surveys. These planes and pilots are usually available to fly aerial pest detection surveys.

The DFO and the SPFO both have experienced sketchmappers in charge of their aerial survey programs, but often times inexperienced, untrained personnel are used to complete the survey crew. This can create problems with the quality of information obtained on the surveys. Greater effort must be made to assure that aerial pest detection surveys are conducted by well-trained, experienced personnel.

With the increased interest in national and regional forest health, there has been a push to standardize aerial surveys and establish minimum pest damage reporting standards. As this effort continues, aerial pest detection survey data collected by different agencies within the Northeastern Area will become more compatible and, therefore, more reliable. With the increased amount of time and money being spent collecting pest damage information, greater effort must be taken to assure that aerial survey personnel are properly trained, and that experienced personnel are available to train and mentor inexperienced surveyors.

AERIAL SURVEY OF FOREST INSECT AND DISEASE ACTIVITY IN ALAKSA

Roy Mask

Forest Health Management, Alaska Region,
USDA Forest Service, Juneau, Alaska 99801

Robert L. Wolfe
Forest Health Management, Alaska Region,
USDA Forest Service, Anchorage, Alaska 99503-3956

Alaska is a vast area with approximately 130,000,000 acres of forest land. Each year, the Alaska Region (Region 10) Forest Health Management Group conducts aerial surveys that cover as much as 32 million acres of Alaska's boreal and coastal forests. Surveys are conducted across all ownerships including federal (Forest Service, Park Service, BIA, BLM, Fish and Wildlife, Department of Defense etc.), state, and private (e.g., native corporation) lands. Surveys are conducted in three segments, covering interior, south-central and southeast Alaska. Surveys begin around mid-July and depending on weather, may continue through the end of August. With limited resources, all of the forested area in Alaska cannot be surveyed in a single year. Therefore, resource managers are polled annually in order to set priorities to obtain the most valuable survey information possible.

Aerial forest pest detection surveys in Alaska have had a "colorful" history. The earliest documented surveys occurred in southeast Alaska, where wide-scale timber management activity first began. Systematic aerial surveys to detect forest insect activity began in interior and southeast Alaska in 1956 and 1952, respectively. For many years, surveys were conducted by research entomologists. State and Private Forestry (FPM) later assumed survey responsibilities following a period of cooperative survey implementation with PNW.

Survey Techniques

Because of rough terrain and often inclimate weather patterns, aerial surveys in Alaska (with the exception of the Kenai Peninsula) are not conducted on a grid pattern. In interior, forests tend to follow narrow bands along river valleys and thus, the survey entails flying many of the major drainages, often in a single pass. Southeast Alaska is made up of a narrow strip of mainland and many islands. Some of the islands rise from sea level to elevations over 3,500 feet. Most of the commercial forest lands in southeast Alaska are located within 2 miles of salt water, the exceptions being some river drainages. Thus, the survey in southeast Alaska can take on a meandering pattern in island areas when ceilings are low.

Survey aircraft vary, but typically include a Cessna 206 amphib or a DeHavilland Beaver. Amphib capabilities are especially beneficial, as refueling sites are often on land or water, but not necessarily on both.

Flying height varies, but is normally from 1,000 to 1,200 feet. For safety reasons, an altitude of 500 feet above "the deck" (water or land) is maintained at all times. Airspeed also varies, depending on survey aircraft and conditions.

Forest pest activity is sketch mapped on 1:250,000 scale maps. Original maps include detail on flight line location and direction.

Defoliator Sampling

In conjunction with the aerial survey of southeast Alaska, periodic stops are made at pre-designated sites (beaches with float plane access) to collect information on western hemlock defoliator species and abundance. This defoliator trend information has been collected during the annual aerial survey since 1971. Approximately 50-60 sites are visited within a 2-week period.

GIS and Airborne Video Application

During the last 2 years, airborne video technology has been deployed to remotely sense spruce beetle activity. This technology is obviously not being used during the entire annual survey, but has proven valuable as a sampling tool. The current airborne video acquisition system is deployed aboard an amphib Dehavilland Beaver that has a pre-existing belly hatch.

In 1993, a cooperative effort between the Forest Service (Forest Health Management) and the Alaska State Division of Forestry was initiated to include annual state-wide insect activity in an ARC INFO database. The information is available to anyone with comparable GIS technology.

Future Work

International Cooperation

Because Alaskan forests have much in common with our neighbors in Canada, there are opportunities to coordinate and share information. Spruce beetle activity northwest of Haines (southeast Alaska) is a prime example, where spruce mortality occurs on both sides of the border.

Aerial Survey and Ecosystem Management

Aerial surveys in Alaska have long included documentation of insect and disease activity among commercial and non-commercial forests alike. As we begin to take an ecosystem level approach in forest management, survey data for all components of forest vegetation will no doubt be elevated in importance. Our historical survey data may provide some baseline information as we begin to look more closely at the ecological role of "non-traditional" forest insects and diseases. In fact, we may determine in many cases that the term "pest" is inappropriate.

AERIAL SURVEY METHODS USED IN THE SOUTHERN REGION

Patrick J. Barry

Forest Health, Asheville Field Office, USDA Forest Service,
Asheville, North Carolina 28802

In the Southern Region, which covers 13 states, our aerial survey program relies heavily on the sketch mapping survey method. Aerial photography in the 9 x 9 format is currently our second most-used method. Airborne videography is becoming very popular with our clients on both National Forest lands and other Federal lands. Our state cooperators are also very interested in the use of videography for documentation of insect and disease occurrences and storm damage.

Our current uses of the aerial sketch map method are:

1. Southern pine beetle (SPB) surveys.
   a. Annual reconnaissance surveys of areas adjacent to known outbreaks or areas having a previous history of SPB activity, for documentation of bark beetle activity.

   b. Detection surveys are usually a 25 percent sketch map survey where numerous active spot infestations were observed during a reconnaissance survey. Detection surveys are also conducted when a land manager reports numerous multiple-tree spot infestations from ground surveillance. On all our aerial sketch map surveys, we estimate spot infestation size by estimating the number of red and fading trees present in the spot. We also use other key codes such as "F" for spots with fading trees and "R" for older spot infestations with only red or brown-colored tree crowns and other helpful codes.

   c. Forest Health Evaluation surveys for SPB are either 50 percent or 100 percent aerial sketch map surveys. Spot size is estimated during evaluation surveys also.

The procedure above is currently used by the Asheville, North Carolina Field Office. The Pineville, Louisiana Field Office relies very heavily on their National Forest Ranger Districts to conduct almost all their aerial sketch map surveys for the SPB. The Asheville Field Office also uses District aerial sketch map surveys where and when possible, especially during continuing suppression projects or where we have trained personnel on the Ranger Districts. For suppression projects on Federal lands, National Forests, and Other Federal, pre-suppression flights are conducted bi-weekly or at least once every 3 weeks.

Our state cooperators conduct two 20 to 25 percent sketch map surveys annually for SPB and other bark beetle detection. Aerial surveys for evaluating outbreak areas are usually 50 to 100 percent surveys. Pre-suppression aerial sketch map surveys are conducted monthly during a cooperative suppression program.

In Region 8, we encourage our Federal land managers to cooperate with State personnel and vice-versa in sharing their aerial sketch map survey results with each other.

2. Gypsy Moth Surveys - Aerial sketch mapping for the detection of gypsy moth defoliation in Region 8 is one of the primary sources for compiling an annual database that depicts the amount and severity of defoliation related to this pest. The data from these surveys are used to form national and regional defoliation maps used in determining the location of new infestations, post-treatment evaluations, amount and severity of defoliation and movement of gypsy moth populations.

3. Other pests surveyed in Region 8 with the aerial sketch map method are:

   a. Other defoliator (pine and hardwood)
   b. Storm damage (tornado, hurricane, ice, etc.)
   c. Oak wilt (Texas and North Carolina)
   d. Littleleaf disease of shortleaf pine
   e. Annosum root rot
   f. Introduced plant species
   g. Balsam woolly adelgid
   h. Hemlock woolly adelgid
   i. Beech bark disease
   j. Air pollution
   k. Fire surveillance
   l. Oak decline
   m. Spruce fir type mapping (etc.)

Current uses of color or IR photography are:

1. Southern pine beetle infestations in special use situations are areas such as wilderness areas when they are threatening bordering state and private lands, or threatened and endangered species their habitat or nesting areas. An example in our Region would be the red-cockaded woodpecker (RCW) its colonies, cavity trees and habitat.

2. Gypsy moth use of aerial photography. The format used for detection of gypsy moth defoliation is either high altitude color infrared or connectional color 9- x 9-inch prints or transparencies of various scales. These photos are used to delineate areas of gypsy moth defoliation. sketch mapping is used to fill in the gaps not covered by photography and the combined results are then entered into a GIS system to produce defoliation maps.

3. Other pests surveyed with aerial photography are:

   a. Oak decline
   b. Oak wilt
   c. Storm damage
   d. Pest in special use areas
   e. Pests threatening T&E species
   f. Balsam woolly adelgid
   g. Hemlock woolly adelgid
   h. Air pollution

We are also making use of satellite imagery and other quads.

Airborne videography is currently used for the following:

1. Monitoring SPB spot infestations in wilderness areas and other special use areas, to determine the rate of spot growth and to document the distance of the individual spot infestations to bordering state and private lands or RCW colonies and cavity trees. The National Forests in Texas and Mississippi are currently using their own aerial videography systems for these purposes. They also have the map and image processing (MIP's) system and GPS. Our field offices also have complete aerial videography and MIP's system.

2. Other planned uses are:

   a. For gypsy moth
   b. Hemlock woolly adelgid
   c. Oak decline
   d. Beech bark disease
   e. Storm damage
   f. Air pollution
   g. Balsam woolly adelgid

ROCKY MOUNTAIN REGION AERIAL SURVEY PROGRAM

Judith E. Pasek

Forest Health Management, Rapid City Service Center,
USDA Forest Service, Rapid City, South Dakota 57701

Approximately 5 years ago, the Rocky Mountain Region decided to curtail much of its regular aerial survey program primarily because of concerns about safety relative to the value of the information to the land manager. Flying at low altitudes over the Rocky Mountains entails problems of sudden downdrafts and hazards of box canyons. Most Forests in the Rocky Mountains require contour flying. We have had to rely on pilots and aircraft that were contracted on a daily basis and often were unfamiliar with the type of flying required to do pest detection surveys. It was often difficult to get the same pilot two days in a row. We use Forest Service dispatchers for flight following, but sometimes have trouble with personnel not being there when we want to start, even after giving them information about our flight plans in advance. We normally must quit flying around noon because the turbulence gets to be too much.

For the past 5 years, each of the three Service Centers in the Region has planned and conducted its own aerial survey program. The Black Hills National Forest (served by the Rapid City Service Center) is surveyed each year primarily for mountain pine beetle damage. The elevation changes are less dramatic in the Black Hills than in the mountainous terrain of most of the rest of the National Forests in the Rocky Mountain Region and can be flown in a grid pattern. Also, the Black Hills National Forest has the largest timber program of any Forest in the Region. Other Forests are surveyed on an as-needed basis, often when an outbreak has already been detected by other means and an estimate of area or volume of damage and extent of infestation is needed. Primary pests of interest are mountain pine beetle, Douglas-fir beetle, western spruce budworm, and spruce beetle. We occasionally survey for infrequent defoliators such as pine sawfly and pine tussock moth. Recently, much of the area surveyed in southern Colorado (served by the Gunnison Service Center) has been prompted by outbreaks of western spruce budworm or bark beetles. The Lakewood Service Center has not conducted any aerial surveys in recent years.

To date, the survey work conducted by Forest Health Management personnel in the Region has entailed sketch mapping. Color and infra-red photography is contracted when needed. For sketch mapping, we use dot symbols to indicate groups of dead trees of various sizes up to 25 trees for bark beetles. We outline larger spots of defoliation and bark beetle damage, including the estimated number of trees killed. Dot symbols are counted and multiplied by an estimate of associated acreage for each symbol type. Acreage of larger, outlined areas is determined using a planimeter. Acreages are then totalled by ownership type (Forest Service, Other Federal, State and Private) to meet national reporting requirements. For bark beetles, estimates of numbers of trees killed are derived by using a sum of the number of each type of dot symbol times a mean number of trees for the corresponding dot symbol, then added to the total estimated number of trees in larger outlined spots.

Conversion factors that vary by tree species and forest are used to estimate volume killed from number of trees killed. Copies of the aerial survey maps are made by hand and sent to affected land management units.

For special project areas, we can generate a computer copy of the sketch map using MIPS software on the PC at the Regional Office. So far, we have not done much digitizing of our aerial survey maps.

A few months ago, a Cessna 206 acquired by Region 2 was outfitted with airborne video equipment. Forest Health Management personnel have yet to use this newer technology. However, the MAG unit in Fort Collins has flown some airborne video projects for Region 2, Forest Health Management in the past couple years. Results were disappointing in that bark beetle (Douglas-fir beetle) damage was not readily discernible on the film. There may be value for its use in recording conditions on permanent plots included in the Forest Health Monitoring program; however, film shot for this purpose has not yet been viewed and interpreted. The availability of the Cessna 206 is likely to improve the aerial survey program for sketch mapping in Region 2 in addition to providing a new technology for our use.

CANADIAN AERIAL SURVEYS FOR PEST DAMAGE ASSESSMENT

G. A. Van Sickle

Forest Insect and Disease Survey, Canadian Forest Service,
Pacific Forestry Centre, 506 West Burnside Road.
Victoria, British Columbia. Canada V8Z 1M5

To complete annual regional and national overviews of forest pest conditions and their implications, the Canadian Forest Service's Forest Insect and Disease Survey (FIDS) has for many years monitored the incidence and damage of insects and diseases in the nation's forests. Aerial reconnaissance and sketch mapping have been a major component of these surveys, especially for mapping some types of defoliation and tree mortality. Across Canada, six similar survey units housed at the federal regional forest centres constitute the national FIDS program. Through cooperation and coordination, regional and national surveys and reports are completed.

At the Pacific Forestry Centre, the 17-member FIDS unit includes field technicians responsible for both ground and aerial surveys throughout the region (British Columbia and Yukon). They are supported by professional and technical diagnostic staff and a geographic information system manager. All are under the general leadership of the Survey Head. Each year more than 225 hours of flying time, much of it in cooperation with the B.C. Ministry of Forests and forest industry, are completed for detection and first-stage mapping of pest-caused damage. Generally, recent bark beetle-killed trees and major defoliator infestations are the specific reasons for the flights, but climatic injury, animal damage, some foliar diseases, or unusually heavy cone crops can often be identified.

The purpose of the aerial survey is to complete a regional and national uniform estimate of yearly changes in pest types, location, area affected and damage intensity. Also of concern are timelines, continuity during and between outbreaks, and support to research and to subsequent more detailed surveys of areas of specific or operational interest.

Aerial Survey and Mapping Methods

Aerial surveys for detection and mapping of forest pests have been quite regular since 1960 and were conducted for selective problems since the late 1940's. Although there are records of aerial mapping from hydroplanes of hemlock looper and mountain pine beetle in British Columbia as early as 1927, most of the earlier cartographic records of infestations were largely limited to mapping from vantage points. For provincial and national overviews, aerial sketch mapping is still the most time and cost-effective procedure for conducting a detection and initial survey over vast areas on a yearly basis. Currently, sketch mapping for a first-stage overview is mostly on 1:100,000 scale maps, occasionally at larger scales and, if necessary because of map availability throughout the region, at smaller scales up to 1:250,000.

Flying is usually best done in late July or August, by which time field staff have a good knowledge of current conditions and can plan the most efficient coverage of known and historically likely outbreaks. Also, the discoloration or loss of foliage caused by bark beetles or defoliators is usually at its most consistent and visible

stage for ease of detection and distiction. With bark beetle-killed pine, experienced observers can usually differentiate between previous year's and older mortality.

There are usually two observers, preferably with the senior observer having at least 5 year's experience. With attention to the plane's altimeter, map contours and natural features, the location, relative size, severity and damage, and probable cause are delineated on topographical maps. If small, the estimated number of currently damaged trees is recorded; otherwise, severity classes are assigned. In mountainous terrain, contour flying is most efficient with one or more passes through the watershed depending on its size and the light conditions. Observers seated in tandem may be best if several passes are made through a drainage, while one on each side of the aircraft is best if only a single pass is made or if a grid pattern is flown.

High-winged aircraft are selcted for safety, ease of forward and lateral visibility (bubble windows greatly improve viewing almost directly below), adequate cruising range and for speed and good performance when mapping is done at elevations of 300 to 500 meters above ground level (depending on terrain) and an air speed of 150 to 175 kph. For best concentration and comfort, individual flights should not greatly exceed 3 hours' duration. The time of day affects lighting and ease of damage detection, especially on north slopes, so mid-morning flights are usually best. Some observers find that amber IR/UV- filtered sunglasses provide better contrast of color changes.

For provincial and national overviews, our preferred map scale is the provincial 1:100,000 topographical series which is currently available for about 40 percent of the province. Alternatives are 1:125,000 or 1:250,000 scale maps. Pre-flight preparations such as lightly marking the previous year's infestation allow staff to check for errors, increases consistency from year to year, improves the accuracy of locating continuing infestations, enables the expansions and changes over time to be checked and better identified, and ensures that major infestations are reflown.

Some oblique, hand-held photography or video is usually obtained for a visual record, a training guide, and sometimes to refine the sketch maps and the assessment of damage. Other photographic and remote sensing techniques have been evaluated (Gimbarzevsky et al., 1992), but it was felt they could not provide as timely, cost effective and complete an overview as the basic sketch mapping procedure. The operating costs for the aerial survey (excluding staff salaries) is about 10 cents per km2 (1/10 of a cent per hectare).

Geographic Information System Outputs - Annual infestation maps and summaries

Development of GIS capabilities has been underway in FIDS at Pacific Forestry Centre (PFC) since 1984. The GIS software used since November 1991 is Environmental System Resource Institute's (ESRI) ARC/INFO. It operates on a Sun Sparcstation 2 platform (32 megabyte (MNB memory, 16-inch colour monitor, 424 MB internal disk drive, 3.5" 1.44 MB floppy disk drive, and Sun Operating System (Sun OS)). Peripheral hardware used includes an Altek AC30 Digitizing Table, a 150 Mb 1/4" SCSI Cartridge Tape Drive, a 1.2 gigabyte (Gb) Wren VII Disk drive, a 758 Hewlett Packard (HP) Pen Plotter, and a QMS-PS 410 Laser Printer. Similar work stations or personal computer-based systems are in place at each of the other Canadian Forest Service laboratories and through the network and cooperation, nation-wide maps can be produced at the Petawawa National Forest Institute.

Upon completion of the aerial surveys each year in August or September, the field technicians return to PFC and enter into the GIS the current infestations by digitizing the polygons and assigning attributes of pest, severity, year, forest region and map reference. From these data, searches or compilations, of any combination of desired attributes can be made.

Also, during digitizing, the current and previous year's infestations can be viewed on the screen and any differences are corrected or accepted by the technician before entry into the database. With the field technicians responsible for input of their own data, errors of missing labels, placement, etc. can be detected and corrected.

Maps are then computer-produced at various scales and distributed to cooperating provincial forest service and forest industry staff, and are available to parks and others. By combining 20 to more than 100 maps, regional and provincial maps are available for review, planning meetings and reports. Using report generators, area and polygon tallies can be derived for selected areas, map sheets, administrative regions or the entire province.

Accuracy of Aerial Sketch Mapping

Aerial sketch mapping is widely used and accepted as an initial survey technique especially for damage by defoliators and bark beetles throughout Canada and the United States. The accuracy of the results is often difficult or costly to assess. Also, the general purpose of the different surveys should not be forgotten. Too often, in the absence of more detailed information, sketch map results are extrapolated beyond reasonable limits and expectations. Conversely, time and effort is often spent on detailed surveys when a simple sketch map would have been just as useful.

With experienced mappers, the detection and location of infestations is generally accurate to the scale of map used. For individual trees or small groups, direct observation can even provide better detection than most overview photography. Our own periodic reviews, as well as Aldrich et al. (1958) with southern pine beetle, have found aerial sketch map detection and location results to compare very favorably with more careful spot checks or complete surveys.

In sketch mapping, the size of infestation is frequently exaggerated, especially when many small pockets are mapped, but the counts of dead trees are usually low. In comparison to aerial photographs obtained for a portion of selected outbreaks, Harris and Dawson (1979) found the total area sketch mapped was 34 percent larger than measured on photographs. An over-estimation of the area affected was also noted by Gimbarzevsky et al. (1992) in an extensive comparison of results from ground plots, aerial sketch mapping and numerous scale and types of remote sensing.

National Standards and Training

While a national workshop such as this one has not been held in Canada (it would be an excellent idea), each regional unit of FIDS has operation manuals (e.g., Forest Insect and Disease Survey 1984) with sections on aerial surveys and safety procedures. Separate manuals exist for the ARNEWS/biomonitoring program

(Magasi 1988). Although national aerial survey standards have not been developed, there is national uniformity in coding and recording forest insect and disease based on procedures established for the computerized database of more than 1.6 million ground-based samples gathered over the last 6 decades (Forestry Canada 1991). GIS data standards and a policy for data sharing still need to be developed.

While each region has its own set of training photos and pest signatures, unfortunately these have not been formalized and there has been too little inter-regional standardization. To partly overcome this, DESTIMAS (defoliation estimation system), a personal computer-based training aid for tree and branch damage assessment has been completed this year (Thomson and Van Sickle 1994) and will be tested. While not intended to replace field or aerial workshops, it does introduce and test the observer's ability to visualize random and known patterns and levels of defoliation or damage as simulated for various tree types.

Conclusion

A large national and regional historical database has been created from ground and aerial surveys over several decades, but only recently has the computer capability of relational database management and geographic information systems enabled fuller analysis. To guide and assist forest protection research and management, the database can be interrogated. A wide range of maps can be stored and produced, and maps can be overlaid, analyzed and summarized in association with pest distribution and history, forest inventory, ecological vegetation zones, administrative boundaries or climatic and other records.

While we continue to seek improved and efficient techniques for timely, annual surveys, we expect that aerial sketch mapping will remain a basic overview method and we will continue to work on improving its consistency and accuracy.

References

Aldrich, R.D., R.C. Heller and W.P. Bailey. 1958. Observation limits for aerial sketch mapping southern pine beetle damage in the southern Appalachians. J. Forest. 56:200-202.

Forestry Canada. 1991. Instruction guide to Forest Insect and Disease Survey general survey form. Petawawa National Forestry Institute. 69 pp.

Forest Insect and Disease Survey. 1984. General instructions manual - Pacific Region. Pacific Forestry Centre. 123 pp.

Gimbarzevsky, P., A.F. Dawson and G.A. Van Sickle. 1992. Assessment of aerial photographs and multispectral scanner imagery for measuring mountain pine beetle damage. Information Report BC-X-333. Pacific Forestry Centre. Victoria, B.C.

Harris, J.W.E. and A.F. Dawson. 1979. Evaluation of aerial forest pest damage survey techniques in British Columbia. Information Report BC-X-198. Canadian Forest Service, Victoria, B.C.

Magasi, L.P. 1988. Acid rain national early warning system. Manual on plot establishment and monitoring. Information Report DPC-X-25. Ottawa, Ontario.

Thomson, A.J. and A. Van Sickle. 1994. Computer-based training in tree damage assessment. A I Applications (in press).

USE OF AERIAL SURVEY FOR MONITORING CYPRESS APHID DAMAGE IN KENYA

J.J. Ngasi

Aerial Survey Specialist, Forest Health Management Centre,
P.O. Box 30241, Nairobi, Kenya

1. *Introduction*

For the best decisions to be made in regards to a forest pest, the extent and magnitude of the damage must be determined. Aerial sketchmap surveys, followed by ground truthing are the most efficient way to obtain good information. In Kenya, an aerial survey became desirable when the cypress aphid outbreak was noticed in 1991 on Mexican cypress plantations.

Detection is done by:

(a) Using a light aircraft to fly over forested areas and sketchmap the locations of damage, and

(b) Ground detection to identify the host, the damage, and the causal agent.

The aerial sketchmapping becomes the only quick way to cover large tracts of remote forest areas in a short period of time.

(a) *Advantages*

(1) Quick assessment of forest damage

(2) Costs per hectare are lower when large areas are involved

(b) *Disadvantages*

(1) Needs highly trained manpower which is expensive to obtain

(2) Sometimes finding a suitable aircraft and a qualified pilot is difficult

(c) *Uses of Aerial Surveys*

Aerial survey is used in detecting and monitoring the location, extent, and intensity of forest damage by a forest pest. The damage is sketchmapped on maps of various scales and then a summary can be made back in the office. Summary information includes the station, block, sub-compartment, age of stand area, and stand volume. This information will quantify the resources at stake and an economic threshold can be determined. The determination of an economic threshold is important as it will tell us how much we can expect to lose in comparison to how much we are going to spend on controlling the pest.

2. *References and Guidelines*

Guidelines for aerial surveys were prepared in February 1992, by Mr. J.G. Denny Ward, FAO/TCP Project Consultant, in collaboration with the project coordinator, Professor Joe Mwangi, and the, then, Deputy Project Coordinator, Mr. J.N. Maina. These guidelines have served as reference material for the execution of aerial surveys in Kenya.

3. *Data Used in the Aerial Survey*

Data used in the aerial survey in Kenya was developed by the relevant branches of the Forest Department and the Kenya Forest Research Institute (KEFRI). This included the following:

(a) Summary of plantation information from Forest Inventory Branch showing:
- District
- Station
- Block
- Sub-compartment No.
- Age
- Area
- Volume of wood in each sub-compartment and the total monetary values

(b) Plantation maps of scales 1:250,000 prepared by the Forest Survey Branch showing the details as above, but without volumes.

(c) Some topographic maps were also brought from the Survey Department of Kenya after several requests and vetting was done by the Defense Department.

4. *Techniques of Aerial Surveys*

Aerial surveys fall under various categories and the technique for each one will depend on the category. The main categories of aerial surveys are:

(a) *Reconnaissance Aerial Survey*

This is a quick survey covering the whole country. The important issue in this kind of survey is that since very large areas are covered every day, small scale maps are desirable. The ideal map scale is 1:250,000 or 1:500,000. The limitation here is that plotting damage accurately is difficult since only a dot on the map will mean several thousands of hectare. Fixed-wing aircraft are used.

(b) *Intensive Operational Aerial Survey*

This is an aerial survey aimed at getting information that can be used for operational purposes, namely spraying, salvaging, biological treatments of stands, silvicultural activities, etc. The map scales used are large scales like 1:10,000, 1:25,000, and 1:50,000. The information is plotted accurately and verification of the same information can be done by spot checking if a helicopter is used in this survey. Helicopters are used in this survey because of the slow speeds required for accurate plotting.

(c) *Post-Treatment Aerial Survey*

This survey is done to determine the effectiveness of a specific treatment done to a stand. This is a site-specific survey and aims to check on mortality or recovery. Both large-scale maps and small-scale maps can be used since the aim is a quick assessment of the results of treatment.

In all the cases, the aerial survey starts with the following:

- Appropriate scale for the purpose.
- All forested areas--marked in green.
- Predetermine flightlines on the maps and drawing them up with appropriate flight intervals and alignment.

At this planning stage, there are numerous considerations to be done; e.g.:

- The type of aircraft that is going to be used (its suitability, carrying capacity, its power, weather conditions, and the financial resources available).

A certified aerial surveyor would require 100 hours of flying time to master the job. There are numerous factors which influence the accuracy of an aerial survey. These factors form a wide subject of discussion and will not be discussed here in this seminar.

After the aerial survey is completed the crew comes back to the office and compiles the following information:

- Date of the flight
- The areas flown
- The block, compartment, sub-compartment, area, age, and volume of stands
- The aerial survey crew--by names
- The aerial survey team leader who signs the document

The aerial survey team leader has several responsibilities which he must ensure that he strictly follows.

5. ***Global Positioning Systems (GPS)***

This is a very important instrument fitted to the aircraft. It is used for navigating both on the ground and in the air, to locations of interest. GPS can be used as an efficient means of updating our GIS database on the cypress aphid.

6. ***Airborne Videography (ABV)***

ABV is an alternate to aerial sketchmapping but it requires highly trained personnel. This is a procedure in which a small video camera and video tape are used in the aircraft to record the desired information. These can be viewed in the office and important features noted. Airborne videography is more accurate than manual sketchmapping. Preservation of the video tapes can be done for many years and stand conditions at the spot can be compared frequently.

7. ***Aerial Survey Results***

The First Aerial Survey

In February 1992, FAO hired a consultant to assist the Kenyan counterparts in developing guidelines for aerial surveys and train the aerial survey crew. The training was done in a seminar held in Muguga and a crew of

four people was thoroughly trained in theory and practice. After the training an aerial survey was done. An actual sketchmapping revealed that about 46,000 ha. of cypress plantations had been severely infested by the aphid. The determination and classification of foliar conditions had been done earlier by Dr. Odera of KEFRI and the sketchmapping was based on this classification.

The conditions of the crown were classified as:

0	healthy
1-25%	light damage
26-50%	moderate
51-75%	heavy
76-100%	severe

The sketchmapping was mainly based on the two conditions: heavy and severe. As the aphids infest the crown from the bottom upwards, it was difficult to register effects in the light and moderate categories.

Maps were developed in the office showing the locations of the severe aphid damage and information was plotted on a GIS in Atlanta, Georgia, U.S.A.

The Second Aerial Survey

The second aerial survey has shown that about 10,000 ha. range between severe effect and mortality. Out of the 10,197 ha., 6,367 ha. have been salvaged, 3,830 ha. have actual mortality, and 1,220 ha. are in the severe state. This means that the area actually needing urgent salvaging is 1,610 ha. These constitute the plantations of 29 years up to 46 years. The figures above are the most recent figures collected from a ground confirmation survey done by the ground survey crew. The reasons given for these plantations not being harvested are:

(a) Inaccessibility
(b) Insecurity, especially in Mt. Elgon
(c) Unavailability of sawmilling industry in certain areas
(d) Political reasons.

8. Ground Survey

In February 1992, after the aerial survey, a ground confirmatory trip was organized and undertaken in April to confirm the aerial survey results. This trip covered Nakuru District, Kericho, Uasin Gishu, Baringo, Nyeri, and Meru. As there were not enough funds, the other Districts were not covered. In July, another trip was organized and covered Kakamega, Nandi, Uasin Gish, Baringo, Nyandarua and Laikipia. Some districts were repeated because the first one was done during the rainy season and it was necessary to compare the information after the long rains. In June and July 1993, two ground surveys were done--one west of the Rift and the other one east of the Rift. This trip was organized to confirm the results of the second aerial survey. The previous data was derived from this confirmatory trip. The trip covered the whole country and all the

districts with host materials were visited, apart from Keiyo Maragwet and Kiambu Districts where a trip is now being organized.

During the survey in western Kenya, intensive sampling was done for mortality counts and most plantations had substantial mortality and the evaluation showed that about Kshs.8 million would be lost in only the 29 plantations that were sampled. This mortality, spread over the whole country, would mean a substantial loss of revenue if the materials are not harvested in time.

Some of the plantations sampled showed that some trees had severe heart rots and the sawmillers were not interesting in harvesting them. Some of the materials which dried up last year have already become unsuitable for sawmilling and many sawmillers are disliking them.

A third aerial and ground survey will be done in November or December 1994.

9. ***Analysis of Aerial and Ground Survey Results***

Introduction

The first question before the aerial survey was done was:

> "What is the extent and location of the cypress aphid damage in the field?"
>
> The sketchmapping surveys showed the locations and the extent of the cypress aphid damage. The actual position of stands severely damaged has been transferred to GIS-generated maps which are now available at the Forest Health Management Centre at Karura.

The second question was:

> "Is the information marked on the maps true?"
>
> This question prompted surveys to be undertaken. The ground survey verified that about 35% of the plantations marked on the map still existed or were harvested due to excessive mortality caused by the aphid or due to the normal harvesting age. It should be noted that the plantation list which was prepared after the aerial survey was used as a checklist and an updated one was produced.
>
> A point worth noting also is that the updated list needs reviewing after six months since the plantations indicated in the previous list are being continuously harvested.

The third question was and is:

"What is the amount of volume loss through mortality?"

This question prompted us to conduct ground surveys to sample the plantations that were viewed from the air as having mortality to determine how many trees were dead due to aphid damage per ha. and per plantation, and the trees' volumes.

Some work has been done on this and the results computed. The ages of the stands sampled ranged from 16 to 46 years and there were numerous gaps in the age ranges. This means that if enough funds were available, sampling could be done in all the stands from age 5 to 46 years to correlate the aphid damage with age. The amount of volume loss has been computed in the test samples and the volumes equivalent to revenue which could accrue if the trees are harvested in time calculated.

B. *Sampling Method*

The sampling method used in this study was the nearest neighbor method. The main advantage of this method is that stratified sampling is done and sample size will depend on the total area of the plantation to be sampled. This means the larger the area, the greater the number of sample plots--up to 20 plots.
This method also limits the number of trees to be assessed to 5 trees per plot and at least 20 plots per plantation so that 100 trees are assessed per plantation.

The trees are assessed by classifying them as:

		0	crown foliar damaged	healthy trees
1	-	25%	crown foliar damaged	light attack
26	-	50%	crown foliar damaged	moderate
51	-	71%	crown foliar damaged	heavy
76	-	100%	crown foliar damaged	severe
Whole tree dried up				dead

When observing mortality it is important to note that other causal agents were noted, e.g., animal damage, human damage, fire damage, and other tree stressors that may have caused the death of the trees.

The fourth question was:

"Is it true that the older the trees the greater the severity of the cypress aphid damage?"

We have tried to prove this by interpolating the figures from the field by comparing severely affected trees in percentages (%) with actual mortality percentages. The trend seems to indicate that the older the tree the greater the effect of the cypress aphid. It is recommended that sampling be done for the whole country and for trees of all age classes to come up with good figures to show the actual relationship between age and damage.

This will also assist in helping us draw up salvage guidelines for the severely affected stands. A decision will be made on which salvage method will be appropriate at what age.

Salvaging can be done in two ways:

(1) Incorporating the harvesting in the usual thinning schedule--selective salvaging.

(2) Salvaging in total: harvesting the whole plantation that is affected.

The advantage of selective salvaging is that the dangers of soil erosion on the salvaged lands is eliminated. There is a tendency of the land on which salvaging has been done to be eroded during the rains before natural regeneration takes place. This is true in stripe slopes.

The disadvantage is that the volumes may not be great enough for money to be made by the sawmillers, so no one would bid on the job.

C. *Recommendations*

We would recommend that whenever the funds are available, monitoring and appraisal of the stand status be done at regular intervals so that stand changes can be registered and the information can be used by managers and decision makers.

AERIAL SURVEYS, THE GOOD, THE BAD, THE BUMPY

David Beckman

Bureau of Private Forestry, Idaho Department of Lands,
Coeur d'Alene, Idaho 83816

I started to learn aerial surveys in the mid-seventies from Ladd Livingston. When I started, it all sounded really neat. I would sit in the back of a Cessna 182, on the passenger side. We sub-contracted a fire patrol aircraft from the Forest Service out of Coeur d'Alene, which contracted from Felts Field Aviation in Spokane, Washington. For the first couple of years, I was just trying to learn to identify the tree species and to locate myself on the maps and keep from getting sick. When I first got started, I can clearly remember that what I saw on the maps was not how it always looked from the air. The maps are large so you had to fold them several times. They have not changed very much over the last 20 years. They are still very large and it is always fun to try to refold them, in a short period of time in these small planes.

Air speed and elevation, with sharp turns at the head of every drainage, were another thing I had to get used to. The first couple of years, sitting in the back seat, was not that easy. You would be looking out the window, then turning your head to look down at your map, then turning your head to look out the window, always trying to keep your location on the map. When you would see a group of dead trees, your head would be going back and forth, back and forth. What tree species is that, how many trees in that group, what is the code for that species? Then, trying to draw a nice little polygon on the map, in perfect location, with a code and a estimated number of dead trees, which was not always right and as you tried to erase the first group or numbers, there came another group of dead trees and another and another. "Oh no, I put it in the wrong spot," or just as you're about to write, the plane hits a turbulence, your head hits the roof of the plane and your pencil hits the map, either making a hole in your map or drawing a long line all over it. In my years of back-seat flying, I can remember trying to map in every dead tree, even the single ones. I would remember having to take motion sickness pills and how they would make me sleepy in the warm afternoons. Trying to keep my concentration as the day wore on, was always hard. Even more so after I got lost on the map.

Usually it would be a different pilot each morning. I would have to get the maps out, explain the procedure, air speed, elevation above the tree tops, staying always on the left side of every drainage, going to the top of the ridge, turning around with a sharp turn, then back down the drainage staying on the left side again, so the bottom of the main drainage was always in view. Then I could see the side drainages coming out of the main drainage and then up the next one. Always going in a clock-wise rotation, so what I wanted to see is always on the right side of the airplane. As I remember, the pilot did some kind of check in; we had no head sets to help keep the noise down. If we had ear plugs, we were lucky. Trying to direct the pilots in the direction I wanted them to go has always been fun in a noisy airplane. I had to make up my own sign language and then hope they were looking when I gave it.

At first, I can remember, if it was cloudy or windy at all, we would not go because of the shadows. It had to be an almost perfect day (not any more). I can remember in the early years I would get pilots who would smoke and would not know where they were or how to get there. They would always have to ask what our location was. They would be using the airplane's radio to do the check ins. The planes are noisy and small, with no

place to go until we landed--usually 3 hours at a flight. After a couple of hours or less, I started to get antsy, and then 9 o'clock comes and the pilot turns on Rush Limbaugh for the next 3 hours.

Some years are always better than others. Some years, one or two of the last 20, we get lucky and the bark beetle populations are very low. The conditions are just right. There are no forest fires, no burning grass fields yet, and you have a good pilot. Most years there are plenty of insects and disease damage to keep one busy and then there forest fires, grass-burning smoke, windy - cloudy days, or something goes wrong with the radio. There seems to be something new every year--a new disease or defoliator or bark beetle. It's never the same.

NORTHERN REGION AERIAL SURVEY PROGRAM

Tim McConnell

Forest Pest Management, Missoula Field Office,
USDA Forest Service, Missoula, Montana 59807

Introduction

Using fixed-wing aircraft to observe forest insect outbreaks in the northern Rocky Mountains began in 1948. At that time few forest access roads were aviailable to detect and monitor insect outbreaks. The post World War II aviation boom provided not only access for forest observations, but also a cost-effective remote sensing technique to observe and record major forest disturbances. Occurring at the same time across most of the northwest United States, was a large western spruce budworm outbreak. As more and more forested areas were flown, more forest disturbances were detected, including Douglas-fir beetle outbreaks and large windthrown areas. Along with the aviation boom came an intensified effort to combat several forest defoliators by using aerial spraying. Much of the "early years" of aerial detection survey mapping supported the aerial spray projects, as well as salvage opportunities for windthrown trees and Douglas-fir beetle caused mortality. These uses of the annual aerial survey are still in effect today. Along with them, is an historical record of major insects and diseases covering a span of over 40 years in some areas. As the Forest Service looks philosophically toward an Ecosystem Management approach to land management, and has a concern for change over time on the land it manages, the aerial detection survey maps have provided a long-term, broadscale record of some of the major components for forest disturbances.

The Program

The Northern Region aerial survey program is conducted annually on all 13 National Forests and one Indian Reservation (Flathead). The survey is flown intermittently on two National Parks and four other Indian Reservations. Areas of low insect disturbance are generally flown every other year due to a limited budget and available trained observers.

Three single-engine aircraft are available for survey flights provided by a private contractor. Survey pilots are the contractor's employees and are carded (certified) by the Forest Service to fly mountain reconnaissance missions. The contract aircraft available the past 6 years has been a Cessna 182, a Cessna 182 RG and a Cessna 206. The contract specifies at least two of the single-engine aircraft will be turbo charged or power boosted. This contract specification is to provide a safety margin for power when flying at the higher altitudes in mountainous terrain.

Two Forest Pest Management (FPM) observers fly approximately 90 percent of the annual survey totaling approximately 375 hours of aircraft time. One summer seasonal (high school biology teacher) and I do all the survey flying for FPM. The approximate aviation contract cost to do the survey each year is $60,000 ($160.00 per hour aircraft time). Most all forested lands are surveyed, except wilderness areas. Since there is a limited amount of dollars and observers, wilderness areas have, for several years, been dropped from the annual aerial survey. This is also due to the fact that one of the primary uses of the survey is to support the timber

aspect of land management and no timber management is currently being conducted in the vast wilderness areas of Montana and northern Idaho. Approximately 26 to 28 million areas are covered by the two observers.

The Idaho Department of Lands, Bureau of Private Forestry personnel fly the other 10 percent of forested lands (4 to 5 million acres) in the Region in Idaho. They are responsible for flying a specific portion each year that is primarily state and private land. Their survey maps are included in the final Regional survey maps.

The Montana Department of State Lands, Forestry Division has a Collection Agreement with the Forest Service to provide funds to cover costs of FPM flying aerial survey on the large, contiguous forested state land holdings. This amounts to approximately $4,500 each year.

Survey Method

Timing

To capture most damage signatures of insects and diseases from the air in a single flight, the survey is conducted during the summer months of July and August. The survey begins in areas where defoliators are not expected and continue to defoliate areas because the pest signatures of western spruce budworm and Douglas-fir tussock moth generally do not show up until late July. Other defoliators such as pine tussock moth need special surveys because the defoliation occurs before the regular survey.

A typical survey day consists of approximately 5.5 to 6.5 hours of flying. The flights occur between 8:00 a.m. and 4:00 p.m. each day. A noon break is usually taken to refuel the aircraft and crew. This break is kept to a 45- to 60-minute maximum to take advantage of optimum sunlight.

Flight Method

Most all aerial surveys are conducted using the contour or drainage-by-drainage method. This method gives a single observer the most thorough view of an area of any first-stage mapping. Terrain often dictates the flying altitude, but generally it is about 1,200 to 2,000 feet above ground level. The estimate is very rough because the terrain is so mountainous.

Flight Following

Positive flight following is practiced in the Northern Region, just as it should be practiced everywhere. Whenever the survey airplane is in the air, someone on the ground knows its location, intention or destination. Flight following is down through the Forest Service dispatch system. Each National Forest has one or more dedicated FM frequency for flight following and other Forest activities. Many dispatch centers are now combined with other National Forests, Bureau of Land Management (BLM) and State agencies for wild fire response efficiency. During the aerial survey, regular check-ins are made every 15 minutes.

Radios used for flight following have been 10 watt 9600's, provided by the Forest Service, which were mounted in the aircraft's instrument panel. The new contract for aerial survey aircraft specify that the contract

aircraft provide their own programmable, 5 watt minimum radio. The benefits of having a programmable radio include being able to contact any National Forest the aircraft is flying over, it offers the flexibility to change frequencies to a fire frequency or to a ground crew's radio frequency, and in eastern Montana where there is less National Forest land, a BLM, State or even wildlife refuge office may be called up for flight following or communication through them to a National Forest.

Survey Flight Maps

Most survey flight maps used for sketch mapping are printed on one side for ease of transferring polygons from the flight map to a final map on a light table. Flight maps are often done in pencil so they can be re-attributed in ink on the ground with the print oriented normally. (An observer normally reads the map oriented to the direction of flight and attributes the polygon in the same way.)

In the past, for the regular aerial surveys, the Forest series (1:126,720) half-inch scale maps were used to sketch map. This map base provides excellent drainage patterns, major grounds features, high points and easily recognizable road systems. As this map base gained additional uses for the Forest such as points of interest, recreation sites and management activity designations, while also providing less and less coverage outside the boundary of the National Forest, the half-inch map became less and less useful to the regular area survey. Since all forested lands are surveyed, a map base that offers complete coverage is necessary. Now, the USDI Geological Survey 1:100,000 scale metric topographical maps are used where needed and available.

Survey Map Processing

Upon completion of a survey map, a master map is made (hand traced) that will be digitized using software developed by our geometronics group. From the digitizing, numerical summaries are made by polygon, attribute and number of trees or intensity. Each polygon is visually checked with a hard copy map for ownership. Ownership information is then combined with the polygon data to produce a final summary by ownership and pest. Land managers are also given photocopies of the master. All surveyor originals and masters are kept on file indefinitely for reference and additional copying.

All the survey maps have been digitized each year since 1988, as well as most maximum-minimum outbreak year maps to support broad-scale analysis projects at both the Forest and Regional level. To support these and other analysis efforts, our map files are usually converted to a MOSS format.

Aerial Pest Detection and Monitoring Questionnaire Results

	Aerial Sketchmap				*Airborne Video*			*Geographic Information System*	
Respondent (Organization)	No. of Aircraft	No. of hrs. flown/year	Aircraft cost/year	No. of personnel in program	No. of hrs. flown/year	No. of aircraft	Image processing (Yes/No)	Yes/No	No. of personnel used
USDA FS R-1 Forest Pest Management	3	375	$65,000	3				Yes	3
USDA FS R-3 Forest Pest Management Flagstaff, AZ	1	200	$20,000	1	40	1	No	Yes	2+
USDA FS R-4 Forest Pest Management	2	350	$55,000	3	26	1	No	Yes	2
USDA FS R-5 Forest Pest Management	2	50	$12,000	Forest personnel	20	1	Yes	Yes	5
USDA FS R-6 Forest Pest Management	2	360	$70,000	5				Yes	2
USDA FS R-8 Forest Health Management Asheville, NC	5	60	$18,000	3	60	1	Yes	Yes	2.5
USDA FS R-8 Forest Health Management Pineville, LA			$5,000		30	5	Yes	No	
USDA FS NA Forest Health Protection Morgantown, WV	6	100	$12,000	1	60	1	Yes	Yes	2
USDA FS NA Forest Health Protection Durham, NH	3	100	?	2	40	2	Yes	Yes	2
USDA FS NA Forest Health Protection St. Paul, MN	1	160		1	20	1	Yes	Yes	2

Respondent (Organization)	No. of Aircraft	No. of hrs. flown/year	Aircraft cost/year	No. of personnel in program	No. of hrs. flown/year	No. of aircraft	Image processing (Yes/No)	Yes/No	No. of personnel used
USDA FS R-10 Forest Health Management Juneau, AK	2	70	$22,000	2	30	1	Yes	Yes	2
USDA FS R-10 Forest Health Management Anchorage, AK	2	100	$35,000	2	2	1	Yes	Yes	1
Idaho Department of Lands Coeur d'Alene, ID	1	65	$12,000	2				No	
Oregon Department of Forestry	1	150	$30,000	2				Yes	USDA FS Personnel
New Mexico State University Cooperative Extension Service	1	35	$3,500	1+					
Texas Forest Service	1-12	350	$35,000	50				No	
Missouri Department of Conservation	3			2				Yes	2
Integrated Forest Pest Management Center, Kenya	1	28	$3,000	2					
TOTALS	42	2,573	$405,500	82	328	15			27.50

1912